Development and application of bioanalytical methodologies based on firefly luciferase (*Photinus pyralis*)

Simone Marin Marques
Doctoral Program in Chemistry
Department of Chemistry and Biochemistry
2014

Supervisor
Joaquim Carlos Gomes Esteves da Silva
Associate Professor with Aggregation, Faculty of Sciences

PhD

This work was supported by a Ph.D. scholarship with the reference **SFRH/BD/65109/2009**, co-funded by the European Social Fund (*Fundo Social Europeu*, *FSE*), through *Programa Operacional Potencial Humano - Quadro de Referência Estratégico Nacional* (*POPH - QREN*), and by national funds from the Ministry of Education and Science through the Portuguese *Fundação para a Ciência e a Tecnologia*, *I.P.* (*FCT*, *I.P.*).

Dedicated to everyone who contributed to it

Acknowledgements

To my scientific supervisor, Professor **Joaquim C.G. Esteves da Silva**, without whom none of this work would exist.

To the **Evaluation Panel** of the Chemistry scientific area of the *Fundação para a Ciência e a Tecnologia*, *I.P.* (*FCT*, *I.P.*) Ph.D. Scholarship Call 2009. They didn't know me, I didn't know them, yet they changed my life.

To ***FCT***, ***I.P.***, for granting the funding for my Ph.D. project.

To my host institution, Chemistry Research Center of the University of Porto (*Centro de Investigação em Química da Universidade do Porto*, *CIQ-UP*), represented by its scientific coordinator, Professor **Manuel A.V. Ribeiro da Silva**, for receiving me as a student and collaborator, and for providing me the conditions to perform my work.

To the Doctoral Program in Chemistry scientific commission, Professor **Manuel A.V. Ribeiro da Silva**, Professor **Maria João Ramos** and Professor **Paula Gomes**. To Professor Gomes my special gratitude for always endure my countless e-mails. To my **schoolfellows** in the Program. To the **teaching staff** from the Department of Chemistry and Biochemistry and the **invited lecturers** who gave their time and their knowledge to enrich the curricular part of the Doctoral Program.

To the **Scientific Council** of Faculty of Sciences, for accepting me as a student and carefully processing all my bureaucracy over these four years with competence and attention.

To Doctor **Valentin N. Petushkov**, for the amazing opportunity of taking part in the elucidation of *Fridericia heliota*'s bioluminescent system.

To **Zélia Azevedo**, for the able assistance in liquid chromatography-mass spectrometry (LC-MS) analysis.

To **Mariana Andrade**, from Materials Center of the University of Porto (*Centro de Materiais da Universidade do Porto*, *CEMUP*), for all the help with the nuclear magnetic resonance (NMR) software. Always available, always so nice.

To the **Department of Chemistry and Biochemistry secretariat** and the **Post-Graduate students office staff**, for all the patience and professionalism to solve all my issues.

To the lab managers **Aurora Leal**, **Maria José Vasconcelos**, **Maria Arminda Silva**, **Maria de Fátima Carvalho** and **Moisés Xavier**, for doing a discrete yet important job.

To my lab buddies **Margarida Miranda, Joel Santos, Diana Gomes, Conceição Mendonça**, **Helena Gonçalves**, **Abel** '**MacGyver**' **Duarte**, **Emanuel Ferreira**, **Ana Reis** and **Marcela Oliveira**, as well as my adoptive lab buddies **Natércia Teixeira**, **Sónia Salomé** and **Isabel Tavares** – always keeping up the fun.

To **Sport Lisboa e Benfica**, for the supreme joy and fun it gave me in the last few weeks of the 2012-2013 soccer season.

To all my **family**. To little misses **Carolina** and **Catarina** big kisses and hugs.

To the new generation of Ph.D. students at lab 2.30 of the Chemometric Research of Chemical, Environmental, Forensic and Biological Systems group, **Eliana Simões**, **Luís Silva**, **Bruno Campos** and **Dilson Pereira** – may the success be with you.

Resumo

Os recentes progressos da química bioanalítica conduziram a diversas aplicações de uso generalizado. Neste âmbito destacam-se as técnicas bioluminescentes, com franco desenvolvimento nos últimos anos, nas quais as luciferases, denominação genérica de enzimas que, agindo sobre o seu substrato natural, luciferina, promovem uma reacção bioquímica na qual ocorre libertação de fotões de luz visível, têm um papel dominante. Este projecto teve como objectivo o desenvolvimento de métodos bioanalíticos visando determinar espécies de interesse biológico, farmacêutico e ambiental baseando-se na luciferase do pirilampo norte-americano *Photinus pyralis* (EC 1.13.12.7) e aplicando metodologias de desenho experimental estatístico. Os analitos escolhidos foram os pesticidas organofosforados, sulfato inorgânico, óxido nítrico (•NO) e ácidos gordos livres. Em paralelo procedeu-se à análise estrutural de compostos semelhantes à luciferina de *Fridericia heliota*, uma minhoca siberiana cujas características bioluminescentes foram recentemente descobertas e que pode constituir um novo sistema bioanalítico de interesse.

O método bioluminescente acoplado para pesticidas organofosforados apresenta uma gama linear entre 2,5-15 μM, com limite de detecção (LD) de 1,5 μM e limite de quantificação (LQ) de 5,0 μM, e foi testado em águas de poços domésticos. O método bioluminescente para sulfato inorgânico, por sua vez, apresenta uma gama linear entre 14-134 $mg \cdot mL^{-1}$, com LD de 10 $mg \cdot mL^{-1}$ e LQ de 34 $mg \cdot mL^{-1}$, e foi testado também em águas de poços domésticos. Relativamente ao •NO, o método desenvolvido apresenta uma gama linear entre 10-100 nM, LD de 4 nM e LQ de 15 nM, e foi testado em saliva humana e meio de cultura de microalgas. Por fim, o método bioluminescente para ácidos gordos livres apresenta uma gama linear entre 1-20 μM, LD de 1,3 e LQ de 4,5 μM, e foi testado em plasma sanguíneo.

Devido à reduzida quantidade de luciferina de *Fridericia heliota* que se consegue extrair, não foi ainda possível estabelecer a sua estrutura química. No entanto, foram realizados estudos utilizando-se compostos semelhantes à luciferina, que serviram como modelos. Estes compostos foram informalmente denominados CompostoX (CompX) e AsLn (acompanhante similar à luciferina). AsLn parece estar intimamente relacionado com a verdadeira luciferina, como um sub-produto ou um intermediário na sua biossíntese, enquanto CompX é um fragmento de AsLn.

Palavras-chave

- Química bioanalítica
- Métodos bioluminescentes
- Ensaio enzimático
- Bioluminescência
- Método de vias enzimáticas acopladas com detecção por bioluminescência
- Luminometria
- Luciferase de pirilampo
- *Photinus pyralis*
- Desenho experimental
- Pesticidas organofosforados
- Sulfato inorgânico (SO_4^{2-})
- Óxido nítrico (•NO)
- Ácidos gordos livres
- Limite de detecção
- Limite de quantificação
- Gama linear
- Curva de calibração
- Método das adições de padrão
- Enquitreídeo
- *Fridericia heliota*
- Luciferina de *Fridericia heliota*
- Compostos relacionados com a luciferina
- CompX
- AsLn(2)
- Determinação da estrutura química
- Cromatografia líquida de alto desempenho
- Espectrometria de massa
- Ressonância magnética nuclear

Abstract

Recent advances in bioanalytical chemistry led to several general purpose applications. In this context the focus is on the bioluminescent techniques, with a fast development in recent years, in which luciferases, generic name for enzymes that, by acting on its natural substrate, luciferin, promote a biochemical reaction which release photons of visible light, have a dominant role. The purpose of this project was the development of bioanalytical methods to determine species of biological, pharmaceutical and environmental interest based on luciferase from the North-American firefly *Photinus pyralis* (EC 1.13.12.7) and applying statistical experimental design methodologies. The chosen analytes were organophosphorus pesticides, inorganic sulfate, nitric oxide (•NO) and free fatty acids. In parallel proceeded the structural analysis of luciferin-related compounds from *Fridericia* heliota, a Siberian earthworm whose bioluminescent features were recently discovered and which may constitute a new interesting bioanalytical system.

The coupled bioluminescent method for organophosphorus pesticides has a linear range between 2.5-15 μM, with a limit of detection (LOD) of 1.5 μM and a limit of quantitation (LOQ) of 5.0 μM, and has been tested in water from domestic wells. The bioluminescent method for inorganic sulfate, in turn, shows a linear range between 14 to 134 $mg \cdot mL^{-1}$, LOD 10 $mg \cdot mL^{-1}$ and LOQ 34 $mg \cdot mL^{-1}$ and was also tested in domestic wells' water. Regarding •NO, the developed method has a linear range of 10-100 nM, LOD 4 nM and LOQ 15 nM and was tested in human saliva and microalgae culture medium. Finally, the bioluminescent method for free fatty acid has a linear range between 1-20 μM, LOD 1.3 μM and LOQ 4.5 μM and was tested in blood plasma.

Due to the reduced amount of *Fridericia heliota* luciferin obtained in extracts, it was not yet possible to establish its chemical structure. However, studies were performed using compounds similar to the luciferin, which served as models. These compounds were informally called CompoundX (CompX) and AsLn (accompanying similar to luciferin). AsLn appears to be closely related to the true luciferin, as either a by-product or an intermediate in its biosynthesis, whereas CompX is a fragment of AsLn.

Keywords

- Bioanalytical chemistry
- Bioluminescent methods
- Enzymatic assay
- Bioluminescence
- Coupled bioluminescent assay
- Luminometry
- Firefly luciferase
- *Photinus pyralis*
- Experimental design
- Organophosphorus pesticides
- Inorganic sulfate (SO_4^{2-})
- Nitric oxide (•NO)
- Free fatty acids
- Limit of detection
- Limit of quantitation
- Linear range
- Calibration curve
- Method of standard additions
- Enchytraeid
- *Fridericia heliota*
- *Fridericia heliota* luciferin
- Luciferin-related compounds
- CompX
- AsLn(2)
- Chemical structure elucidation
- High-performance liquid chromatography (HPLC)
- Mass spectrometry (MS)
- Nuclear magnetic resonance (NMR)

Structure of the Thesis

This Thesis is divided into four sections, the introduction, the presentation of the developed methods, the studies made on *Fridericia heliota*'s luciferin-related compounds, and a conclusion and future perspectives. Each section, by its turn, is composed of chapters, corresponding to papers already published or manuscripts intended to be submitted for publication in specialized peer-reviewed international journals.

The introduction section presents one chapter (Chapter one), in which photochemical concepts, luciferases' reaction mechanisms and bioluminescent techniques principles are described, together with selected examples of applications. This section ends with a brief description of the main objectives of the project that led to the Thesis.

The second section encompasses four chapters corresponding to the bioluminescent methods for organophosphorus pesticides (Chapter two), inorganic sulfate (Chapter three), nitric oxide (Chapter four) and free fatty acids (Chapter five).

The third section has three chapters, dealing with preliminary analyses on AsLn (Chapter six) and the structural characterization of CompX (Chapter seven) and AsLn(2) (Chapter eight).

The fourth and last section presents the main conclusions of the performed work, as well as a book chapter addressing the development of novel bioluminescent methods using nanomaterials (Chapter nine).

Table of contents

Section one

Introduction

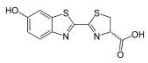

Chapter one

There´s plenty of light at the bottom: Bioanalytical and biomedical applications of luciferases

Simone M. Marques, Joaquim C.G. Esteves da Silva

Glob. J. Anal. Chem. 2 (2011) 241-271

The text was integrally written and the figures were integrally made by Simone Marques within the host institution, the Chemometric Research of Chemical, Environmental, Forensic and Biological Systems group, from the Chemistry Research Center of the University of Porto (*Centro de Investigação em Química da Universidade do Porto*, *CIQ-UP*), Department of Chemistry and Biochemistry, Faculty of Sciences, University of Porto, under the supervision of Joaquim Esteves da Silva.

GLOBAL JOURNAL OF ANALYTICAL CHEMISTRY

There´s plenty of light at the bottom: Bioanalytical and biomedical applications of luciferases

Simone M. Marques, Joaquim C.G. Esteves da Silva*

Centro de Investigação em Química da Universidade do Porto (CIQ-UP), Department of Chemistry and Biochemistry, Faculty of Sciences, University of Porto, Rua do Campo Alegre, no. 687, 4169-007 Porto, Portugal

**Author for correspondence: Joaquim C.G. Esteves da Silva, email: jcsilva@fc.up.pt*
Received 2 Mar 2011; Accepted 19 Apr 2011; Available Online 18 May 2011

Abstract

Bioanalytical chemistry has been attracting much attention in recent years due to the growing interest in biomolecules in the biochemical, biological, biomedical, pharmaceutical and environmental contexts, allowing detailed and sensitive analysis from the molecular up to the whole-body level. This review focuses on the application of luciferases, a generic name for enzymes whose biochemical reactions lead to a particular phenomenon called bioluminescence, concerning bioanalytical chemistry and biomedicine. Several powerful techniques employing luciferases were developed, among which bioluminescence resonance energy transfer (BRET) assays, split luciferase assays and bioluminescence imaging (BLI) stand out. Luciferase bioluminescent methods were successfully applied to gain insights into drug screening, gene-mediated therapy evaluation, infection progression, cancer therapy, cell tracking, biosensors, basic research and biomedical engineering, which will be illustrated through representative examples.

Keywords: Luciferase; Bioluminescence; Bioanalytical chemistry; Biomedicine; Bioluminescence imaging; Bioluminescence resonance energy transfer; Split luciferase; Quantum dot

Abbreviations: BLI, bioluminescence imaging; BRET, bioluminescence resonance energy transfer; λ_{max}, wavelength of maximum emission

1. Introduction

1.1. When analytical chemistry meets life sciences

Bioanalytical chemistry can be regarded, in simple terms, as the result of applying the concepts and techniques of "classical" analytical chemistry towards the study of biomolecules like nucleic acids, proteins, lipids, drugs and antibodies [1]. It is an interdisciplinary field, meeting the interest of chemistry, biochemistry, molecular and cell biology, biomedicine and clinical analysis, environmental toxicology, forensic sciences, food chemistry, industrial and pharmaceutical research, and so forth. Some well-established analytical techniques such as chromatography, mass spectrometry, spectrophotometry and nuclear magnetic resonance are also employed in bioanalysis, taking into account the specificities of biomolecules. Other techniques were developed owing to biomolecule studies, namely the enzyme linked immunosorbent assay (ELISA), the polymerase chain reaction (PCR) and electrophoresis [1].

Bioanalytical methods have to meet essential requirements in order to be suitable for bioanalysis, namely an enhanced sensitivity, robustness and specificity. Nowadays, with their widespread use in clinical and pharmaceutical analysis, it is also desirable that they can be suitable for high-throughput screening, ease to perform, commercially available and moderate-to low-cost. In this context the enzyme luciferase is an invaluable tool [2], and this review aims to present its most recent application in outstanding research areas.

2. Bioluminescence and luciferases

2.1. Basic photochemical and photophysical concepts

Before focusing attention to the bioluminescence phenomenon itself, it may be convenient to expose some basic concepts on photochemistry and photophysics.

There are two relevant forms of electromagnetic radiation (light) emission, incandescence and luminescence. Originally they were called "hot light" and "cold light" respectively, since incandescence involves the conversion of vibrational energy into radiant energy as a consequence of a raise in the temperature [3], whereas luminescence is about

GLOBAL JOURNAL OF ANALYTICAL CHEMISTRY

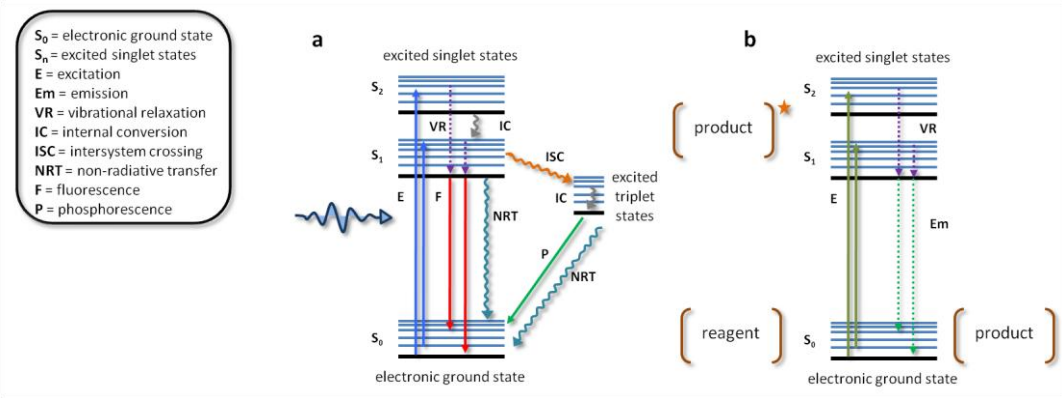

Figure 1. Jablonski diagrams for (a) photoluminescence and (b) bioluminescence. Photoluminescenc (a) is initiated by the absorption of electromagnetic radiation (wavy blue arrow), whereas in bioluminescence (b) an excited state product is generated in a biochemical reaction; its decay to the ground state releases photons of visible light. See text for more details.

electronic transitions [4]. But actually, the main differentiation criterion between incandescence and luminescence should not be heat, but instead whether the light emission involves transitions in electronic energy levels among atoms or molecules, in the case of incandescence, or transitions in electronic energy levels within atoms or molecules, in the case of luminescence [5].

Regarding the energy source responsible for the formation of the electronically excited state, luminescence can be classified into different types. For example, photoluminescence is the result of absorption of photons and re-emission of photons of lower energy; electroluminescence occurs due to an electric current; and crystalloluminescence refers to the release of light as a result of the crystallization of a substance [6]. Chemiluminescence designates the process in which a chemical reaction produces the electronically excited substance. When these reactions are encountered in biological systems the effect is then known as bioluminescence [6].

All processes which occur within excited substances can be graphically presented through a Jablonski diagram (Figures 1a and 1b) [4]. In photoluminescence, an electron in the electronic ground state (S_0, Figure 1a) is excited (E, Figure 1a) to one of the many vibrational levels in the electronic excited state (S_1 and S_2, Figure 1a) as a consequence of absorption of photons. Typically, those are excited singlet states (S), so that the electrons remain spin-paired. Once in the excited electronic state, there are many possible ways in which energy can be released to return the electron to its ground state. A molecule in an excited state can lose energy to other molecules through collisions, or distribute its excess energy to its own vibrations and rotations (VR, Figure 1a) [4]. The electron can also undergo internal conversion (IC, Figure 1a), placing it from a higher vibrational level (S_2) to a lower one (S_1). It is also possible that the molecule loses its energy in other processes that do not lead to light emission, called non-radiative transfer of energy (NRT, Figure 1a). Finally, an electron in excited singlet states can also return to the ground state by emitting a photon (F, P, Figure 1a). If the emission comes from singlet states it is called fluorescence (F, Figure 1a). The other possibility for the electron is to change its spin in a process called intersystem crossing (ISC, Figure 1a). This results in a triplet excited state. From the triplet state the electron must change its spin again before returning to the ground state. If this is done along with the emission of a photon, the process is called phosphorescence (P, Figure 1a). It is also possible for the triplet state to return to the ground state by non-radiative transfer (NRT, Figure 1a) [4]. Analogous processes occur in bioluminescence (Figure 1b), except that the initial excited state is created by a biochemical reaction. The corresponding emission of photons (Em, Figure 1b) is regarded as bioluminescence emission, although it is indistinguishable from fluorescencent emission.

Another important concept is the quantum yield (Φ). It can be defined as the number of defined events occurring *per* photon absorbed by the system (1) [6]:

$$\Phi = \frac{(number\ of\ events)}{(number\ of\ photons\ absorbed)} \quad (1)$$

For example, in fluorescence processes it can be specifically stated as the ratio between the number of photons emitted to the number of photons absorbed, and in chemiluminescence or

bioluminescence it is the amount of photons emitted to the amount of reactant consumed or product formed [6]. In those latter cases, Φ can be divided into three components: (1) the fraction of the reaction that produces the light emitter, Φ_r; (2) the fraction of emitter that is formed in a excited state, Φ_{ex}; and (3) the fraction of those excited states that emit light, Φ_{fl} (quantum yield for fluorescence) [7, 8]; the overall efficiency resulting is then $\Phi = \Phi_r \Phi_{ex} \Phi_{fl}$ [7, 8]. In this sense, the quantum yield can be viewed as a measure of the efficiency of the system.

2.2. It is only bioluminescence with luciferases

As it was seen above, bioluminescence can be regarded as a particular case of chemiluminescence. The main difference is that bioluminescent chemical reactions must be catalyzed by specific enzymes. These enzymes are generally called luciferases, whose name is derived from the Latin words *lucem ferre*, meaning "light-bearer". In the same sense, the corresponding substrates are the luciferins. All bioluminescent reactions are oxidations with molecular oxygen, and they may also require co-factors such as adenosine-5'-triphosphate (ATP), magnesium ions or reduced flavin mononucleotides (riboflavin-5'-phosphate, $FMNH_2$). Some reactions involve additional proteins, which will be described later.

Bioluminescence is ubiquitous in nature. Several creatures developed their luciferase-luciferin systems, for example bacteria (*Photobacterium*, *Xenorhabdus*, *Vibrio*), dinoflagellates (*Gonyaulax*, *Noctiluca*, *Pyrocystis*), coelenterates (*Aequorea*, *Renilla*), annelids (*Diplocardia*, *Fridericia*), mollusks (*Latia*), crustaceans (*Cypridina*, *Metridia*, *Gaussia*), fungi (*Panellus*, *Mycena*, *Omphalotus*) and insects (*Photinus*, *Photuris*, *Luciola*, *Pyrophorus*, *Phrixothrix*, *Pyrearinus*, *Arachnocampa*) [9-12].

However, for practical purposes, the main luciferases in use are those from bacteria, from the marine copepod crustaceans *Gaussia princeps*, *Cypridina noctiluca* and *Cypridina hilgendorfii*, from the coelenterate *Renilla reniformis* and from the North American firefly *Photinus pyralis*, which will be the focus from this point on.

3. Bacterial luciferase

Bacterial luciferase is classified as alkanal, $FMNH_2$: oxygen oxidoreductase (1-hydroxylating, luminescing), EC 1.14.14.3. All bacterial luciferases isolated so far are heterodimers composed of two non-identical subunits, an α subunit with molecular weights between 40-42 kDa and a β subunit between 37-39 kDa, giving a global molecular weight about 76 kDa [10, 12]. The bioluminescent reaction involves the oxidation of $FMNH_2$ and a saturated long-chain aliphatic aldehyde with more than ten carbon atoms, preferably tetradecanal [12]. The aldehyde is considered to be the bacterial luciferin, producing the corresponding carboxylic acid, oxidized flavin (FMN), a molecule of water and light in the blue region of the visible spectrum [wavelength of maximum emission (λ_{max}) = 490 nm] *in vitro*, with a quantum yield between 0.10 and 0.16 [10, 12].

For the bioluminescent reaction to begin, $FMNH_2$ must be produced in bacterial cells from FMN, by reduction with the enzyme flavin reductase using nicotinamide adenine dinucleotide reduced (NADH) as the reducing agent (Figure 2a) [10, 12, 13]. The free form of $FMNH_2$ is extremely unstable in the presence of oxygen, being instantly oxidized. In the presence of bacterial luciferase, however, $FMNH_2$ bounds to it and is deprotonated at a nitrogen atom, forming an $FMNH_2$-luciferase complex that is more stable than free $FMNH_2$ (Figure 2a). The deprotonated flavin in the complex is readily attacked by molecular oxygen, giving a hydroperoxide (intermediate I, Figure 2a). In the presence of a long-chain aldehyde (bacterial luciferin), intermediate I is converted into intermediate II, which contains a peroxyhemiacetal of flavin (Figure 2a). The decomposition of intermediate II, through several steps, yields the excited-state hydroxyflavin-luciferase complex (intermediate III) and the corresponding fatty acid. Although the aldehyde is regarded as the luciferin, the light emitter is considered to be the luciferase-bound hydroxyflavin (intermediate III, Figure 2a). Light is emitted when the excited state intermediate III falls to the ground state, generating water and FMN, which is regenerated by flavin reductase to enter a new reaction cycle [10, 12]. In the same way, the produced carboxylic acid can be reduced again to the corresponding aldehyde. With purified bacterial luciferases, the maximum emission is similar for different species and occurs at 490 nm, but a completely different pattern is seen *in vivo* [10, 12]. In fact, *in vivo* emission maxima range from 472 to 545 nm, depending on the bacterium species [12]. This phenomenon is explained by the presence of accessory proteins, namely bacterial blue fluorescent lumazine protein (LumP) and bacterial yellow fluorescent protein (YFP), which absorb the light energy produced by bacterial luciferases and re-emits in longer wavelengths [10, 12]. This process,

GLOBAL JOURNAL OF ANALYTICAL CHEMISTRY

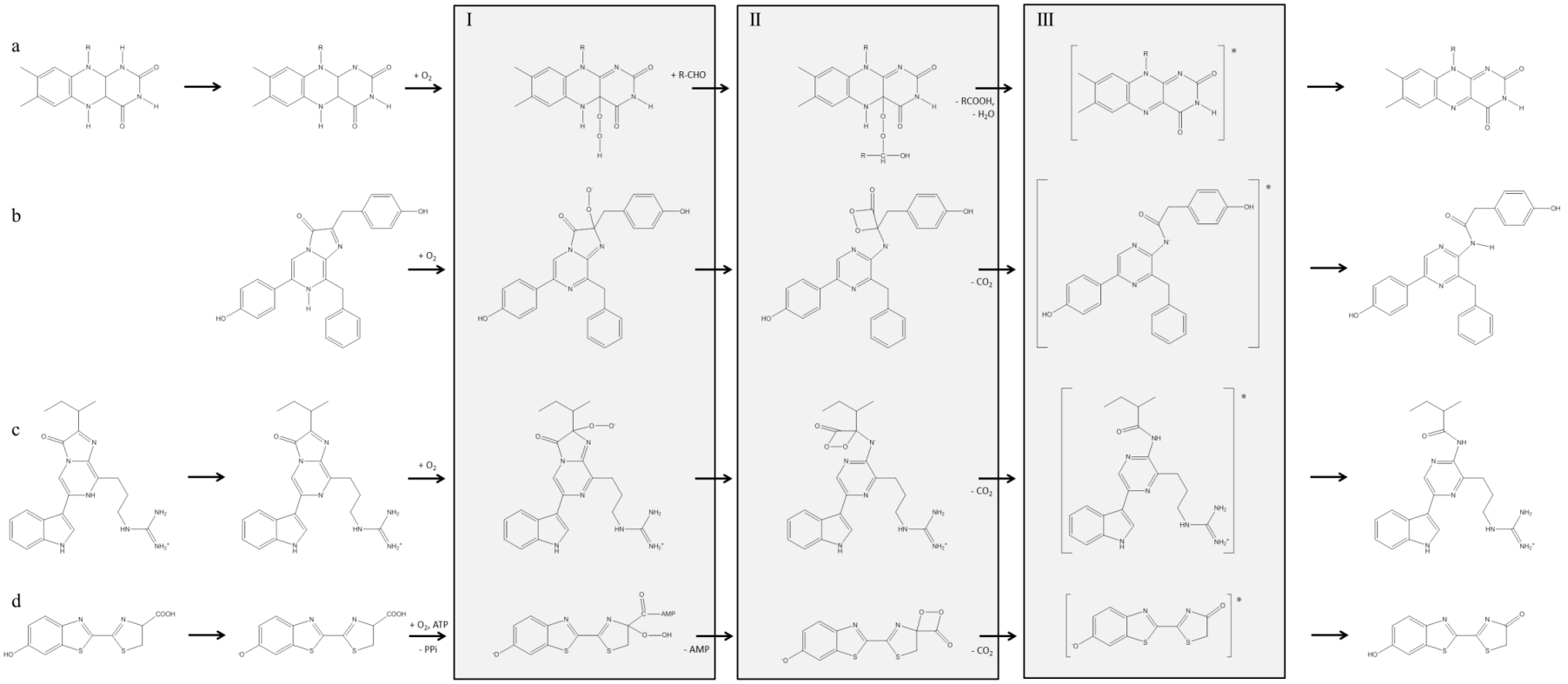

Figure 2. Schematic biochemical reactions catalyzed by (a) bacterial luciferase, (b) Renilla and Gaussia luciferases, (c) Cypridina luciferase and (d) firefly luciferase. In general terms, those reactions involve specific substrate, luciferins, which react with molecular oxygen to generate intermediates I; afterwards, those intermediates originate the energy-rich intermediates II, either by the reaction with long-chain aldehydes (a) or by the formation of four-membered ring dioxetatones (b-d); finally, the excited state light emitter intermediates III are produced, which release photons of light and leads to the oxidized ground-state final products.

bioluminescence resonance energy transfer (BRET), will be explained in section 8.6.

Bacterial luciferase genes (*lux* genes) are arranged in an operon, *lux*CDABE [14]. The *lux*A and *lux*B genes code for the subunits of bacterial luciferase, whereas *lux*C, D and E code for an enzyme, fatty acid reductase, responsible for the biosynthesis of the aldehyde. Other *lux* genes may be found in certain species, like the regulatory genes *lux*I and *lux*R, or *lux*H involved in riboflavin synthesis [14]. This genetic organization of the bioluminescent system genes in bacteria opens up the interesting possibility of constructing self-illuminating cells and organisms through the introduction of the whole *lux*CDABE operon, as it codes for both bacterial luciferase itself and the enzymes to synthesize bacterial luciferin [15].

4. *Renilla reniformis* (Renilla) luciferase

The luciferase from the sea pansy *Renilla reniformis* is one of the best characterized luciferase-luciferin system from a marine organism. Its systematic name is *Renilla*-luciferin: oxygen 2-oxidoreductase (decarboxylating), EC 1.13.12.5. Purified Renilla luciferase has a molecular weight of about 35 kDa [10, 12]. *In vitro*, the bioluminescent reaction presents a $pH_{optimal}$ at 7.4, at 32 ºC and in the presence of a salt like NaCl or KCl. It generates photons in the blue range (λ_{max} = 480 nm) with a quantum yield of about 0.06-0.07 [10, 12]. Renilla luciferin is coelenterazine, an imidazopyrazinone common to other bioluminescent and non-bioluminescent marine organisms [12, 16].

Regarding the *in vivo* bioluminescent reaction, coelenterazine is stored in the form of coelenterazine enol-sulfate [12]. Part of the coelenterazine sulfate stock is subjected to sulfate removal by a luciferin sulfokinase, allowing coelenterazine to bind to coelenterazine-binding protein, a protein akin to calmodulin in its capacity to bind calcium ions. When calcium concentration is raised, by nerve stimulation, three calcium ions bind to coelenterazine-binding protein, triggering the release of coelenterazine [12]. From this point coelenterazine binds to Renilla luciferase, where it will react with oxygen producing a peroxide intermediate (intermediate I, Figure 2b) [12]. This intermediate undergoes a cyclization to form an energy-rich dioxetanone intermediate (intermediate II, Figure 2b), whose breakage leads to carbon dioxide (CO_2) and the oxidized form of coelenterazine, coelenteramide, in the excited state (intermediate III, Figure 2b) [10, 12]. Like in the bacterial bioluminescent system, in Renilla's system there is also an accessory protein, Renilla green fluorescent protein (Not to confuse with the better known green fluorescent protein from the jellyfish *Aequorea victoria*, whose discovery and development granted the Nobel Prize in Chemistry in 2008) [10, 12]. In the presence of Renilla green fluorescent protein, the energy of the excited state coelenteramide is transferred, by BRET, to the fluorescent protein, resulting in the emission of green light (λ_{max} = 509 nm); in the absence of the fluorescent protein or in *in vitro* conditions, however, blue light (λ_{max} = 480 nm) is emitted [10, 12].

5. *Gaussia princeps* (Gaussia) luciferase

Gaussia luciferase, from the homonymous marine crustacean species *Gaussia princeps*, is one of the latest luciferases being used in bioanalytical applications. It is the smallest luciferase found to date, with a molecular weight about 19.9 kDa [12, 17-19]. It is naturally secreted, *in vivo* and *in vitro*, due to a secretory sequence peptide. Moreover, Gaussia luciferase is a coelenterazine-dependent luciferase, and its bioluminescent reaction mechanism is believed to equal that of Renilla luciferase, namely the oxidative decarboxilation of coelenterazine to yield excited-state coelenteramide and photons of blue light (λ_{max} = 470 nm) (Figure 2b) [12, 17-19]. Like other coelenterazine-dependent luciferases, this luciferase has a tendency to self-aggregate into inactive forms [12]. *In vitro*, the bioluminescent reaction presents a $pH_{optimal}$ at 7.7, and its activity is highly dependent upon the concentration of monovalent cations. Nonetheless, Gaussia luciferase is very resistant to high temperatures (that is, it is a thermostable enzyme) and to extreme acidic and basic conditions, which is important for technological applications [12, 17-19].

Contrary to early discovered luciferases, which were subjected to decades of studies before cloning, genetic engineering improvements and assignement to molecular biology and bioanalytical applications, Gaussia was readily recruited to practical applications. Indeed, Gaussia luciferase is currently commercially available as plasmids (Figure 3). Furthermore, it was already subjected to genetic enhancements. One such important feature includes a recombinant biotinylated version of Gaussia luciferase [20]. Biotin is a small vitamin which is used in laboratorial studies as a biological "hook" to separate proteins [21]. This compound is chemically linked to a protein of interest. After that, the sample with the biotinylated protein is incubated with

GLOBAL JOURNAL OF ANALYTICAL CHEMISTRY

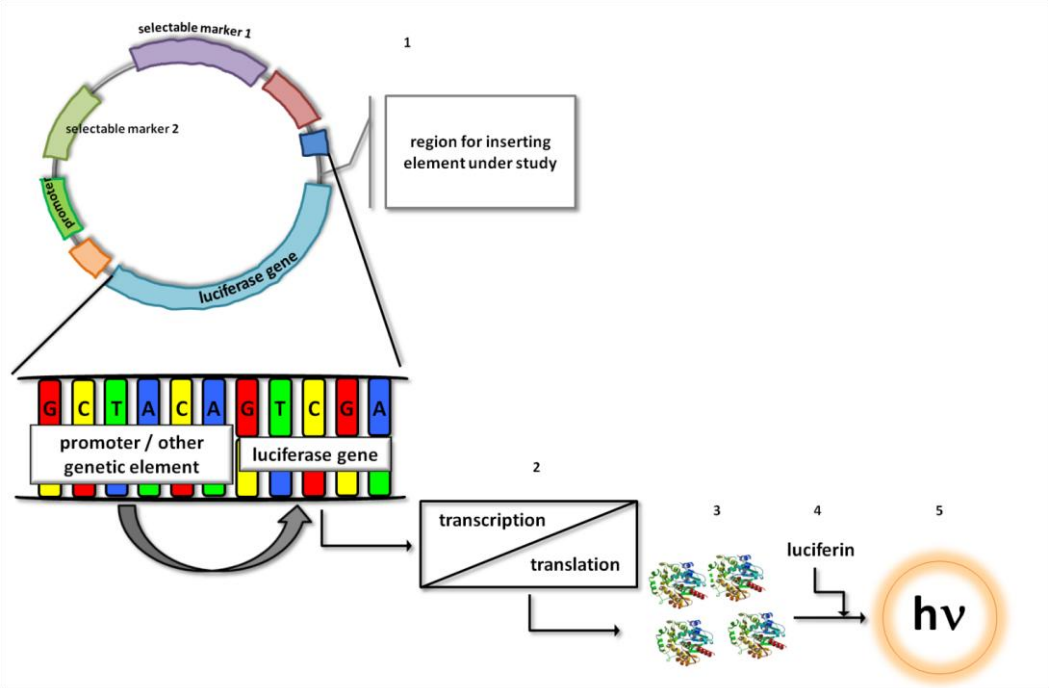

Figure 3. Principle of luciferase reporter gene assay. A plasmid containing the luciferase gene and the genetic element under study is constructed (1). These plasmids also contain several genetic elements to allow the correct processing of luciferase gene, like selectable markers and promoters. Once this plasmid is processed by the the cell's DNA replication machinery, luciferase is transcribed (that is, an mRNA is produced) and translated (2) into functional luciferase (3). By adding luciferin (4), light is emitted (5).

straptavidin or avidin immobilized into a support. Both of them bind strongly and specifically to biotin, allowing the separation of the biotinylated protein from solution [21]. A biotinylated Gaussia luciferase facilitate its purification, reduces its inactivation due to conjugation with other molecules and facilitates its use as a bioprobe [20]. Another improved Gaussia luciferase is a "humanized", codon-optimized version which produces 200- (*in vivo*) to 1000-fold (*in vitro*) higher bioluminescence signals in mammalian cells compared to Renilla and firefly luciferases [22].

6. Cypridina luciferase

Cypridina luciferase is obtained from marine crustaceans (sea fireflies) of the species *Cypridina noctiluca* [23] and *Cypridina hilgendorfii* (also known as *Vargula hilgendorfii*) [12, 24]. Its classification is *Cypridina*-luciferin: oxygen 2-oxidoreductase (decarboxylating), EC 1.13.12.6. The bioluminescent substrate is Cypridina luciferin, sometimes called vargulin, an imidazopyrazinone chemical compound distinct from the other luciferins described so far [12]. The bioluminescent reaction also requires molecular oxygen, yielding CO_2 and oxidized vargulin [12]. Cypridina luciferase is a 61-62-kDa enzyme, emitting blue light (λ_{max} = 452 nm) *in vivo*, although the color can vary *in vitro* according to the buffer used. The $pH_{optimal}$ is 7.7 and the optimum temperature is about 30 ºC [12]. Salts like NaCl or $CaCl_2$ are important to enhance the reaction output. *In vivo*, it is secreted to the medium [12], as well as in *in vitro* assays [25].

The Cypridina bioluminescenct reaction proceeds according to the scheme shown in Figure 2c [12]; the imidazopyrazinone part of Cypridina luciferin is negatively charged when the luciferin is bound to luciferase, making it easily oxygenated by molecular oxygen, and leading to a peroxide anion (intermediate I, Figure 2c). Analogously to Renilla biolumescent reaction, the peroxide cyclizes, forming a dioxetanone ring (intermediate II, Figure 2c), which instantly decomposes by a concerted splitting of the 4-membered ring into CO_2 plus an amide oxidized Cypridina luciferin in an excited state (intermediate III, Figure 2c). Light is emitted when the excited state falls to its ground state. The quantum yield is about 0.3 [12].

7. *Photinus pyralis* (firefly) luciferase

Firefly luciferase, or *Photinus*-luciferin: oxygen 4-oxidoreductase (decarboxylating,

ATP-hydrolysing), EC 1.13. 12.7, from the North American firefly (*Photinus pyralis*), is the most popular luciferase so far regarding bioanalytical applications. It is also one of the best studied and characterized luciferase, thanks to the work of William McElroy and colleagues during several decades, although some details regarding its biochemical mechanism are not yet clear [26].

Firefly luciferase is a 62-kDa [27, 28] enzyme bearing a peroxisome targeting peptide in its native form [29]. The firefly luciferin is the D- enantiomer of a benzothiazolyl-thiazole, [(S)-2-(6'- hydroxy-2'-benzothiazolyl)-2-thiazoline-4-carboxylic acid], or simply D-luciferin [30]. The same way coelenterazine is common to several marine organisms, so all the bioluminescent beetles (order *Coleoptera*; families *Elateridae*, for example click beetles; *Phengodidae*, like railroad-worms; and *Lampyridae*, the fireflies) share this luciferin in their bioluminescent reaction [10, 12, 26, 30, 31].

Contrary to the other luciferases described so far, firefly luciferase requires ATP, along with a divalent metallic cation, most frequently magnesium ions, to proceed. Unlike the common sense, however, ATP does not have an energetic role, but rather to provide a good leaving group, adenosine-5´-monophosphate (AMP), which facilitates the subsequent steps of the bioluminescent reaction [10]. *In vivo*, yellow-green light is emitted; *in vitro*, however, the emission peak can be the same as *in vivo* (λ_{max} = 562 nm), as firefly's bioluminescent system does not have accessory fluorescent proteins, but only at basic media (pH about 7.5-7.8) [10, 12, 26, 30, 31]. In fact, firefly luciferase is pH-sensitive, and acidic media (pH about 5-6) can shift the emission to the red (λ_{max} = 620 nm), along with higher temperatures or heavy metal cations [10, 12, 26, 30, 31]. The $pH_{optimal}$ is about 7.8 at 23-25 ºC. The formation of inhibitory by-products can hamper the emission from luciferase. The addition of coenzyme A (CoA) leads to the conversion of these inhibitory by-products to a less inhibitory form, thus stabilizing and prolonging the light emission [10, 12, 26, 30-32].

The detailed mechanism of the bioluminescent reaction catalyzed by firefly luciferase is somewhat complex, and its full presentation is not under the remit of this review (interested readers may consult ref. [26, 30, 31]). In short, the reaction emcompasses the activation of D-luciferin by ATP-Mg^{2+}, generating inorganic pyrophosphate (PPi) and a luciferase-bound adenylated intermediate (Figure 2d), an anhydride formed between the carboxyl group of D-luciferin and the phosphate group of AMP [10, 12, 26, 30, 31]. The adenylate is oxidated by oxygen in the air, forming a hydroperoxide intermediate (intermediate I, Figure 2d) which, by its turn, produces the dioxetanone ring-bearing intermediate II by the departure of AMP. As this high-energy ring is very unstable, it quickly breaks down, yielding CO_2 and oxyluciferin in an excited state (intermediate III, Figure 2d). The excited state oxyluciferin release its energy as photons, leaving oxyluciferin in the ground state [10, 12, 26, 30, 31]. The quantum yield of this reaction is about 0.41-0.48 [33, 34].

8. Bioanalytical methodologies based on luciferases – then and now

This section aims to present the basic principles underlying the diversified luciferase-based methods established for bioanalytical purposes, preceding the presentation of demonstrative examples of their application.

8.1. Luciferase assay

In initial studies about luciferase, as early as 1947, McElroy observed that the duration of the emitted light by firefly luciferase *in vitro* was directly proportional to the amount of ATP added [35]. Although at that time the role of ATP in the bioluminescent reaction was unknown, and only a qualitative relationship between light and ATP could be inferred [35], it was a hint of the potential of luciferase for ATP assay. And indeed this was the case. In the incoming years, the major application of firefly luciferase was in luciferase assays for ATP [36]. In the simplest assays, a reaction mixture is prepared, composed of luciferase, luciferin and magnesium cations (like $MgCl_2$) in a buffer system at pH 7.6-7.8. Sometimes CoA is also added to stabilize the light emission. A calibration curve with ATP is obtained and the sample is tested. The emitted light is recorded on luminometers, a specific device equipped with photomultiplier tubes with variable degrees of sensitivity. With time, a more complete knowledge of firefly luciferase bioluminescent reaction was achieved, and thus more sophisticated methods were developed [2], for example the ATP measurement inside cells with genetically encoded luciferases (see next section), along with the development of assays for other analytes which participate in the reaction, namely CoA [37] and PPi [38]. Likewise, analytes other than ATP could be assessed with bacterial luciferase, as its reaction allows the assay of long-chain aldehydes [39], NADH [40, 41] and FMN [40].

8.2. Luciferase reporter gene assay

Reporter gene can be defined as "a gene with a readily measurable phenotype that can be distinguished easily over a background of endogenous proteins" [42, 46]. Reporter gene technology is, then, a molecular biology tool in which a reporter gene is introduced into cells, together with a genetic entity of interest and, once it is translated into protein, it can be readily detected, giving information about molecular or cellular events under study (Figure 3) [43]. The reporter gene and the genetic entity under study are placed together in the same DNA construct, usually in the form of a circular DNA molecule called a plasmid (Figure 3), prior to their introduction into cells. The most commonly studied processes are the following [42, 43]: 1) the expression of a gene of interest. In this case the reporter is directly attached to the gene of interest, being the two genes under the control of the same promoter elements and being transcribed into a single messenger RNA (mRNA). The mRNA is then translated into the protein, and the localization of the protein can be traced by assaying the reporter, for example by adding its substrate when the reporter is an enzyme; and 2) the activity of a particular promoter or other regulatory element, like an enhancer. In this case there is no separate "gene of interest"; the reporter gene is simply placed under the control of the target promoter or element, and its transcriptional strength is then estimated quantitatively from the *in vitro* activity of the reporter gene product, considering that the action of the promoter upon the reporter will be the same as that upon the native gene [42, 43].

The onset of this technology dates back early 1980's, for both prokaryotic and eukaryotic cells [44, 45]. At this time popular reporter genes were the enzymes chloramphenicol acetyltransferase, β-galactosidase and alkaline phosphatase [46, 47]. Firefly luciferase was introduced as a reporter gene a few years after its cloning in 1985 [28], for example in plant cells and transgenic whole plants [48], for the study of the cauliflower mosaic virus 35s RNA promoter [49], for the analysis of the interleukin-2 promoter [50] and for the study of estrogen regulatory elements in a *Xenopus* (aquatic frog) model [51]. In the same sense, bacterial luciferase was then applied as reporter, for example in the study of genetic recombinatory mechanisms in prokaryotes [52].

8.3. Bioluminescent Enzyme Immunoassay (BLEIA)

An enzyme immunoassay (EIA) is a biochemical technique used mainly in immunology to detect the presence of an antibody or an antigen in a sample. In simple terms, a specific antibody is added to a sample with an unknown amount of the antigen or *vice-versa*. This antibody is linked to an enzyme and, in the final step, a substrate is added so that the enzyme can convert it into some detectable signal, most commonly a color change [53, 54]. When the enzyme is luciferase, the assay is called bioluminescent enzyme immunoassay (BLEIA) [55].

Regarding the most common procedure, a buffered solution of the antigen to be tested is added to each well of a microtiter plate, where the antigen will adhere. A solution of a non-reacting protein, such as bovine serum albumin (BSA) or casein, is added to block any plastic surface in the well that remains uncoated by the antigen. Next, a primary antibody is added, which binds specifically to the test antigen that is coating the well. This primary antibody could also be in the serum of a donor, in which case it will be tested for reactivity towards the antigen. Afterwards, a secondary antibody is added, which will bind the primary antibody. This secondary antibody often has an enzyme attached to it, which should have a negligible effect on the binding properties of the antibody. A substrate for this enzyme is then added. Often, this substrate changes color upon reaction with the enzyme. The color change shows that secondary antibody has bound to primary antibody, which strongly implies that the donor has had an immune reaction to the test antigen. The higher the concentration of the primary antibody which was presented in the sample, the stronger is the color change [53, 54]. Often a spectrometer is used to give quantitative values for color strength. In other formulations the primary antibodies can be added to the microtiter plate first, followed by the antigen sample and the secondary antibodies. Also, chemically modified antigens can be marked with the enzyme, instead of the antibody, and mixed to an antigen sample. The labeled antigen competes for primary antibody binding sites with the corresponding sample antigen (unlabeled). The more antigens in the sample, the less labeled antigen is retained in the well and weaker is the signal [53, 54].

8.4. Coupled Bioluminescent Assay (CBA)

A coupled enzymatic assay refers to the determination of a substrate or enzyme activity by coupling one or more enzymatic reaction with another one whose final product is more easily detected. The product of the first reaction is the substrate for the subsequent reaction, and so forth, until the last reaction. In coupled bioluminescent assays, luciferase catalyzes the

GLOBAL JOURNAL OF ANALYTICAL CHEMISTRY

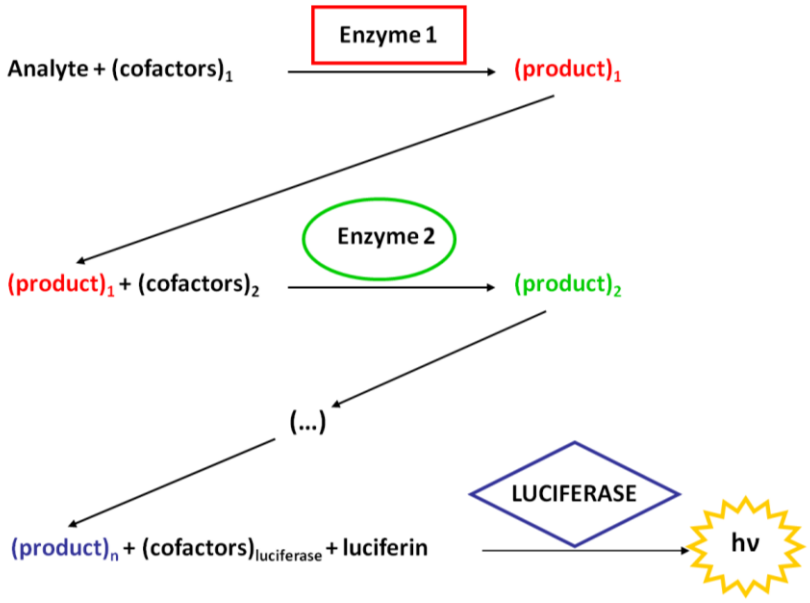

Figure 4. Principle of coupled bioluminescent assay. In a chemical or biochemical reaction, catalyzed by enzyme 1, product 1 is formed. Product 1 will enter into a second reaction cycle with enzyme 2, by its turn generating product 2. The last reaction in the sequence is catalyzed by a luciferase, and the emitted light is measured. A correlation between the intensity of the emitted light and the concentration of the initial reagent (analyte) is inferred and quantitative results can be calculated.

last reaction, and the final output is the measurement of the emitted photons (Figure 4) [55]. This method is often applied when the enzyme-catalyzed reaction or product of interest is difficult to assay directly.

Regarding luciferase, this method is well-established, both in custom-made developed assay, for example for the assay of enolase [56], as well as commercial standard kits [55].

8.5. Bioluminescence Imaging (BLI)

Bioluminescence imaging (BLI) is a technology developed over the past decades which allows the study of the light emitted from living entities to produce an image, where a profile of the emitted light can be visualized and biological information can be inferred [57-60]. This concept was first sketched in early 1990's for single cell measurements [61] and evolved up to the whole body imaging in small laboratory animals in 1995 [62]. It encloses, therefore, molecular imaging, which is "the visualization, characterization, and measurement of biological processes at the molecular and cellular levels in humans and other living systems" [63], to whole-body imaging in small animals. Today it has a widespread use.

Conceptually, it can be viewed as a fusion between bioluminescent reporter gene and optical imagiology (Figure 5a). First, the gene encoding the luciferase is incorporated into a plasmid (Figure 5a, 1), which is then inserted into cells or other genetic material carriers, like liposomes or viruses (Figure 5a, 2). Then they are transferred to living small animals like mice (Figure 5a, 3). It is given time for functional luciferase to be produced from the gene and the image is taken [57-60]. The animals are placed in light-tight chambers and, immediately before imaging, they are anesthetized to keep them still. Gas anesthesia with isoflurane or intraperitoneal injection of ketamine and xylazine are safe methods for short-term immobilization, as it is the case of BLI [57-60]. Luciferin, when necessary, is then injected (Figure 5a, 4). Generally, D-luciferin is injected intraperitoneally, whereas coelenterazine is administered via lateral tail vein [57-60]. A normal photography of the animal, in grayscale, is acquired under weak illumination to serve as an anatomic reference. After that, the bioluminescent signal is captured in complete darkness by an ultra-sensitive charge-coupled device (CCD) camera mounted on the top of the chamber (Figure 5a, 5) [57-60]. The duration of the imaging is variable, ranging from a few seconds up to several minutes (maximum of 2 minutes for Renilla luciferase, and 5 minutes for firefly luciferase) [57-60]. The signal intensity is computationally recorded, treated by specific softwares and finally represented as a pseudocolor image superimposed on the greyscale reference photo. The signal intensity is normally quantified as photons per second per cm^2 per steradian with a color scale from blue (lowest intensity) to red (highest intensity) [57-60].

GLOBAL JOURNAL OF ANALYTICAL CHEMISTRY

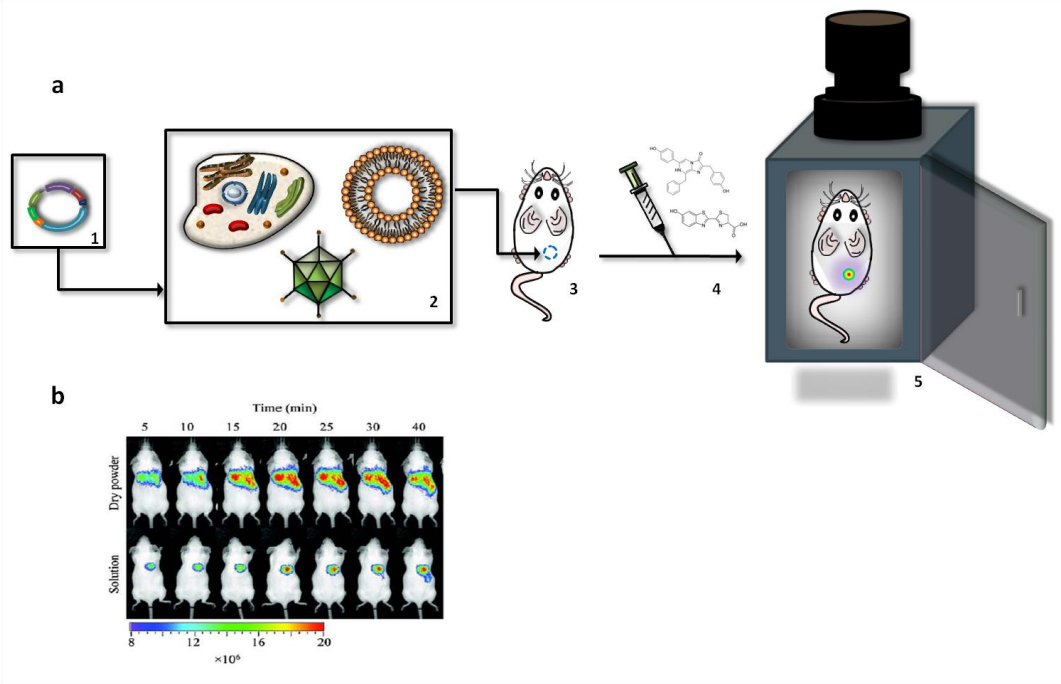

Figure 5. Bioluminescence imaging (BLI). (a) Principle of BLI. A plasmid (1) containing a luciferase gene is introduced into vectors, such as cells, viruses or liposomes (2). These vectors are injected into a living test animal (3). Prior to the analysis, luciferin is injected (4) and the animal is transferred to a chamber mounted with a camera (5). The emitted photons are registered by the device's software and displayed as colored spots upon the animal's picture. (b) An example of a BLI analysis. In this study, mice were treated with a powder formulated for pulmonary gene delivery, containing luciferase as a reporter gene. Both its dry and soluble form were tested and, through a BLI analysis, it was verified that the dry powder is more efficient in delivering the gene to the lungs. Figure 5b adapted from ref. [103] and reproduced with permission from Elsevier.

The distinctive component of this technology is the CCD cameras, since they must be capable of detecting very low levels of emitted light [64]. This sensitivity can be enhanced by, for example, cooling the CCD chip to below -100°C, which significantly reduces background dark current signals, and are referred as cooled CCD [57, 64]. Several systems are commercially available; moreover, some models were specifically designed to measure light emission from small animals, for example the IVIS™ imaging system (Xenogen Corporation) with improved functionalities, like the imaging of groups of several animals simultaneously or the incorporation of nose cones to deliver gaseous anesthetics to animals during the course of imaging [57, 58].

8.6. Bioluminescence Resonance Energy Transfer (BRET)

8.6.1. The BRET phenomemon

In sections 3 and 4, it was stated that there are marked differences among the various bacterial species and strains concerning the *in vivo* bioluminescence spectra *versus* the *in vitro* one. The emission maxima are spread mostly in a range from 472 to 545 nm *in vivo*, whereas the *in vitro* bioluminescence spectra measured with purified luciferases obtained from various bacterial species and strains are all similar (λ_{max} about 490 nm) [12]. Likewise, the Renilla's bioluminescent system emits blue light (λ_{max} = 480 nm) *in vitro*, a value that is shifted to green light (λ_{max} = 509 nm) *in vivo* [12]. These spectral shifts of light emission could indicate the occurrence of some energy transfer process involving the luciferase and a chromophore. Today it is known that such process is resonance energy transfer (RET).

RET was observed in the laboratorial context as well as biological systems, like the carotenoid-to-chlorophyll RET in marine diatoms [65]. A theory of RET was proposed by the German scientist Theodor Förster in the 1940's [66], and hence the common acronym Förster resonance energy transfer (FRET) by which this phenomenon is also known. According to the theory, RET is a photophysical process involving two chromophores, a "donor" and an "acceptor". The "donor", initially in an electronically excited state, can transfer excitation energy to an "acceptor" molecule.

GLOBAL JOURNAL OF ANALYTICAL CHEMISTRY

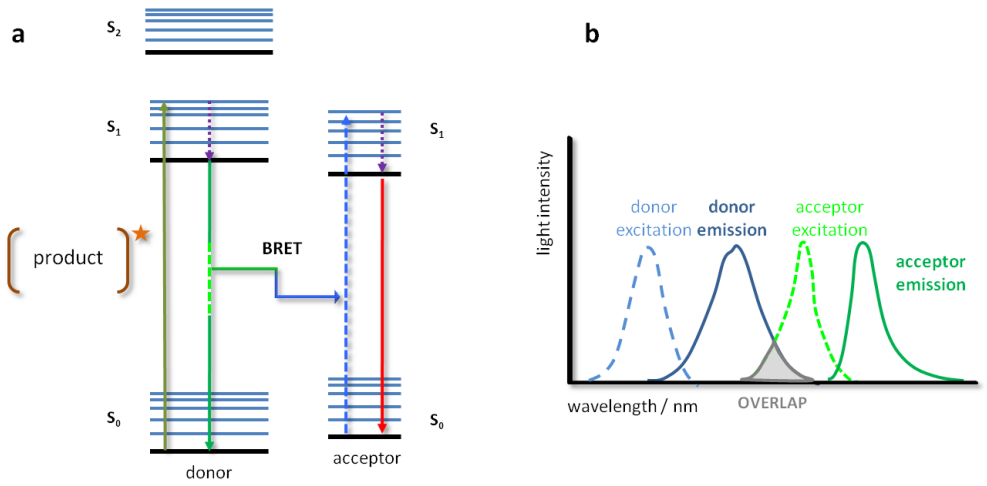

Figure 6. The bioluminescence resonance energy transfer (BRET) principles. (a) Jablonski diagram showing the "donor" and "acceptor" coupling and resonance energy transfer. (b) Spectral overlap requirement for the occurrence of BRET. A "donor" molecule is excited at its specific wavelength and light emission will occur. If the "donor" emission matches the energy required for a nearby molecule to be excited, energy transfer by BRET will occur and the "acceptor" will posteriorly re-emit this energy as photons.

This intermolecular energy transfer occurs by dipole-dipole coupling, and not by electron transfer, whereby it is non-radiative [65-67] (Figure 6a).

Bioluminescence resonance energy transfer (BRET) is a particular case of RET in which the "donor" molecule is a luciferase [67] (Figure 6a). *In vivo*, the "acceptor" is a fluorescent protein, like the bacterial blue fluorescent proteins (LumPs), containing lumazine as their chromophores, and bacterial yellow fluorescent proteins (YFPs), containing a chromophore of FMN or riboflavin [12], or the green fluorescent protein from *Renilla reniformis* [12].

In order to RET occur, at least two conditions must be fulfilled: firstly, the emission spectrum of the "donor" must overlap with the excitation spectrum of the "acceptor" (Figure 6b); secondly, the two molecules must be in close proximity, from 1 to 10 nm at maximum [65, 67]. This last requirement was readily recognized as a possible application to evaluate protein-protein interactions.

8.6.2. The BRET technology

As an analytical method, the first RET methods involved a fluorescent protein coupled to another fluorescent protein capable of emitting at a different wavelength [68]. In this case, the method is called fluorescent resonance energy transfer (FRET). This denomination refers, hence, to the nature of the "donor"-"acceptor" pairs, and not to the mechanism of light transfer. In both FRET and BRET, to investigate protein-protein interactions, one protein of the pair is genetically fused to the "donor", and the second protein to the "acceptor" (Figure 7a). The "donor" protein is excited and, if the two proteins do not interact, only one light signal, corresponding to the "donor" emission, is registered (Figure 7a, 1); however, when the two proteins interact, RET can occur and an additional light signal, corresponding to the "acceptor" emission, is detected (Figure 7a, 2) [69]. The "donor" and "acceptor" reporters can be fused to a single protein, and in this case an intramolecular signal can be monitored, which is useful to study conformational changes upon the binding of a ligand, for example (Figure 7b) [70]. The RET signal can be displayed in several formats, depending on the purpose of the study (Figure 7c).

Although the occurrence of BRET in nature is established a long time ago [71], technological applications of BRET in bioanalysis was not done until 1999, when it was used to demonstrate that the circadian clock protein KaiB, from a cyanobacterium, forms homodimers, by genetically fusing it to Renilla luciferase and a modified green fluorescent protein [72]. Since then, a "boom" of applications based on BRET were developed. For example, FRET- and BRET-based method were extensively applied to study the interactions of cellular receptors with their corresponding ligands, for example the interaction between G protein-coupled receptors (GPCR) and trimeric G protein upon addition of the receptor's agonist, norepinephrine [73], or to verify receptor's dimerization [74, 75].

A variant of the BRET methodology recently described is the conjugation of luciferases and quantum dots [76]. Quantum dots

GLOBAL JOURNAL OF ANALYTICAL CHEMISTRY

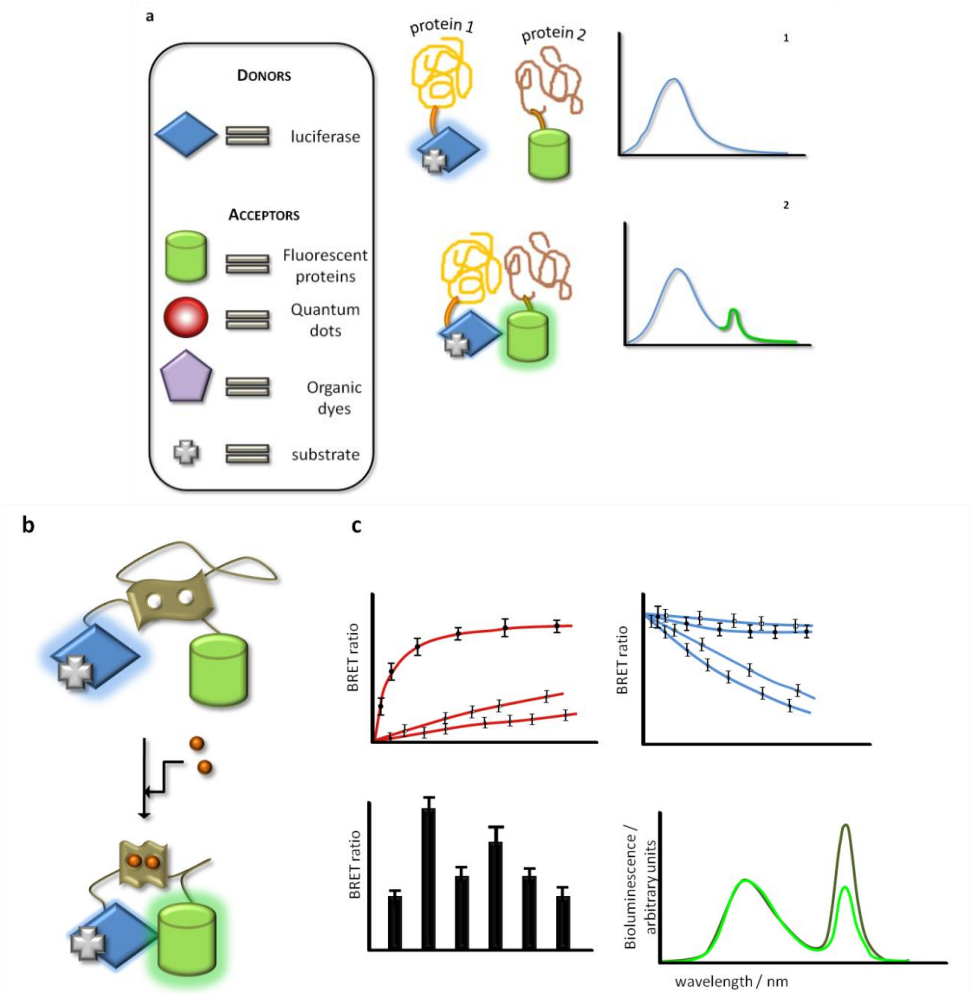

Figure 7. The BRET technology. (a) To assess protein-protein interactions, each protein of the presumably interacting pair is genetically fused to a luciferase and to an "acceptor", which can be a fluorescent protein, a quantum dot or an organic dye (in this scheme, a fluorescent protein is represented). If the two proteins do not interact, or if they are far apart from each other, BRET will not occur and a single signal, corresponding to the luciferase, will be registered (1); on the other hand, when the two proteins interact, BRET will occur between the luciferase and the "acceptor" and two signals will be recorded, one from the luciferase and a novel peak corresponding to the emission of the "acceptor" (2). (b) Schematic representation of intramolecular BRET. Two BRET pairs are genetically fused to the same protein. By adding its agonist (orange circles), for example, the protein will undergo structural changes, bringing the two BRET pairs into close proximity and allowing the occurrence of BRET. (c) BRET data representation. According to the purpose of the analysis, the BRET results can be displayed under several formats.

are tiny fluorescent and semiconductor crystals of inorganic elements, like cadmium and tellurium, with dimensions in the nanoscale, typically from 3 to 100 nm [77-79]. At this scale, quantum dots present properties differing from the bulk material they came from. In fact, quantum dots have unique optical properties like high quantum yields, large molar extinction coefficients, large excitation spectra, narrow emission spectra, size-dependent tunable emission and high photostability, which make them appealing fluorescent probes for imaging [77-79].

The principle of luciferase-quantum dots BRET is the same as already described (Figure 8a). The first reported protocol was published in 2006, using a genetically modified Renilla luciferase with improved stability and light output [80]. To obtain such luciferase, eight mutations were performed, and so this mutant was called Renilla luciferase8 [81, 82].

The major advantage is that quantum dots can be produced within a wide emission wavelength, from blue to near-infrared [77-79], which is the desired range for BLI in small living animals. In fact, the interaction of light with tissues involves several kinds of processes (Figure 9). When light is emitted in a bioluminescent reaction inside a living animal, photons passing through the tissues can be scattered by cell and organelles membranes or absorbed by intrinsic cellular chromophores like

GLOBAL JOURNAL OF ANALYTICAL CHEMISTRY

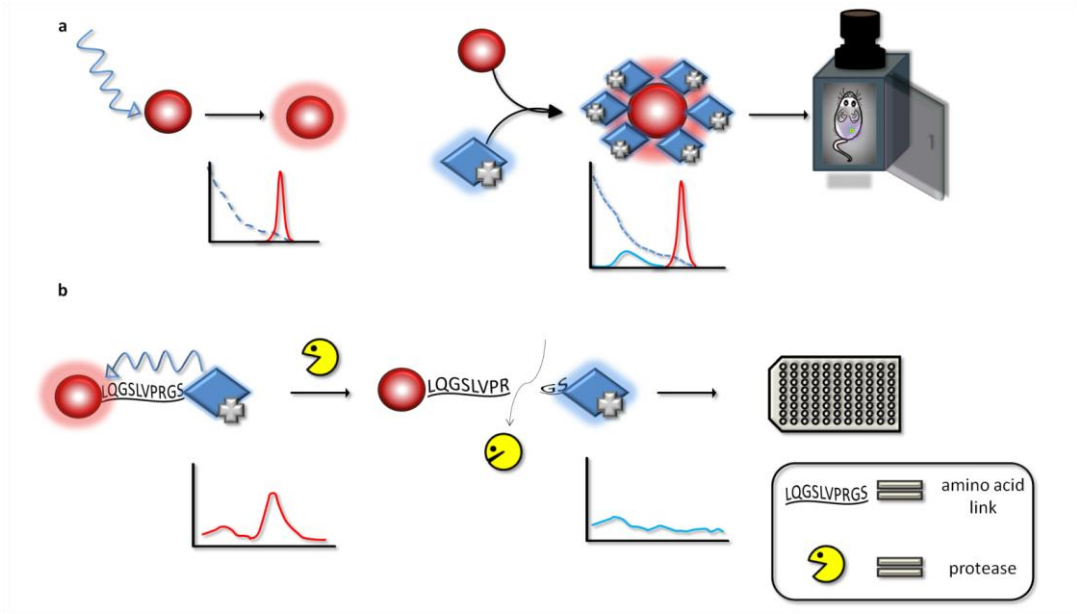

Figure 8. Luciferase-quantum dot conjugates for BRET. (a) A quantum dot is excited by an external light source (dotted blue line in the graph) and emits at a characteristic wavelength (red line). By coupling it to luciferases, and adding luciferin, the luciferase will emit light (blue line), and part of this energy will be transferred to the quantum dot, thus avoiding the need for external illumination. By introducing this luciferase-quantum dot conjugate into an animal, an image can be obtained. (b) Schematic representation of a protease assay based on luciferase-quantum dot BRET. A luciferase is genetically fused to an amino acid link recognized by a protease under study. Later, this luciferase is chemically coupled to a quantum dot and BRET will occur (red line graph). In the presence of the protease, the amino acid link will be cleaved, luciferase and the quantum dot will get far apart and the BRET signal will disappear, being registered only the emission from the luciferase (blue line graph). This assay can be performed in a microplate format.

water, hemoglobin, collagen, flavins and melanin, leaving lesser light to be transmitted [57, 58, 83]. Furthermore, fluorescent proteins and quantum dots require external excitation by a laser beam (Figure 8a). This beam will not only be scattered by tisses but it will also induce their autofluorescence, generating a strong background which lowers the sensitivity of the assay [57, 58]. This way, little light will be available for excite quantum dots and fluorescent proteins, thus limiting imaging at superficial locations inside the animal, as the more tissue between the reporter and the detector, the more light is lost [57, 58]. Blue and green light (shorter wavelengths) are largely absorbed by tissues, especially by hemoglobin, but red light (longer wavelengths) is less affected. So, shifting the emission to the red region of the spectrum and above would be greatly beneficial for all optical imagiology modalities.

Originally described as a proof-of-principle method for BLI [80], luciferase-quantum dot bioconjugate also found application as protease and nucleic acid biosensor (see section 9.6.).

8.7. Split luciferase / Protein Complementation Assay (PCA)

Protein-fragment complementation assay (PCA) consists in the splitting of a monomeric reporter protein into two separate fragments [84-87]. These fragments are, consequently, inactive, but the reporter can regain its function by non-covalent reassembly and folding when the fragments are brought in close proximity. If a pair of interacting proteins is genetically fused to each of the fragments, the reporter will be reactivated upon association of the proteins (Figure 10a) [84-87]. This way, PCA is another technique to assay protein-protein interactions. In parallel, if the split reporter is fused to a single protein, it can monitor conformational changes (Figure 10b). If the reporter is a luciferase, the technique is called split luciferase, and when it involves the reconstitution of fluorescent proteins it is named bimolecular fluorescence complementation (BiFC) [84-87].

This technology resembles the yeast two-hybrid system (Y2H) screening, a molecular biology technique to assay protein-protein interactions and protein-DNA interactions [85, 88]. This method consists in the activation of transcription of a downstream reporter gene by the binding of a transcription factor onto an upstream activating sequence that will drive the transcription of the reporter gene. For two-hybrid

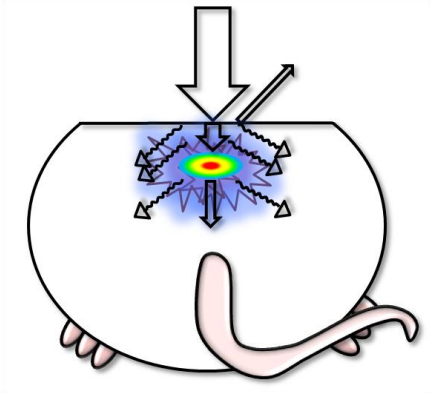

Figure 9. Schematic representation of light-tissues interactions. When a beam of light (thick arrow) is applied upon a living animal, part of the light can be refracted (thin arrow). When the light penetrates deeper into the animal, another part of it can be scattered (wavy arrows) or absorbed by chromophores (short thick arrow). Light will also provoke autofluorescence (purple shaded area). Finally, a fraction of the initial light will reach the fluorescent target and result in luminescence (colored circle), being registered by the detector (long thin arrow). Bioluminescence produced by luciferases within the animal is also subjected to these phenomena.

screening, the transcription factor is split into two separate fragments, called the binding domain (BD) and activating domain (AD) [88]. The BD is the domain responsible for binding to the activating sequence, whereas the AD is the domain responsible for the activation of transcription itself. One protein under study is fused to the BD domain ("bait"), the other protein partner to the AD domain ("prey"). By their own, none of these constructs are sufficient to activate the transcription of the reporter gene, but when the proteins interact the AD and BD of the transcription factor are brought together, it became functional, the reporter is transcribed and a signal is measured [88]. Such a system using Cypridina luciferase as the reporter gene is described in the literature [89].

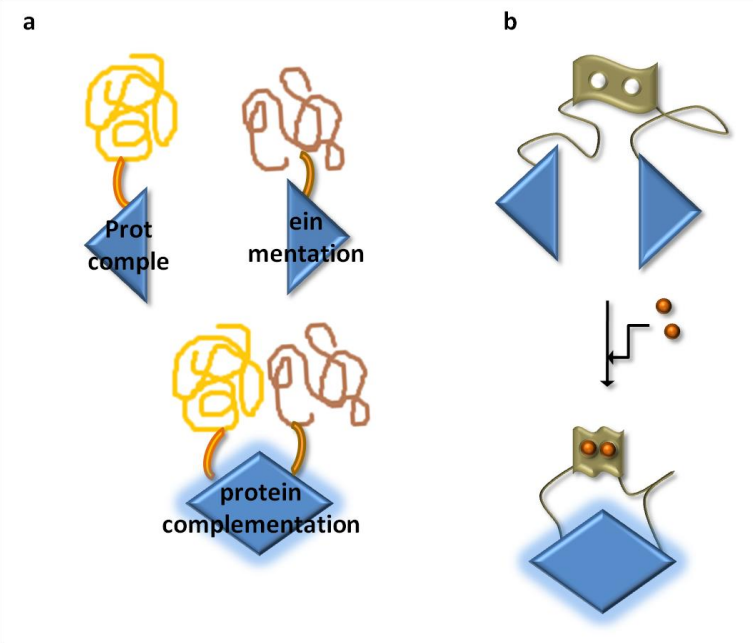

Figure 10. Principle of the split luciferase assy for protein-protein interactions and protein structural changes. (a) Intermolecular split luciferase assay. A luciferase is genetically dissected into two separate fragments and fused to each protein from a pair of interacting proteins. When the two proteins are not interacting, luciferase cannot emit light. When the two proteins interact, luciferase regains its activity and light is emitted. (b) Intramolecular split luciferase assay. Split luciferase fragments are genetically fused to one protein. By adding the protein's ligand (orange circles), the protein will undergo structural changes, bringing the two fragments close enough to luciferase regain its activity.

GLOBAL JOURNAL OF ANALYTICAL CHEMISTRY

9. Bioanalytical and biomedical applications of luciferases

9.1. Drug screening

The need for new-generation drugs is paramount in today's world, to account for 1) cases of drug resistance, 2) cases of emerging new diseases and 3) to improve already-existing therapies. The pharmaceutical industry demands a combination of a high number of tested compounds in lesser time and with minimum costs, the so-called high-throughput screening. In this context, the development of luciferase bioanalytical methods for drug screening can be a good option [90-92].

Such bioluminescent methods were applied in the screening of inhibitors compounds for West Nile virus, a pathogen that causes meningoencephalitis and whose presence is spreading through both developed and developing countries [93]. It is a cell-based assay in which Vero cells were transfected with West Nile virus genes and Renilla luciferase gene. Then test compounds were added, along with the luciferase substrate coelenterazine, and bioluminescence was measured. The more active the compound in inhibiting West Nile virus replication, the more reduced was the emitted light. Beginning with almost 100,000 test compounds, at the end only five of them were selected and further tested to identify their mode of action by other techniques. Other targets include other viruses like dengue virus [94] and human immunodeficiency virus (HIV) [95], and parasites such as *Plasmodium*, the causative of malaria [96], or *Leishmania*, the agent of leishmaniasis [97, 98].

Besides the drug screening at the cellular level, one line of investigation aims the therapeutics at the molecular level. BRET-based methods are being adopted for such purpose, for example in the quest for cyclic AMP (cAMP) antagonists as the enzyme it regulates, cAMP-dependent protein kinase, is associated with several diseases [99], or to the study of insulin receptors interaction, which are potential targets for improved diabetes therapies [100,101].

9.2. Gene-mediated therapy evaluation

The possibility of correct or modulate genetic defects that leads to maladies, instead of treating their outcome, the so-called gene therapy, may be the ultimate achievement in medicine in the XXI century. Much work is being made in this field due to progresses in molecular biology and genetic engineering. Luciferase reporter gene systems coupled with BLI are valuable tools for assessing therapy efficacy, namely gene expression and localization inside target cells, where luciferase replaces the therapeutic gene [102]. For example, to test a new formulation of a dry powder for pulmonary gene therapy, firefly luciferase activity was measured *in vivo* and in real time in mice (Figure 5b) [103]. Unlike *in vitro* assays, all the complexity of a living organism was maintained, which allows the scientists to obtain results much closer to the real situation.

A branch of gene therapy is gene-mediated therapy, which follows the principles of gene therapy but with other gene entities. An entity that has granted a lot of attention in recent years is RNA interference (RNAi) [104, 105]. This is a novel gene control mechanism in which fragments generated from RNA can locate sequences complementary to its own in mRNA and establish base-pairing, preventing the translation of the RNA and the consequent production of proteins [104, 105]. Sometimes the RNA fragment is the target itself, and in this case anti-RNAi oligonucleotides were developed [106]. It is known that some microRNAs (miRNAs) inhibit the synthesis of tumor suppressor proteins by binding to their corresponding mRNA, which leads to cancer proliferation. However, anti-microRNA oligonucleotides bind to microRNAs and abrogate their effect (Figure 11). Such oligonucleotides were synthesized and tested [106]. A nucleotidic sequence recognized by the tested microRNA was fused to luciferase, and their processing resulted in the corresponding mRNA molecule (Figure 11, 1). When the microRNA binds to this sequence in the mRNA, luciferase synthesis is inhibited and no light is measured (Figure 11, 2). By contrast, when adding anti-microRNA, the microRNA is inactivated, luciferase synthesis is re-started and light output increases (Figure 11, 3) [106]. This was a proof-of-principle study but, recently, it was demonstrated that RNAi could indeed be observed in human cells [107, 108], thereby opening the possibility to a new cancer therapy based on RNAi inhibition and with luciferase assessment [109, 110].

9.3. Infection progression

To obtain better clinical treatments, it is important to know how precisely a disease-causing agent, either viruses, bacteria or protozoan, spreads inside an organism. The standard procedure consists of inoculating test animals (mice) with the studied agent and follow its spread over time through the sacrifice of the animals and analyzing the contaminated tissues *ex vivo*. This approach, however, has several drawbacks: firstly, lots of animals need to be inoculated and killed to obtain useful statistical

GLOBAL JOURNAL OF ANALYTICAL CHEMISTRY

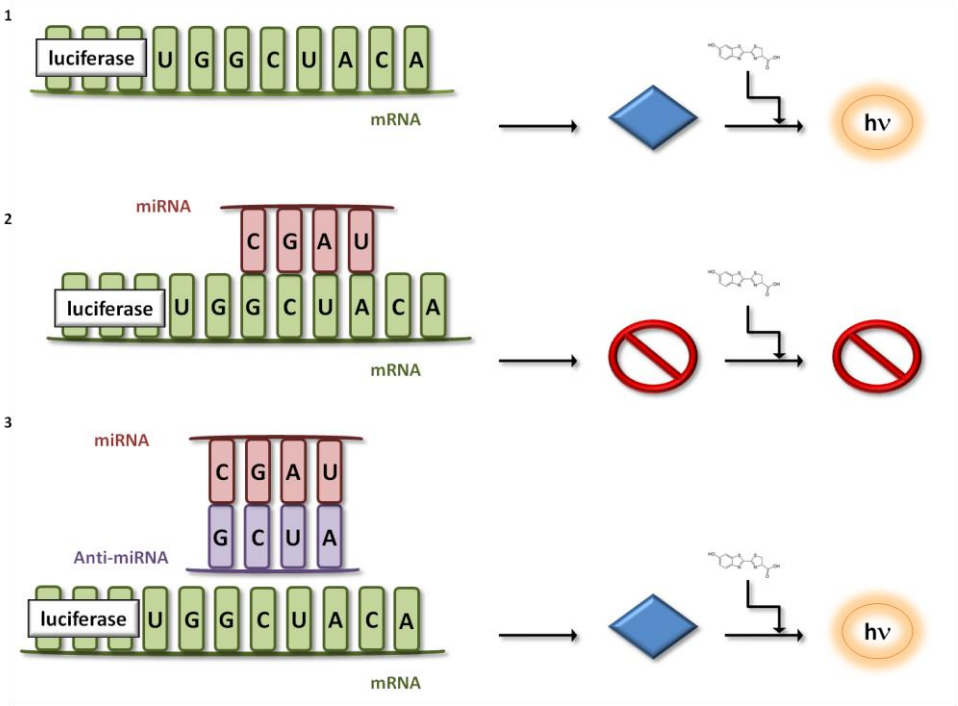

Figure 11. Principle underlaying the luciferase reporter gene assay applied to RNA interference (RNAi). A messenger RNA (mRNA) molecule (green structure) is produced based on the luciferase gene. Luciferase is produced from mRNA and addition of luciferin leads to light emission (1). If the mRNA contains a nucleotide sequence complementar to a micro RNA (miRNA) fragment (red structure), this miRNA will bind to it and hamper the production of functional luciferase and, hence, the light emission (2). An *in vitro* synthesized anti-miRNA molecule (purple structure), with the same sequence of the mRNA, will bind the miRNA, freeing the mRNA to be processed and produce luciferase (3). RNAi could be the basis for novel gene-mediated therapies.

data which, besides the ethical issues raised, is expensive and time-consuming; secondly, if a disease is already characterized, and its target organs are well-known, only they will be the focus of detailed analysis, thus missing unexpected sites of attack. BLI can overcome at least part of these issues; a whole-body analysis ensures that all sites of infection are detected, and statistical analyses are facilitated since only one animal can be followed in the course of the experiment [58, 111-115]. Such approach was employed to visualize the germination of *Bacillus anthracis* spores in living mice using engineered *Bacillus* that express bacterial luciferase [116]. It was possible not only to detect the primary site of infection - the lungs - but also to discover the germination onset (about 18 h in living animals but as early as 30 minutes if the animals are immediately euthanized) [116]. Furthermore, it was demonstrated that macrophages play an important role in the infection process since these cells are recruited to deal with spores, which in fact germinate inside macrophages [116]. Other relevant target is *Mycobacterium tuberculosis*, the causative agent of tuberculosis. The complete host-parasite dynamics was monitored *in vivo* with genetically modified bioluminescent mycobacteria [117]. Recently, three luciferase genes, those from Gaussia, bacteria and firefly, were optimized towards their application with mycobacteria [118]. Good results were obtained, namely the production of self-illuminating mycobacteria with *lux* genes [118].

Viruses can also be monitorized this way. A murine gammaherpesvirus was engineered to express firefly luciferase, as a model for human viruses that can persist for a lifetime in the organism leading to several diseases, like Epstein-Barr and Kaposi's sarcoma-associated herpesvirus [119]. When introduced into mice, the host-parasite dynamics could be studied in a prolonged way, leading to the discovery of new sites of infection, the process of local organs clearance and the possibility of infection reactivation by immunosupressors [119].

9.4. Cancer therapy

Cancer has always been a field of intense research. The major focuses have been the localization of tumors and metastasis, the follow up of the disease's evolution and the assessment of the response to treatment. The use

of animal models is a standard procedure, which now can be improved with BLI [120-122]. For instance, the synthetic analogue of hemiasterlin - a natural product of a marine sponge with antiproliferation properties - was tested as a potential novel chemotherapeutic agent against bladder cancer [123]. Human cancer cells were transfected with firefly luciferase and an *in vivo* study demonstrated that the bioluminescent signal decreased in a time- and dose-responsive manner to hemiasterlin analogue, thus indicating the compound's efficacy. In another application, several tumors and metastasis were imaged by injecting bioluminescent *Escherichia coli* in living mice [124]. Taking into account that bacteria were indeed found in excised tumors from patients, this could be a selective probe for early detection of malignancies [125].

As already described for drug screening (see section 9.1.), in cancer research much attention is being paid to molecular targets, like the chemokine receptors CXCR4 [126] and CXCR7 [127], the heat shock protein 90 [128, 129], the protease furin [130], the apoptose effector caspases 3/7 [131] and microtubules [132]. Alternatives to "classical" chemotherapy are also being pursued, for example with a biopolymer gel for controlled delivery of drugs [133] and the establishment of immune cell therapies [134], both of which can be assessed by BLI in living animals.

9.5. Cell tracking

The fate of single cells or even molecules can be tracked through modern technology, using luciferases as biomarkers. This tracking is especially important in cell-based therapies like T-cell traffic toward tumor sites [135] or in the recent field of stem cell technology [136-139]. In the first example, mice were inoculated with several tumors and firefly luciferase-bearing T cells were injected into them. Bioluminescence was detected *in vivo* and co-localized with tumors [135]; in the second one, myoblasts were removed from genetically modified mice expressing luciferase [139]. When transferred to muscle-challenged mice, it was possible to monitor, by BLI, not only 1) their correct localization but also 2) the proliferation of such cells, due to an increase in the bioluminescent signal, and 3) the minimal number of cells that must be transferred to allow their self-renewal [139].

9.6. Biosensors

The detection and quantification of biologically relevant analytes or cellular processes is often accomplished by biosensors. Strictly speaking, a biosensor is "a device that uses specific biochemical reactions mediated by isolated enzymes, immunosystems, tissues, organelles or whole cells to detect chemical compounds usually by electrical, thermal or optical signals" [140]. Luciferase acts as the biological sensing element, either directly interacting with the analytes or consuming a by-product generated by coupled reactions, generating a bioluminescence output proportional to the concentration of the analyte or to the extension of the cellular and molecular process under study.

Perhaps one of the most popular biosensor utilizes either genetically engineered bioluminescent bacteria or natural bioluminescent bacteria to sense pollutants in toxicological and environmental contexts, for instance in drinking water [141-143].

The classical architecture of a biosensor may not always follow the expected pattern, as the biological sensing element could be added in solution to the sample or be genetically coded, and so it will not be integrated within the transducer or detector. Such biosensor methodologies include luciferase reporter gene assays, coupled bioluminescent assays, bioluminescent immunoassay, BRET and split luciferase assays.

Several luciferase-based biosensors for analytes of biological concern are described in the literature. They include extracellular adenosine [144], carcinogens [145], prostaglandin E_2 [146], ADP-ribose [147], L-cysteine [148], calcium [149], S-Equol (an estrogenic compound) [150], nitric oxide [151], stress hormones [152], c-Myc (a transcription factor protein) [153], rapamycin (an immunosuppressant drug) [154], cAMP [154], 2', 5'-oligoadenylate 5'-triphosphate (an effector in the interferon antiviral system) [155], interferon–α [156], glycans in the cell membrane [157], glucose [158] and nucleic acids [159-161]. Regarding this latter example, it is curious to note that there are methods for nucleic acid detection based on RET [159], luciferase-quantum dot BRET [160] and split luciferase [161], althought these concepts are traditionally applied to assay protein-protein interactions. In the luciferase-quantum dot BRET method, two oligonucleotide probes are constructed *in vitro*, one coupled to Renilla luciferase and the other, with a complementary sequence of the target nucleic acid, is coupled to a quantum dot [160]. In the absence of the target nucleic acid, the two probes will hybridize, under certain conditions, and a BRET signal will be measured after addition of coelenterazine. In the presence of target nucleic acid, this and the luciferase probe will compete to bind to the quantum dot probe.

The more nucleic acid in the sample, the more extense will be the hybridization with the quantum dot probe and the weaker will become the BRET signal [160]. The split luciferase method is similar, except that the two probes each contain a fragment of a Renilla luciferase [161], instead of a complete luciferase and a quantum dot.

In the medical context the focus is on monitoring pathogenic compounds, for instance bacterial endotoxin [162] and hepatitis B virus surface antigen [163], as well as whole organism like lytic bacteriophages [164] and to differentiate bacterial strains [165].

The activity of numerous enzymes can be assayed with luciferase biosensors. To quote a few, there are biosensors for acetate kinase [166], pyruvate phosphate dikinase [166], thymidylate kinase [167], glutathione S-transferase [168], protein methyltransferases [169], plant α-oxidase [170], phospholipase C [171] and proteasome enzymes, namely chymotrypsin, trypsin and caspases [172]. Proteases have been receiving much attention, as it was demonstrated that their activity is generally disregulated in several types of cancer. Some biosensors are based on split luciferase assays [173, 174], but another series of such biosensors are based on the BRET technology, either with sole genetically encoded sensing elements, the luciferase and a fluorescent protein [175], or with the chemical coupling of luciferases with nanomaterials, namely quantum dots [176] and gold nanoparticles [177]. In the former case, a thrombin assay was created by generating a plasmid containing a thrombin-cleavage sequence between the "donor" (Renilla luciferase) and the "acceptor" (green fluorescent protein) genes. When coelenterazine was added, the emitted light was specific of the "acceptor" protein due to the occurrence of BRET but, in the presence of thrombin, the sequence that links the two proteins was cleavaged, the two proteins got apart from each other and the emitted light became specific of the luciferase. By quantifying the ratio of "acceptor" / "donor" emission, the concentration of thrombin could be calculated. In regard of luciferase-quantum dots, a similar procedure was pursued, except that the plasmid only contains the protease amino acid sequence fused with Renilla luciferase8 gene [176] (Figure 8b). *In vitro*, this fused protein was bioconjugated to the selected quantum dot. This strategy was applied for the quantification of matrix metalloproteinases. The luciferase-gold nanoparticles biosensor presents a different principle. Herein, the gold nanoparticles quench the emission from Renilla luciferase8, and hence little or no light is detected. Cleavage of the amino acid sequence between the nanoparticles and luciferase8 diminishes the quenching, enhancing the bioluminescent emission. Once more, this biosensor was constructed towards measurement of a matrix metalloproteinase activity [177].

In cellular biology, the study of physiological processes within living cells and organisms is very relevant, and so is the construction of specific biosensors for protein-protein interactions and dynamics [178-182], sodium channel activity [183] and mitochondrial fusion [184], among others. Also, the post-translational regulation of proteins, which tags these proteins to specific fates or functions in the cellular environment, deserves special consideration. Such well-studied modification is protein ubiquination by the covalent attachment of the small peptide ubiquitin. A BRET-based assay involves the fusion of green fluorescent protein to ubiquitin and Renilla luciferase to the target protein, for example β-arrestin [185]. When β-arrestin is ubiquitinated, Renilla luciferase and green fluorescent protein become close to each other and a BRET signal (emission of green light by the fluorescent protein instead of emission of only blue light by luciferase) is detected [185]. Recently, a novel ubiquitin-like post-translational entity was discovered, the small ubiquitin-like modifier (SUMO) [186, 187], followed by a BRET-based biosensor for SUMOylation using Renilla luciferase fused to SUMO and enhanced yellow fluorescent protein fused to the target protein [188].

9.7. Basic research

Basic, fundamental or pure research aims to increase knowledge about the principles underlying a field of research [189]. As a consequence of its definition, basic research does not seek to obtain a direct applied output. Nevertheless, it is a proven fact that many techniques, products and new lines of investigation owe their existence to basic research [189].

Many methods applied in basic research rely upon luciferases. For example, as a gene reporter, firefly luciferase was applied to study gene regulation in the parasitic protozoan *Leishmania* [190]. In this study, it was discovered a novel genetic element responsible to control gene expression, at the mRNA level, leading to a differential gene expression pattern according to the developmental stage of the parasite, either in its obligatory intracellular stage or extracellular free-live stage [190]. This was possible by constructing plasmids in which firefly luciferase gene was placed under the control of this genetic element, transfecting

Leishmania cells and performing luciferases assays after active luciferase was produced *in vivo* [190]. In another interesting study, it was discovered a single mRNA molecule in an insect (silkworm) that codes for three proteins, that is, a polycistronic mRNA [191]. Although this phenomenon is common in prokaryotes, it is relatively rare in eukaryotes and, whenever it occurs, it is mainly in the form of dicistronic mRNA. Each of these three genes was replaced with firefly luciferase in an artificially constructed mRNA molecule and translated *in vitro* [191]. Likewise, firefly luciferase was used as a reporter gene in studies regarding higher eukaryotes, such as for the study of genetic regulatory elements within mRNAs of the rat brain-derived neurotrophic factor (BDNF) gene [192] and human dihydrofolate reductase gene [193].

Another important line of investigation is related to receptor-ligand associations and structural organization, which allows their subsequent study as therapeutic targets. In this context, BRET-based assays are the choice *par excellence*. For example, such studies demonstrated dimerization of the human follitropin receptor [194], the interaction of dopamine and 5-hydroxytryptamine receptors to constitute a heteromer [195], the assembly of Kir3 channels with G protein [196] and conformational changes in the TrkB receptor by binding of its agonist [197].

In immunological studies, bioluminescent *Escherichia coli* with bacterial *lux* gene was applied to analyze the complement system [198], which is a defence mechanism against bacterial invasion [199].

The mechanism of action of anesthetics is not fully understood. Fundamental research in this area has been relying upon model proteins. Firefly luciferase was first introduced as a model in 1984 [200, 201] and, since then, it is one of the best model systems for studying anesthetic-protein interactions [202]. It has several interesting features such as the ability to bind a large range of anesthetics at over a 100,000-fold range of potencies and displaying concentration sensitivities very close to those found in anesthetized animals [200-202]. Computational simulation with luciferase and other proteins, based on previously obtained crystallographic data of the protein-anesthetic complexes, will also bring new insights to this theme [203, 204].

9.8. Biomedical engineering

The area of bioengineering can be defined in the following way: “Bioengineering integrates physical, chemical, or mathematical sciences and engineering principles for the study of biology, medicine, behavior, or health. It advances fundamental concepts, creates knowledge for the molecular to the organ systems levels, and develops innovative biologics, materials, processes, implants, devices, and informatics approaches for the prevention, diagnosis, and treatment of disease, for patient rehabilitation, and for improving health" [205]. Under this definition it is clear the focus on biomedicine, albeit this discipline has a broader scope, covering other areas of life science [205].

Examples of luciferase application in biomedical engineering can be found in the literature. They include the BLI of luciferases in bone-tissue engineering [206], the evaluation of bacterial infection in bioengineered materials, also by BLI [207], and the evaluation of an enhanced system to produce recombinant proteins with pharmacological applications, using luciferase as a reporter gene [208].

10. Final remarks on luciferases in bioanalytical chemistry

10.1. Advantages and drawbacks of Luciferase methodologies

This review presented representative examples of applications of luciferase systems in bioanaytical and biomedical research, as well as some of the principles underlying them. It is not intended to be a thorough compendium of all the possible applications of luciferases, as more and more examples are published almost every day, but rather to state the potential of luciferase in modern bioanalytical chemistry and biomedicine.

The advantages of any luciferase assay are the high sensitivity and selectivity, the absence of luciferase activity background in non-bioluminescent organisms, the wide dynamic range for analyte quantification, reduced assay time, low costs of both reagents and equipments and no special training to perform analysis. Furthermore, each luciferase presents specific interesting features. Gaussia and Cypridina luciferases are naturally secreted, which avoid the cell lysis to assay luciferase’s bioluminescence; Gaussia is the smallest luciferase cloned so far, which diminishes steric hindrance when fused to other proteins, like in BRET assays; bacterial luciferases do not require the exogenous supply of luciferin, as do the other luciferases.

From the initial research with firefly luciferase it did not take long for scientists to realize the potential of this enzyme in ATP assays. In fact, as an ubiquitous energy source in living organisms, ATP quantification is important for detection of bacterial

contamination in food [209], for diagnostic purposes [210] and to study metabolic shifts in living cells [211]. The reporter gene technology was also greatly benefited with luciferases, so that countless applications of luciferase reporter genes were reported. The luciferases described in this review require no post-translational modification for enzymatic activity, are non-toxic, and can be expressed in both prokaryotic and eukaryotic systems.

BLI is becoming a widespread-use technique, especially for the study of biological processes in small laboratory animals [212]. This technology combines the advantages of a reporter gene assay with the possibility of non-invasive, real-time and *in vivo* whole-body optical imaging [57-59], which makes it competitive with other well-established imaging techniques like magnetic resonance imaging (MRI), computerized tomography (CT) or positron-emission tomography (PET) for animal use [137]. However, in markedly contrast with these techniques, BLI is not prone to be used in human patients due to low transmission of the generated photons through tissues and concerns about luciferin dynamics in humans. However, even if BLI never reaches human diagnostics, at least it has the merit of decrease the demand for experimental animals. The only invasive steps in BLI are the anesthesia and the luciferin injection, and after the imaging the animals are removed from the chamber and allowed to recover [27-59]. As signals from the same animal can be measured over a number of time points, the animals serve as their own controls [57-59]. This way, being impossible to completely abolish animal testing in scientific experiments, at least more animals are spared.

BRET is another successful example of a bioanalytical method employing luciferases. Sundry studies have shown that BRET is superior to FRET, the most widespread RET method, regarding sensitivity [175, 213, 214]. However, as any bioanalytical technique, it has some drawbacks. A BRET assay requires a careful planning and data treatment to obtain reliable results, for example to discard BRET signals due to non-specific interactions [69]. But as long as these requirements are fulfilled, a rigorous experiment can be performed. In the same sense, split luciferase assays present a crucial requirement: the splitted fragments should not associate spontaneously in the absence of the binding proteins, as this would render the method less reliable due to the presence of false positives [86]. Studying the self-assembly of fragmented reporters, it has been concluded that, if they are expressed at high levels, in certain cases, the fragments can indeed self-associate with each other regardless of the protein-protein interaction [86]. Thus, it is important to perform appropriate controls in split luciferase assays to ensure the specificity of the detected signal and to express the protein fusions at low levels, close to those of the endogenous counterparts to avoid self-association [86].

Albeit the great utility of luciferases as biomarkers, there are other important alternatives, namely fluorescent proteins [215-217], organic dyes [218] and quantum dots [78, 219, 220]. Fluorescent proteins have the drawback of requiring an external light excitation, which can elicit tissue autofluorescence, and requires a certain time period for its intrinsic chromophore to be formed inside living cells [215-217]. Organic dyes, like fluorescein or Cy3, are generally small molecules and, hence, present less steric hindrance, combined with interesting chemical and photophysical properties [218]. Nonetheless, they lack the specificity conferred by an enzymatic reaction and cannot be genetically coded, thus limiting their range of applications. Finally, quantum dots are attracting much attention for bioanalytical applications [219, 220], but there are serious concerns about their biostability and toxicity, demanding more studies on it (see section 10.2.3.). Like organic dyes, quantum dots cannot be genetically coded.

The contribution of luciferases in biomedical applications is astonishing. However, many of the publications are proof-of-principles studies. There is a pressing need for luciferases methods to be validated and become standard procedures.

10.2. Current and future improvements

10.2.1. Novel luciferases

Currently the most used luciferases are those from firefly and Renilla, but this scenario is probably going to change as new luciferases are cloned and characterized, by one hand, or previously described luciferases with scarce applications regain attention, by the other hand. The most promising ones include:

1) Fridericia luciferase – This luciferase was discovered in *Fridericia heliota*, a Siberian bioluminescent earthworm [221]. Little is known about its bioluminescent system, but studies are currently being made. For example, it is already known that this is an ATP-dependent luciferase, which suggests a novel biosensor for ATP like firefly luciferase, emitting a blue-green light with a maximum at 478 nm [222]. The presence of anions, cations of divalent metals, detergents and certain lipids, as well as changes in pH and temperature, may alter the emission

profile *in vitro* [223]. The structures of both luciferase (a 70-kDa enzyme [224]) and luciferin also need to be clarified, and these studies are on their way regarding luciferin [225].

2) Dinoflagellate luciferase – Dinoflagellate luciferase, obtained from the species *Pyrocystis lunula*, is a 140-kDa luciferase emitting blue light (λ_{max} = 474 nm) with dinoflagellate luciferin, a tetrapyrrole ring similar to chlorophyll [226, 227]. Its cloning and expression in mammalian cells suggest that this could be a novel luciferase reporter gene [227].

3) Metridia luciferases – Metridia luciferase comes from the marine crustaceans *Metridia longa* [228] and *Metridia pacifica* [229]. Both organisms emitt blue light (λ_{max} = 485 nm) with coelenterazine. *Metridia longa* possesses a sole luciferase with a molecular weight about 24 kDa [228], whereas in *Metridia pacifica* two luciferase genes were cloned, resulting in two luciferase isoforms of about 20 and 23 kDa and a remarkable thermostability [229]. They are secreted *in vivo* and *in vitro*, a fact that prompted their use as reporter gene in non-disruptive conditions, that is, without the need to cell lysis in order to detect luciferase activity [228, 229].

4) Railroad-worm luciferases (Phrixothrix) – Railroad-worms of the genus *Phrixothrix* are peculiar creatures in the sense that a sole specimen naturally displays two bioluminescent colors, yellow-green and red. In fact, a green luciferase was cloned from *Phrixothrix vivianii* (λ_{max} = 542 nm), and a red one from *Phrixothrix hirtus* (λ_{max} = 636 nm) [12, 230]. These luciferases were subjected to genetic engineering to allow and improve their expression in mammalian cells [231] and proposed as reporter gene in the analysis of clock gene transcription [232]. It would be expected that the red-emitting luciferase from *Phrixothrix hirtus* would have a widespread use, as it is one of the rare naturally red-emitting luciferase, but that is not the case, dut to its low activity and stability [233]. However, recently this luciferase was subjected to site-directed mutagenesis to produce mutants with both enhanced activity and better stability [233]. Also, its quantum yield was measured, and a value of 0.15 was obtained [234]. This way, this railroad-worm luciferase is prone to gain popularity.

5) Click beetle luciferases (Pyrophorus, Pyrearinus) – A representative species of click beetle is the Jamaican click beetle *Pyrophorus plagiophthalamus*. Just like *Phrixothrix*, individual specimens *in vivo* display two sets of colors, green to yellow-green in the head and green to orange in the abdomen [235]. In 1989 four isoforms of luciferase were cloned form the abdomen of specimens of *Pyrophorus plagiophthalamus*, yielding luciferases with emission of green (λ_{max} = 546 nm, molecular weight of 61 kDa), yellow-green (λ_{max} = 560 nm, molecular weight 60 kDa), yellow (λ_{max} = 578 nm, molecular weight 60 kDa) and orange light (λ_{max} = 593 nm, molecular weight 60 kDa) [235]. The major interest in such a variety of colors is the possibility of formulating multicolor assays to detect several analytes at the same time. For instance, a biosensor to evaluate the action of agonists and antagonists upon their binding in the corresponding receptors was developed with green (λ_{max} = 540 nm) and orange (λ_{max} = 610 nm) Pyrophorus luciferases [236]. A split luciferase assay for protein-protein interactions was also reported with those same luciferases [237].

In the meantime, another Brazilian click beetle species, *Pyrearinus termitilluminans*, was studied [238]. It possess a 61-kDa green light-emitting luciferase (λ_{max} = 538 nm) [238], which is also pH-insensitive in the range of pH 8 to pH 10 and with higher thermostability compared to other beetle luciferases, like firefly's [238]. But the most remarkable feature is its quantum yield, calculated as 0.61 [234], one of the highest among the known luciferases. This luciferase was genetically modified to enhance its expression level and brightness compared to firefly luciferase in mammalian cells [239], thus increasing its versatility in bioanalysis.

It is worth to remember that railroad-worm and click beetle luciferases use firefly D-luciferin as a substrate. This fact avoid the purchase of different luciferin in laboratories where firefly luciferase is well-established and facilitate the use of these luciferases with firefly luciferase in multiplex analysis, as the addition of the substrate will activate all the luciferases at once.

10.2.2. Luciferase and luciferin improvements

The improvement of current-use luciferases and the corresponding luciferins is always a goal to keep in mind. Some of the most important improvements are listed below.

1) Luciferin derivatives and their delivery – The chemical synthesis of derivatives of firefly D-luciferin aimed to improve its stability and bioacculation *in vivo* [240], to augment its light output in the bioluminescent reaction [241], to alter the color emission, especially for red-shifted wavelengths [242, 243] and to produce "caged" luciferins that require an activation step in order to react with firefly luciferase at a defined time and cellular localization [244]. Besides firefly D-luciferin, native coelenterazine underwent several

chemical modifications, yielding successful analogues as coelenterazine 400-a (DeepBlue C™), coelenterazine-*v*, coelenterazine-*h*, coelenterazine-*f*, coelenterazine-*e*, ViviRen™, among others [245-248], with higher resistance to oxidation, higher bioaccumulation and red-shifted light colors.

Actually, the extended availability of luciferins *in vitro* and *in vivo* is a hot topic of research, as it leads to longer analysis times. Two main approaches are used to achieve this goal: accessory proteins to recycle firefly oxyluciferin or to help stabilize coelenterazine; and novel delivery systems. The recycling of oxyluciferin by a luciferin regenerating enzyme (LRE) was reported some years ago [249]. Such enzyme was cloned from the bioluminescent Japanese fireflies *Luciola cruciata* and *Luciola lateralis* [250], the Iranian firefly *Lampyris turkestanicus* [251] and the North American firefly *Photinus pyralis* [252]. In an *in vitro* study, it was showed that this enzyme can indeed induce a more prolonged light emission [251]. Other possibility reported is the coupling of coelenterazine to a coelenterazine-binding protein [253]. As it was demonstrated, not only this protein did avoid the oxidation of coelenterazine but also increased the sensitivity of the assay: since low concentrations of coelenterazine are required, lower background interference is produced [253].

The development of safer and more biocompatible delivery systems are useful in bioluminescent assays. As examples, polyethylene glycol (PEG) molecules were covalently attached to 6-amino-D-luciferin [254], or D-luciferin was encapsulated into liposomes [255]. In both cases, light was registered for several hours after injection of these conjugates.

2) Additives to improve luciferase's activity – CoA was one of the first compounds added to firefly luciferase's reaction mixture to promote or alter the light emission pattern. It participates in a side-reaction where inhibitory compounds, generated in the bioluminescent reaction, react with CoA, leading to less inhibitory products and freeing luciferase for another reactional cycle [32]. Other compounds include ethylenediaminetetraacetic acid (EDTA, a quelant agent for metal ions such as Ca^{2+} and Fe^{3+}), glycerol (an anti-freeze and cryoprotectant), bovine serum albumin (to stabilize enzymes) or sodium azide (a preservative). Recently a research paper showed that α–synuclein, a small protein whose accumulation in neuronal tissues has been associated to Parkinson's disease, Alzheimer's disease, and several other neurodegenerative illnesses [256], can interact and bind to firefly luciferase, leading to an enhancement in the light emission [257]. On the other hand, some chemicals act by structurally stabilizing firefly luciferase, namely trehalose and magnesium sulfate [258], or by protecting it against proteolytic degradation, an effect exerted by osmolites like sucrose, glycine and dimethyl sulfoxide (DMSO) [259].

Another line of research deals with the identification of inhibitors of firefly luciferase [260]. A detailed list of inhibitors, together with their potency and mode of action, can aid in eliminating interferences from reaction mixtures and samples.

3) Genetic engineering and site-directed mutagenesis – The application of genetic engineering techniques to firefly luciferase aims to improve features like thermostability [261-264], pH tolerance [262, 264], protease resistance [265] and catalytic activity [266, 267]. These objectives also hold true for other luciferases like Renilla [81, 268] and Gaussia [269, 270], in which increased stability, photon emission rate and catalytic activity were achieved.

The most recent interventions are concerned with producing red-shifted luciferases for BLI applications, in order to raise the number of photons that can cross cells and tissues and reach the detector. To this end, sundry firefly luciferase mutants were engineered with maximum wavelength emissions ranging from 610 to 617 nm [271-273]. Likewise, a mutant of Renilla luciferase had its natural light color shifted from blue (λ_{max} = 480 nm) to green with natural coelenterazine (λ_{max} = 547 nm) and even to orange with coelenterazine-*v* (λ_{max} = 588 nm), and also presented greater stability and higher light emission than native Renilla luciferase [253, 274].

Finally, bacterial luciferase was subjected to genetic improvements. For a long time, the use of bacterial luciferase as reporter gene was restricted to prokaryotic systems. Recently, however, an efficient expression in mammaliam cells was presented [275]. After this great achievement, other features like self-bioluminescence in mammalian cells [276] and an "upgrade" in its performance through the splitting of the *lux* operon [277] were reported, thus expanding its analytical potential.

4) Luciferases' immobilization – Traditionally, luciferase assays are performed with free luciferase in solution or, when genetically coded, luciferase is soluble in the cytoplasm. However, several studies have shown that the immobilization of luciferases in specific supports could lead to an increase in their stability along time and increased light output.

For example, as early as 1976, bacterial luciferase and FMN reductase were immobilized on glass beads and used as a biosensor for NADH [278]. Other common matrices include polymer gels of starch and gelatine for bacterial luciferase [279], and agarose gels (Sepharose) [280], glass strips [281], and cationic liposomes with cholesterol [282, 283], all for firefly luciferase. A slightly different strategy involves the engineering of luciferases to be expressed with biotin, which can then be coupled to streptavidin, resulting in firefly's immobilization. In an elegant experiment, derived from this basic concept, firefly luciferase was genetically fused to a biotin-ligand protein, expressed in cells and chemically biotinylated. Later, this luciferase was attached to streptavidin beads of about 1 μm in diameter. Finally, those biotinylated luciferase-streptavidin beads were added to cells previously biotinylated. The beads became attached to the cells' surface through uncovered streptavidin sites on the beads. The whole conjugate was applied in the measurement of ATP release from astrocyte cells using a CCD camera in real time and with improved sensitivity [284].

The fabrication of optical biosensors and microfluidics devices offers favourable features like the cost-effectiveness, the optimization of reaction's conditions, the portability and ease of use. Whole-cell biosensors with naturally or genetically modified bioluminescent bacteria are being tested in regard to the best material and protocol for immobilization. For this purpose, fibers like cotton, polyester, viscose, rayon and silk were tested [285]. Also, the optical properties of bacterial luciferase were studied in a biochip model [286]. Firefly luciferase was reported to be immobilized in optical fibers for ATP detection [287], and incorporated into a microfluidic device [288]. Further developments in biosensors fabrication must focus on obtaining longer sensing operation, faster response time and good signal reproducibility.

The rise of nanochemistry and nanotechnology will bring benefits to this area (see also section 10.2.3.). For example, firefly luciferase was incorporated into nanostructured monolayers of colloidal poly(dimethyldiallyl ammonium chloride), which were simultaneously deposited onto 520 nm-diameter polystyrene beads and tested for their ability to assay ATP [289]. Enhanced time stability and activity compared to bare luciferase were found [289].

5) Improved methodologies – Taking into account the growing interest in the BRET technology, researches have been applying a lot of effort in finding novel and improved BRET pairs. Such pairs involve green-emitting luciferases as "donors", rather than the blue-emitting Renilla luciferase, and red fluorescent proteins as "acceptor", for example in the combination firefly luciferase-Discosoma red fluorescent protein [290, 291] and click bettle luciferase-tdTomato [292]. Returning to Renilla and Renilla luciferase8 systems, their coupling with yellow fluorescent proteins and Renilla green fluorescent protein, rather than the widespread *Aequorea victoria* green fluorescent protein, have been reported [293]. These novel systems displayed superior sensitivity compared to established BRET pairs [293]; Likewise, the stability of the well-known Renilla luciferase8-quantum dot conjugate was improved by encapsulating the luciferase into polymeric polyacrylamide gel [294]. Interesting recent proposals involve intramolecular BRET by chemically labeled luciferases with red or infrared fluorescent organic dyes, for instance between Cypridina luciferase and an indocyanine derivative with an emission maximum of 675 nm [295] or between recombinant firefly luciferase and Alexa Fluor near-infrared dyes derivatives with emission maxima of 705 and 780 nm [296]. The discovery in nature of novel fluorescent proteins [297], even in the near infrared range [298], will certainly boost the design of new BRET pairs.

The improvement of BLI in small animals also attracts attention. For example, it was analyzed a better way of administering luciferin [299], whereas other study shed light on luciferin dynamics in plasma [300].

A better understanding of the complexity of whole cellular and molecular physiology, like in proteomics, genomics, lipidomics and metabolomics, can only be achieved by the combination of several techniques at a single analysis to monitor multiple events simultaneously, the so-called multiplex screening. In this regards, several studies were published concerning multiplex imaging in BRET and BLI [176, 301, 302], the combination of BLI and split luciferase assay [174], the combination of BRET and split luciferase assay [178] and a sequential BRET-FRET technique (SRET) [303].

10.2.3. Luciferases and nanomaterials

Nanomaterials are the result of the technological application of nanochemistry concepts. They are designed, synthesized or fabricated for specific purposes, and arise from conventional bulk materials like carbon, metals or semiconductors, but their dimensions are restricted to the nanoscale, where the substances

are governed by quantum mechanics phenomena and, this way, their properties are notably different from the starting bulk materials [304]. Actually, improved or even novel properties are obtained. These materials have innumerable applications, having been recruited in bioanalysis [305, 306] and suggested in biomedicine [307-309].

The coupling of luciferase-nanomaterials is a fruitful field. Some significant examples includes the luciferase-quantum dot BRET conjugates for BLI [80] and biosensing of nucleic acids [160] and proteases [176], luciferase-gold nanoparticles biosensor for proteases [177], all already described, and firefly luciferase-carbon nanotubes for detection of ATP [310]. Curiously, the benefits are mutual: Renilla luciferase8 was used as a scaffold to mediate the growing of PbS quantum dots capable of emitting near infrared light by BRET with the luciferase [311]. This way, this hybrid nanostructure not only allowed the attainment of the desired quantum dot but also resulted as a novel BRET-based sensor with luciferase.

In spite of those promising features, the application of nanomaterials inside cells has raised relevant questions regarding biosafety and biocompatibility [312, 313]. Some studies point out to cellular damages to the nucleus and mitochondria in cell cultures by exposure to quantum dots [313]. The synthesis of quantum dots with more biocompatible materials like carbon, instead of the "traditional" metals like cadmium or selenium, can overcome part of this drawback [314, 315]. Another strategy is the capping of quantum dots with biocompatible molecules [306, 316]. A bioassay using bioluminescent bacteria was already proposed to evaluate the toxicity of quantum dots [317]. This method could become potentially useful if the utilization of quantum dots become more and more widespread. And this looks like to be exactly the case, as several nanobiotechnological companies have been created to commercialize these nanoproducts. Such an example is Zymera, Inc, which sells the Renilla luciferase8-red-emitting quantum dot under the trademark BRET-Qdot® [318].

11. Conclusions

Nowadays, luciferases stand out as versatile tools in bioanalytical chemistry. Several luciferases are well-characterized and have found distinctive applications, namely bacterial, firefly, Renilla, Gaussia or Cypridina luciferases. Beginning with simple ATP assays with firefly luciferase, a plethora of techniques was developed, like luciferase reporter gene technology, BLI, coupled bioluminescent assay, split luciferase and BRET. In biomedicine, luciferases proved their importance with indispensable features like cost-effectiveness, easiness to perform, freedom from radioactive substrates and high sensitivity and selectiveness. They also allow non-invasive and real-time imaging in living animals. With luciferases, the foundations for improved bioanalytical techniques and corresponding astonishing discoveries are assured.

Acknowledgements

This work was supported by grant PTDC/QUI/71366/2006 from the Portuguese *Fundação para a Ciência e a Tecnologia* (*FCT*-Lisbon) of the Ministry of Science, Technology and Higher Education. Simone M. Marques also wishes to acknowledge a Ph.D. studentship (SFRH/BD/65109/2009) co-funded by the European Social Fund (*Fundo Social Europeu*, *FSE*, through *Programa Operacional Potencial Humano* of the *Quadro de Referência Estratégico Nacional* [*POPH-QREN*]) and by *FCT*.

References

1. A. Manz, N. Pamme, D. Iossifidis, Bioanalytical Chemistry, Imperial College Press, Singapore (2004).
2. A. Roda, M. Guardigli, E. Michelini, M. Mirasoli, Trends Anal. Chem. 28 (2009) 307.
3. A.K. Campbell, Chemiluminescence - Principles and Applications in Biology and Medicine, Wiley-VCH, Chichester (1988).
4. J.R. Lakowicz, Principles of Fluorescence Spectroscopy, 3rd ed., Springer, Singapore (2006).
5. http://www.chem.leeds.ac.uk/delights/texts/Appendix.htm. Accessed 03. Feb. 2011.
6. J.W. Verhoeven, Pure Appl. Chem. 68 (1996) 2223.
7. F. McCapra, Accounts Chem. Res. 9 (1976) 201.
8. E.H. White, M.G. Steinmetz, J.D. Miano, P.D. Wildes, R. Morland, J. Am. Chem. Soc. 102 (1980) 3199.
9. J.W. Hastings, J. Mol. Evol. 19 (1983) 309.
10. T. Wilson, J.W. Hastings, Annu. Rev. Cell Dev. Biol. 14 (1998) 197.
11. D.E. Desjardin, A.G. Oliveira, C.V. Stevani, Photochem. Photobiol. Sci. 7 (2008) 170.
12. O. Shimomura, Bioluminescence – Chemical Principles and Methods, World Scientific Publishing, Singapore (2006).
13. S.-C. Tu, Photochem. Photobiol. Sci. 7 (2008) 183.

14. E.A. Meighen, Faseb J. 7 (1993) 1016.
15. M.S. Waidmann, F.S. Bleichrodt, T. Laslo, C.U. Riedel, Bioeng. Bugs 2 (2011) 8.
16. K. Hori, H. Charbonneau, R.C. Hart, M.J. Cormier, Proc. Natl. Acad. Sci. U.S.A. 74 (1977) 4285.
17. C. Szent-Gyorgyi, B.T. Ballou, E. Dagnal, B. Bryan, Proc. SPIE 3600 (1999) 4.
18. B. Ballou, C. Szent-Gyorgyi, G. Finley, Properties of a new luciferase from the copepod *Gaussia princeps*, 11th International Symposium on Bioluminescence and Chemiluminescence, Asilomar, CA (2000) pp. 34.
19. B.J. Bryan, C. Szent-Gyorgyi, Luciferases, fluorescent proteins, nucleic acids encoding the luciferases and fluorescent proteins and the use thereof in diagnostics, high throughput screening and novelty items, U.S. Patent 6,232,107 (2001).
20. M. Verhaegen, T.K. Christopoulos, Anal. Chem. 74 (2002) 4378.
21. O.H. Laitinen, V.P. Hytönen, H.R. Nordlund, M.S. Kulomaa, Cell. Mol. Life Sci. 63 (2006) 2992.
22. B.A. Tannous, D.-E. Kim, J.L. Fernandez, R. Weissleder, X.O. Breakefield, Mol. Ther. 11 (2005) 435.
23. Y. Nakajima, K. Kobayashi, K. Yamagishi, T. Enomoto, Y. Ohmiya, Biosci. Biotechnol. Biochem. 68 (2004) 565.
24. E.M. Thompson, S. Nagata, F.I. Tsuji, Proc. Natl. Acad. Sci. U.S.A. 86 (1989) 6567.
25. S. Inouye, Y. Ohmiya, Y. Toya, F.I. Tsuji, Proc. Natl. Acad. Sci. U.S.A. 89 (1992) 9584.
26. H. Fraga, Photochem. Photobiol. Sci. 7 (2008) 146.
27. K.V. Wood, J.R. de Wet, N. Dewi, M. DeLuca, Biochem. Biophys. Res. Commun. 124 (1984) 592.
28. J.R. de Wet, K.V. Wood, D.R. Helinski, M. DeLuca, Proc. Natl. Acad. Sci. U.S.A. 82 (1985) 7870.
29. S.J. Gould, G.-A. Keller, S. Subramani, J. Cell Biol. 105 (1987) 2923.
30. S.M. Marques, J.C.G. Esteves da Silva, IUBMB Life 61 (2009) 6.
31. S. Inouye, Cell. Mol. Life Sci. 67 (2010) 387.
32. H. Fraga, D. Fernandes, R. Fontes, J.C.G. Esteves da Silva, FEBS J. 272 (2005) 5206.
33. Y. Ando, K. Niwa, N. Yamada, T. Enomoto, T. Irie, H. Kubota, Y. Ohmiya, H. AKiyama, Nat. Photonics 2 (2008) 44.
34. K. Niwa, Y. Ichino, Y. Ohmiya, Chem. Lett. 39 (2010) 291.
35. W.D. McElroy, Proc. Natl. Acad. Sci. U.S.A. 33 (1947) 342.
36. B.L. Strehler, W.D. McElroy, Methods Enzymol. 3 (1957) 871.
37. S.M. Marques, J.C.G. Esteves da Silva, Anal. Bioanal. Chem. 391 (2008) 2161.
38. S.M. Marques, F. Peralta, J.C.G. Esteves da Silva, Talanta 77 (2009) 1497.
39. E.A. Meighen, K.N. Slessor, G.G. Grant, J. Chem. Ecol. 8 (1982) 911.
40. P.E. Stanley, Anal. Biochem. 39 (1971) 441.
41. N.L. Jocoy, D.J. Butcher, Spectr. Lett. 31 (1998) 1589.
42. L.H. Naylor, Biochem. Pharmacol. 58 (1999) 749.
43. B.E. Tropp, Molecular Biology - Genes to Proteins, 3rd ed., Jonas and Bartlett Publishers, Kendallville (2008).
44. Y. Murooka, I. Mitani, J. Biotechnol. 2 (1985) 303.
45. M.R. Montminy, K.A. Sevarino, J.A. Wagner, G. Mandel, R.H. Goodman, Proc. Natl. Acad. Sci. U.S.A. 83 (1986) 6682.
46. J. Alam, J.L. Cook, Anal. Biochem. 188 (1990) 245.
47. C.-M. Ghim, S.K. Lee, S. Takayama, R.J. Mitchell, BMB Rep. 43 (2010) 451.
48. D.W. Ow, K.V. Wood, M. DeLuca, J.R. de Wet, D.R. Helinski, S.H. Howell, Science 234 (1986) 856.
49. D.W. Ow, J.D. Jacobs, S.H. Howell, Proc. Natl. Acad. Sci. U.S.A. 84 (1987) 4870.
50. T.M. Williams, J.E. Burlein, S. Ogden, L.J. Kricka, J.A. Kant, Anal. Biochem. 176 (1989) 28.
51. M. Pons, D. Gagne, J.C. Nicolas, M. Mehtali, Biotechniques 9 (1990) 450.
52. A. Nussbaum, A. Cohen, J. Mol. Biol. 203 (1988) 391.
53. R.A. Goldsby, T.J. Kindt, B.A. Osborne, Kuby Immunology, 4th ed., W.H. Freeman and Company, New York (2000) pp. 162.
54. J.M. Berg, J.L. Tymoczko, L. Stryer, Biochemistry, 5th ed., W.H. Freeman and Company, New York (2002) pp. 101-102.
55. M.J. Corey, Coupled Bioluminescent Assays - Methods, Evaluations, and Applications, John Wiley and Sons, Hoboken (2009).
56. J.L. Viallard, M.R.V. Murthy, B. Dastugue, Neurochem. Res. 10 (1985) 1555.
57. C.H. Contag, M.H. Bachmann, Annu. Rev. Biomed. Eng. 4 (2002) 235.
58. T.C. Doyle, S.M. Burns, C.H. Contag, Cell. Microbiol. 6 (2004) 303.
59. O. Gheysens, F.M. Mottaghy, Methods 48 (2009) 139.
60. D.M. Close, T. Xu, G.S. Sayler, S. Ripp, Sensors 11 (2011) 180.
61. C.E. Hooper, R.E. Ansorge, H.M. Browne, P. Tomkins, J. Biolumin. Chemilumin. 5 (1990) 123.

62. C.H. Contag, P.R. Contag, J.I. Mullins, S.D. Spilman, D.K. Stevenson, D.A. Benaron, Mol. Microbiol. 18 (1995) 593.
63. D. Mankoff, J. Nucl. Med. 48 (2007) 18N.
64. M. Oshiro, Methods Cell Biol. 56 (1998) 45.
65. G.D. Scholes, Annu. Rev. Phys. Chem. 54 (2003) 57.
66. T. Förster, Ann. Phys.-Berlin 437 (1948) 55.
67. A. Roda, M. Guardigli, E. Michelini, M. Mirasoli, Anal. Bioanal. Chem. 393 (2009) 109.
68. T.E. Hébert, C. Galés, R.V. Rebois, Cell Biochem. Biophys. 45 (2006) 85.
69. J. Bacart, C. Corbel, R. Jockers, S. Bach, C. Couturier, Biotechnol. J. 3 (2008) 311.
70. P. G. Charest, S. Terrillon, M. Bouvier, EMBO Rep. 6 (2005) 334.
71. H. Morise, O. Shimomura, F.H. Johnson, J. Winant, Biochemistry 13 (1974) 2656.
72. Y. Xu, D.W. Piston, C.H. Johnson, Proc. Natl. Acad. Sci. U.S.A. 96 (1999) 151.
73. A. Prinz, G. Reither, M. Diskar, C. Schultz, Proteomics 8 (2008) 1179.
74. K.A. Eidne, K.M. Kroeger, A.C. Hanyaloglu, Trends Endocrinol. Metab. 13 (2002) 415.
75. M.A. Ayoub, K.D.G. Pfleger, Curr. Opin. Pharmacol. 10 (2010) 44.
76. Z. Xia, J. Rao, Curr. Opin. Biotechnol. 20 (2009) 37.
77. A.M. Smith, S. Nie, Accounts Chem. Res. 43 (2010) 190.
78. G.P.C. Drummen, Int. J. Mol. Sci. 11 (2010) 154.
79. A.M. Smith, H. Duan, A.M. Mohs, S. Nie, Adv. Drug Deliv. Rev. 60 (2008) 1226.
80. M.-K. So, C. Xu, A.M. Loening, S.S. Gambhir, J. Rao, Nat. Biotechnol. 24 (2006) 339.
81. A.M. Loening, T.D. Fenn, A.M. Wu, S.S. Gambhir, Protein Eng. Des. Sel. 19 (2006) 391.
82. A.M. Loening, T.D. Fenn, S.S. Gambhir, J. Mol. Biol. 374 (2007) 1017.
83. V. Tuchin, Tissue Optics – Light Scattering Methods and Instruments for Medical Diagnosis, 2nd ed., SPIE Press, Bellingham (2007).
84. T. Ozawa, Anal. Chim. Acta 556 (2006) 58.
85. V. Villalobos, S. Naik, D. Piwnica-Worms, Annu. Rev. Biomed. Eng. 9 (2007) 321.
86. M. Morell, S. Ventura, F.X. Avilés, FEBS Lett. 583 (2009) 1684.
87. S.B. Kim, T. Ozawa, Supramol. Chem. 22 (2010) 440.
88. P.L. Bartel, S. Fields (Eds.), The Yeast Two-Hybrid System, Oxford University Press, New York (1997).
89. Y. Tochigi, N. Sato, T. Sahara, C. Wu, S. Saito, T. Irie, W. Fujibuchi. T. Goda, R. Yamaji, M. Ogawa, Y. Ohmyia, S. Ohgiya, Anal. Chem. 82 (2010) 5768.
90. A. Roda, M. Guardigli, P. Pasini, M. Mirasoli, Anal. Bioanal. Chem. 377 (2003) 826.
91. F. Fan, K.V. Wood, Assay Drug Dev. Technol. 5 (2007) 127.
92. M. Rudin, Curr. Opin. Chem. Biol. 13 (2009) 360.
93. F. Puig-Basagoiti, M. Qing, H. Dong, B. Zhang, G. Zou, Z. Yuan, P.-Y. Shi, Antiviral Res. 83 (2009) 71.
94. M. Qig, W. Liu, Z. Yuan, F. Gu, P.Y. Shi, Antiviral Res. 86 (2010) 163.
95. T.G. Edmonds, H. Ding, X. Yuan, Q. Wei, K.S. Smith, J.A. Conway, L. Wieczorek, B. Brown, V. Polonis, J.T. West, D.C. Montefiori, J.C. Kappes, C. Ochsenbauer, Virology 408 (2010) 1.
96. L. Cui, J. Miao, J. Wang, Q. Li, L. Cui, Exp. Parasitol. 120 (2008) 80.
97. A. Dube, R. Gupta, N. Singh, Trends Parasitol. 25 (2009) 432.
98. T. Lang, H. Lecoeur, E. Prina, Trends Parasitol. 25 (2009) 464.
99. F. Gesellchen, A. Prinz, B. Zimmermann, F.W. Herberg, Eur. J. Cell Biol. 85 (2006) 663.
100. T. Issad, N. Boute, S. Boubekeur, D. Lacasa, K. Pernet, Diabetes Metab. 29 (2003) 111.
101. C. Blanquart, J. Achi, T. Issad, Biochem. Pharmacol. 76 (2008) 873.
102. J.A. Prescher, C.H. Contag, Curr. Opin. Chem. Biol. 14 (2010) 80.
103. T. Mizuno, K. Mohri, S. Nasu, K. Danjo, H. Okamoto, J. Control. Release 134 (2009) 149.
104. C.C. Mello, D. Conte Jr., Nature 431 (2004) 338.
105. M. Jinek, J.A. Doudna, Nature 457 (2009) 405.
106. Y. Lu, J. Xiao, H. Lin, Y. Bai, X. Luo, Z. Wang, B. Yang, Nucleic Acids Res. 37 (2009) e24.
107. J. Kurreck, Angew. Chem. Int. Edit. 49 (2010) 6258.
108. M.E. Davis, J.E. Zuckerman, C.H.J. Choi, D. Seligson, A. Tolcher, C.A. Alabi, Y. Yen, J.D. Heidel, A. Ribas, Nature 464 (2010) 1067.
109. G.J. Hannon, J.J. Rossi, Nature 431 (2004) 371.
110. J. Guo, K.A. Fisher, R. Darcy, J.F. Cryan, C. O'Driscoll, Mol. Biosyst. 6 (2010) 1143.
111. L.F. Greer III, A.A. Szalay, Luminescence 17 (2002) 43.

112. M. Hutchens, G.D. Luker, Cell. Microbiol. 9 (2007) 2315.
113. K.E. Luker, G.D. Luker, Antiviral Res. 78 (2008) 179.
114. K.E. Luker, G.D. Luker, Antiviral Res. 86 (2010) 93.
115. N. Andreu, A. Zelmer, S. Wiles, Fems Microbiol. Rev. 35 (2011) 360.
116. P. Sanz, L.D. Teel, F. Alem, H.M. Carvalho, S.C. Darnell, A.D. O'Brien, Infect. Immun. 76 (2008) 1036.
117. F. Heuts, B. Carow, H. Wigzell, M.E. Rottenberg, Microbes Infect. 11 (2009) 1114.
118. N. Andreu, A. Zelmer, T. Fletcher, P.T. Elkington, T.H. Ward, J. Ripoll, T. Parish, G.J. Bancroft, U. Schaible, B.D. Robertson, S. Wiles, PLoS One 5 (2010) e10777.
119. S. Hwang, T.-T. Wu, L.M. Tong, K.S. Kim, D. Martinez-Guzman, A.D. Colantonio, C.H. Uittenbogaart, R. Sun, J. Virol. 82 (2008) 12498.
120. C.H. Contag, D. Jenkins, P.R. Contag, R.S. Negrin, Neoplasia 2 (2000) 41.
121. A.L. Kung, Drug Discov. Today 2 (2005) 153.
122. S. Gross, D. Piwnica-Worms, Cancer Cell 7 (2005) 5.
123. B.A. Hadaschik, H. Adomat, L. Fazli, Y. Fradet, R.J. Andersen, M.E. Gleave, A.I. So, Clin. Cancer Res. 14 (2008) 1510.
124. J.-J. Min, H.-J. Kim, J.H. Park, S. Moon, J.H. Jeong, Y.-J. Hong, K.-O. Cho, J.H. Nam, N. Kim, Y.-K. Park, H.-S. Bom, J.H. Rhee, H.E. Choy, Mol. Imaging Biol. 10 (2008) 54.
125. Y.A. Yu, T. Timiryasova, Q. Zhang, R. Beltz, A.A. Szalay, Anal. Bioanal. Chem. 377 (2003) 964.
126. K.E. Luker, M. Gupta, G.D, Luker, Anal. Chem. 80 (2008) 5565.
127. K.E. Luker, M. Gupta, J.M. Steele, B.R. Foerster, G.D. Luker, Neoplasia 11 (2009) 1022.
128. G. Niu, X. Chen, Eur. J. Radiol. 70 (2009) 294.
129. C.T. Chan, R. Paulmurugan, O.S. Gheysens, J. Kim, G. Chiosis, S.S. Gambhir, Cancer Res. 68 (2008) 216.
130. A. Dragulescu-Andrasi, G. Liang, J. Rao, Bioconjugate Chem. 20 (2009) 1660.
131. M. Scabini, F. Stellari, P. Cappella, S. Rizzitano, G. Texido, E. Pesenti, Apoptosis 16 (2011) 198.
132. F. Li, Y. Lu, W. Li, D.D. Miller, R.I. Mahato, J. Control. Release 143 (2010) 151.
133. M.K. Kwak, K. Hur, J.E. Yu, T.S. Han, K. Yanagihara, W.H. Kim, S.M. Lee, S.-C. Song, H.-K. Yang, Invest. New Drugs 28 (2010) 284.
134. M. Edinger, Y.-A. Cao, M.R. Verneris, M.H. Bachmann, C.H. Contag, R.S. Negrin, Blood 101 (2003) 640.
135. C.E. Brown, R.P. Vishwanath, B. Aguilar, R. Starr, J. Najbauer, K.S. Aboody, M.C. Jensen, J. Immunol. 179 (2007) 3332.
136. X. Wang, M. Rosol, S. Ge, D. Peterson, G. McNamara, H. Pollack, D.B. Kohn, M.D. Nelson, G.M. Crooks, Blood 102 (2003) 3478.
137. S.C. Li, L.M.L. Tachiki, J. Luo, B.A. Dethlefs, Z. Chen, W.G. Loudon, Stem Cell Rev. Rep. 6 (2010) 317.
138. K.J. Ransohoff, J.C. Wu, Thromb. Haemost. 104 (2010) 13.
139. A. Sacco, R. Doyonnas, P. Kraft, S. Vitorovic, H.M. Blau, Nature 456 (2008) 502.
140. http://goldbook.iupac.org/. Accessed 18. Feb. 2011.
141. S. Girotti, E.N. Ferri, M.G. Fumo, E. Maiolini, Anal. Chim. Acta 608 (2008) 2.
142. M. Woutersen, S. Belkin, B. Brouwer, A.P. van Wezel, M.B. Heringa, Anal. Bioanal. Chem. 400 (2011) 915.
143. Y. Song, G. Li, S.F. Thornton, I.P. Thompson, S.A. Banwart, D.N. Lerner, W.E. Huang, Environ. Sci. Technol. 43 (2009) 7931.
144. S.F.M. Häusler, M. Ossadnik, E. Horn, S. Heuer, J. Dietl, J. Wischhusen, J. Immunol. Methods 361 (2010) 51.
145. R. Zhang, Y. Niu, H. Du, X. Cao, D. Shi, Q. Hao, Y. Zhou, Toxicol. Vitro 23 (2009) 158.
146. C. Wu, S. Irie, S. Yamamoto, Y. Ohmiya, Luminescence 24 (2009) 131.
147. J.L. Furman, P.-W. Mok, S. Shen, C.I. Stains, I. Ghosh, Chem. Commun. 47 (2011) 397.
148. K. Niwa, Y. Nakajima, Y. Ohmiya, Anal. Biochem. 396 (2010) 316.
149. K. Saito, N. Hatsugai, K. Horikawa, K. Kobayashi, T. Matsu-ura, K. Mikoshiba, T. Nagai, PLoS One 5 (2010) e9935.
150. T. Minekawa, A. Kambegawa, K. Shindome, H. Ohkuma, K. Abe, H. Maekawa, H. Arakawa, Chem. Pharm. Bull. 59 (2011) 84.
151. Y.Y. Woldman, J. Sun, J.L. Zweier, V.V. Khramtsov, Free Radic. Biol. Med. 47 (2009) 1339.
152. S.B. Kim, M. Sato, H. Tao, Anal. Chem. 81 (2009) 3760.
153. H. Fan-Minogue, Z. Cao, R. Paulmurugan, C.T. Chan, T.F. Massoud, D.W. Felsher, S.S. Gambhir, Proc. Natl. Acad. Sci. U.S.A. 107 (2010) 15892.

154. F. Fan, B.F. Binkowski, B.L. Butler, P.F. Stecha, M.K. Lewis, K.V. Wood, ACS Chem. Biol. 3 (2008) 346.
155. Y. Seto, K. Abe, M. Itoh, H. Sawai, Bioconjugate Chem. 13 (2002) 303.
156. C. Wu, K. Kawasaki, Y. Ogawa, Y. Yoshida, S. Ohgiya, Y. Ohmiya, Anal. Chem. 79 (2007) 1634.
157. A.S. Cohen, E.A. Dubikovskaya, J.S. Rush, C.R. Bertozzi, J. Am. Chem. Soc. 132 (2010) 8563.
158. A. Taneoka, A. Sakaguchi-Mikami, T. Yamazaki, W. Tsugawa, K. Sode, Biosens. Bioelectron. 25 (2009) 76.
159. K.A. Cissell, E.A. Hunt, S.K. Deo, Anal. Bioanal. Chem. 393 (2008) 125.
160. K.A. Cissell, S. Campbell, S.K. Deo, Anal. Bioanal. Chem. 391 (2008) 2577.
161. K.A. Cissell, Y. Rahimi, S. Shrestha, S.K. Deo, Bioconjugate Chem. 20 (2009) 15.
162. K. Noda, H. Goto, Y. Murakami, A.B.F. Ahmed, A. Kuroda, Anal. Biochem. 397 (2010) 152.
163. T. Minekawa, H. Ohkuma, K. Abe, H. Maekawa, H. Arakawa, Luminescence 24 (2009) 394.
164. S. Kim, B. Schuler, A. Terekhov, J. Auer, L.J. Mauer, L. Perry, B. Applegate, J. Microbiol. Methods 79 (2009) 18.
165. M. Nakamura, M. Mie, E. Kobatake, Analyst 136 (2011) 71.
166. K. Ito, K. Nakagawa, S. Murakami, H. Arakawa, M. Maeda, Anal. Sci. 19 (2003) 105.
167. C.-M. Hu, Z.-F. Chang, Anal. Biochem. 398 (2010) 269.
168. A. Yasgar, J. Shultz, W. Zhou, H. Wang, F. Huang, N. Murphy, E.L. Abel, J. DiGiovanni, J. Inglese, A. Simeonov, Assay Drug Dev. Technol. 8 (2010) 200.
169. G. Ibáñez, J.L. McBean, Y.M. Astudillo, M. Luo, Anal. Biochem. 401 (2010) 203.
170. K.W. Cho, J. Biochem. Mol. Biol. 33 (2000) 353.
171. K.W. Cho, S. Mo, H.-S. Lee, J.-R. Rho, J. Shin, J. Microbiol. 38 (2000) 150.
172. R.A. Moravec, M.A. O'Brien, W.J. Daily, M.A. Scurria, L. Bernad, T.L. Riss, Anal. Biochem. 387 (2009) 294.
173. S.S. Shekhawat, J.R. Porter, A. Sriprasad, I. Ghosh, J. Am. Chem. Soc. 131 (2009) 15284.
174. L. Wang, Q. Fu, Y. Dong, Y. Zhou, S. Jia, J. Du, F. Zhao, Y. Wang, X. Wang, J. Peng, S. Yang, L. Zhan, Antiviral Res. 87 (2010) 50.
175. H. Dacres, M.M. Dumancic, I. Horne, S.C. Trowell, Biosens. Bioelectron. 24 (2009) 1164.
176. Z. Xia, Y. Xing, M.-K. So, A.L. Koh, R. Sinclair, J. Rao, Anal. Chem. 80 (2008) 8649.
177. Y.-P. Kim, W.L. Daniel, Z. Xia, H. Xie, C.A. Mirkin, J. Rao, Chem. Commun. 46 (2010) 76.
178. R.V. Rebois, M. Robitaille, D. Pétrin, P. Zylbergold, P. Trieu, T.E. Hébert, Methods 45 (2008) 214.
179. S.B. Kim, M. Sato, H. Tao, Bioconjugate Chem. 20 (2009) 2324.
180. C.I. Stains, J.L. Furman, J.R. Porter, S. Rajagopal, Y. Li, R.T. Wyatt, I. Ghosh, ACS Chem. Biol. 5 (2010) 943.
181. T. Otsuji, E. Okuda-Ashitaka, S. Kojima, H. Akiyama, S. Ito, Y. Ohmiya, Anal. Biochem. 329 (2004) 230.
182. S.B. Kim, M. Sato, H. Tao, Anal. Chem. 81 (2009) 67.
183. A. Kaihara, A. Sunami, J. Kurokawa, T. Furukawa, J. Am. Chem. Soc. 131 (2009) 4188.
184. H. Huang, S.-Y. Choi, M.A. Frohman, Mitochondrion 10 (2010) 559.
185. J. Perroy, S. Pontier, P.G. Charest, M. Aubry, M. Bouvier, Nat. Methods 1 (2004) 203.
186. E.S. Johnson, Annu. Rev. Biochem. 73 (2004) 355.
187. R.J. Dohmen, Biochim. Biophys. Acta 1695 (2004) 113.
188. Y.-P. Kim, Z. Jin, E. Kim, S. Park, Y.-H. Oh, H.-S. Kim, Biochem. Biophys. Res. Commun. 382 (2009) 530.
189. http://www.lbl.gov/Education/ELSI/research-main.html. Accessed 21. Feb. 2011.
190. N. Boucher, Y. Wu, C. Dumas, M. Dubé, D. Sereno, M. Breton, B. Papadopoulou, J. Biol. Chem. 277 (2002) 19511.
191. Y. Kanamori, Y. Hayakawa, H. Matsumoto, Y. Yasukochi, S. Shimura, Y. Nakahara, M. Kiuchi, M. Kamimura, J. Biol. Chem. 285 (2010) 36933.
192. M. Fukuchi, M. Tsuda, J. Neurochem. 115 (2010) 1222.
193. N. Tai, J.C. Schmitz, T.-M. Chen, M.B. O´Neill, E. Chu, Biochem. Biophys. Res. Commun. 369 (2008) 795.
194. R. Guan, X. Wu, X. Feng, M. Zhang, T.E. Hébert, D.L. Segaloff, Cell. Signal. 22 (2010) 247.
195. D.O. Borroto-Escuela, W. Romero-Fernandez, A.O. Tarakanov, D. Marcellino, F. Ciruela, L.F. Agnati, K. Fuxe, Biochem. Biophys. Res. Commun. 401 (2010) 605.
196. M. Robitaille, N. Ramakrishnan, A. Baragli, T.E. Hébert, Cell. Signal. 21 (2009) 488.

197. L. De Vries, F. Finana, F. Cachoux, B. Vacher, P. Sokoloff, D. Cussac, Cell. Signal. 22 (2010) 158.
198. M.K. Kilpi, J.T. Atosuo, E.-M.E. Lilius, Dev. Comp. Immunol. 33 (2009) 1102.
199. K.A. Joiner, E.J. Brown, M.M. Frank, Annu. Rev. Immunol. 2 (1984) 461.
200. N.P. Franks, W.R. Lieb, Nature 310 (1984) 599.
201. N.P. Franks, W.R. Lieb, Anesthesiology 101 (2004) 235.
202. N.P. Franks, A. Jenkins, E. Conti, W.R. Lieb, P. Brick, Biophys. J. 75 (1998) 2205.
203. E.J. Bertaccini, J.R. Trudell, N.P. Franks, Anesth. Analg. 104 (2007) 318.
204. S. Vemparala, C. Domene, M.L. Klein, Accounts Chem. Res. 43 (2010) 103.
205. M.R. Riley, J. Biol. Eng. 1 (2007) 1.
206. J. de Boer, C. van Blitterswijk, C. Löwik, Biomaterials 27 (2006) 1851.
207. J. Sjollema, P.K. Sharma, R.J.B. Dijkstra, G.M. van Dam, H.C. van der Mei, A.F. Engelsman, H.J. Busscher, Biomaterials 31 (2010) 1984.
208. F. Krammer, J. Pontiller, C. Tauer, D. Palmberger, A. Maccani, M. Baumann, R. Grabherr, PLoS One 5 (2010) e13265.
209. J.-M. Hawronskyj, J. Holah, Trends Food Sci. Technol. 8 (1997) 79.
210. M. Levin, T. Björnheden, M. Evaldsson, S. Walenta, O. Wiklund, Arterioscler. Thromb. Vasc. Biol. 19 (1999) 950.
211. G. Di Tomaso, R. Borghese, D. Zannoni, Arch. Microbiol. 177 (2001) 11.
212. N. Blow, Nat. Methods 6 (2009) 465.
213. N. Boute, R. Jockers, T. Issad, Trends Pharmacol. Sci. 23 (2002) 351.
214. H. Dacres, M.M. Dumancic, I. Horne, S.C. Trowell, Anal. Biochem. 385 (2009) 194.
215. R.Y. Tsien, Annu. Rev. Biochem. 67 (1998) 509.
216. Y. Wang, J.Y.-J. Shyy, S. Chien, Annu. Rev. Biomed. Eng. 10 (2008) 1.
217. M. Zimmer, Chem. Soc. Rev. 38 (2009) 2823.
218. L.D. Lavis, R.T. Raines, ACS Chem. Biol. 3 (2008) 142.
219. E. Tholouli, E. Sweeney, E. Barrow, V. Clay, J.A. Hoyland, R.J. Byers, J. Pathol. 216 (2008) 275.
220. W.R. Algar, A.J. Tavares, U.J. Krull, Anal. Chim. Acta 673 (2010) 1.
221. E. Rota, N.T. Zalesskaja, N.S. Rodionova, V.N. Petushkov, J. Zool. 260 (2003) 291.
222. N.S. Rodionova, V.S. Bondar', V.N. Petushkov, Dokl. Biochem. Biophys. 392 (2003) 253.
223. N.S. Rodionova, V.N. Petushkov, J. Photochem. Photobiol. B-Biol. 83 (2006) 123.
224. V.N. Petushkov, N.S. Rodionova, J. Photochem. Photobiol. B-Biol. 87 (2007) 130.
225. S.M. Marques, V.N. Petushkov, N.S. Rodionova, J.C.G. Esteves da Silva, J. Photochem. Photobiol. B-Biol.102 (2011) 218.
226. J.C. Dunlap, J.W. Hastings, Biochemistry 20 (1981) 983.
227. C. Suzuki, Y. Nakajima, H. Akimoto, C. Wu, Y. Ohmiya, Gene 344 (2005) 61.
228. S.V. Markova, S. Golz, L.A. Frank, B. Kalthof, E.S. Vysotski, J. Biol. Chem. 279 (2004) 3212.
229. Y. Takenaka, H. Masuda, A. Yamaguchi, S. Nishikawa, Y. Shigeri, Y. Yoshida, H. Mizuno, Gene 425 (2008) 28.
230. V.R. Viviani, E.J.H. Bechara, Y. Ohmiya, Biochemistry 38 (1999) 8271.
231. Y. Nakajima, T. Kimura, C. Suzuki, Y. Ohmiya, Biosci. Biotechnol. Biochem. 68 (2004) 948.
232. Y. Nakajima, M. Ikeda, T. Kimura, S. Honma, Y. Ohmiya, K.-I. Honma, FEBS Lett. 565 (2004) 122.
233. X. Li, Y. Nakajima, K. Niwa, V.R. Viviani, Y. Ohmiya, Protein Sci. 19 (2010) 26.
234. K. Niwa, Y. Ichino, S. Kumata, Y. Nakajima, Y. Hiraishi, D.-I. Kato, V.R. Viviani, Y. Ohmiya, Photochem. Photobiol. 86 (2010) 1046.
235. K.V. Wood, Y.A. Lam, H.H. Seliger, W.D. McElroy, Science 244 (1989) 700.
236. S.B. Kim, Y. Umezawa, K.A. Kanno, H. Tao, ACS Chem. Biol. 3 (2008) 359.
237. V. Villalobos, S. Naik, M. Bruinsma, R.S. Dothager, M.-H. Pan, M. Samrakandi, B. Moss, A. Elhammali, D. Piwnica-Worms, Chem. Biol. 17 (2010) 1018.
238. V.R. Viviani, A.C.R. Silva, G.L.O. Perez, R.V. Santelli, E.J.H. Bechara, F.C. Reinach, Photochem. Photobiol. 70 (1999) 254.
239. Y. Nakajima, T. Yamazaki, S. Nishii, T. Noguchi, H. Hoshino, K. Niwa, V.R. Viviani, Y. Ohmiya, PLoS One 5 (2010) e10011.
240. R. Shinde, J. Perkins, C.H. Contag, Biochemistry 45 (2006) 11103.
241. G.R. Reddy, W.C. Thompson, S.C. Miller, J. Am. Chem. Soc. 132 (2010) 13586.
242. B.R. Branchini, M.H. Murtiashaw, R.A. Magyar, N.C. Portier, M.C. Ruggiero, J.G. Stroh, J. Am. Chem. Soc. 124 (2002) 2112.
243. H. Takakura, K. Sasakura, T. Ueno, Y. Urano, T. Terai, K. Hanaoka, T. Tsuboi, T. Nagano, Chem.- Asian J. 5 (2010) 2053.

244. Q. Shao, T. Jiang, G. Ren, Z. Cheng, B. Xing, Chem. Commun. (2009) 4028.
245. O. Shimomura, B. Musicki, Y. Kishi, Biochem. J. 261 (1989) 913.
246. S. Inouye, O. Shimomura, Biochem. Biophys. Res. Commun. 233 (1997) 349.
247. H. Zhao, T.C. Doyle, R.J. Wong, Y. Cao, D.K. Stevenson, D. Piwnica-Worms, C.H. Contag, Mol. Imaging 3 (2004) 43.
248. E. Hawkins, J. Unch, N. Murphy, J. Vidugiriene, M. Scurria, D.H. Klaubert, K.V. Wood, Promega Notes 90 (2005) 10.
249. K. Gomi, N. Kajiyama, J. Biol. Chem. 276 (2001) 36508.
250. K. Gomi, K. Hirokawa, N. Kajiyama, Gene 294 (2002) 157.
251. R. Emamzadeh, S. Hosseinkhani, R. Hemati, M. Sadeghizadeh, Enzyme Microb. Technol. 47 (2010) 159.
252. J.C. Day, M.J. Bailey, Insect Mol. Biol. 12 (2003) 365.
253. G.A. Stepanyuk, J. Unch, N.P. Malikova, S.V. Markova, J. Lee, E.S. Vysotski, Anal. Bioanal. Chem. 398 (2010) 1809.
254. S.S. Chandran, S.A. Williams, S.R. Denmeade, Luminescence 24 (2009) 35.
255. A. Kheirolomoom, D.E. Kruse, S. Qin, K.E. Watson, C.-Y. Lai, L.J.T. Young, R.D. Cardiff, K.W. Ferrara, J. Control. Release 141 (2010) 128.
256. J.M. George, Genome Biol. 3 (2001) reviews 3002.1.
257. J. Kim, C.H. Moon, S. Jung, S.R. Paik, Biochim. Biophys. Acta-Proteins Proteomics 1794 (2009) 309.
258. M.R. Ganjalikhany, B. Ranjbar, S. Hosseinkhani, K. Khalifeh, L. Hassani, J. Mol. Catal. B-Enzym. 62 (2010) 127.
259. F. Ataei, S. Hosseinkhani, K. Khajeh, J. Biotechnol. 144 (2009) 83.
260. J.M.M. Leitão, J.C.G. Esteves da Silva, J. Photochem. Photobiol. B-Biol. 101 (2010) 1.
261. L.C. Tisi, P.J. White, D.J. Squirrell, M.J. Murphy, C.R. Lowe, J.A.H. Murray, Anal. Chim. Acta 457 (2002) 115.
262. G.H.E. Law, O.A. Gandelman, L.C. Tisi, C.R. Lowe, J.A.H. Murray, Biochem. J 397 (2006) 305.
263. B.R. Branchini, D.M. Ablamsky, M.H. Murtiashaw, L. Uzasci, H. Fraga, T.L. Southworth, Anal. Biochem. 361 (2007) 253.
264. M. Imani, S. Hosseinkhani, S. Ahmadian, M. Nazari, Photochem. Photobiol. Sci. 9 (2010) 1167.
265. A. Riahi-Madvar, S. Hosseinkhani, Protein Eng. Des. Sel. 22 (2009) 655.
266. J.F. Thompson, K.F. Geoghegan, D.B. Lloyd, A.J. Lanzetti, R.A. Magyar, S.M. Anderson, B.R. Branchini, J. Biol. Chem. 272 (1997) 18766.
267. H. Fujii, K. Noda, Y. Asami, A. Kuroda, M. Sakata, A. Tokida, Anal. Biochem. 366 (2007) 131.
268. J. Woo, A.G. von Arnim, Plant Methods 4 (2008) DOI:10.1186/1746-4811-4-23.
269. J.P. Welsh, K.G. Patel, K. Manthiram, J.R. Swartz, Biochem. Biophys. Res. Commun. 389 (2009) 563.
270. T. Rathnayaka, M. Tawa, S. Sohya, M. Yohda, Y. Kuroda, Biochim. Biophys. Acta-Proteins Proteomics 1804 (2010) 1902.
271. B.R. Branchini, T.L. Southworth, N.F. Khattak, E. Michelini, A. Roda, Anal. Biochem. 345 (2005) 140.
272. H. Caysa, R. Jacob, N. Müther, B. Branchini, M. Messerle, A. Söling, Photochem. Photobiol. Sci. 8 (2009) 52.
273. B.R. Branchini, D.M. Ablamsky, A.L. Davis, T.L. Southworth, B. Butler, F. Fan, A.P. Jathoul, M.A. Pule, Anal. Biochem. 396 (2010) 290.
274. A.M. Loening, A.M. Wu, S.S. Gambhir, Nat. Methods 4 (2007) 641.
275. S.S. Patterson, H.M. Dionisi, R.K. Gupta, G.S. Sayler, J. Ind. Microbiol. Biotechnol. 32 (2005) 115.
276. D.M. Close, S.S. Patterson, S. Ripp, S.J. Baek, J. Sanseverino, G.S.Sayler, PLoS One 5 (2010) e12441.
277. S. Yagur-Kroll, S. Belkin, Anal. Bioanal. Chem. 400 (2011) 1071.
278. E. Jablonski, M. DeLuca, Proc. Natl. Acad. Sci. U.S.A. 73 (1976) 3848.
279. E.N. Esimbekova, I.G. Torgashina, V.A. Kratasyuk, Biochem. -Moscow 74 (2009) 695.
280. M. Yousefi-Nejad, S. Hosseinkhani, K. Khajeh, B. Ranjbar, Enzyme Microb. Technol. 40 (2007) 740.
281. A.R. Ribeiro, R.M. Santos, L.M. Rosário, M.H. Gil, J. Biolumin. Chemilumin. 13 (1998) 371.
282. N. Nakata, T. Kamidate, Luminescence 16 (2001) 263.
283. N. Nakata, A. Ishida, H. Tani, T. Kamidate, Anal. Sci. 19 (2003) 1183.
284. Y. Zhang, G.J. Phillips, Q. Li, E.S. Yeung, Anal. Chem. 80 (2008) 9316.
285. Y.-F. Chu, C.-H. Hsu, P.K. Soma, Y.M. Lo, Bioresour. Technol. 100 (2009) 3167.
286. H. Ben-Yoav, T. Elad, O. Shlomovits, S. Belkin, Y. Shacham-Diamand, Biosens. Bioelectron. 24 (2009) 1969.

287. M. Iinuma, Y. Ushio, A. Kuroda, Y. Kadoya, Electr. Commun. Jpn. 92 (2009) 53.
288. Q. Mei, Z. Xia, F. Xu, S.A. Soper, Z.H. Fan, Anal. Chem. 80 (2008) 6045.
289. L. Pastorino, S. Disawal, C. Nicolini, Y.M. Lvov, V.V. Erokhin, Biotechnol. Bioeng. 84 (2003) 286.
290. M.V. Matz, A.F. Fradkov, Y.A. Labas, A.P. Savitsky, A.G. Zaraisky, M.L. Markelov, S.A. Lukyanov, Nat. Biotechnol. 17 (1999) 969.
291. R. Arai, H. Nakagawa, A. Kitayama, H. Ueda, T. Nagamune, J. Biosci. Bioeng. 94 (2002) 362.
292. S.T. Gammon, V.M. Villalobos, M. Roshal, M. Samrakandi, D. Piwnica-Worms, Biotechnol. Prog. 25 (2009) 559.
293. M. Kamal, M. Marquez, V. Vauthier, A. Leloire, P. Froguel, R. Jockers, C. Couturier, Biotechnol. J. 4 (2009) 1337.
294. Y. Xing, M.-K. So, A.L. Koh, R. Sinclair, J. Rao, Biochem. Biophys. Res. Commun. 372 (2008) 388.
295. C. Wu, K. Mino, H. Akimoto, M. Kawabata, K. Nakamura, M. Ozaki, Y. Ohmiya, Proc. Natl. Acad. Sci. U.S.A. 106 (2009) 15599.
296. B.R. Branchini, D.M. Ablamsky, J.C. Rosenberg, Bioconjugate Chem. 21 (2010) 2023.
297. A. Miyawaki, Cell Struct. Funct. 27 (2002) 343.
298. X. Shu, A. Royant, M.Z. Lin, T.A. Aguilera, V. Lev-Ram, P.A. Steinbach, R.Y. Tsien, Science 324 (2009) 804.
299. Y. Inoue, S. Kiryu, K. Izawa, M. Watanabe, A. Tojo, K. Ohtomo, Eur. J. Nucl. Med. Mol. Imaging 36 (2009) 771.
300. M. Keyaerts, C. Heneweer, L.O.T. Gainkam, V. Caveliers, B.J. Beattie, G.A. Martens, C. Vanhove, A. Bossuyt, R.G. Blasberg, T. Lahoutte, Mol. Imaging Biol. 13 (2011) 59.
301. E. Michelini, L. Cevenini, L. Mezzanotte, D. Ablamsky, T. Southworth, B. Branchini, A. Roda, Anal. Chem. 80 (2008) 260.
302. B. Breton, E. Sauvageau, J. Zhou, H. Bonin, C. Le Gouill, M. Bouvier, Biophys. J. 99 (2010) 4037.
303. P. Carriba, G. Navarro, F. Ciruela, S. Ferré, V. Casadó, L. Agnati, A. Cortés, J. Mallol, K. Fuxe, E.I. Canela, C. Lluís, R. Franco, Nat. Methods 5 (2008) 727.
304. H. Goesmann, C. Feldmann, Angew. Chem. Int. Edit. 49 (2010) 1362.
305. J. Gao, B. Xu, Nano Today 4 (2009) 37.
306. M.F. Frasco, N. Chaniotakis, Anal. Bioanal. Chem. 396 (2010) 229.
307. W. Cai, A.R. Hsu, Z.-B. Li, X. Chen, Nanoscale Res. Lett. 2 (2007) 265.
308. W.H. Suh, K.S. Suslick, G.D. Stucky, Y.-H. Suh, Prog. Neurobiol. 87 (2009) 133.
309. P. Zrazhevskiy, X. Gao, Nano Today 4 (2009) 414.
310. J.-H. Kim, J.-H. Ahn, P.W. Barone, H. Jin, J. Zhang, D.A. Heller, M.S. Strano, Angew. Chem. Int. Edit. 49 (2010) 1456.
311. N. Ma, A.F. Marshall, J. Rao, J. Am. Chem. Soc. 132 (2010) 6884.
312. A.M. Derfus, W.C.W. Chan, S.N. Bhatia, Nano Lett. 4 (2004) 11.
313. J. Lovrić, S.J. Cho, F.M. Winnik, D. Maysinger, Chem. Biol. 12 (2005) 1227.
314. Y.-P. Sun, B. Zhou, Y. Lin, W. Wang, K.A.S. Fernando, P. Pathak, M.J. Meziani, B.A. Harruff, X. Wang, H. Wang, P.G. Luo, H. Yang, M.E. Kose, B. Chen, L.M. Veca, S.-Y. Xie, J. Am. Chem. Soc. 128 (2006) 7756.
315. S.N. Baker, G.A. Baker, Angew. Chem. Int. Edit. 49 (2010) 6726.
316. A. Hoshino, K. Fujioka, T. Oku, M. Suga, Y.F. Sasaki, T. Ohta, M. Yasuhara, K. Suzuki, K. Yamamoto, Nano Lett. 4 (2004) 2163.
317. L. Wang, H. Zheng, Y. Long, M. Gao, J. Hao, J. Du, X. Mao, D. Zhou, J. Hazard. Mater. 177 (2010) 1134.
318. http://www.zymera.com/images/Technology_Description.pdf. Accessed 28. Feb. 2011.

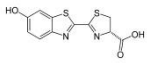

Objectives

This project encompasses two major objectives, the development and application of novel bioanalytical methods based on firefly luciferase and the study of *Fridericia heliota*'s bioluminescent system.

For each of the proposed methods, aiming the detection and quantitation of organophosphorus pesticides, inorganic sulfate, nitric oxide and free fatty acids, multi-enzymatic reactions that produce or consume ATP, thus enhancing or decreasing the bioluminescent signal catalyzed by firefly luciferase, will be presented. Posteriorly, the bioluminescent methods will be characterized in terms of limits of detection and quantitation, linear range, repeatability and interferences, and finally tested in samples selected by their biological, environmental or clinical interest.

Purified extracts of *Fridericia heliota*, obtained by Valentin N. Petushkov and co-workers, will be subjected to instrumental techniques such as high-performance liquid chromatography, mass spectrometry and nuclear magnetic resonance, to uncover the ultraviolet-visible properties and chemical structure of its luciferin. Later on, the proposed structure will be confirmed by chemical synthesis. Finally, luminometric studies with purified *F*. *heliota*'s luciferase will determine their potential application in novel bioluminescent methods.

Section two

Methods set up and application

Chapter two

Quantitative analysis of organophosphorus pesticides in freshwater using an optimized firefly luciferase-based coupled bioluminescent assay

Simone M. Marques, Joaquim C.G. Esteves da Silva

Luminescence DOI 10.1002/bio.2556

The scientific work leading to this paper was integrally performed within the host institution, the Chemometric Research of Chemical, Environmental, Forensic and Biological Systems group, from the Chemistry Research Center of the University of Porto (*Centro de Investigação em Química da Universidade do Porto*, *CIQ-UP*), Department of Chemistry and Biochemistry, Faculty of Sciences, University of Porto. Simone Marques was responsible for bibliographic search, protocols set up, experimental execution, data treatment and paper writing, under the supervision of Joaquim Esteves da Silva.

LUMINESCENCE
The Journal of Biological and Chemical Luminescence

Received: 8 January 2013, Revised: 23 May 2013, Accepted: 26 May 2013 Published online in Wiley Online Library

(wileyonlinelibrary.com) DOI 10.1002/bio.2556

Quantitative analysis of organophosphorus pesticides in freshwater using an optimized firefly luciferase-based coupled bioluminescent assay

SM Marques and JCG Esteves da Silva*

ABSTRACT: In this paper, a coupled bioluminescent assay, relying on the coupling of the enzymes acetylcholinesterase, *S*-acetyl-coenzyme A synthetase and firefly luciferase, for the detection and quantitation of organophosphorus pesticides, is presented. Using malathion as a model organophosphorus pesticide, the assay was optimized through statistical experimental design methodology, namely Plackett–Burman and central composite designs. The optimized method requires only 20 μL of sample. The linear range for the assay was 2.5–15 μM of malathion, with limits of detection and quantitation of 1.5 and 5.0 μM, respectively. This simple, fast and robust method allows samples to be analyzed at room temperature and without any pretreatment. Copyright © 2013 John Wiley & Sons, Ltd.

Supporting Information may be found in the online version of this article.

Keywords: bioanalytical chemistry; enzymatic assay; bioluminescence; luminometry; experimental design

Introduction

Organophosphorus pesticides are a wide class of synthetic derivatives of phosphorus and thiophosphorus acids with organic substituents. Their main application is in insect control, both in crops and in urban areas, and include the commercial pesticides malathion (Fig. 1), parathion, phosmet and trichlorfon (1,2). They act by inhibiting acetylcholinesterase, the enzyme responsible for hydrolyzing the neurotransmitter acetylcholine, thus interfering with the normal nerve impulse finalization (3). Because of their widespread use, many concerns about safety and toxic exposure are raised, and therefore their detection and quantitation, as well as their degradation subproducts in food and in the environment, are of great importance. The use of domestic wells intended for consumption and recreation is still common in both developed and developing countries, especially in less urbanized areas. However, this practice presents risks because this water may not be subjected to regular analysis by official agencies. As many domestic wells are close to or within cultivation fields, possible contamination with pesticides is relevant. Alternatives to the use of pesticides are being proposed, for example, biopesticides (4). Nonetheless, it is not known whether they may replace the current pesticides in the near future. In fact, although malathion has been banned by the European Union since 2008, it was reintroduced into the market in 2010 (5), demonstrating that more research is needed in this area.

Many of the analytical methods used in pesticide identification, separation and quantitation are based on instrumental techniques, especially gas (6,7) and liquid chromatography (8,9), sometimes coupled to mass spectrometry (10–12). They often also include sample pretreatment and concentration by solid- or liquid-phase extraction. Despite their high sensitivity and the possibility of high-throughput analysis, these techniques are time-consuming and not suitable for the *in situ* evaluation of samples. Furthermore, theoretical knowledge and training are required.

Other methods rely on biochemical reactions, either acetylcholinesterase-catalyzed reactions (13) or immunoassays (14,15). For example, a very simple assay was created by immobilizing acetylcholinesterase in commercial pH indicator strips, where the presence of the pesticides is detected by colorimetry due to pH changes conferred by the reaction products (16). Another approach employs electrochemical biosensors, with acetylcholinesterase immobilized in appropriate matrices (17,18). These methods have the sensitivity and specificity associated with either enzymatic assays or antibodies, but biosensors may become nonresponsive over time due to loss of enzyme activity, loss of the enzyme itself or saturation with debris. Immunoassays may be time-consuming and expensive. Recently, the use of nanomaterials has led to a novel class of biosensors, for example, using gold nanoparticles (19), carbon nanotubes (20) and enzyme-coupled quantum dots loaded onto carbon electrodes (21). However, laboratory synthesis and characterization can be problematic , and they may also lose stability over time due to degradation. This last point is of

* Correspondence to: J. C. G. Esteves da Silva, Centro de Investigação em Química da Universidade do Porto (CIQ-UP), Department of Chemistry and Biochemistry, Faculty of Sciences, University of Porto, Rua do Campo Alegre, no. 687, 4169–007 Porto, Portugal. Email: jcsilva@fc.up.pt

Centro de Investigação em Química da Universidade do Porto (CIQ-UP), Department of Chemistry and Biochemistry, University of Porto, Porto, Portugal

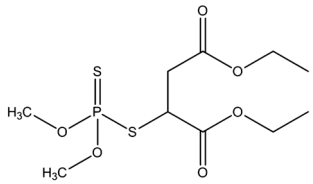

Figure 1. Chemical structure of malathion.

utmost importance because many studies suggest that they may lead to biological and environmental contamination (22,23).

This paper presents the establishment and optimization of a coupled bioluminescent assay (24) for organophosphorus pesticides using malathion, diethyl 2-[(dimethoxyphosphorothioyl) sulfanyl]succinate (Fig. 1), as a model pesticide and the reaction catalyzed by *S*-acetyl-coenzyme A synthetase as a consumer of ATP. In this coupled bioluminescent assay, the first reaction is catalyzed by acetylcholinesterase, generating acetate and choline (equation 1). Acetate, the product of this first reaction, is one of the substrates for *S*-acetyl-coenzyme A synthetase, along with ATP and coenzyme A (equation 2). The final coupled reaction is catalyzed by firefly luciferase, requiring the substrate firefly luciferin and ATP. However, because ATP was consumed in the previous reaction, the bioluminescent reaction is impaired (equation 3). The presence of an organophosphorus pesticide will inhibit the first reaction, thus favoring the bioluminescent reaction. Some reports suggest that herbicides (25) and aromatic pesticides (26) can also inhibit the bioluminescent reaction, as well as fatty acids, alcohols, anesthetics, luciferin analogues and side-products of the bioluminescent reaction (27).

$$\text{Acetylcholine} + H_2O \xrightarrow{\text{acetylcholinesterase}} \text{acetate} + \text{choline} \quad (1)$$

$$\text{Acetate} + \text{ATP-Mg}^{2+} + \text{coenzyme A} \xrightarrow{\text{S-acetyl-coenzyme A synthetase}} \text{acetyl-coenzyme A} + \text{AMP-Mg}^{2+} + \text{PPi-Mg}^{2+} \quad (2)$$

$$\text{AMP-Mg}^{2+} + \text{firefly luciferin} + O_2 \xrightarrow{\text{firefly luciferase}} \textit{no light produced} \quad (3)$$

A multivariate experimental design methodology based on computational software was used for the method's optimization (28,29).

Experimental

Reagents

The enzymes firefly luciferase (from *Photinus pyralis*, EC 1.13.12.7; product code L9506, lot 014K7430), acetylcholinesterase (from *Electrophorus electricus* type VI-S, EC 3.1.1.7; product code C3389, lot 047K7010) and *S*-acetyl-coenzyme A synthetase (from baker's yeast, EC 6.2.1.1; product code A1765, lot 31K1717), as well as the reagents acetylcholine chloride (product code A6625), coenzyme A sodium salt hydrate (from yeast, product code C3144), 4-(2-hydroxyethyl)piperazine-1-ethanesulfonic acid (Hepes, product code H3375), adenosine 5′-triphosphate disodium salt (ATP, from a bacterial source, product code A2383) and firefly luciferin (synthetic firefly D-luciferin, product code L9504) were purchased from Sigma (Steinheim, Germany). Magnesium chloride hexahydrate (product code 63064) and malathion (Pestanal® analytical standard, product code 36143) were purchased from Fluka (Buchs, Switzerland). All reagents were used without further purification. A stock solution of firefly luciferase was prepared by dissolving the whole content of the flask (~ 43 mg of lyophilized powder, corresponding to 10 mg of pure luciferase, or ~ 21% protein/mg powder, according to the manufacturer's information) in Hepes buffer 0.5 M, pH 7.5. The concentration was checked by UV/Vis spectroscopy using the molar extinction coefficient of 39,310 L/mol cm^{-1} at a wavelength (λ_{max}) of 280 nm and considering a molar mass of 60,745 g/mol. Analogously, a stock solution of acetylcholinesterase was prepared by dissolving the whole content of the flask (~ 4.7 mg of lyophilized powder, ~ 62% protein/mg powder, according to the manufacturer's information) in Hepes buffer 0.5 M, pH 7.5. The concentration was confirmed by UV/Vis spectroscopy using the molar extinction coefficient of 505,120 L/mol cm^{-1} at λ_{max} = 280 nm and considering a molar mass of 287,204 g/mol. Finally, the stock solution of *S*-acetyl-coenzyme A synthetase was prepared by dissolving the whole content of the flask (~ 5 mg of protein, or ~ 21% protein/mg powder, according to the manufacturer's information) in Hepes buffer 0.5 M, pH 7.5. The concentration was checked by UV/Vis spectroscopy using a molar extinction coefficient of 336,570 L/mol cm^{-1} at λ_{max} = 280 nm and considering a molar mass of 237,386 g/mol. The molar masses were calculated by gathering information from the BRENDA database (30,31) and the UniProt Protein Knowledgebase (32,33). The values of the molar extinction coefficients were calculated using the ProtParam tool (protein physical and chemical parameters) from the ExPASy Proteomics Server (34,35). The values of molar masses were also confirmed using this software. Hepes was prepared by dissolving the corresponding mass in deionized water, and the pH was adjusted to 7.5 by adding drops of a 10 M sodium hydroxide solution. Firefly luciferin stock solutions were prepared in deionized water with intense stirring for ~ 1 h, protected from the air and light. The concentration was confirmed by UV/Vis spectroscopy using a molar extinction coefficient of 18,200 L/mol cm^{-1} at λ_{max} = 327 nm (36). Stock solutions of malathion, acetylcholine, coenzyme A, magnesium chloride and ATP were prepared in deionized water without pH adjustment. The concentrations of ATP and coenzyme A were confirmed by UV/Vis spectroscopy using a molar extinction coefficients of 15,400 L/mol cm^{-1} at λ_{max} = 259 nm (37) and 14,328 L/mol cm^{-1} at λ_{max} = 258 nm (38), respectively. To ensure that the same conditions are used throughout the development and optimization of the method, and to avoid multiple freeze–thaw cycles, stock solutions were prepared in large volumes and subsequently aliquoted in small volumes and stored at −20°C with the exception of malathion, which was stored at 4°C. A commercial acetylcholinesterase assay kit (aCella™, AchE bioluminescence non-radioactive assay for monitoring acetylcholinesterase activity) was purchased from Cell Technology, Inc. (Mountain View, CA, USA).

Experimental design formulation

Experimental designs were created using The Unscrambler® version 9.2 (CAMO AS, Oslo, Norway). Screening designs were performed using Plackett–Burman designs from scratch with ten continuous design variables at two level values (see Table 1) and one nondesign (response) variable, which was set as malathion at 1, 5, 10 and 20 μM (initial concentration). For the experimental procedure, it was set at one replication

Table 1. Selected factors and the corresponding levels analyzed in Plackett–Burman and central composite designs

Factor	Levels				
Plackett–Burman design					
Acetylcholinesterase concentration (nM)	10	20		30	
Preincubation time (min)	2:30	5:00		7:30	
S-Acetyl-coenzyme A synthetase concentration (nM)	15	30		45	
Acetylcholine concentration (μM)	20	40		60	
Coenzyme A concentration (μM)	30	60		90	
ATP concentration (μM)	30	60		90	
Incubation time (min)	5	10		15	
Temperature of incubation (°C)	room	25		35	
Firefly luciferase concentration (nM)	10	15		20	
Firefly luciferin concentration (μM)	30	45		60	
Central composite design					
ATP concentration (μM)	17.5736	30	60	90	102.4264
Firefly luciferase concentration (nM)	7.9289	10	15	20	22.0711

per experiment, three centre (control) experiments and without randomization, with a total of twelve testing experiments plus the three control experiments. Optimization designs were performed using central composite designs from scratch with two continuous design variables at two level values (see Table 1) and one nondesign (response) variable, which was set as malathion at 5 μM (initial concentration). The star point distance from centre was settled at 1.41. For the experimental procedure, it was set at one replication per experiment, five centre experiments and without randomization, with a total of eight testing experiments plus the five control experiments.

Coupled bioluminescent assays

Screening and optimization designs. Bioluminescent assays were performed in a homemade luminometer using a photomultiplier tube (HCL35, Hamamatsu, Middlesex, New Jersey, USA) inside a light-tight dark chamber coupled to an automatic microburette (Crison MicroBU Model 2030, Crison Instruments, Barcelona, Spain) equipped with a 2.5-mL glass syringe (GASTIGHT® Syringes 1000 Series, Model 1002, Hamilton Bonaduz AG, Bonaduz, Switzerland). The stock solutions of reagents and enzymes were diluted in deionized water or Hepes buffer 0.5 M, pH 7.5, respectively, and kept on ice until use. Coupled reactions were performed in three steps (Fig. 2). The first, preincubation, was performed by adding 2 μL of acetylcholinesterase to 20 μL of malathion standards in 0.6-mL boil-proof microcentrifuge tubes and maintaining them at room temperature for the times and concentrations indicated in Table 1. Preincubation was stopped by transferring the tubes onto ice. The second step was the coupled reaction in which 2 μL of *S*-acetyl-coenzyme A synthetase was added to the acetylcholinesterase–malathion tubes, followed by the reaction mixture (3 mM magnesium chloride, ATP, coenzyme A and acetylcholine, at the concentrations indicated in Table 1, 4 μL each. Total volume added 16 μL, intermediate reaction volume 40 μL). Tubes were incubated at the temperatures and times indicated in Table 1. For temperatures other than room temperature, tubes were incubated in a water bath using an immersion thermostat (ET Basic Yellow Line, IMLAB, Boutersem, Belgium). The reaction was stopped by transferring the tubes onto ice. The third and final step consisted of the bioluminescent detection. To the mixture, 10 μL of firefly luciferase was added at the concentrations indicated in Table 1, the mixture was transferred to transparent test tubes, introduced into the dark chamber at room temperature and the baseline was recorded (t = 00:30 seconds, Fig. 2) at a integration interval of 0.1 s. At T = 1 minute, 50 μL of firefly luciferin, at the concentrations listed in Table 1, was injected from the automatic burette (final reaction volume 100 μL). The light output was recorded for another 30 s. Concentration values refer to the intermediate reaction volume for steps 1 and 2 and to the final reaction volume for step 3.

Optimized coupled assays. The optimized assays were performed as described above, using the following optimized conditions: 10 nM acetylcholinesterase, 2 min preincubation time, 15 nM *S*-acetyl-coenzyme A synthetase, 80 μM ATP;

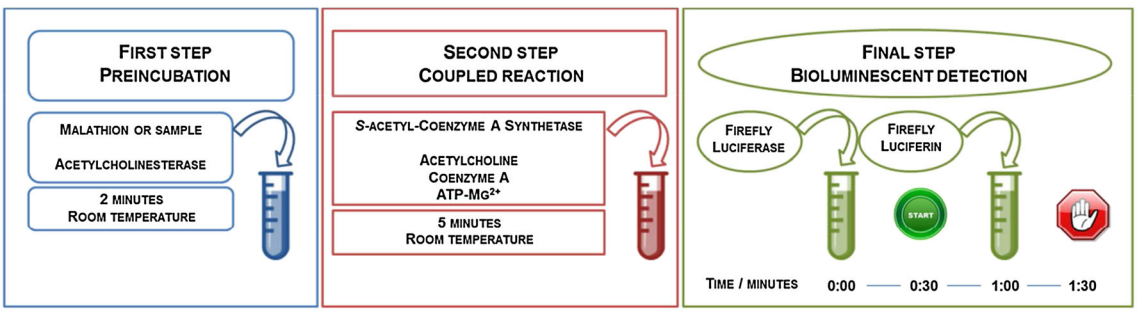

Figure 2. Schematic representation of the experimental steps of the optimized coupled bioluminescent assay.

30 μM coenzyme A; 20 μM acetylcholine; incubation at room temperature, 5 min reaction time, 10 nM firefly luciferase and 30 μM firefly luciferin. Magnesium chloride maintained a fixed concentration of 3 mM. Calibration curves were made using malathion standards from 0 to 25 μM (20 experimental points), to screen the linear range, and from 0 to 15 μM (six experimental points for each curve) to obtain figures of merit and samples' assays. To test the influence of malathion on firefly luciferase activity, malathion standards ranging from 1 to 150 μM were prepared in deionized water. Pure deionized water was used as a control. Twenty microliters of each standard was added to 20 μL of a reaction mixture containing ATP and magnesium chloride in the optimized concentrations. Bioluminescent detection was performed as in the final step of Fig. 2 using optimized concentrations of firefly luciferin and firefly luciferase.

Sample assay. Water was collected in polypropylene flasks from three domestic wells within the municipalities of Matosinhos (one well) and Maia (two wells), and stored at room temperature protected from light. Samples were assayed without any pretreatment under the conditions previously described. Using the method of standard additions, 20 μL aliquots of sample were added to 4 μL of malathion standard solutions from 0 to 15 μM (initial concentrations). The volumes of magnesium chloride, ATP, coenzyme A and acetylcholine were reduced to 3 μL each. For the spike-and-recovery assay, 20 μL of samples were spiked with 4 μL of malathion standards at 3, 9 and 15 μM and assayed as described above. A calibration curve was simultaneously made under the same conditions for 3–20 μM of malathion standards ($n = 5$). For the comparative kit assay, a calibration curve was set up with malathion standards from 0 to 15 μM. To 50 μL of either samples or malathion standards was added 50 μL of component A (which contains acetylcholinesterase), the mixture was transferred to transparent test tubes, introduced into the dark chamber at room temperature and preincubated for 2 min, at a intermediate reaction volume of 100 μL. After that, 50 μL of component B (which contains detection reagent, acetylcholine and coupled enzyme reaction) was injected from an automatic burette, at a final reaction volume of 150 μL. Baseline recording began at 1 min 30 s after the addition of component A and stopped 5 min after addition of component B. Integration time was set at 0.1 s.

Statistical analysis

Data obtained from the experimental designs were analyzed using The Unscrambler® software. For the screening designs (Plackett–Burman), an analysis of effect was performed. Results were expressed as an effects overview, using the significance testing methods higher order interaction effects (HOIE) and Center. For the optimization designs (central composite) a response surface analysis, which includes a two-way analysis of variance (ANOVA) table, residuals calculation and response surface, was applied. All those parameters were evaluated through the *F*-ratios and *p* values. Regarding the variables, the B coefficients and their corresponding standard errors were also taken into account. Residuals were evaluated through a normal probability plot. Linear regression was performed with a Microsoft® Excel® spreadsheet. Each experimental point corresponds to the peak of the bioluminescent signal, defined as the point when firefly luciferin is injected into the reaction mixture, from which the baseline, defined as the average of signal registered previously to the addition of firefly luciferin, was subtracted (Fig. 3 inset). Results were expressed as relative light units (RLU). From calibration curves set up using the method of least squares, the limits of detection (LOD) and quantitation (LOQ) were calculated using the following criteria: $LOD = (a + 3S_{y/x})$ and $LOQ = (a + 10S_{y/x})$, where a is the intercept of the calibration curves and $S_{y/x}$ is the random error in the y-direction (29). When the method of standard additions was used, the concentration of pesticide was given as the ratio between the intercept and the slope of the regression line. Recovery (R) was calculated using the expression:

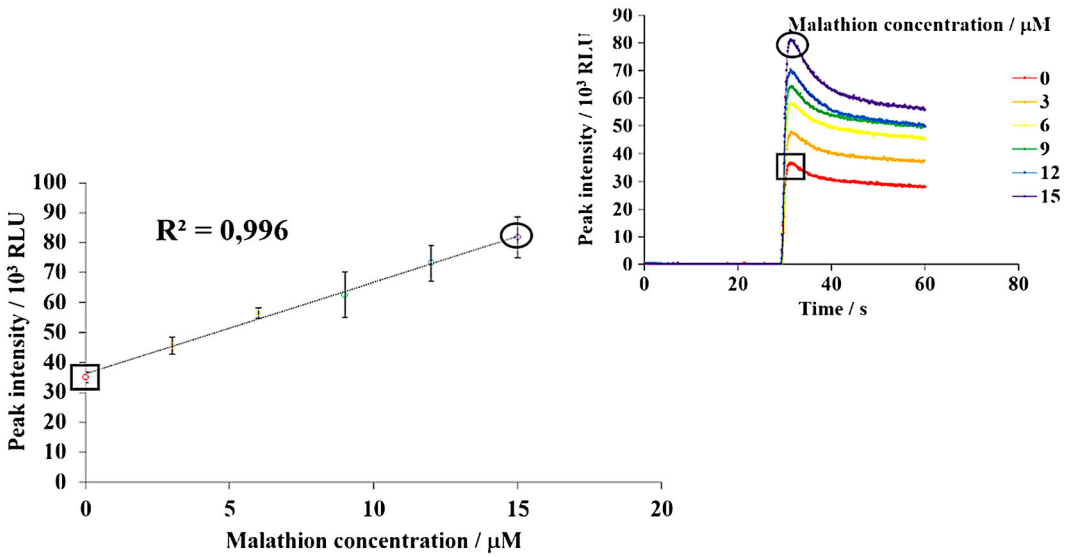

Figure 3. Typical calibration curve for malathion using the optimized coupled bioluminescent assay. (Inset) The corresponding raw luminogram, in which each of the peak maxima correspond to individual points in the calibration curve (see Experimental section). RLU, relative light units.

$$R(\%) = [(\text{Concentration of fortified sample} - \text{Concentration of sample}) / \text{Concentration of fortification}] \times 100.$$

To analyze statistically significant differences between firefly luciferase activity with or without malathion, one-way ANOVA and Student's *t*-test were performed (29). Results are expressed as pesticide concentration ± 95% confidence limits (95% CL) of the concentration ($n = 5$ for this assay and $n = 3$ for the kit assay) for the assay of pesticides in samples, or as mean ± standard deviation (SD) for recoveries values. A value of $p < 0.05$ was considered as statistically significant.

Results and discussion

Experimental designs

The overall optimization process included two steps, screening to identify which factors have statistically the most influence on the method's response and the subsequent determination of the levels at which these factors must be kept to optimize the method's response. Taking into account the various reagents and steps in the method, 10 factors were selected for screening and, to keep the number of experiments to a minimum, a Plackett–Burman design was selected (Table 1). The concentrations of the factors were selected by considering time and solubility constraints and to conserve the most expensive reagents, specifically the enzymes. After the experiments were performed the results showed that, in the presence of 5 μM malathion and using the testing method Center, the concentrations of ATP and firefly luciferase were likely the most significant factors (see Table S1). Using the significance testing method HOIE none of the factors were considered significant (Table S1).

With this information, a central composite optimization design was established to uncover the best ATP and firefly luciferase concentrations, and to determine if their interactions are also important for the method's response, which was not possible with the previous design. The remaining factors were kept to their most convenient values, in this case the lowest values of concentration, the shortest times of preincubation and incubation and the performing of the assay at room temperature. From the ANOVA table (Table 2) it was confirmed that ATP and firefly luciferase concentrations are important factors, showing significant *F*-ratios ($p < 0.05$) and presenting standard errors of the regression coefficient lower than the regression coefficient itself. Besides, the interaction ATP vs. firefly luciferase (A-B in Table 2) and the quadratic response firefly luciferase × firefly luciferase (BB in Table 2) are also significant. According to their *F*-ratios, the model is significant, whereas the lack of fit is not ($p < 0.05$ and $p > 0.05$, respectively), which shows that the experimental measurements fit the model. Finally, a normal probability plot of the residues showed that they lie along a straight line, meaning that there are no outliers (Fig. S1). The response surface curve (Fig. 4) shows that the concentrations of ATP and firefly luciferase should be kept at the highest values tested to obtain the maximum bioluminescent signal. However, although higher concentrations of firefly luciferase are desirable whenever high sensitivity is needed, it also raises the cost of the assay. Taking that into consideration, the concentrations of both ATP and firefly luciferase were set to the saddle values

Table 2. Analysis of variance (ANOVA) for the central composite optimization design

	SS	df	MS	*F*-ratio	*p*	*B* coefficient	SE_b	Saddle point
Summary								
Model	6.746×10^{10}	5	1.349×10^{10}	45.924	0.0000			
Error	2.057×10^{9}	7	2.938×10^{8}					
Adjusted Total	6.952×10^{10}	12	5.793×10^{9}					
Variable								
Intercept	8.214×10^{10}	1	8.214×10^{10}	279.601	0.0000	1.282×10^{5}	7.665×10^{3}	
ATP (A)	3.254×10^{10}	1	3.254×10^{10}	110.755	0.0000	2.126×10^{3}	201.999	79.026
Firefly luciferase (B)	2.588×10^{10}	1	2.588×10^{10}	88.084	0.0000	1.137×10^{4}	1.212×10^{3}	6.687
AB	4.627×10^{9}	1	4.627×10^{9}	15.750	0.0054	2.267×10^{4}	5.713×10^{3}	
AA	2.257×10^{8}	1	2.257×10^{8}	0.768	0.4098	-3.798×10^{3}	4.332×10^{3}	
BB	3.871×10^{9}	1	3.871×10^{9}	13.177	0.0084	1.573×10^{4}	4.332×10^{3}	
Model Check								
Main	5.842×10^{10}	2	2.921×0^{10}	15.750	0.0054			
Int	4.627×10^{9}	1	4.627×10^{9}	7.516	0.0181			
Int + Squ	4.416×10^{9}	2	2.208×10^{9}	7.516	0.0181			
Squ	4.416×10^{9}	2	2.208×10^{9}					
Error	2.057×10^{9}	7	2.938×10^{8}					
Lack of Fit								
Lack of Fit	8.783×10^{8}	3	2.928×10^{8}	0.994	0.4810			
Pure Error	1.178×10^{9}	4	2.946×10^{8}					
Total Error	2.057×10^{9}	7	2.938×10^{8}					

SS, Sum of Squares; df, degrees of freedom; MS, Mean Squares (ratio between SS and df); *F*-ratio, ratio between 'between-measurements' MS and 'within-measurements' (residual) MS; *p*, probability of getting the *F*-ratio under the null hypothesis at 95%; B coefficient, regression coefficient from a multiple linear regression analysis; SE_b, standard error of b.

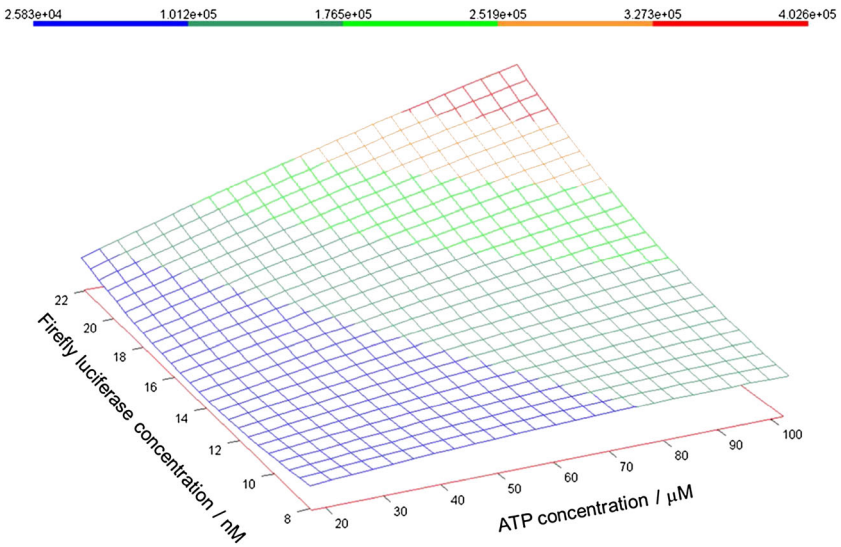

Figure 4. Response surface landscape plot for the most important method's factors, ATP and firefly luciferase concentrations, tested in a central composite design.

suggested by the ANOVA table rounded up, that is 80 μM and 10 nM, respectively.

Method figures of merit

Using the optimized conditions, the coupled bioluminescent assay was characterized in terms of linear range, LOD and LOQ and precision at several concentrations of malathion standards.

The linear response interval was obtained through calibration curves with malathion standards. Because no previous information was available for this interval, calibration curves with a relatively broad concentration range, 0–25 μM of malathion, were tested. It was verified that below 1 μM and above 15 μM malathion the signals were not proportional to the malathion concentration (data not shown). Below 1 μM the concentration of malathion may be too low to quantitatively inhibit acetylcholinesterase using the method's optimized conditions, and above 15 μM there is saturation, since the increase in malathion concentration leads to a constant signal. In the 1–15 μM malathion range the response was directly proportional to the concentration of the standards. Calibration curves covering only this interval were obtained and the results were confirmed. From these calibration curves (Fig. 3), the linear range was settled from 2.5 to 15 μM malathion. Using also calibration curves, the LOD and LOQ were calculated as 1.5 and 5.0, respectively (r^2 varying from 0.989 to 0.996, average of three independent measurements, see Experimental section). The precision of the method was estimated from relative standard deviation, and showed values of 3.8% at 3 μM malathion, 7.4% at 6 μM malathion and 5.1% at 15 μM malathion (average of two independent experiments, each concentration value measured in triplicate).

The inhibitory effect of malathion on firefly luciferase activity was tested. The bioluminescent reaction catalyzed by firefly luciferase will produce the detected signal, therefore it is important to assure that it will not be affected. The results showed that, using the optimized conditions, no statistically significant (at the significant level of 5%) inhibitory effect was observed (Fig. S2).

Sample assay

Water collected from residential wells within the Metropolitan Area of Porto was assayed for the presence of organophosphorus pesticides using this new optimized method. The results showed that the malathion content is below either the LOD or LOQ (data not shown). To confirm that the method is capable of detecting pesticides in contaminated samples, a spike-and-recovery assay was performed, the results of which are presented in Table 3. Good recoveries were obtained, with average values above 80%.

The same samples were tested using a commercial acetylcholinestease assay kit and the results are in good agreement with the optimized method.

To assess the possible interference of the matrix, samples were also assayed by the method of standard additions. No interferences were found (data not shown).

It is important to highlight that, although the method was developed using malathion, in real samples other pesticides may be present in the same sample. The method is based on the inhibition of acetylcholinesterase and, in this sense, it is specific for any pesticide able to inhibit acetylcholinesterase, namely organophosphorus. Other pesticides, even at higher concentrations, would not interfere with the assay if they cannot inhibit acetylcholinesterase. However, if the sample contains several different organophosphorus pesticides, the method will respond, but will be unable to quantify each separately. In this case, and if needed, other techniques, like chromatographic separation, should be employed following the bioluminescence assay.

Table 3. Spike-and-recovery of malathion standards in well water samples

Sample	Low spike (3 μM)	Medium spike (9 μM)	High spike (15 μM)
Matosinhos well	87.0	86.1	101.7
Maia well #1	85.7	89.6	91.6
Maia well #2	75.7	87.6	83.4
Mean recovery (± SD)	82.8 ± 6.2	87.8 ± 1.8	92.2 ± 9.2

Conclusions

This paper presented the establishment and optimization of a coupled bioluminescent assay for organophosphorus pesticides.

The significance of this works stands in its portability and its optimization through statistical experimental design methodology.

Instrumental methods such as chromatography and electrophoresis have high sensitivity and the possibility of high-throughput analysis, but may be time-consuming, not suitable for the *in situ* evaluation of samples, and demand specialized apparatus and personnel training. In the case of assays employing nanomaterials, there is the risk of toxicity, as suggested by several studies. Enzymatic assays have the advantages of being sensitive and specific, but may become expensive if large volumes of enzyme are necessary, or when commercial kits are to be used. Furthermore, to the best of our knowledge, few of these methods were subjected to optimization. Experimental design methodology makes it possible to determine the variables needed to obtain the most sensitive and robust method, requesting a relatively small number of experiments to achieve it. In fact, using optimized conditions, even small deviations from the optimal values will not seriously affect the response. The optimized method, relying on the acetylcholinesterase-catalyzed reaction, is also specific towards organophosphorus pesticides, safe, simple to perform and economic, despite the use of several enzymes and reagents, because of their reduced volumes. Although the volumes of reagents and the reaction mixture were not proposed for optimization because since they were considered adequate already, users can still adapt them to their needs, for example, if too little sample is available.

The portability of the method is due to the fact that it does not require any sample pretreatment, uses low volumes of both sample and reagents, all reagents and a portable luminometer are commercially available, the reagents do not need further purification prior to use and their solutions are stable for several months when stored at −20°C and also stable at room temperature. Although we used a single-tube luminometer, the method is also suitable for multiplate assays, thus allowing the simultaneous testing of several samples. One major disadvantage of this method is its relatively reduced sensitivity, in the order of μM. This, however, is adequate for the proposed application, that is, the *in situ* analysis of organophosphorus pesticides in freshwater. Furthermore, the loss in sensitivity is compensated for by the other features, such as simplicity and reduced costs. If necessary, more sensitive assays may be performed in the laboratory. Finally, the validation with water from domestic wells confirmed the applicability of the method to real samples.

Supporting Information

Supporting Information may be found in the online version of this article.

Figure S1. Normal probability plot of the residuals of the central composite optimization design.

Figure S2. Evaluation of the inhibitory effect of malathion on firefly luciferase activity. RLU, relative light units.

Table S1. HOIE and Center significance testing methods results for the Plackett–Burman screening designs at several malathion levels.

Acknowledgements

SM Marques wishes to thank her PhD scholarship (reference SFRH/BD/65109/2009), co-funded by the European Social Fund (Fundo Social Europeu, FSE), through Quadro de Referência Estratégico Nacional-Programa Operacional Potencial Humano (QREN-POPH), and by national funds from the Ministry of Education and Science through the Portuguese Fundação para a Ciência e a Tecnologia (FCT).

References

1. Costa LG. Current issues in organophosphate toxicology. Clin Chim Acta 2006;366:1–13.
2. International Programme on Chemical Safety (IPCS). Hamilton: The Canadian Centre for Occupational Health and Safety, International Programme on Chemical Safety (IPCS), 1996. http://www.inchem.org/documents/pims/chemical/pimg001.htm [updated September 2012; accessed 7 January 2013].
3. Guyton AC, Hall JE. *Textbook of medical physiology*. 11th ed. Beijing: Elsevier Saunders, 2006.
4. Glare T, Caradus J, Gelernter W, Jackson T, Keyhani N, Köhl J et al. Have biopesticides come of age? Trends Biotechnol 2012;30:250–8.
5. The European Commission. Commission Directive 2010/17/EU, of 9 March 2010. Off J Eur Union 2010;53:17–9.
6. Pinheiro AS, Andrade JB. Development, validation and application of a SDME/GC-FID methodology for the multiresidue determination of organophosphate and pyrethroid pesticides in water. Talanta 2009;79:1354–9.
7. Samadi S, Sereshti H, Assadi Y. Ultra-preconcentration and determination of thirteen organophosphorus pesticides in water samples using solid-phase extraction followed by dispersive liquid–liquid microextraction and gas chromatography with flame photometric detection. J Chromatogr A 2012;1219:61–5.
8. Buonasera K, D'Orazio G, Fanali S, Dugo P, Mondello L. Separation of organophosphorus pesticides by using nano-liquid chromatography. J Chromatogr A 2009;1216:3970–6.
9. Wang C, Wu Q, Wu C, Wang Z. Determination of some organophosphorus pesticides in water and watermelon samples by microextraction prior to high-performance liquid chromatography. J Sep Sci 2011;34:3231–9.
10. García-Valcárcel AI, Tadeo JL. A combination of ultrasonic assisted extraction with LC-MS/MS for the determination of organophosphorus pesticides in sludge. Anal Chim Acta 2009;641:117–23.
11. Liang Y, Wang W, Shen Y, Liu Y, Liu XJ. Effects of home preparation on organophosphorus pesticide residues in raw cucumber. Food Chem 2012;133:636–40.
12. Mao X, Wan Y, Yan A, Shen M, Wei Y. Simultaneous determination of organophosphorus, organochlorine, pyrethriod and carbamate pesticides in Radix astragali by microwave-assisted extraction/dispersive-solid phase extraction coupled with GC–MS. Talanta 2012;97:131–41.
13. Rhouati A, Istamboulie G, Cortina-Puig M, Marty J-L, Noguer T. Selective spectrophotometric detection of insecticides using cholinesterases, phosphotriesterase and chemometric analysis. Enzyme Microb Technol 2010;46:212–6.
14. Xu Z-L, Wang Q, Lei H-T, Eremin SA, Shen Y-D, Wang H et al. A simple, rapid and high-throughput fluorescence polarization immunoassay for simultaneous detection of organophosphorus pesticides in vegetable and environmental water samples. Anal Chim Acta 2011;708:123–9.
15. Xu Z-L, Deng H, Deng X-F, Yang J-Y, Jiang Y-M, Zeng D-P et al. Monitoring of organophosphorus pesticides in vegetables using monoclonal antibody-based direct competitive ELISA followed by HPLC–MS/MS. Food Chem 2012;131:1569–76.
16. Pohanka M, Karasova JZ, Kuca K, Pikula J, Holas O, Korabecny J et al. Colorimetric dipstick for assay of organophosphate pesticides and nerve agents represented by paraoxon, sarin and VX. Talanta 2010;81:621–4.
17. Andreescu S, Marty J-L. Twenty years research in cholinesterase biosensors: from basic research to practical applications. Biomol Eng 2006;23:1–15.

18. Mishra RK, Dominguez RB, Bhand S, Muñoz R, Marty J-L. A novel automated flow-based biosensor for the determination of organophosphate pesticides in milk. Biosens Bioelectron 2012;32:56–61.
19. Liu D, Chen W, Wei J, Li X, Wang Z, Jiang X. A highly sensitive, dual-readout assay based on gold nanoparticles for organophosphorus and carbamate pesticides. Anal Chem 2012;84:4185–91.
20. Zeng Y, Yu D, Yu Y, Zhou T, Shi G. Differential pulse voltammetric determination of methyl parathion based on multiwalled carbon nanotubes–poly(acrylamide) nanocomposite film modified electrode. J Hazard Mater 2012;217–218:315–22.
21. Du D, Chen W, Zhang W, Liu D, Li H, Lin Y. Covalent coupling of organophosphorus hydrolase loaded quantum dots to carbon nanotube/Au nanocomposite for enhanced detection of methyl parathion. Biosens Bioelectron 2010;25:1370–5.
22. Lapresta-Fernández A, Fernández A, Blasco J. Nanoecotoxicity effects of engineered silver and gold nanoparticles in aquatic organisms. Trends Anal Chem 2012;32:40–59.
23. Sharifi S, Behzadi S, Laurent S, Forrest ML, Stroeve P, Mahmoudi M. Toxicity of nanomaterials. Chem Soc Rev 2012;41:2323–43.
24. Corey MJ. *Coupled bioluminescent assays – Methods, evaluations, and applications*. Hoboken, NJ: Wiley, 2009.
25. Rusness DG, Still GG. Firefly luciferase inhibition by isopropyl-3-chlorocarbanilate and isopropyl-3-chloro-hydroxycarbanilate analogues. Pestic Biochem Physiol 1974;4:109–19.
26. Trajkovska S, Tosheska K, Aaron JJ, Spirovski F, Zdravkovski Z. Bioluminescence determination of enzyme activity of firefly luciferase in the presence of pesticides. Luminescence 2005;20:192–6.
27. Leitão JMM, Esteves da Silva JCG. Firefly luciferase inhibition. J Photochem Photobiol B 2010;101:1–8.
28. Antony J. *Design of experiments for engineers and scientists*. Oxford: Elsevier Butterworth-Heinemann, 2003.
29. Miller JN, Miller JC. *Statistics and chemometrics for analytical chemistry*. 5th ed. Gosport: Pearson Prentice Hall, 2005.
30. Schomburg I, Chang A, Schomburg D. BRENDA, enzyme data and metabolic information. Nucleic Acids Res 2002;30:47–9.
31. BRENDA. The comprehensive enzyme information system. Braunschweig: Institute of Biochemistry and Bioinformatics, Technical University of Braunschweig, 2013. http://www.brenda-enzymes.org [updated July 2012; accessed 7 January 2013].
32. The UniProt Consortium. Reorganizing the protein space at the Universal Protein Resource (UniProt). Nucleic Acids Res 2012;40: D71–5.
33. The Universal Protein Resource (UniProt). Cambridge/Geneva/Washington, DC: European Bioinformatics Institute/Swiss Institute of Bioinformatics/Protein Information Resource; 2002–2013. http://www.uniprot.org/ [accessed 7 January 2013].
34. Gasteiger E, Gattiker A, Hoogland C, Ivanyi I, Appel RD, Bairoch A. ExPASy: the proteomics server for in-depth protein knowledge and analysis. Nucleic Acids Res 2003;31:3784–8.
35. ExPASy Bioinformatics Resource Portal. Geneva: Swiss Institute of Bioinformatics, 2012. http://www.expasy.org/ [updated April 2012; accessed 7 January 2013].
36. Bowie LJ. Synthesis of firefly luciferin and structural analogs. Methods Enzymol 1978;57:15–28..
37. Bock RM, Ling N-S, Morell SA, Lipton SH. Ultraviolet absorption spectra of adenosine-5′-triphosphate and related 5′-ribonucleotides. Arch Biochem Biophys 1956;62:253–64.
38. Giljanović J, Prkić A. Determination of coenzyme A (CoASH) in the presence of different thiols by using flow-injection with a UV/Vis spectrophotometric detector and potentiometric determination of CoASH using an iodide ISE. Molecules 2010;15:100–13.

Quantitative analysis of organophosphorus pesticides in freshwater using an optimized firefly luciferase-based coupled bioluminescent assay

SM Marques and JCG Esteves da Silva

SUPPORTING INFORMATION

Table S1. HOIE and Center significance testing methods results for the Plackett-Burman screening designs at several malathion levels

	Malathion 1 μM		Malathion 5 μM		Malathion 10 μM		Malathion 20 μM	
	HOIE*	Center	HOIE	Center	HOIE	Center	HOIE	Center
Acetylcholinesterase concentration	NS	NS	NS	NS	NS	NS	NS	NS
Preincubation time	NS	NS	NS	NS	NS	NS	NS	NS
S-Acetyl-coenzyme A synthetase concentration	NS	NS	NS	NS	NS	NS	NS	NS
Acetylcholine concentration	NS	NS	NS	NS	NS	NS	NS	NS
Coenzyme A concentration	NS	NS	NS	NS	NS	NS	NS	NS
ATP concentration	NS	NS	NS	+	NS	NS	NS	NS
Incubation time	NS	NS	NS	NS	NS	NS	NS	NS
Temperature of incubation	NS	NS	NS	NS	NS	NS	NS	NS
Firefly luciferase concentration	NS	NS	NS	+	NS	NS	NS	NS
Firefly luciferin concentration	NS	NS	NS	NS	NS	NS	NS	NS

*HOIE, Higher Order Interaction Effects

Significance of each effect at 95% level: NS, not significant; from + to +++, positive effect; from - to - - -, negative effect

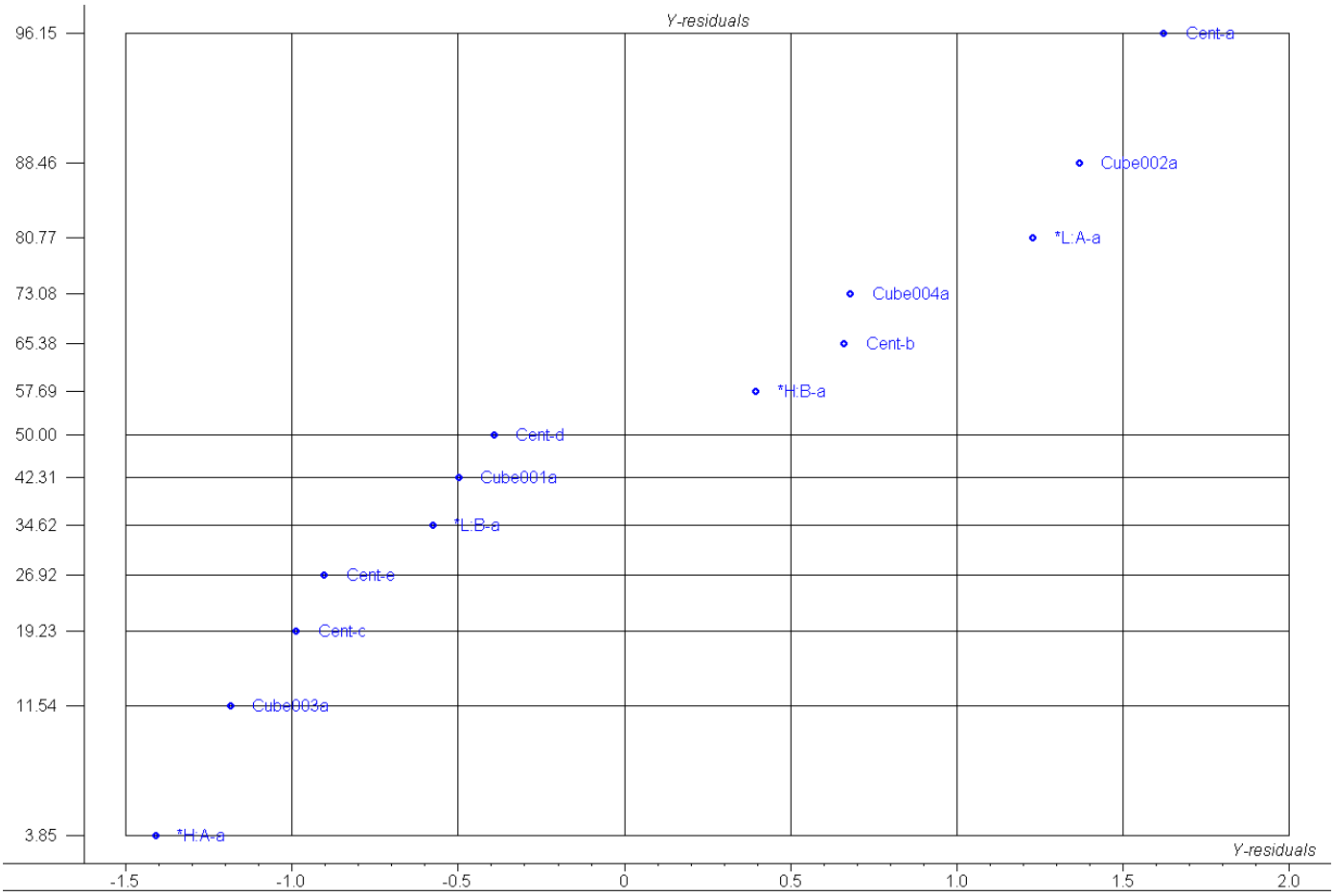

Figure S1. Normal probability plot of the residuals of the Central Composite optimization design.

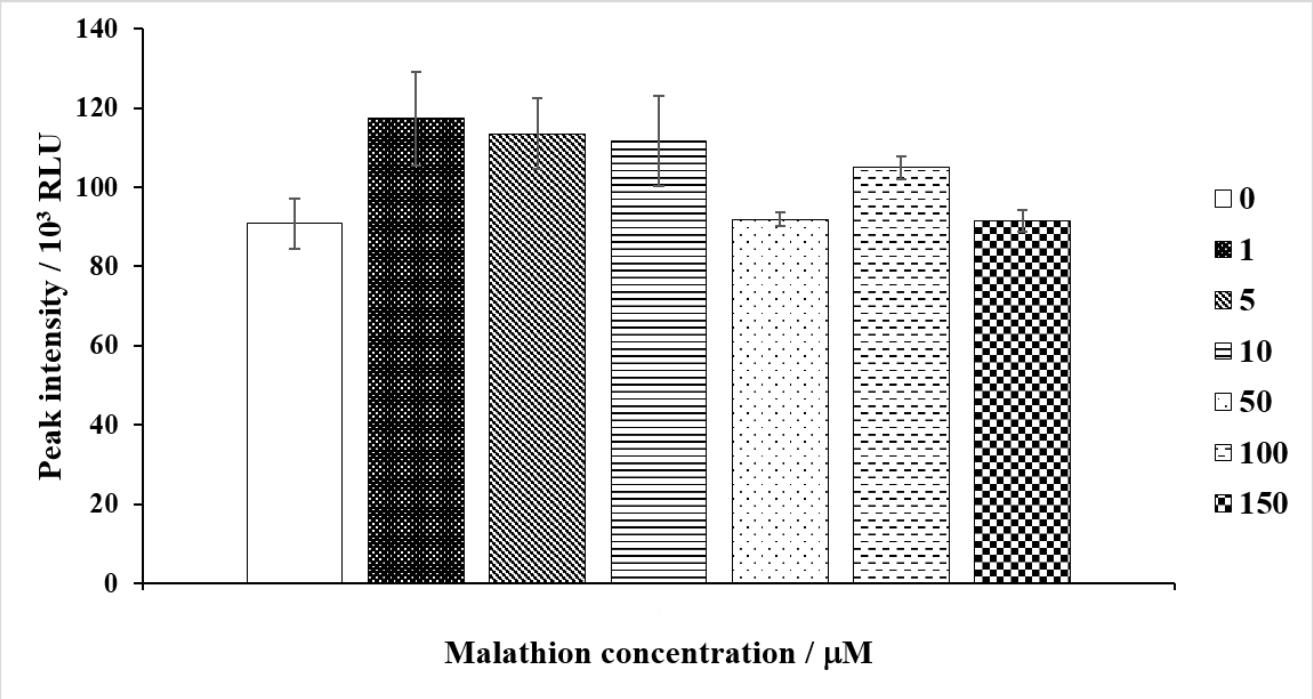

Figure S2. Evaluation of the inhibitory effect of malathion on firefly luciferase activity. RLU, Relative Light Units.

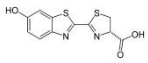

Chapter three

An optimized bioluminescent assay for inorganic sulfate quantitation in freshwater

Simone M. Marques, Joaquim C.G. Esteves da Silva

Anal. Methods 5 (2013) 1317-1327

The scientific work leading to this paper was integrally performed within the host institution, the Chemometric Research of Chemical, Environmental, Forensic and Biological Systems group, from the Chemistry Research Center of the University of Porto (*Centro de Investigação em Química da Universidade do Porto*, *CIQ-UP*), Department of Chemistry and Biochemistry, Faculty of Sciences, University of Porto. Simone Marques was responsible for bibliographic search, protocols set up, experimental execution, data treatment and paper writing, under the supervision of Joaquim Esteves da Silva.

Analytical Methods

RSC Publishing

PAPER

View Article Online
View Journal | View Issue

An optimized bioluminescent assay for inorganic sulfate quantitation in freshwater†

Cite this: *Anal. Methods*, 2013, **5**, 1317

Simone M. Marques and Joaquim C. G. Esteves da Silva*

In this paper an optimized enzymatic assay for inorganic sulfate (SO_4^{-2}) detection and quantitation in freshwater, relying on adenosine-5′-triphosphate sulfurylase catalyzed reaction coupled to bioluminescent detection by firefly luciferase, is described. Inorganic sulfate is converted, by adenosine-5′-triphosphate sulfurylase, into adenosine-5′-phosphosulfate and inorganic pyrophosphate, with consumption of adenosine-5′-triphosphate. The remaining adenosine-5′-triphosphate is used as a co-factor in the reaction catalyzed by firefly luciferase generating, as a co-product, photons of visible light. The light output is inversely proportional to the inorganic sulfate content. Using sodium sulfate as a model, the assay was optimized through a statistical experimental design methodology and validated in water samples from domestic wells from two municipalities within the Metropolitan Area of Porto plus tap water as control. The optimized method requires 20 μL of sample in a final reaction volume of 100 μL. It is linear in the range from 14 to 134 mg L^{-1} of inorganic sulfate, with limits of detection and quantitation of 10 and 34 mg L^{-1}, respectively. Repeatability, expressed as relative standard deviation, is 7.23% at 34 mg L^{-1}, 6.87% at 68 mg L^{-1} and 4.67% at 96 mg L^{-1}. The inorganic sulfate concentration in the wells is approximately 124, 182 and 182 mg L^{-1}, whereas it was found to be a value of about 200 mg L^{-1} in tap water. Samples can be quantified by calibration curves without any pre-treatment other than dilution. The optimized method is fast, simple to perform and robust.

Received 23rd October 2012
Accepted 9th January 2013

DOI: 10.1039/c3ay26255c

www.rsc.org/methods

Introduction

Firefly luciferase [*Photinus*-luciferin: oxygen 4-oxidoreductase (decarboxylating, adenosine-5′-triphosphate-hydrolysing)], from the North-American firefly species *Photinus pyralis*, catalyzes the conversion of its natural substrate, firefly D-luciferin, in the presence of adenosine-5′-triphosphate complexed with magnesium ions (ATP-Mg^{2+}) and molecular oxygen (O_2) into oxyluciferin and the by-products adenosine-5′-monophosphate (AMP), inorganic pyrophosphate (PPi), carbon dioxide (CO_2) and photons of visible light (eqn (1)).[1]

$$\text{D-Luciferin} + \text{ATP–Mg}^{2+} + \text{O}_2 \xrightarrow{\text{luciferase}} \text{oxyluciferin} + \text{AMP–Mg}^{2+} + \text{PPi–Mg}^{2+} + \text{CO}_2 + \text{photon} \quad (1)$$

Firefly luciferase is an invaluable tool in bioanalytical chemistry, either in single reactions, for example as a reporter gene or in quantifying analytes which direct or indirectly participate in the bioluminescent reaction, such as ATP and coenzyme A, or coupled to other enzymes whose reactions generate or consume ATP, a method called coupled bioluminescent assay.[2] Such an example of this coupling is the enzymatic luminometric inorganic pyrophosphate detection assay (ELIDA)[3] for the quantitation of inorganic pyrophosphate. It relies on the conversion, by adenosine-5′-triphosphate sulfurylase, of adenosine-5′-phosphosulfate (APS) and inorganic pyrophosphate into inorganic sulfate (SO_4^{-2}) and ATP (eqn (2)). The produced ATP is then consumed in the bioluminescent reaction (eqn (1)).

$$\text{APS} + \text{PPi–Mg}^{2+} \xleftrightarrow{\text{ATP sulfurylase}} \text{SO}_4^{2-} + \text{ATP–Mg}^{2+} \quad (2)$$

ELIDA is also the base of Pyrosequencing®,[4,5] a method for real-time sequencing of DNA[6] and DNA-related products,[7] since the formation of new nucleic acid chains releases inorganic pyrophosphate.

In this paper an optimized bioluminescent method for sulfate quantitation in freshwater, relying on the enzymes adenosine-5′-triphosphate sulfurylase and firefly luciferase, is presented. The method is based on the reverse of eqn (2) (eqn (3)). The remaining ATP is used in the reaction catalyzed by firefly luciferase (eqn (4)). Thus, the more sulfate in the sample, the greater is the ATP consumption, and lower is the light output.

$$\text{SO}_4^{2-} + \text{ATP–Mg}^{2+} \xleftrightarrow{\text{ATP sulfurylase}} \text{APS} + \text{PPi–Mg}^{2+} \quad (3)$$

Centro de Investigação em Química da Universidade do Porto (CIQ-UP), Department of Chemistry and Biochemistry, Faculty of Sciences, University of Porto, Rua do Campo Alegre, no. 687, 4169-007 Porto, Portugal. E-mail: jcsilva@fc.up.pt; Fax: +351 220 402 659; Tel: +351 220 402 569

† Electronic supplementary information (ESI) available. See DOI: 10.1039/c3ay26255c

$$\text{D-Luciferin} + \text{remaining ATP–}Mg^{2+} + O_2 \xrightarrow{\text{luciferase}} \text{light output proportional to ATP} \quad (4)$$

The World Health Organization, through the publication 'International Standards for Drinking-Water' in 1958, proposed sulfate concentration limits between 200 and 400 mg L^{-1}, or between 500 and 1000 mg L^{-1} if magnesium and sodium sulfate coexist in a sample.[8] In this document, sulfate was considered as a chemical which may affect the potability of water, but it is not dangerous or toxic. By its turn, the European Union, through the Council Directive 98/83/EC, of November 3rd 1998, proposed the monitoring of sulfate with a parametric value of 250 mg L^{-1}.[9] This Directive was transposed into the Portuguese national Law in 2001[10] and revised in 2007.[11] In its more recent report, 'Guidelines for Drinking-Water Quality', the World Health Organization confirmed that sulfate is 'not of health concern at levels found in drinking water'.[12] It is also mentioned, however, that some people reported a noticeable or even unpleasant taste when sulfate is present at concentrations above 250 mg L^{-1}, as well as laxative effects above 1000 mg L^{-1}, especially in the sensitive sub-population such as the elderly, children and travelers.

Inorganic sulfate levels in water depend on several factors, such as the geographical location and the type of water reservoir (groundwater, rivers and lakes, among others). Values of 0 to 230 mg L^{-1} sulfate in groundwater are reported.[13] Another study reported Finnish deep (213–891 m) groundwater sulfate levels between 2.27 and 795 mg L^{-1}, but no correlation was found between the depth and sulfate level.[14] In the Metropolitan Area of Porto, for example, the average groundwater sulfate content ranges between 5 and 30 mg L^{-1}.[15] Although tap water is subjected to regulation, other non-tested common water sources may expose the users to high levels of sulfate. For instance, wells are a source of drinking water in Portugal, especially in less urbanized areas, and in many developing countries as well.

The analytical methods available for sulfate quantitation are based on gravimetry,[16] volumetry,[17,18] potentiometry,[19] spectrophotometry/turbidimetry,[20–23] ion chromatography[24–26] and capillary[14,27] and microchip electrophoresis.[28] In line with the recent evolution in nanomaterials, a colorimetric assay using gold nanoparticles capped with cysteamine was proposed.[29] Bioluminescent assays for sulfate are also described, for example a whole-cell biosensor using non-bioluminescent bacteria engineered with the bacterial luciferase gene cassette *luxCDABE* from *Photorhabdus luminescens*[30] or the photoprotein aequorin genetically split into two fragments and attached to a sulfate binding protein.[31] When sulfate binds to the protein, the two fragments come together, and light is emitted.

Instrumental methods such as chromatography and electrophoresis have high sensitivity and the possibility of high-throughput analysis, but may be time-consuming, not prone to *in situ* evaluation of samples, and demand specialized apparatus and personnel training. In the case of assays employing nanomaterials, there is the risk of their toxicity, as suggested by several studies.[32] Enzymatic assays have the advantages of being sensitive and specific, but may become expensive if large volumes of enzymes are necessary, or when commercial kits are to be used. Furthermore, to the best of our knowledge, few of these methods were subjected to optimization. By using this methodology, with a relatively small number of experiments, it is possible to determine the variables which must be taken into account to obtain the most sensitive and robust method. In fact, using the optimized conditions, even small deviations from the optimal values will not seriously affect the response.

Using sodium sulfate as a model, the assay was optimized through a statistical experimental design methodology and validated in water samples from domestic wells from two municipalities within the Metropolitan Area of Porto plus tap water as control, which rendered a fast, simple to perform and robust method.

Experimental

Chemicals and reagents

The enzymes (see Table 1) and the reagents 4-(2-hydroxyethyl) piperazine-1-ethanesulfonic acid (HEPES, Product Code H3375), ATP disodium salt hydrate (from bacterial source, Product Code A2383) and firefly D-luciferin (synthetic firefly D-luciferin free acid, Product Code L9504) were purchased from Sigma (Steinheim, Germany). Magnesium chloride hexahydrate (Product Code 63064) was purchased from Fluka (Buchs, Switzerland) and sodium sulfate was obtained from Pronalab (Lisbon, Portugal).

All reagents were used without further purification. Stock solutions of the enzymes were prepared by dissolving the whole content of the flasks in HEPES buffer 0.5 M, pH 7.5. Concentrations were checked by ultraviolet-visible spectroscopy considering the molar extinction coefficient and molar masses in Table 1. Molar mass values were calculated using the information from the BRENDA database[33,34] and the Universal Protein Resource (UniProt).[35,36] The values of molar extinction coefficients were calculated using the ProtParam tool (protein physical and chemical parameters) from the ExPASy Proteomics

Table 1 Commercial and physico-chemical properties of the enzymes used in the bioluminescent method for sulfate quantitation in freshwater

Enzyme	Source	EC	Product code	Lot	Molar extinction coefficient/L mol^{-1} cm^{-1} (λ_{max} = 280 nm)	Molar mass/ g mol^{-1}	References
Firefly luciferase	*Photinus pyralis*	1.13.12.7	L9506	060M7400	39 310	60 745	33–38
ATP sulfurylase	*Saccharomyces cerevisiae*	2.7.7.4	A8957	129K7680V	367 860	346 257	
Inorganic pyrophosphatase	*Saccharomyces cerevisiae*	3.6.1.1	I1891	057K8618	98 780	64 581	

Server.[37,38] Molar mass values were also confirmed using this software.

HEPES was prepared by dissolving the corresponding mass in deionized water, and the pH was adjusted to 7.5 using 10 mM sodium hydroxide solution. A stock solution of ATP was prepared in deionized water and the concentration was confirmed by ultraviolet-visible spectroscopy using a molar extinction coefficient of 15 400 L mol^{-1} cm^{-1} at $\lambda_{max} = 259$ nm.[39] Stock solutions of magnesium chloride were prepared in deionized water without pH adjustment. Firefly D-luciferin stock solutions were prepared in deionized water with intense stirring for about 1 hour protected from the air and light. The concentration was confirmed by ultraviolet-visible spectroscopy using a molar extinction coefficient of 18 200 L mol^{-1} cm^{-1} at $\lambda_{max} = 327$ nm.[40] Finally, for the preparation of sodium sulfate stock solutions, the salt was previously heated in an oven at 100 °C for 12 hours, then transferred to a desiccator filled with cobalt(II) chloride until it cooled to room temperature and the corresponding mass was weighed and dissolved in deionized water.

All the stock solutions were aliquoted in small volumes and stored at −20 °C.

Experimental design formulation

Experimental designs were created using The Unscrambler® version 9.2 (CAMO AS, Oslo, Norway) and performed according to Scheme 1.

Bioluminescent assays

Preliminary studies. Bioluminescent assays were performed in a homemade luminometer using a photomultiplier tube (HCL35, Hamamatsu, Middlesex, USA) inside a light-tight dark chamber coupled to an automatic microburette (Crison MicroBU Model 2030, Crison Instruments, Barcelona, Spain) equipped with a 2.5 mL glass syringe (GASTIGHT® Syringes 1000 Series, Model 1002, Hamilton Bonaduz AG, Bonaduz, Switzerland).

The stock solutions of reagents and enzymes were diluted in deionized water or HEPES buffer, 0.5 M, pH 7.5, respectively, and kept in ice until use. Assays were performed according to Scheme 2.

To test the influence of sodium sulfate on firefly luciferase, sodium sulfate standards ranging from 0 to 96 mg L^{-1} were prepared and assayed in triplicate. Deionized water was used as control and adenosine-5′-triphosphate sulfurylase was replaced by deionized water. To test the influence of the enzymes adenosine-5′-triphosphate sulfurylase and inorganic pyrophosphatase on firefly luciferase, the following mixtures were prepared: 2 μL deionized water plus 2 μL adenosine-5′-triphosphate sulfurylase 0–50 nM; 2 μL deionized water plus 2 μL inorganic pyrophosphatase 0–50 nM; 2 μL adenosine-5′-triphosphate sulfurylase 0–50 nM plus 2 μL inorganic pyrophosphatase 0–50 nM; and 4 μL deionized water as control. Finally, to test the method's response to sulfate, two assays were performed using the conditions described in Scheme 2 with 0 to 96 mg L^{-1} of sodium sulfate standards (high range) or with 0 to 19 mg L^{-1} of sodium sulfate standards (low range), plus 2 μL of adenosine-5′-triphosphate sulfurylase 20 nM and 2 μL of inorganic pyrophosphatase 30 nM.

Screening and optimization designs. The screening and optimization of assays were performed as described in Scheme 2, using the concentrations in Table 2. For temperatures other than the room temperature, tubes were incubated in a water bath using an immersion thermostat (ET Basic Yellow Line, IMLAB, Boutersem, Belgium).

Method's characterization. The optimized assays were performed as described in Scheme 2.

Calibration curves were made using sodium sulfate standards from 0 to 134 mg L^{-1} (eight experimental points for each curve, each point measured in triplicate). In parallel, control

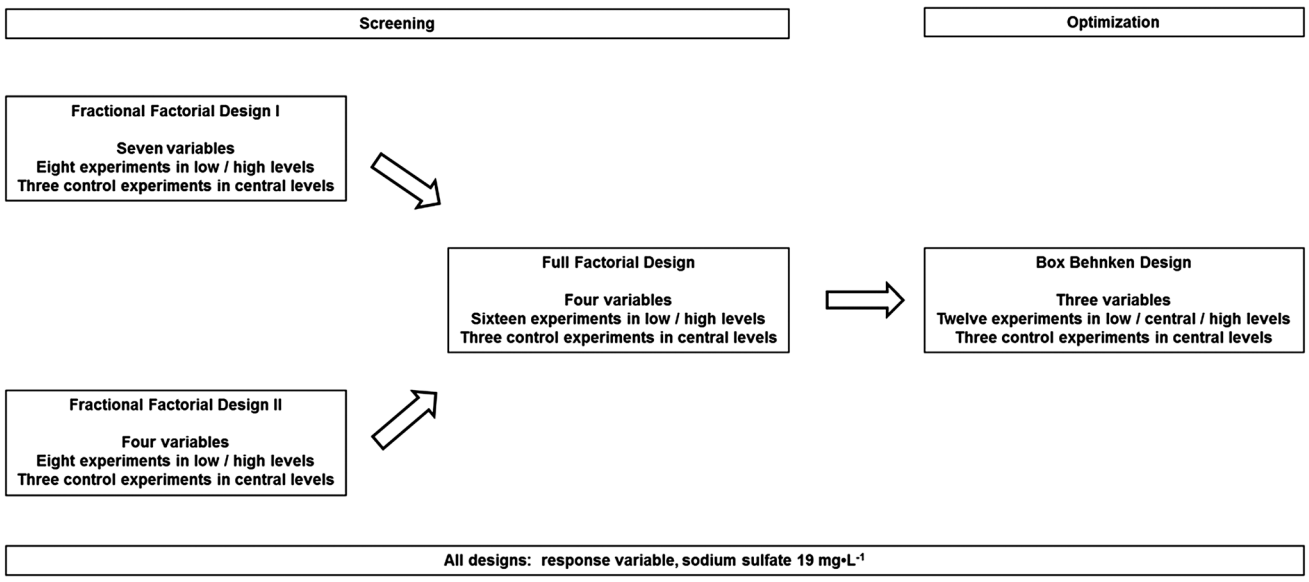

Scheme 1 Experimental design formulation flowchart.

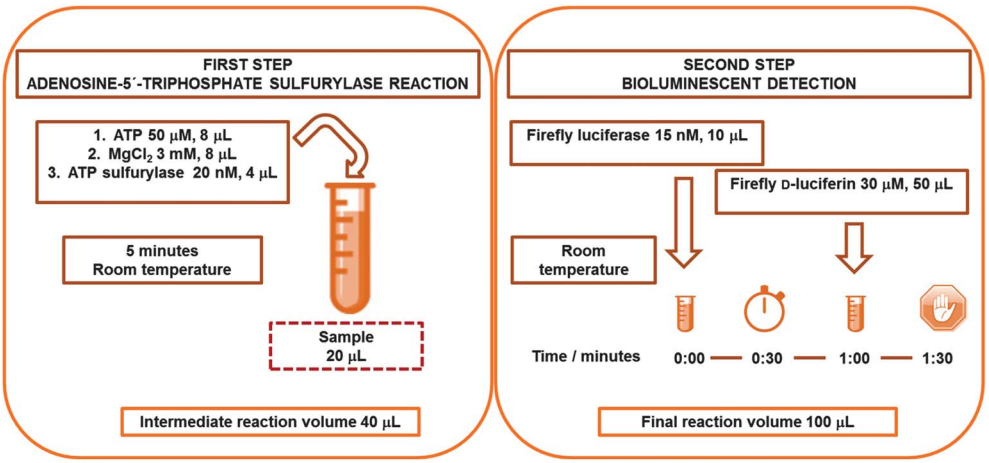

Scheme 2 Bioluminescent assay flowchart.

Table 2 Selected factors and the corresponding levels analyzed in Fractional Factorials, Full Factorial and Box Behnken designs

	Levels		
Factor	Low	Central	High
Fractional Factorial design I			
ATP concentration/μM	25	50	75
ATP sulfurylase[a] concentration/nM	10	20	30
Inorganic pyrophosphatase concentration/nM	0	15	30
Incubation time/minutes	5	10	15
Temperature of incubation/°C	Room	25	30
Firefly luciferase concentration/nM	10	15	20
Firefly D-luciferin concentration/μM	25	37.5	50
Fractional Factorial design II			
ATP sulfurylase concentration/nM	10	20	30
Inorganic pyrophosphatase concentration/nM	0	15	30
Incubation time/minutes	5	10	15
Temperature of incubation/°C	Room	25	30
Full Factorial design			
ATP concentration/μM	25	50	75
ATP sulfurylase concentration/nM	10	20	30
Firefly luciferase concentration/nM	10	15	20
Firefly D-luciferin concentration/μM	25	37.5	50
Box Behnken design			
ATP concentration/μM	25	50	75
Firefly luciferase concentration/nM	10	15	20
Firefly D-luciferin concentration/μM	25	37.5	50

[a] ATP sulfurylase, adenosine-5′-triphosphate sulfurylase.

tubes with deionized water without sulfate and HEPES buffer 0.5 M, pH 7.5 in place of adenosine-5′-triphosphate sulfurylase were assayed, in triplicate, before and after the measurement of the calibration points.

For the estimation of the method's repeatability, assays were made using the optimized conditions with sodium sulfate standards at 34, 68 and 96 mg L^{-1} (each concentration measured in quintuplicate).

Sample assay. Water was collected in polypropylene flasks from three domestic wells within the municipalities of Matosinhos (one well) and Maia (two wells), and stored in room temperature protected from light.

Prior to performing the assay, samples were tested for the order of magnitude of their sulfate content with test strips (MQuant™ 110019 Sulfate Test, Merck, Darmstadt, Germany) and diluted with deionized water. Assays were performed under the conditions described in Scheme 2 through calibration curves and the method of standard additions. Analysis with calibration curves was performed by using sodium sulfate standards from 0 to 134 mg L^{-1} (five experimental points for each curve, each point measured in triplicate) and 20 μL of each sample was measured in quintuplicate.

Using the method of standard additions, 20 μL aliquots of sample were added to 4 μL of sodium sulfate standard solutions so that the combined concentrations (sample plus standard) ranged from 0 to 134 mg L^{-1}, approximately (five experimental points for each curve, each point measured in triplicate). The volumes of magnesium chloride and ATP were reduced to 6 μL each. For the spike-and-recovery assay, 10 μL of water from Maia well #1 was spiked with 10 μL of sodium sulfate standards at 34, 68 and 96 mg L^{-1} (each concentration measured in quintuplicate). A calibration curve was made within the spike-and-recovery assay from 0 to 134 mg L^{-1} (five experimental points for each curve, each point measured in triplicate).

Samples were assayed, for comparison purposes, according to the method described in ref. 41 with the following modification: the concentration range of the calibration curve was settled to 0 to 35 mg L^{-1}, because above this value a deviation from linearity was verified.

Statistical analysis

Data obtained from the experimental designs were analyzed using The Unscrambler® software. For the screening designs, an Analysis of Effect was performed. Results were expressed as

Effects Overview, using the significance testing methods Comparison with a Scale-Independent Distribution (COSCIND) and Center for Fractional Factorial designs, and Higher Order Interaction Effects (HOIE) and Center for the Full Factorial design. For the Box Behnken optimization design, a Response Surface Analysis, which includes a two-way Analysis of Variance (ANOVA) table, residuals calculation and response surface, was applied. From the ANOVA table, the analyzed parameters were the Summary (evaluation of the global model), the Variable (evaluation of the significance of the variables tested), the Model Check (evaluation of the global quadratic model) and the Lack of Fit (degree of misfitting of the experimental data to the model). All those parameters were evaluated through the *F*-ratios and the *p*-values. Regarding the variables, the *B*-coefficients and their corresponding standard errors were also taken into account. Residuals were evaluated through a normal probability plot.

Linear regression was performed with a Microsoft® Excel® spreadsheet. Each experimental point corresponds to the peak of the bioluminescent signal, defined as the point when firefly D-luciferin is injected into the reaction mixture, from which the baseline, defined as the average of signals registered previously to the addition of firefly D-luciferin, was subtracted (see Fig. 3, inset). Results were expressed as Relative Light Units (RLUs). From calibration curves settled by the method of least squares, the limits of detection (LOD) and quantitation (LOQ) were calculated using the following criteria: $\mathrm{LOD} = (a + 3S_{y/x})$ and $\mathrm{LOQ} = (a + 10S_{y/x})$, where a is the intercept of the calibration curves and $S_{y/x}$ is the random error in the y-direction.[42] When the method of standard additions was used, curves were settled by calculating corrected signal values using the expression corrected signal = [average signal of blank (in triplicate) − average signal of sample plus sulfate standard (in triplicate)]/average signal of blank, wherein the blank was prepared with deionized water without sulfate addition. The concentration of inorganic sulfate was given as the ratio between the intercept and the slope of the regression lines. Recovery (R) was calculated using the expression $R(\%) = [(\text{concentration of fortified sample} - \text{concentration of sample})/\text{concentration of fortification}] \times 100$. To test whether there is a significant difference between the results obtained by this method and the reference, a paired *t*-test was performed.[42]

Results are expressed as sulfate concentration ± 95% confidence limits of the concentration ($n = 5$). A p-value <0.05 was considered as statistically significant.

Results and discussion

Overview

This paper presented the establishment of an optimized bioluminescent assay for inorganic sulfate quantitation in freshwater, relying on adenosine-5′-triphosphate sulfurylase and firefly luciferase. The novelty of this assay is not only the use of adenosine-5′-triphosphate sulfurylase to quantify inorganic sulfate instead of inorganic pyrophosphate, but most importantly its optimization based on the experimental design methodology. This optimized method is safe, simple to perform and economic despite the use of several enzymes and reagents because of the reduced volumes of enzymes required. All reagents are commercially available, do not need further purification prior to use and their solutions are stable for several months when stored at −20 °C. Although we used a single-tube luminometer, the method is applicable to multiplate assays, thus allowing the simultaneous testing of multiple samples. Also, as no pre-treatment of the samples other than dilution is necessary, and regarding the low volumes needed, *in situ* analyses are possible with portable commercial luminometers. Two possible disadvantages were considered. On one hand, the assay has a higher detection limit compared to some other methods (μg L^{-1} *versus* mg L^{-1} for this method). The loss in sensitivity, however, is compensated by the other described features, like simplicity and possibility of *in situ* analyses. Another concern with the use of enzymes is that they may lose activity over time. This problem is common to all methods employing enzymes, and may also vary according to the enzyme in use. For example, firefly luciferase is sensitive to long-term assays at room temperature, whereas adenosine-5′-triphosphate sulfurylase is not. The use of additives during the preparation of solutions of firefly luciferase enhances its stability. For the sake of simplicity, we chose not to add any additive to our firefly luciferase stock preparation, but readers can add them if necessary, especially when longer assay times are to be applied (over two hours).

Preliminary assays

Preliminary assays were done to study the possible influence of inorganic sulfate on firefly luciferase activity in the absence of adenosine-5′-triphosphate sulfurylase. It was verified that a spike in luminescence occurs both in deionized water and at a low concentration of sulfate (Fig. 1A). This feature is not uncommon in firefly luciferase catalyzed reactions, and may be due to the natural variability of its enzymatic activity. A recent report demonstrated that the addition of magnesium sulfate to the reaction mixture could stabilize firefly luciferase.[43] However, the present results did not reveal any significant influence of sulfate (Fig. 1A). This could be explained by a difference in experimental conditions, for example in the concentration values. They used firefly luciferase at 6 μg mL^{-1} (about 99 nM) with a magnesium sulfate concentration ranging from 0 to 1.2 M (0 to 115 276 mg mL^{-1}), with an average of 10 mM of magnesium sulfate (about 960 mg mL^{-1}). Furthermore, they performed medium- to long-term analysis, where firefly luciferase was assayed for its bioluminescence over a one hour period, whereas in the present work the bioluminescent recording lasts only 1 minute and 30 seconds (see Experimental section). Both firefly luciferase and inorganic pyrophosphatase require magnesium ions to function. In this regard, we have chosen to use magnesium chloride as a source of magnesium ions, instead of magnesium sulfate, to avoid a double acting of the latter. The influence of the enzymes adenosine-5′-triphosphate sulfurylase and inorganic pyrophosphatase on firefly luciferase activity, in the absence of their substrates, was also tested. Inorganic pyrophosphatase catalyzes the cleavage of

inorganic pyrophosphate into two phosphate ions. In this regard, the coupling of this reaction could aid in driving the reaction catalyzed by adenosine-5′-triphosphate sulfurylase into completion. The results showed no differential response to the presence of these enzymes (Fig. 1B), either alone or as a couple.

The subsequent step was to verify preliminary working ranges for sulfate quantitation. Two concentration intervals were assayed, 0 to 96 mg L^{-1} of sodium sulfate standards (high range) and 0 to 19 mg L^{-1} of sodium sulfate standards (low range). No response was detected below 14 mg L^{-1}, but the decrease of the bioluminescent signal was proportional to the sulfate concentration above this value (data not shown). Therefore, a provisory range of 0 to 96 mg L^{-1} was settled for the method.

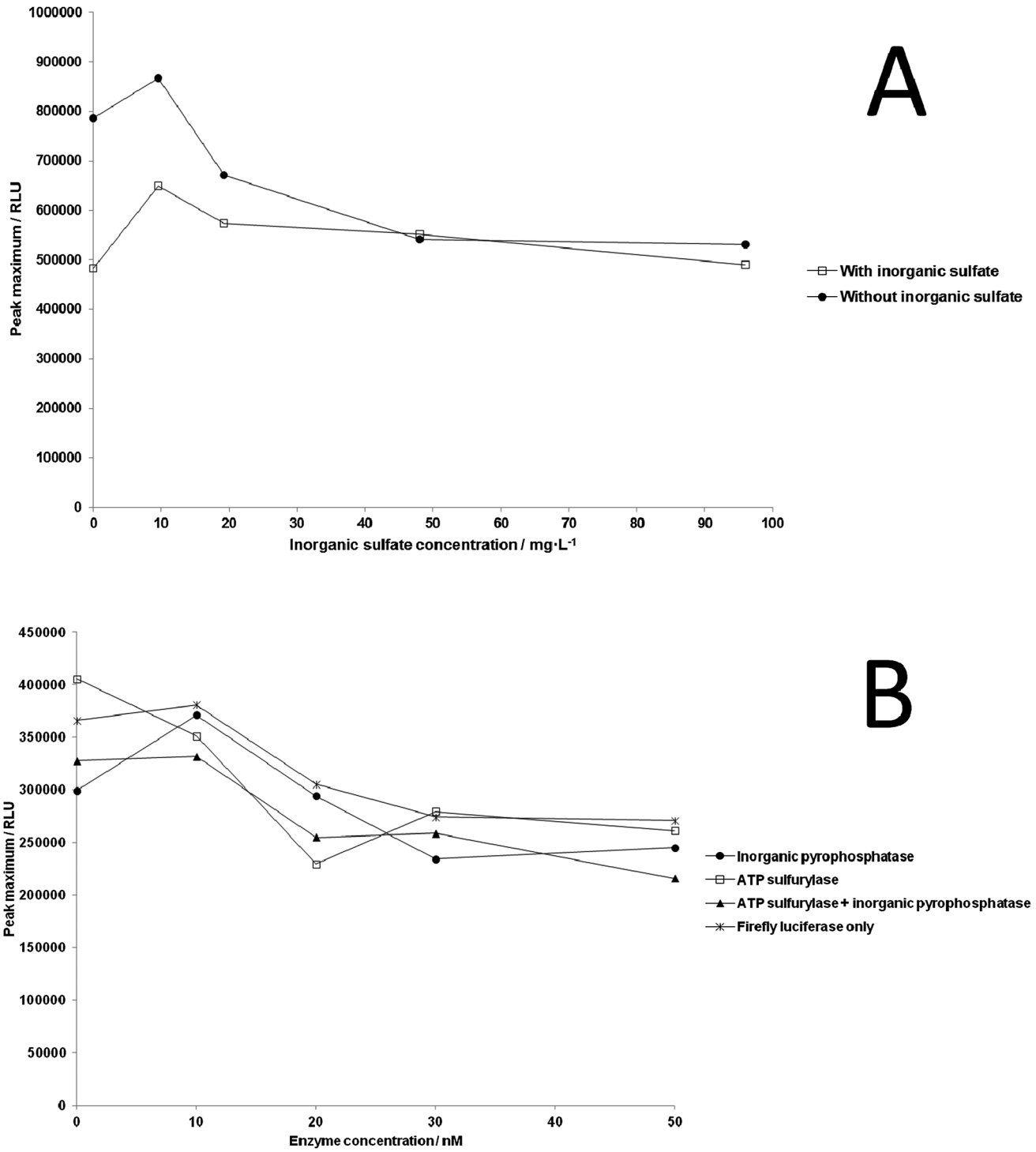

Fig. 1 Response of firefly luciferase to the presence of (A) inorganic sulfate and (B) the enzymes adenosine-5′-triphosphate sulfurylase and inorganic pyrophosphatase. RLU, Relative Light Units; ATP sulfurylase, adenosine-5′-triphosphate sulfurylase.

Experimental designs

On the basis of these results the method was optimized using the experimental design methodology. The overall optimization process included two steps: a screening to identify which factors have statistically the most influence on the method's response and the subsequent determination of the levels at which these factors must be kept to optimize the method's response. Taking into account the various reagents and steps in the method, seven factors were initially selected for screening and a Fractional Factorial design was selected (Table 2). The concentrations of the factors were selected by considering time and solubility constraints and to conserve the most expensive reagents, in this case the enzymes. In the case of magnesium chloride, the value of 3 mM was selected based on the literature as the best value for adenosine-5′-triphosphate sulfurylase activity.[44] Results showed that, in the presence of 19 mg L^{-1} of inorganic sulfate and using the testing method Center, the concentrations of ATP, firefly luciferase and firefly D-luciferin were likely the most significant factors (ESI, Table S1†). Furthermore, they exert a positive influence, that is, the higher are the concentrations, the higher is the response (the plus signal for the factors, see ESI, Table S1†). Using the significance testing method COSCIND, none of the factors were considered significant (ESI, Table S1†). The significant factors were more related to the bioluminescent detection, which can be explained as the response was the light output. To evaluate the factors more related to the adenosine-5′-triphosphate sulfurylase reaction, a second Fractional Factorial design with four factors was built (Table 2). In the presence of 19 mg L^{-1} of inorganic sulfate and using the testing method Center, the concentration of adenosine-5′-triphosphate sulfurylase was likely the most significant factor with a negative influence: the lower is its concentration, the higher is the response (the minus signal for the factors, see ESI, Table S1†). Using the significance testing method COSCIND, adenosine-5′-triphosphate sulfurylase concentration was also determined to be significant (ESI, Table S1†). Once again, as adenosine-5′-triphosphate sulfurylase causes depletion of ATP, higher concentrations lead to reduced light emission, thus the need to lower its concentration. Before the optimization step, a Full Factorial design with these four factors was created to confirm the results (Table 2). Results showed that, in the presence of 19 mg L^{-1} of inorganic sulfate and using the testing method HOIE, the concentrations of ATP, firefly luciferase and firefly D-luciferin were again the most significant factors, as well as the interaction ATP concentration × firefly luciferase concentration (ESI, Table S1†), meaning that a change in one of these two factors has a positive influence on the response. Using the significance testing method Center none of the factors were considered significant (ESI, Table S1†).

Table 3 Analysis of Variance (ANOVA) table for the Box Behnken optimization design

	SS[a]	DF	MS	*F*-ratio	*p*-value	*B*-coefficient	SE_b	Saddle point
Summary								
Model	8.109×10^9	9	9.011×10^8	5.176	0.0425			
Error	8.705×10^8	5	1.741×10^8					
Adjusted total	8.980×10^9	14	6.414×10^8					
Variable								
Intercept	1.466×10^{10}	1	1.466×10^{10}	84.190	0.0003	6.990×10^4	7.618×10^3	
ATP (A)	2.787×10^7	1	2.787×10^7	0.160	0.7056	74.665	186.597	46.952
Luciferase (B)	1.737×10^9	1	1.737×10^9	9.976	0.0251	2.947×10^3	932.984	15.953
Luciferin (C)	4.574×10^9	1	4.574×10^9	26.274	0.0037	1.913×10^3	373.194	26.164
AB	5.558×10^5	1	5.558×10^5	3.192×10^{-3}	0.9571	−213.000	3.770×10^3	
AC	4.533×10^6	1	4.533×10^6	2.604×10^{-2}	0.8781	608.286	3.770×10^3	
BC	8.370×10^8	1	8.370×10^8	4.808	0.0798	8.266×10^3	3.770×10^3	
AA	4.280×10^7	1	4.280×10^7	0.246	0.6410	1.946×10^3	3.924×10^3	
BB	7.003×10^7	1	7.003×10^7	0.402	0.5538	-2.489×10^3	3.924×10^3	
CC	7.905×10^8	1	7.905×10^8	4.541	0.0863	8.361×10^3	3.924×10^3	
Model check								
Main	6.339×10^9	3	2.113×10^9	1.612	0.2984			
Int	8.421×10^8	3	2.807×10^8	1.778	0.2675			
Int + Squ	9.287×10^8	3	3.096×10^8	1.778	0.2675			
Squ	9.287×10^8	3	3.096×10^8					
Error	8.705×10^8	5	1.741×10^8					
Lack of Fit								
Lack of Fit	6.428×10^8	3	2.143×10^8	1.883	0.3654			
Pure error	2.276×10^8	2	1.138×10^8					
Total error	8.705×10^8	5	1.741×10^8					

[a] SS, Sum of Squares; DF, degrees of freedom; MS, Mean Squares (ratio between SS and DF); *F*-ratio, ratio between 'between-measures' MS and 'within-measures' (residual) MS; *p*-value, probability of getting the *F*-ratio under the null hypothesis at 95%; *B*-coefficient, regression coefficient from a multiple linear regression analysis; SE_b, Standard Errors of b.

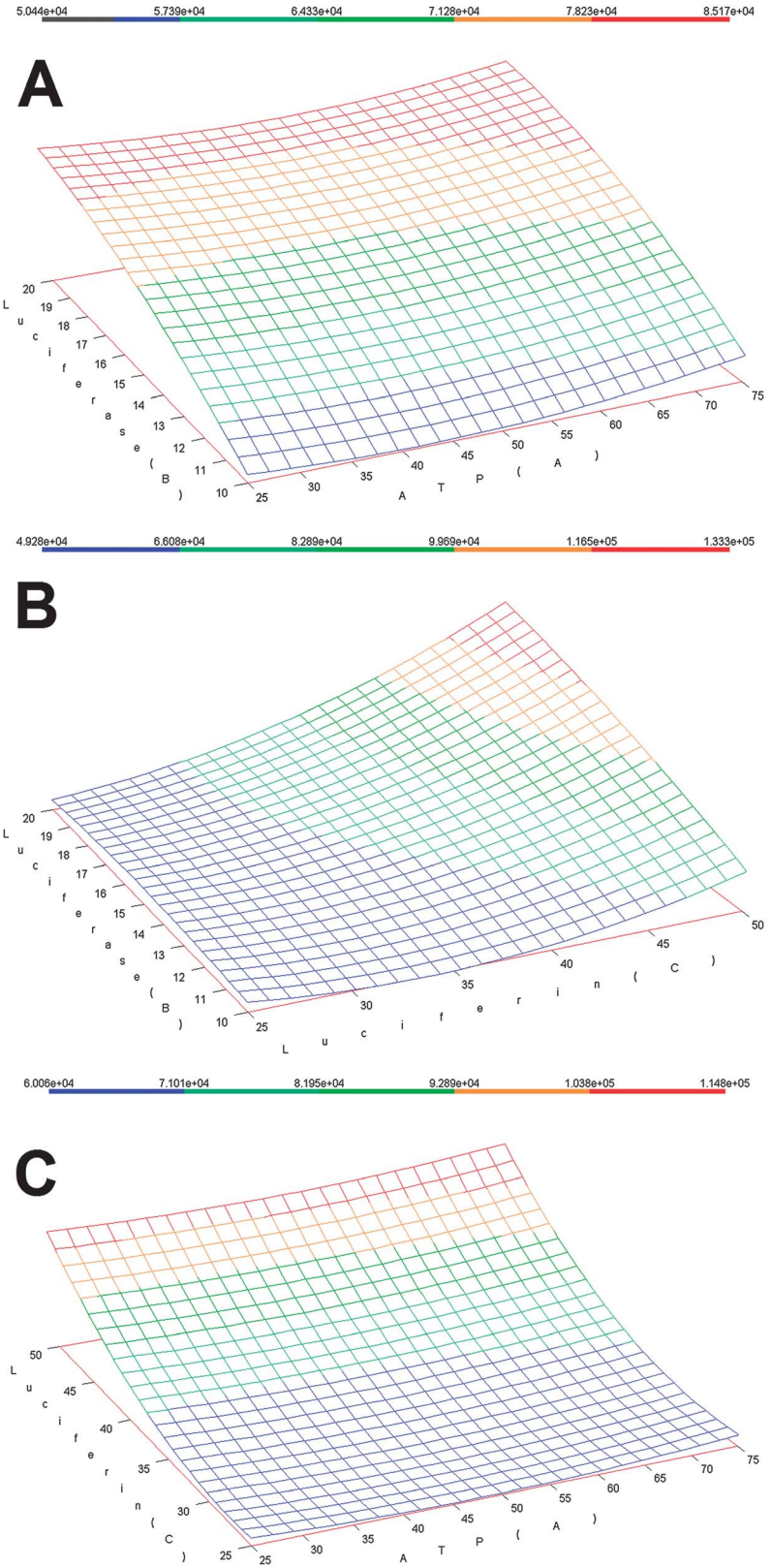

Fig. 2 Response surface landscape plots for the most important method's factors, ATP, firefly luciferase and firefly D-luciferin concentrations, tested in a Box Behnken Design. (A) Firefly luciferase concentration *vs.* ATP concentration; (B) Firefly luciferase concentration *vs.* firefly D-luciferin concentration; (C) Firefly D-luciferin concentration *vs.* ATP concentration.

With this information, a Box Behnken optimization design was built to uncover the best ATP, firefly luciferase and firefly D-luciferin concentrations (Table 2), and to discover if their interactions are also important for the method's response. The remaining factors were kept of lowest concentration, the shortest time of incubation and to perform the assay at room temperature. From the ANOVA table (Table 3) it was confirmed that firefly luciferase (B) and firefly D-luciferin (C) concentrations are important factors, showing significant *F*-ratios ($p < 0.05$) and presenting standard errors of the regression coefficient lower than the regression coefficient itself. On the other hand, the ATP concentration (A), the interaction between factors (AB, AC and BC) and the quadratic responses (AA, BB and CC) were not significant. According to their *F*-ratios, the Model is significant whereas the Lack of Fit is not ($p < 0.05$ and $p > 0.05$, respectively), which shows that the experimental measurements fit the model. Finally, a normal probability plot of the residues showed that they lie along a straight line, meaning that there are no outliers (ESI, Fig. S1†). The response surface curves (Fig. 2) show that the concentrations of firefly luciferase and firefly D-luciferin should be kept at the highest values tested to obtain the maximum signal (bioluminescence emission), whereas any concentration of ATP can be chosen since it is not a significant factor in this design. However, although higher concentrations of firefly luciferase are desirable whenever high sensitivity is needed, it also raises the cost of the assay. Taking that into consideration, the concentrations of ATP, firefly luciferase and firefly D-luciferin were settled to the saddle values suggested by the ANOVA table rounded up, that is 50 μM of ATP, 15 nM of firefly luciferase and 30 μM of firefly D-luciferin.

Furthermore, although the volumes of reagents and the reaction mixture were not proposed for optimization, since they were considered already adequate, the users can still adapt them according to their needs, for example if too little sample is available.

Method figures of merit

Using the optimized conditions, the bioluminescent assay was characterized in terms of linear range, limits of detection and quantitation and repeatability at several concentrations of inorganic sulfate.

To obtain the linear interval, calibration curves using a concentration range from 14 to 134 mg L^{-1} of inorganic sulfate were analyzed. It was verified that a linear trend occurs at this interval [product–moment correlation coefficient (r^2) varying from 0.989 to 0.999, an average r^2 of 0.996; average of seven independent measurements] (Fig. 3). Based on calibration curves, the limits of detection and quantitation were estimated as 10 and 34 mg L^{-1}, respectively. The repeatability of the method was estimated from the relative standard deviation, and showed values of 7.23% at 34 mg L^{-1}, 6.87% at 68 mg L^{-1} and 4.67% at 96 mg L^{-1} of inorganic sulfate (average of three independent experiments). As a method based on ATP depletion, it is important to assure that the loss of signal is not due to enzyme deactivation over time, since firefly luciferase is relatively unstable at prolonged use in room temperature.[43] In this regard, control tubes were assayed at the beginning and at the ending of every calibration curve assay. It was verified that firefly luciferase has indeed lost some of its activity, even with utmost care, in the order of 27%, based on differences in the peak maximum, during a one hour period of use. On the other hand, when coupled to adenosine-5′-triphosphate sulfurylase catalyzed reaction, the reduction in the bioluminescent signal with the raise in sulfate concentration was about 43%, thus demonstrating the effect of ATP depletion.

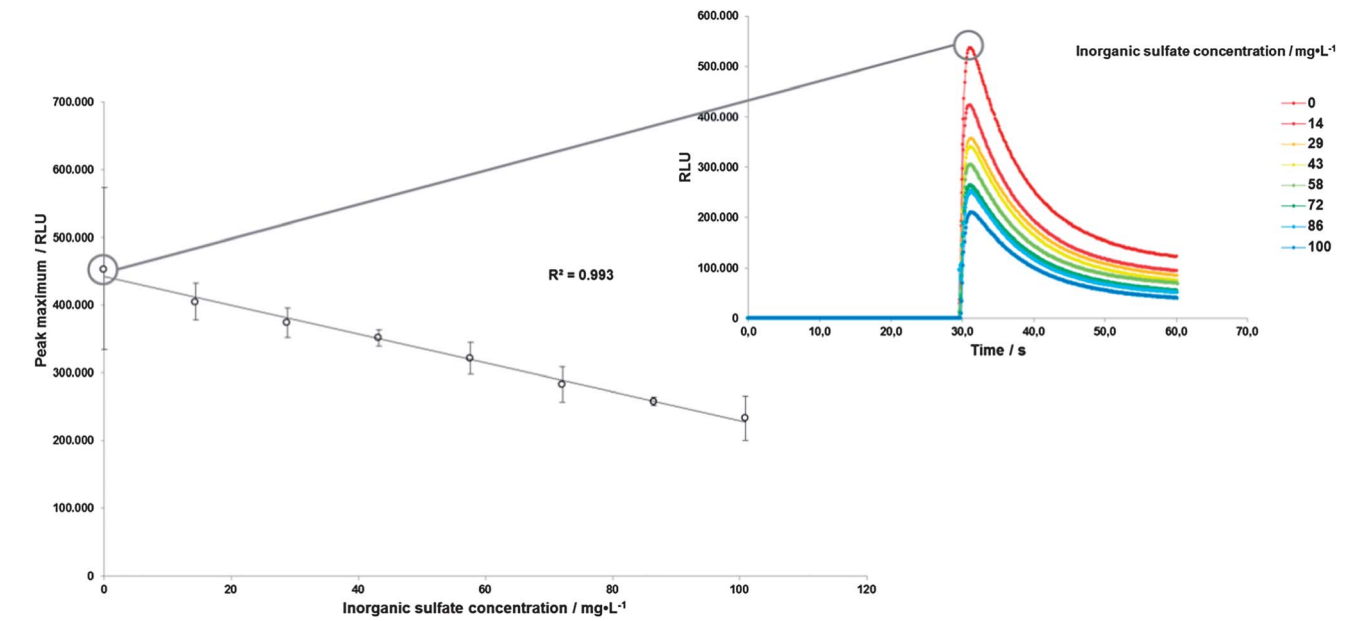

Fig. 3 Representative standard calibration curve for inorganic sulfate in the optimized bioluminescent assay. *Inset*: the corresponding luminogram. RLU, Relative Light Units.

Table 4 Inorganic sulfate quantitation in well and tap water and corresponding data quality parameters

	Sulfate concentration/mg L^{-1}			
	This method		Comparison method	
Sample	Calibration curve	Standard additions	Spectrophotometry	Turbidimetry
Matosinhos well	182.17 ± 0.33	182.43 ± 0.48	182.35 ± 0.29	182.42 ± 0.27
Maia well #1	123.85 ± 0.32	123.56 ± 0.45	124.07 ± 0.24	123.57 ± 0.36
Maia well #2	182.27 ± 0.57	182.14 ± 0.82	182.10 ± 0.42	182.44 ± 0.32
Tap water	201.48 ± 0.46	201.67 ± 0.53	201.49 ± 0.43	201.87 ± 0.37

Sample assay

Water collected from residential wells within the Metropolitan Area of Porto was assayed for their content of inorganic sulfate using this new optimized method. Results are presented in Table 4. The content of inorganic sulfate is between 124 and 183 mg L^{-1}. On the other hand, the tap water sulfate concentration was below the regulated level of 250 mg L^{-1},[10,11] indicating that the water is suitable for consumption.

To assess the possible interference of the matrix, samples were also assayed by the method of standard additions. No interferences were found ($p < 0.05$) (Table 4). To further confirm these results, a spike-and-recovery assay was performed with the Maia #1 water well. Good recoveries were obtained, with 86.7% for a spike of 34 mg L^{-1} (low spike), 95.6% for a spike of 68 mg L^{-1} (medium spike) and 94.5% for a spike of 96 mg L^{-1} (high spike). Besides matrix effects, endogenous ATP is an interfering compound and must be eliminated prior to the assay. Our samples were assayed for the presence of endogenous ATP, with negative results (data not shown). However, if a sample is suspected to contain ATP, adenosine-5′-triphosphatase (EC 3.6.1.3) may be added to the sample, incubated and denaturated by high temperatures prior to the assay.

Finally, the bioluminescent method was compared to another method described in the literature and commonly used for sulfate analysis. This method uses barium sulfate, which makes the sample cloudy and raises its absorbance. Samples were quantified by both turbidimetry and spectrophotometry at λ_{max} 420 nm. As can be seen in Table 4, no significant differences were found among the methods ($p < 0.05$). Although the spectrophotometric/turbidimetric determinations are easy to perform, they require much higher sample and reagent volumes (100 mL *versus* 20 μL with our method).

Conclusions

In this work the optimization of a bioluminescent assay for inorganic sulfate quantification was achieved. It is linear in the range from 14 to 134 mg L^{-1} of inorganic sulfate, with limits of detection and quantitation of 10 and 34 mg L^{-1}, respectively. Samples can be quantified by calibration curves without any pre-treatment other than dilution. The optimized method is fast, simple to perform and robust. Validation with water from domestic wells confirmed the applicability of the method to real samples.

Acknowledgements

Simone M. Marques is grateful for a Ph.D. scholarship (reference SFRH/BD/65109/2009), co-funded by the European Social Fund (Fundo Social Europeu, FSE), through Quadro de Referência Estratégico Nacional-Programa Operacional Potencial Humano (QREN-POPH), and by national funds from the Ministry of Education and Science through the Portuguese Fundação para a Ciência e a Tecnologia (FCT).

References

1 S. M. Marques and J. C. G. Esteves da Silva, *IUBMB Life*, 2009, **61**, 6–17.
2 S. M. Marques and J. C. G. Esteves da Silva, *Glob. J. Anal. Chem.*, 2011, **2**, 241–271.
3 P. Nyrén and A. Lundin, *Anal. Biochem.*, 1985, **151**, 504–509.
4 M. Ronaghi, *Genome Res.*, 2001, **11**, 3–11.
5 P. Nyrén, *The History of Pyrosequencing®*, in *Methods in Molecular Biology™ – Pyrosequencing® Protocols, 373*, ed. S. Marsh, Humana Press, Totowa, 2007.
6 M. Ronagui, S. Karamohamed, B. Pettersson, M. Uhlén and P. Nyrén, *Anal. Biochem.*, 1996, **242**, 84–89.
7 Y. Sun, K. J. Gregory, N. G. Chen and V. Golovlev, *Anal. Biochem.*, 2012, **429**, 11–17.
8 The World Health Organization, *International Standards for Drinking Water*, Geneva, 1958.
9 The Council of the European Union, Council Directive 98/83/EC, of 3 November 1998, Official Journal L 330, 5.12.1998, 1998, p. 32.
10 The XIV Portuguese Constitutional Government, Law-Decree no. 243/2001, of September 5th, The Portuguese Official Gazette I Series-A No. 206 of 5th September 2001.
11 The XVII Portuguese Constitutional Government, Law-Decree no. 306/2007, of August 27th, The Portuguese Official Gazette I Series No. 164 of 27th August 2007.
12 The World Health Organization, *Guidelines for Drinking-Water Quality*, 4th edn, Gutenberg Press,Tarxien,2011.
13 The World Health Organization, *Sulfate in Drinking-Water – Background Document for Development of WHO Guidelines for Drinking-Water Quality*, 2004, http://www.who.int/water_sanitation_health/dwq/chemicals/sulfate.pdf, accessed 15 October 2012.
14 T. Hiissa, H. Sirén, T. Kotiaho, M. Snellman and A. Hautojärvi, *J. Chromatogr., A*, 1999, **853**, 403–411.

15 Digital Environmental Atlas – Chemical Quality of Groundwater, Content of Sulfate (mg L^{-1} SO_4^{2-}), The Portuguese Environment Agency of the Ministry of Agriculture, Sea, Environment and Spatial Planning, Lisbon, http://www.apambiente.pt/, accessed 15 October 2012.
16 T. W. Vetter, K. W. Pratt, G. C. Turk, C. M. Beck and T. A. Butler, *Analyst*, 1995, **120**, 2025–2032.
17 B. Carvalho e Silva, L. M. Moreira de Campos and G. A. Pianetti, *Quim. Nova*, 2005, **28**, 54–56.
18 D. Belle-Oudry, *J. Chem. Educ.*, 2008, **85**, 1269–1270.
19 M. Mazloum-Ardakani, A. D. Manshadi, M. Bagherzadeh and H. Kargar, *Anal. Chem.*, 2012, **84**, 2614–2621.
20 M. I. Farooqi, J. Anwar, S. A. Nagra and A. Hussain, *J. Chem. Soc. Pak.*, 1989, **11**, 37–40.
21 A. Roy, B. K. Das and J. Bhattacharya, *Mine Water Environ.*, 2011, **30**, 169–174.
22 I. P. A. Morais, A. O. S. S. Rangel and M. R. S. Souto, *J. AOAC Int.*, 2001, **84**, 59–64.
23 N. Zárate, R. Pérez-Olmos and B. Freire dos Reis, *J. Braz. Chem. Soc.*, 2011, **22**, 1009–1014.
24 D. E. C. Cole and J. Evrovski, *J. Chromatogr., A*, 1997, **789**, 221–232.
25 G. Schminke and A. Seubert, *J. Chromatogr., A*, 2000, **890**, 295–301.
26 E. C. Figueiredo, J. C. Dias, L. T. Kubota, M. Korn, P. V. Oliveira and M. A. Z. Arruda, *Talanta*, 2011, **85**, 2707–2710.
27 E. A. Pereira, A. Stevanato, A. A. Cardoso and M. F. M. Tavares, *Anal. Bioanal. Chem.*, 2004, **380**, 178–182.
28 M. Masár, B. Bomastyk, R. Bodor, M. Horčičiak, L. Danč, P. Troška and H.-M. Kuss, *Microchim. Acta*, 2012, **177**, 309–316.
29 M. Zhang, Y.-Q. Liu and B.-C. Ye, *Analyst*, 2011, **136**, 4558–4562.
30 A. Ivask, T. Rõlova and A. Kahru, *BMC Biotechnol.*, 2009, **9**, 41, DOI: 10.1186/1472-6750-9-41.
31 K. T. Hamorsky, C. M. Ensor, P. Pasini and S. Daunert, *Anal. Biochem.*, 2012, **421**, 172–180.
32 S. Sharifi, S. Behzadi, S. Laurent, M. L. Forrest, P. Stroeve and M. Mahmoudi, *Chem. Soc. Rev.*, 2012, **41**, 2323–2343.
33 I. Schomburg, A. Chang and D. Schomburg, *Nucleic Acids Res.*, 2002, **30**, 47–49.
34 BRENDA – The comprehensive enzyme information system, Institute of Biochemistry and Bioinformatics, Technical University of Braunschweig, Braunschweig, http://www.brenda-enzymes.org, accessed 25 June 2012.
35 The UniProt Consortium, *Nucleic Acids Res.*, 2012, **40**, D71–D75.
36 The Universal Protein Resource (UniProt), European Bioinformatics Institute, Cambridge, Swiss Institute of Bioinformatics, Geneva, Protein Information Resource, Washington, DC, http://www.uniprot.org/, accessed 25 June 2012.
37 E. Gasteiger, A. Gattiker, C. Hoogland, I. Ivanyi, R. D. Appel and A. Bairoch, *Nucleic Acids Res.*, 2003, **31**, 3784–3788.
38 ExPASy Bioinformatics Resource Portal, Swiss Institute of Bioinformatics, Geneva, http://www.expasy.org/, accessed 25 June 2012.
39 R. M. Bock, N.-S. Ling, S. A. Morell and S. H. Lipton, *Arch. Biochem. Biophys.*, 1956, **62**, 253–264.
40 L. J. Bowie, *Methods Enzymol.*, 1978, **57**, 15–28.
41 *Standard Methods for the Examination of Water and Wastewater*, 20th edn, ed. L. S. Clesceri, A. E. Greenberg and A. D. Eaton, American Public Health Association, Baltimore, 1999.
42 J. N. Miller and J. C. Miller, *Statistics and Chemometrics for Analytical Chemistry*, 5th edn, Pearson Prentice Hall, Gosport, 2005.
43 M. R. Ganjalikhany, B. Ranjbar, S. Hosseinkhani, K. Khalifeh and L. Hassani, *J. Mol. Catal. B: Enzym.*, 2010, **62**, 127–132.
44 M. Heinzel and H. G. Trüper, *Arch. Microbiol.*, 1976, **107**, 293–297.

Electronic Supplementary Material (ESI) for Analytical Methods

An optimized bioluminescent assay for inorganic sulfate quantitation in freshwater

Simone M. Marques, Joaquim C.G. Esteves da Silva*

Centro de Investigação em Química da Universidade do Porto *(*CIQ-UP*), Department of Chemistry and Biochemistry, Faculty of Sciences, University of Porto, Rua do Campo Alegre, no. 687, 4169-007 Porto, Portugal.*

E-mail: jcsilva@fc.up.pt; Fax: +351 220 402 659; Tel: +351 220 402 569

Supplemental information

Table S1 Center, COSCIND[a] and HOIE[b] significance testing methods results for the screening designs

	Fractional Factorial Design I		Fractional Factorial Design II		Full Factorial Design	
	Center	COSCIND	Center	COSCIND	Center	HOIE
ATP concentration / μM (A)	+	NS			NS	++
ATP sulfurylase[c] concentration / nM (B)	NS	NS	-	5%	NS	NS
Inorganic pyrophosphatase concentration / nM	NS	NS	NS	NS		
Incubation time / minutes	NS	NS	NS	NS		
Temperature of incubation / ºC	NS	NS	NS	NS		
Firefly luciferase concentration / nM (C)	+	NS			NS	++
Firefly D-luciferin concentration / μM (D)	+	NS			NS	++
AB					NS	NS
AC					NS	+
AD					NS	NS
BC					NS	NS
BD					NS	NS
CD					NS	NS

[a]COSCIND, Comparison with a Scale-Independent Distribution

[b]HOIE, Higher Order Interaction Effects

[c] ATP sulfurylase, adenosine-5´-triphosphate sulfurylase

Significance of each effect at 95% level: NS, not significant; from + to +++, positive effect; from - to - - -, negative effect

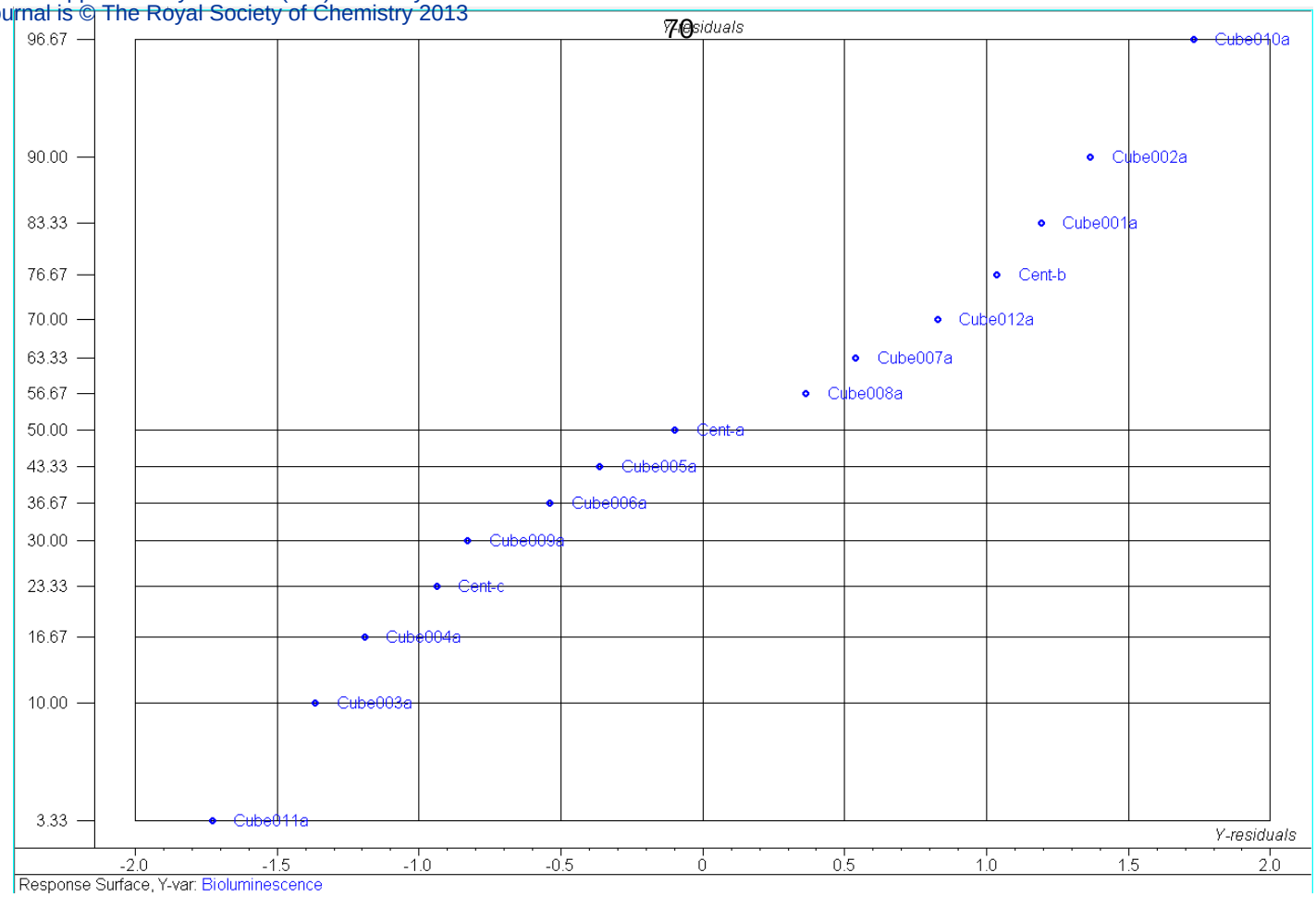

Fig. S1. Normal probability plot of the residuals of the Box Behken optimization design.

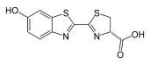

Chapter four

Nitric oxide quantitative assay by a glyceraldehyde 3-phosphate dehydrogenase/phosphoglycerate kinase/firefly luciferase optimized coupled bioluminescent assay

The scientific work leading to this chapter was integrally performed within the host institution, the Chemometric Research of Chemical, Environmental, Forensic and Biological Systems group, from the Chemistry Research Center of the University of Porto (*Centro de Investigação em Química da Universidade do Porto*, *CIQ-UP*), Department of Chemistry and Biochemistry, Faculty of Sciences, University of Porto. Simone Marques was responsible for bibliographic search, protocols set up, experimental execution, data treatment and manuscript writing, under the supervision of Joaquim Esteves da Silva.

Nitric oxide quantitative assay by a glyceraldehyde 3-phosphate dehydrogenase/phosphoglycerate kinase/firefly luciferase optimized coupled bioluminescent assay

A novel optimized coupled bioluminescent assay for nitrogen monoxide free radical (nitric oxide, •NO), an important environmental and physiological molecule, is presented. The method is based on the reaction catalyzed by glyceraldehyde 3-phosphate dehydrogenase (GAPDH), whose product is used as a substrate for phosphoglycerate kinase (PGK), generating adenosine 5'-triphosphate (ATP), which is an essential cofactor for the firefly luciferase (LUC) bioluminescent reaction. Inhibition of GAPDH by •NO hampers the coupled reactions, leading to a depletion of ATP and hence a decrease in the bioluminescent signal. Using diethylamine NONOate (DEA-NONOate) as the •NO donor, the assay was optimized through statistical experimental design methodology, namely Plackett-Burman (screening) and Box Behnken (optimization) designs. The optimized method requires 5 μL of sample *per* tube in a final reaction volume of 100 μL. It is linear in the range from 10 to 100 nM of •NO, with limits of detection and quantitation of 4 and 15 nM, respectively. As a proof-of-principle, human saliva and microalgae culture medium were assayed by the method of standard additions. Major features include its simplicity of execution, low reagent volumes, sensitivity and robustness, and the possibility to adapt it to multiplate assay and *in situ* analysis.

Keywords: Analytical biochemistry; Luminometry; Experimental design; Enzymatic assay

1. Introduction

Nitrogen monoxide, commonly known as nitric oxide (•NO), is a small gaseous and free radical molecule containing one unpaired electron with an enormous importance in the environmental, biological and pathological contexts.[1-4] It is mainly recognized as an atmospheric pollutant, along with its derivative nitrogen dioxide (NO_2), and as an intra- and extracellular signaling molecule with relevant roles in inflammatory, carcinogenic, cardiovascular, immune response, neurodegenerative and neurotransmission, and pain generation processes.[1-4]

Methods for •NO detection and quantitation may be direct or indirect. In indirect methods, the •NO amount is estimated through its derivatives, nitrite (NO_2^-), nitrate (NO_3^-) or NO_2. Assuming that all the •NO in a sample tends to be converted into the more stable products nitrate and nitrite, a widespread indirect method is the Griess test for nitrite.[5] Nitrate may also be quantified by its previous conversion to nitrite, for example by using nitrate reductase. Although simple to perform, this methodology may not reflect the endogenous •NO content, which originates from nitric oxide synthase reactions with the amino acid L-arginine,[2] because other sources may affect the results, for example dietary intake.[6] Other popular methods are based on fluorescence,[7] ultraviolet-visible (UV-vis) spectrophotometry,[8] electrochemical sensors,[9-11] chemiluminescence with ozone,[12, 13] spin trapping coupled to electron paramagnetic resonance (EPR) spectroscopy[14, 15] and membrane inlet mass spectrometry (MS).[16] Recent approaches for •NO quantitation include the use of nanomaterials to create novel electrochemical sensors,[17-21] the synthesis of novel fluorescent probes, [22, 23] the bioimaging of •NO in living cells and small animals,[23, 24] and coupled enzymatic assays.[25] Those methods are in general highly sensitive, with limits of detection (LOD) varying from the nanomolar range, 0.31[17] up to 95 nM,[21] to the low micromolar range, 0.1[20] up to 3 μM.[7] However, some problems are worthy to note. EPR and MS equipment are not portable, involve high costs of acquisition and maintenance, and may require specialized personnel to operate. The dyes used in fluorescent and UV-vis methods may participate in side reactions, either reducing their free amount to react with •NO or leading to other fluorescent or coloured products which interfere with the assay.[26, 27] The use of nanomaterials is very promising, but some concerns regarding their toxicity are still under discussion. [28, 29] Lastly, most of the proposed new methods were not tested in real samples, nor they were subjected to optimization. In this chapter, an optimized coupled bioluminescent assay for •NO will be presented.

Coupled enzymatic assays refer to analytical methods in which several enzymatic reactions, one of which using the desired analyte, occur sequentially to generate a

measurable signal.[30] A first reaction generates one product that will be used in a second coupled reaction as a substrate. The second reaction will generate another product that may be used as substrate in a third coupled reaction and so on, until a final product that is measured. When the measured product are photons, the assay is termed coupled bioluminescent assay.[30] Coupled enzymatic assays are useful when the enzymatic reaction consuming or producing the desired analyte does not lead to an easily measurable product. Furthermore, they may lead to signal amplification. On the other hand, if one of the enzymes is inactivated, or the concentration of one of the reagents is too low, the coupling is hampered, which requires the careful evaluation of each enzyme and reagent prior to the assay.

In the presented method, the first reaction of the coupling is catalyzed by glyceraldehyde 3-phosphate dehydrogenase (GAPDH), producing 1,3-bisphosphoglycerate (1,3-BPG) in the presence of its substrate, glyceraldehyde 3-phosphate (G3P), and the cofactors β-nicotinamide adenine dinucleotide (NAD^+) and phosphate ions (Pi) (Scheme 1). The product, 1,3-BPG, is used as a substrate for phosphoglycerate kinase (PGK), producing 3-phosphoglycerate (3-PG). In the course of this reaction its cofactor, adenosine 5'-diphosphate (ADP), is phosphorylated into adenosine 5'-triphosphate (ATP), which is an essential cofactor for the bioluminescent reaction catalyzed by firefly luciferase (LUC). In the presence of ATP, molecular oxygen (O_2) and its natural substrate, firefly D-luciferin (D-LH_2), LUC generates adenosine-5'-monophosphate (AMP), inorganic pyrophosphate (PPi), carbon dioxide (CO_2), oxyluciferin and photons of visible light which are recorded in a luminometer. •NO is known to inhibit GAPDH, presumably by acting on a thiol group from an enzyme's active site cysteine, albeit this is still under discussion.[31-36] By inhibiting GAPDH, the production of ATP is impaired, decreasing the light output.

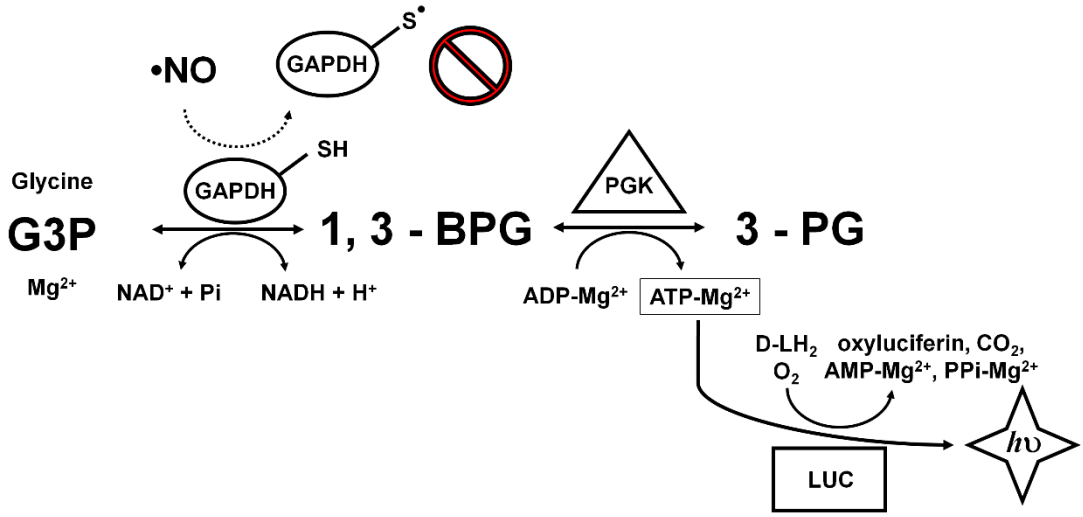

Scheme 1. Coupled enzymatic reactions. •NO, nitric oxide; G3P, glyceraldehyde 3-phosphate; Mg^{2+}, magnesium ions; GAPDH, glyceraldehyde 3-phosphate dehydrogenase; NAD^+, β-nicotinamide adenine dinucleotide; Pi, phosphate ions; NADH + H^+, β-nicotinamide adenine dinucleotide (reduced form); 1,3-BPG, 1,3-bisphosphoglycerate; PGK, phosphoglycerate kinase; 3-PG, 3-phosphoglycerate; ADP-Mg^{2+}, adenosine 5'-diphosphate complexed with magnesium ions; ATP-Mg^{2+}, adenosine 5'-triphosphate complexed with magnesium ions; LUC, firefly luciferase; D-LH_2, firefly D-luciferin; O_2, molecular oxygen; CO_2, carbon dioxide; AMP-Mg^{2+}, adenosine 5'-monophosphate complexed with magnesium ions; PPi-Mg^{2+}, inorganic pyrophosphate complexed with magnesium ions; *h*υ, photons; -SH, GAPDH thiol group; -S•, GAPDH thiyl radical.

With the exceptions of LUC and D-LH_2, the reagents and enzymes in this method are abundant in cells. Several strategies must be taken into account to avoid interference, especially from ATP, since the detection method is based on ATP depletion. Centrifugation may be used to separate cells, which contain the bulk of biological compounds, from supernatant. The remaining ATP may be removed through enzymatic reactions that consume or degrade ATP. An example of such reaction is catalyzed by ATP sulfurylase in the presence of sulfate ions (SO_4^{2-}), giving adenosine 5'-phosphosulfate (APS) and PPi (equation 1).[37]

$$SO_4^{2-} + \text{ATP-}Mg^{2+} \xleftrightarrow{\text{ATP sulfurylase}} \text{APS} + \text{PPi-}Mg^{2+} \quad (1)$$

By its turns, PPi must also be removed, not only to favor the consumption of ATP but also because PPi interferes with the bioluminescent reaction. [38] This can be achieved by adding inorganic pyrophosphatase (PPase) to the medium (equation 2).[37]

$$\text{PPi-}Mg^{2+} + H_2O \xleftrightarrow{\text{PPase}} 2\ \text{Pi-}Mg^{2+} \quad (2)$$

Another approach consists of using the method of standard additions.[39] This is a type of data analysis in which several standards of rigorously known concentration of the analyte are added to all but one aliquots of samples. The signal is measured for all samples and a calibration curve is obtained. The original concentration of the analyte is obtained by reading the absolute value of the *x*-intercept for the zero signal. The method has some disadvantages, namely it is more time-consuming because every sample has to have its own curve, it demands larger quantities of samples and most of the time it is not possible to separate samples from the standards after the procedure. Nevertheless, it is the method of choice for biological samples where matrix effects often occur.

The compound (*Z*)-1-[*N*,*N*-diethylamino]diazen-1-ium-1,2-diolate (diethylamine NONOate, DEA-NONOate, Figure 1) was used as a •NO donor. NONOates are prepared in alkaline solutions and, by lowering the pH, under defined temperature and concentration conditions, they dissociate to the free amino and •NO according to a defined stoichiometry. These features make them a versatile and convenient choice for an ever greater number of studies.[40, 41]

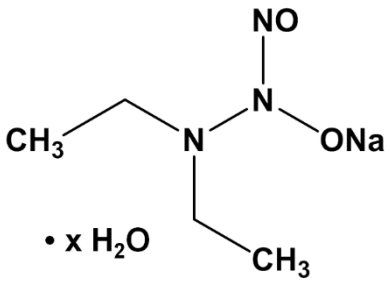

Figure 1. Chemical structure of DEA-NONOate in its sodium salt hydrate formulation.

2. Experimental

Note: All experiments were performed at room temperature (approximately 20 ºC). Concentration values are final.

2.1. Reagents and solutions

2.1.1. Reagents

The enzymes (see Table 1) and the reagents 4-(2-hydroxyethyl)piperazine-1-ethanesulfonic acid (HEPES, product code H3375), G3P (G5251), NAD^+ (N0632), DEA-

NONOate (D184), ADP (A5285), ATP (A2383), D-LH_2 (L9504), glycine (410225) and magnesium chloride ($MgCl_2$, 63064) were purchased from Sigma-Aldrich® (Steinheim, Germany). Sodium sulfate (Na_2SO_4) was obtained from Pronalab (Lisbon, Portugal). Sodium hydroxide (NaOH) was purchased from Moura Drugstore (Porto, Portugal). Sodium dihydrogen phosphate monohydrate ($NaH_2PO_4 \cdot H_2O$) was obtained from Merck (Darmstadt, Germany). Nitrogen (Alphagaz™ Smartop N_2) was obtained from Air Liquide Portugal (Algés, Portugal).

A commercial •NO assay kit, 'Nitric Oxide Assay Kit (Colorimetric)', ab65328, was purchased from Abcam® (Cambridge, U.K.).

Table 1. Commercial references of the enzymes used in the method

Enzyme	Source	EC	Product code	Lot
Glyceraldehyde 3-phosphate dehydrogenase	*Saccharomyces cerevisiae*	1.2.1.12	G5537	030M7715V
Phosphoglycerate kinase	*Saccharomyces cerevisiae*	2.7.2.3	P7634	061M7674V
Firefly luciferase	*Photinus pyralis*	1.13.12.7	L9506	060M7400
ATP sulfurylase	*Saccharomyces cerevisiae*	2.7.7.4	A8957	129K7680V
Inorganic pyrophosphatase	*Saccharomyces cerevisiae*	3.6.1.1	I1891	057K8618

2.1.2. Solutions

All reagents were used without further purification. Stock solutions of the enzymes were prepared by dissolving the whole content of the flasks in HEPES buffer 0.5 M, pH 7.5, with the exception of PGK, which was purchased as an ammonium sulfate suspension.

HEPES was prepared by dissolving the corresponding mass in deionized water, and the pH was adjusted to 7.5 using a 10 M NaOH solution. Phosphate buffer 150 mM, pH 6.9 was prepared by dissolving the corresponding mass of $NaH_2PO_4 \cdot H_2O$ in deionized water and adjusting the pH to 6.9 using a 10 M NaOH solution. G3P was purchased as an aqueous solution. Stock solutions of NAD^+, ADP, ATP, $MgCl_2$ and glycine were prepared

in deionized water without pH adjustment. D-LH_2 stock solutions were prepared in deionized water with intense stirring for about 1 hour protected from the air and from the light. Concentration was confirmed by UV-vis spectrophotometry using an Unicam Helios γ spectrophotometer (Cambridge, U.K.) and considering a molar extinction coefficient of 18,200 $L \cdot mol^{-1} \cdot cm^{-1}$ at the maximum wavelength (λ_{max}) of 327 nm.[42] For the preparation of Na_2SO_4 stock solutions, the salt was previously heated in an oven at 100 ºC for 12 hours, then transferred to a desiccator filled with cobalt (II) chloride until it cooled to room temperature and the corresponding mass was weighted and dissolved in deionized water. DEA-NONOate solutions were freshly prepared by dissolving the corresponding mass in a 10 mM NaOH solution previously bubbled with a nitrogen stream in capped polypropylene tubes. Concentration was confirmed by UV-vis spectrophotometry using the molar extinction coefficient of 6,500 $L \cdot mol^{-1} \cdot cm^{-1}$ at λ_{max} 250 nm, according to the manufacturer's information.

To ensure that the same conditions were achieved throughout the work, and also to avoid multiple freezing-thawing cycles, stock solutions were prepared in large volumes, aliquoted in small volumes and stored at -20 ºC with the exception of PGK, which was stored at 2 ºC.

2.2. Preliminary assays

2.2.1. UV-vis spectrophotometric assays

2.2.1.1. GAPDH and PGK activity assay

GAPDH and PGK activities were assayed by a spectrophotometric assay based on the 'Enzymatic Assay of 3-Phosphoglyceric Phosphokinase (EC 2.7.2.3) from Baker's Yeast' protocol available from the manufacturer with modifications. Briefly, the test, GAPDH blank and PGK blank reaction mixtures contained 1,725 μL of phosphate buffer 50 mM, pH 6.9 (Pi), 75.0 μL of G3P 0.83 mM, 37.5 μL of NAD^+ 0.3 mM, 37.5 μL of ADP 0.2 mM, 188 μL of $MgCl_2$ 4.2 mM, and 750 μL of glycine 133 mM in a 3,500-μL Hellma® QS Suprasil® quartz cuvette (Müllheim, Germany). To the reaction mixtures, 37.5 μL of GAPDH 3.9 $\mu g \cdot mL^{-1}$ (test and PGK blank) or Pi (GAPDH blank) was added. The reagents were mixed by inverting the cuvette and introduced into the spectrophotometer. The absorbance was monitored at λ_{max} 340 nm until constant. One hundred and fifty microliters of PGK 0.011 $\mu g \cdot mL^{-1}$ (test and GAPDH blank) or Pi (PGK blank) was added. Absorbance was recorded for 30 minutes.

2.2.1.2. DEA-NONOate releasing assay

DEA-NONOate releasing was assayed by a spectrophotometric assay. Briefly, 3,325 μL of Pi was pipetted to the cuvette. Then 175 μL of DEA-NONOate in NaOH 10 mM, corresponding to a concentration of 10 μM •NO, was added, the reagents were mixed by inverting the cuvette and introduced into the spectrophotometer. The absorbance was monitored at λ_{max} 250 nm until no further changes in the absorbance values were observed.

2.2.2. Bioluminescent assays

2.2.2.1. ATP contamination in reagents and enzymes

ATP contamination in reagents and enzymes was evaluated by luminometry using a homemade luminometer with a Hamamatsu HCL35 photomultiplier tube (Middlesex, N.J., U.S.A) inside a light-tight dark chamber coupled to a Crison MicroBU 2030 automatic microburette (Barcelona, Spain) equipped with a 2.5 mL Hamilton GASTIGHT® 1002 glass syringe (Bonaduz, Switzerland).

The stock solutions of reagents were diluted in deionized water, DEA-NONOate standard solutions were diluted in NaOH 10 mM, and the enzymes were diluted in HEPES buffer 0.5 M, pH 7.5, and kept on ice until use.

Briefly, 10.00 μL of $MgCl_2$ 4.2 mM was added to 30.0 μL of each of the reagents and enzymes in polypropylene transparent test tubes. Concentrations of the regents were as follow: DEA-NONOate 1 mM, Pi 50 mM, G3P 0.83 mM, NAD^+ 0.3 mM, ADP 0.2 mM, glycine 133 mM, GAPDH 3.9 $\mu g \cdot mL^{-1}$ and PGK 0.011 $\mu g \cdot mL^{-1}$. Controls were made by assaying ATP 0.2 mM without the reagents or enzymes and adding LUC and D-LH_2, by replacing $MgCl_2$, the reagents and the enzymes with deionized water and adding LUC and D-LH_2, and by replacing $MgCl_2$, the reagents and the enzymes with deionized water and adding only D-LH_2. Ten microliters of either LUC 6 $\mu g \cdot mL^{-1}$ or deionized water (controls) was added to the mixtures, the tubes were introduced into the dark chamber and the baseline register by the equipment was turned on, at an integration interval of 0.1 seconds. After 30 seconds, 50 μL of D-LH_2 8.7 μM was injected from the automatic burette. The light output was recorded for more 30 seconds.

2.2.2.2. Reagents and enzymes influence on LUC activity

The influence of the reagents and enzymes on LUC activity was assayed by luminometry as described in subsection 2.2.2.1. with the following alterations: 10.00 μL of $MgCl_2$ 4.2 mM plus 10.00 μL of ATP 0.2 mM were added to 20.0 μL of each of the reagents and enzymes. NaOH 10 mM was also tested. Controls were made by assaying ATP and $MgCl_2$ without the reagents or enzymes and adding LUC and D-LH_2, by replacing ATP and $MgCl_2$ with deionized water and adding LUC and D-LH_2, and by replacing ATP and $MgCl_2$ with deionized water and adding only D-LH_2.

2.2.2.3. Evaluation of the enzymatic reactions coupling and the effect of •NO on GAPDH

To confirm the reactions coupling and the effect of •NO on GAPDH, a bioluminescent assay was performed. Briefly, DEA-NONOate solutions with final concentrations corresponding to 1 nM, 1 μM and 1 mM of •NO, considering a ratio of 1.5 moles of •NO *per* parent compound, according to the manufacturer's information, were prepared in NaOH 10 mM in capped polypropylene tubes. The solutions were diluted 1:20 in Pi in capped tubes and incubated at room temperature for 20 minutes before starting the assay to allow the release of •NO. Controls were made by replacing DEA-NONOate with deionized water (positive control) and by replacing GAPDH with deionized water (negative control). Reaction mixtures contained 450 μL of Pi, 25.0 μL of G3P 0.83 mM, 12.5 μL of NAD^+ 0.3 mM, 12.5 μL of ADP 0.2 mM, 62.5 μL of $MgCl_2$ 4.2 mM, 250 μL of glycine 133 mM, 12.5 μL of GAPDH 3.9 $\mu g \cdot mL^{-1}$ or deionized water, 50.0 μL of D-LH_2 8.7 μM and 25.0 μL of LUC 6 $\mu g \cdot mL^{-1}$. Fifty microliters of each DEA-NONOate solutions or deionized water was transferred to transparent test tubes, the reaction mixture was added and the tubes were introduced into the dark chamber, one at a time. The baseline register by the equipment was turned on, at an integration interval of 1 second. After 50 seconds, 50 μL of PGK 0.011 $\mu g \cdot mL^{-1}$ was injected from the automatic burette. The light output was recorded for more 10 minutes.

2.3. Experimental designs

2.3.1. Experimental design formulation

Experimental designs were created using The Unscrambler® version 9.2 from CAMO (Oslo, Norway). Screening designs were created using Plackett-Burman designs with eleven continuous variables at two levels and one nondesign (response) variable, which was set as •NO 5 nM (Table 2). For the experimental procedure, it was chosen one replication *per* experiment and three centre (control) experiments, with a total of twelve testing experiments plus the three control experiments. Optimization designs were created using Box Behnken designs with five continuous variables at two levels and one nondesign variable, which was set as •NO 5 nM (Table 2). For the experimental procedure, it was chosen one replication *per* experiment and five centre experiments, with a total of forty testing experiments plus the five control experiments.

Table 2. Selected factors and the corresponding levels analyzed in the Plackett-Burman screening design and the Box Behnken optimization design

	Levels		
Factor	low	central	high
Plackett-Burman Design			
[Pi] / mM	9	50	90
[G3P] / mM	0.15	0.83	1.5
[NAD^+] / mM	0.05	0.3	0.50
[ADP] / mM	0.036	0.20	0.36
[$MgCl_2$] / mM	0.76	4.2	7.6
[Glycine] / mM	24	133	240
[GAPDH] / $\mu g \cdot mL^{-1}$	0.71	3.9	7.1
[D-LH_2] / μM	1.58	8.7	15.8
[LUC] / $\mu g \cdot mL^{-1}$	1	6	11
[PGK] / $\mu g \cdot mL^{-1}$	0.0020	0.011	0.020
Preincubation time / minutes	0	5	15
Box Behnken Design			
[Pi] / mM	9	50	90
[G3P] / mM	0.15	0.83	1.5
[ADP] / mM	0.036	0.20	0.36
[$MgCl_2$] / mM	0.76	4.2	7.6
Preincubation time / minutes	0	5	15

2.3.2. Experimental design execution

Experimental designs were performed by luminometry. Briefly, a DEA-NONOate solution with concentration corresponding to 5 nM of •NO was prepared in NaOH 10 mM in a capped polypropylene tube. The solution was diluted 1:20 in Pi in capped tubes and incubated at room temperature for 20 minutes. The reaction mixture contained 25.0 μL of Pi, 2.50 μL of G3P, 1.25 μL of NAD^+, 1.25 μL of ADP, 6.25 μL of $MgCl_2$, 20.0 μL of glycine, 5.00 μL of D-LH_2 and 2.50 μL of LUC, which were prepared at the concentrations indicated in Table 2. Five microliters of DEA-NONOate solution was transferred to a transparent test tube and preincubated with 1.25 μL of GAPDH at the concentrations and for the times indicated in Table 2. The reaction mixture was added and the tube was introduced into the dark chamber. The baseline register by the equipment was turned on, at an integration interval of 1 second. After 30 seconds, 30 μL of PGK at the concentrations indicated in Table 2 was injected from the automatic burette. The light output was recorded for more 3 minutes. The Box Behnken design was performed using the concentrations in Table 2 for Pi, G3P, ADP, $MgCl_2$ and preincubation time plus the following reagents and enzymes: NAD^+ 0.3 mM, glycine 133 mM, GAPDH 3.9 $\mu g \cdot mL^{-1}$, D-LH_2 8.7 μM, LUC 6 $\mu g \cdot mL^{-1}$ and PGK 0.011 $\mu g \cdot mL^{-1}$.

2.4. Optimized coupled bioluminescent assays

2.4.1. General optimized protocol

The optimized assays were performed as described in Scheme 2. Briefly, DEA-NONOate solutions were prepared in NaOH 10 mM in capped polypropylene tubes. Solutions were diluted 1:20 in Pi in capped tubes and incubated at room temperature for 20 minutes. The reaction mixture contained 25.0 μL of Pi 30 mM, 2.50 μL of G3P 0.83 mM, 1.25 μL of NAD^+ 0.3 mM, 1.25 μL of ADP 0.3 mM, 6.25 μL of $MgCl_2$ 4.2 mM, 20.0 μL of glycine 133 mM, 1.25 μL of GAPDH 3.9 $\mu g \cdot mL^{-1}$, 5.00 μL of D-LH_2 8.7 μM and 2.50 μL of LUC 6 $\mu g \cdot mL^{-1}$. Five microliters of the DEA-NONOate solutions was transferred to transparent test tubes, the reaction mixture was added and the tubes were introduced into the dark chamber, one at a time. The baseline register by the equipment was turned on, at an integration interval of 1 second. After 30 seconds, 30 μL of PGK 0.011 $\mu g \cdot mL^{-1}$ was injected from the automatic burette. The light output was recorded for more 3 minutes.

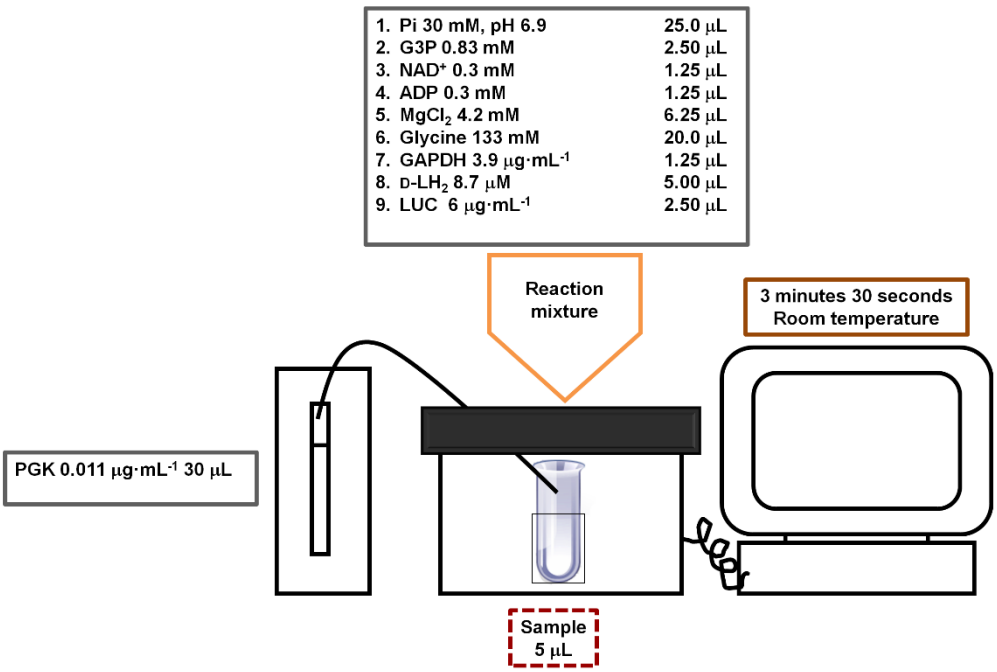

Scheme 2. Optimized coupled bioluminescent assay flowchart.

2.4.2. Method figures of merit

Preliminary calibration curves were made according to the procedure described in subsection 2.4.1. using DEA-NONOate standards corresponding to •NO concentrations from 0 to 1,000 µM (ten experimental points for each curve, each point measured in triplicate). To evaluate precisely the linear range of the method, calibration curves were made using DEA-NONOate standards corresponding to •NO concentrations from 0 to 100 nM (eleven experimental points for each curve, each point measured in triplicate). For the estimation of the method's repeatability, assays were made with DEA-NONOate standards corresponding to •NO concentrations at 10, 50 and 100 nM (each concentration measured in quintuplicate in each assay).

2.4.3. Samples' assays

2.4.3.1. Sample handling and maintenance

Resting whole saliva was freshly collected using a swab at least 90 minutes after a morning meal and stored in capped polypropylene tubes. A laboratorial culture of *Chlorella vulgaris* was inoculated in a 250-mL glass Erlenmeyer previously boiled in deionized water with Z8 medium, constant aeration and a 16h light / 8h dark photoperiod. Freshly prepared

culture medium was added to the Erlenmeyer once a week to replace evaporated medium. Aliquots were taken when the microalgae reached the exponential grown phase.

2.4.3.2. ATP quantitation assay

ATP was quantified in samples by luminometry through a calibration curve of ATP standard solutions. Briefly, ATP standard solutions ranging from 0 to 50 μM were prepared. To 5.00 μL of either samples or ATP standards 35.0 μL of $MgCl_2$ 4.2 mM was added in polypropylene transparent test tubes. Ten microliters of LUC 6 $\mu g \cdot mL^{-1}$ was added to the mixtures, the tubes were introduced into the dark chamber and the baseline register by the equipment was turned on, at an integration interval of 0.1 seconds. After 30 seconds, 50 μL of D-LH_2 8.7 μM was injected from the automatic burette. The light output was recorded for more 30 seconds.

2.4.3.3. Samples influence on LUC activity

The influence of the samples on LUC activity was assayed by luminometry as described in subsection 2.2.2.2. with the following alterations: 17.5 μL of $MgCl_2$ 4.2 mM and 17.5 μL of ATP 0.2 mM was added to 5.00 μL of either samples or deionized water as control.

2.4.3.4. •NO quantitation

2.4.3.4.1. Removal of endogenous ATP

Endogenous ATP in samples was removed by an enzymatic reaction using ATP sulfurylase, PPase and inorganic sulfate.[37] Eight microliters of $MgCl_2$ 3 mM, 4.00 μL of ATP sulfurylase 20 nM, 8.00 μL of PPase 30 nM and 10.00 μL of Na_2SO_4 500 μM were added to 20.0 μL of samples in a capped polypropylene tube for 5 minutes. Reaction was stopped by transferring the tubes to ice. The tubes were boiled in a water bath using an IMLAB ET Basic Yellow Line immersion thermostat (Boutersem, Belgium) for 2 minutes. Afterwards the tubes were allowed to cool, centrifuged (10,000 *x g*, 15 minutes) in an Eppendorf 5415D workbench centrifuge (Hamburg, Germany) and the supernatants were transferred to novel tubes. The remaining ATP was assayed according to the procedure described in subsection 2.4.3.2. with ATP standards ranging from 0 to 50 nM.

2.4.3.4.2. •NO quantitation using the optimized coupled bioluminescent assay

Assays were performed under the conditions described in subsection 2.4.1. through calibration curves and the method of standard additions. Analysis with calibration curves were performed by using DEA-NONOate standards corresponding to •NO concentrations from 0 to 100 nM (eleven experimental points for each curve, each point measured in triplicate) and 5.00 μL of each sample was measured in triplicate. Using the method of standard additions, 5.00 μL aliquots of sample were added to 5.00 μL of DEA-NONOate standards corresponding to •NO concentrations from 0 to 60 nM (seven experimental points for each curve, each point measured in triplicate). The volume of PGK was reduced to 25 μL. A blank, in which the sample plus DEA-NONOate standard was replaced with deionized water, was measured in triplicate.

2.4.3.4.3. •NO quantitation using a commercial kit

One hundred and fifty microliters of samples was pipetted to 5-mL capped polypropylene tubes and 700 μL of assay buffer was added. Blank tubes were made by replacing the samples with 850 μL of assay buffer. A calibration curve ranging from 0 to 31.75 μM of nitrate was made by pippeting 0, 20, 40, 60, 80 or 100 μL of the 1-mM nitrate standard solution to the tubes and completing the volume to 850 μL with assay buffer. The blank tubes received 1,150 μL of assay buffer and were put aside. To convert nitrate to nitrite, 50.0 μL of nitrate reductase and 50.0 μL of enzyme cofactor were added to the sample and calibration curve standard tubes. The tubes were covered and incubated for 1 hour. Fifty microliters of enhancer was added and the tubes were incubated for another 10 minutes. Finally, the reaction of nitrite to produce color was achieved by adding 500 μL of Griess reagent R1 plus 500 μL of Griess reagent 2 and incubating for 10 minutes. The content of each tube was transferred to a cuvette and the absorbance was read at λ_{max} 540 nm.

2.5. Statistical analysis

2.5.1. Preliminary assays

Note: Data treatment and calculations were performed with a Microsoft® Excel® spreadsheet.

2.5.1.1. Bioluminescent assays

2.5.1.1.1. ATP contamination in reagents and enzymes

Evaluation of the amount of ATP in reagents and enzymes was achieved by calculating, for each of them, the corrected peak of bioluminescence, expressed in relative light units (RLU). This value is obtained by selecting the maximum of the luminogram, corresponding to the moment at which D-LH_2 is injected into the mixture, and subtracting the baseline, defined as the average registered bioluminescence in the first 30 seconds of record (Figure 2A). Results are presented as mean ± standard deviation (SD) (*n* = 3), and percent of light emission compared to the control with ATP, of two independent assays.

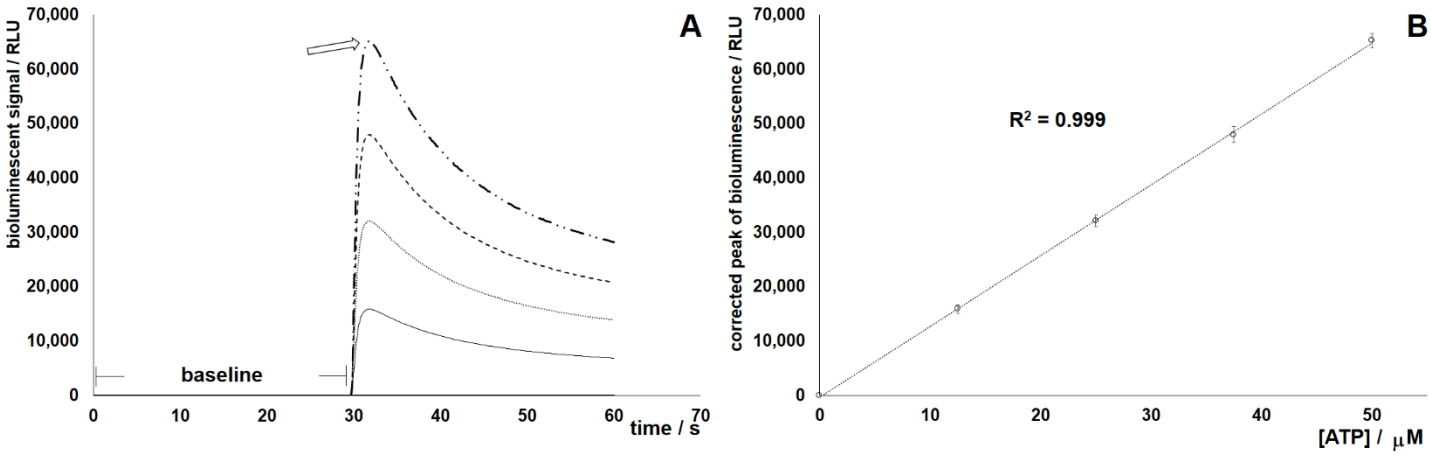

Figure 2. Bioluminescent ATP quantitation assay. (A) Typical luminogram and (B) the corresponding ATP calibration curve. The arrow in (A) indicates the peak of bioluminescence due to D-LH_2 injection. RLU, relative light units.

2.5.1.1.2. Reagents and enzymes influence on LUC activity

Evaluation of the influence of the reagents and enzymes on LUC activity was achieved by calculating, for each of them, the corrected peak of bioluminescence as defined in subsection 2.5.1.1.1.. Results are presented as mean ± SD (*n* = 3), and percent of light emission compared to the control with ATP, of two independent assays. Differences between the values were evaluated by one-way analysis of variance (ANOVA) followed by the Dunnett's multiple-comparison test.

2.5.1.1.3. Evaluation of the coupling

Evaluation of the inhibitory effect of •NO was achieved by calculating the initial rate of bioluminescence generation. The initial rate of bioluminescence generation was obtained by plotting the recorded bioluminescence, after the subtraction of the baseline, as a function of time (in seconds), and calculating the slope of the linear portion of the plot, which corresponds to the first 60 seconds of reaction (Figure 3A). Baseline was defined as the average recorded bioluminescence prior to the injection of PGK, which corresponds to the first 30 seconds of record. Results are presented as mean ± SD (n = 3), and percent of light emission compared to the positive control without DEA-NONOate, of two independent assays. Differences among the values were evaluated by one-way ANOVA followed by the Dunnett's multiple-comparison test.

2.5.2. Experimental designs calculations

Data obtained from the experimental designs was analyzed using The Unscrambler® software. For the Plackett-Burman screening design, an analysis of effect was performed. Results were expressed as effects overview, using the significance testing method center. For the Box Behnken optimization design, a response surface analysis, which includes a two-way ANOVA table, residuals calculation and response surface, was applied. From the ANOVA table, the analyzed parameters were the summary (evaluation of the global model), the variable (evaluation of the significance of each of the variables tested), the model check (evaluation of the global quadratic model) and the lack of fit (degree of misfitting of the experimental data to the model). All those parameters were evaluated through the F-ratios and the corresponding p-values. A p-value <0.05 was considered as statistically significant.

2.5.3. Optimized coupled bioluminescent assays

Note: Data treatment and calculations were performed with a Microsoft® Excel® spreadsheet.

2.5.3.1. General optimized protocol

Quantitation of •NO is achieved through calibration curves, set up by the method of least squares, by plotting the initial rate of bioluminescence generation, as described in subsection 2.5.1.1.3., as a function of the concentration of •NO standard solutions. Results

are presented as •NO concentration ± 95% confidence limits (95% CL) of the concentration, of at least two independent assays.

2.5.3.2. Method figures of merit

The method figures of merit linear range, LOD and limit of quantitation (LOQ) were obtained through calibration curves settled by the method of least squares (Figure 4). LOD and LOQ were calculated using the following criteria: LOD = (a + 3$S_{y/x}$) and LOQ = (a + 10$S_{y/x}$), where a is the intercept of the calibration curves and $S_{y/x}$ is the random error in the y-direction.[39] Precision was expressed as relative standard deviation (RSD) calculated with the expression (SD / mean) x 100 (n = 3), of two independent assays.

2.5.3.3. Samples' assays

2.5.3.3.1. ATP quantitation assay

Calibration curves were set up by the method of least squares by plotting the values of corrected peak of bioluminescence, as described in subsection 2.5.1.1.1., as a function of the concentration of the ATP standards (Figure 2B). Results are presented as ATP concentration ± 95% CL of the concentration, of two independent assays.

2.5.3.3.2. Samples influence on LUC activity

Evaluation of the influence of the samples on LUC activity was achieved as described in subsection 2.5.1.1.2..

2.5.3.3.3. •NO quantitation

2.5.3.3.3.1. Removal of endogenous ATP

Assessment of the remaining ATP in samples after enzymatic treatment was achieved as described in subsection 2.5.3.3.1..

2.5.3.3.3.2. •NO quantitation using the optimized coupled bioluminescent assay

The •NO content in samples was assayed by both calibration curves and the method of standard additions. Calibration curves were settled as described in subsection 2.5.3.1.. When the method of standard additions was used, curves were settled by plotting either the initial rate of bioluminescence generation as a function of the concentration of NO standard added (Figure 5A), as defined in subsection 2.5.1.1.3., or by calculating and plotting the corrected initial rate of bioluminescence generation using the expression {corrected initial rate of bioluminescence generation = [average signal of blank (in triplicate) – average signal of sample plus DEA-NONOate standard (in triplicate)]/average signal of blank}, wherein the blank was prepared without DEA-NONOate addition and without sample (Figure 5B). The concentration of •NO was given as the ratio between the intercept and the slope of the regression line in Figure 5B. Differences in the curves obtained from both methods were evaluated through *F*-tests using the slopes variances. Results are expressed as •NO concentration ± 95% CL of the concentration ($n = 3$), for two independent assays. Concentrations values obtained from both methods were compared through *t*-tests. A *p*-value <0.05 was considered as statistically significant.

2.5.3.3.3.3. •NO quantification using a commercial kit

The •NO content in samples was assayed by calibration curves, set up by the method of least squares, by plotting the corrected absorbance as a function of the concentration of nitrate standards. The corrected absorbance is defined as the measured value of absorbance to which the blank signal was subtracted. Results are presented as total nitrate/nitrite concentration ± 95% CL of the concentration, of two independent assays.

3. Results and discussion

3.1 Preliminary assays

The proposed method is based on the coupling of three enzymatic reactions, with the detection based on the linear decrease of bioluminescent signal due to a reduction in ATP generation. Before proceeding to its optimization, characterization and application to samples, preliminary assays were made.

The activity of both of the enzymes GAPDH and PGK, as well as the release of •NO from DEA-NONOate, were evaluated through UV-vis spectrophotometry. The GAPDH

catalyzed reaction produces NADH + H^+ (Scheme 1), which presents an absorption band at λ_{max} 340 nm. The continuous production of NADH + H^+ leads to an increase in absorbance monitored at this wavelength. In the absence of GAPDH and the presence of PGK (blank GAPDH), the absorbance is constant and the values are reduced to a minimum, indicating no production of NADH + H^+ (Supplementary data, Figure S1). In the presence of GAPDH and the absence of PGK (blank PGK), the absorbance is still constant, but with values about ten times higher. This may indicate that some NADH + H^+ was produced by GAPDH, but because PGK was not available to further drive the reaction, the concentration remained constant. Only with both GAPDH and PGK in the reaction mixture (test) an increase in absorbance over time was observed, indicating continuous production of NADH + H^+. It was then confirmed the integrity and correct coupling of the enzymes.

Intact DEA-NONOate has an absorption band at λ_{max} 250 nm. When the molecule dissociates to the free amine and •NO, the absorbance registered at this wavelength decreases over time. In Supplementary data Figure S2, a representative DEA-NONOate decomposition spectrum of a solution corresponding to 10 μM of •NO diluted 1:20 in Pi is shown. The compound is completed dissociated within 15 minutes, as the absorbance reaches zero, indicating that DEA-NONOate solution is in good conditions.

As already mentioned, it is mandatory to avoid exogenous ATP because it will interfere with the assay. Furthermore, because the method involves decrease in light detection, it is important to verify that this is not due to an inhibitory effect of some of the reagents or enzymes on LUC. With this aim, two bioluminescent assays were devised. One of the assays aimed to verify any interference of the emitted light in the presence of reagents or enzymes compared to a control without them. The other was done without exogenously added ATP, so that any produced light would be due to ATP contamination within reagents or enzymes. Results showed no contamination of ATP in reagents and enzymes (Supplementary data, Table S1). The maximum value registered was from ADP but, even so, it was only 0.71% of the control. Regarding the influence on LUC activity, it was detected a slightly inhibition of light production from Pi (90% of the light emitted by the control) and DEA-NONOate (93% of the light emitted by the control) (Supplementary data, Figure S3). Because pure NAOH was not interfering (Figure S3), the effect was due to DEA-NONOate itself or some •NO released upon contact to LUC, since the enzyme is at a lower pH value (7.5) compared to the DEA-NONOate solution (about 12). It was reported that •NO could inhibit the transcription of the *luc* gene,[43] but no reports of its action on the mature enzyme is available, to the best of our knowledge. Furthermore, it was demonstrated that •NO activate the flashing of fireflies *in vivo*, but only through the inhibition of O_2 usage by mitochondria in photocytes, and not due to a direct action upon the

enzyme.[44-48] The inhibition of Pi was not expected, since this buffer is used in bioluminescent assays with LUC.[49] The effect may be due to the Pi-induced precipitation of Mg^{2+} cations.[50] Pi has three functions in this assay, as a source of phosphate ions for the coupled reaction, as a preferential buffer for GAPDH and as a medium to DEA-NONOate dissociation. Its substitution for another buffer with all these features was not possible. The last preliminary assay was to evaluate, by luminometry, the enzymatic reactions coupling and the effect of •NO on GAPDH (Figure 3). The choice for D-LH_2 and LUC concentration values was based on solubility constraints of D-LH_2 and the costs of the enzyme, respectively. The concentrations of the remaining reagents and enzymes were based on the 'Enzymatic Assay of 3-Phosphoglycerate Phosphokinase (EC 2.7.2.3) from Baker's Yeast' protocol by the manufacturer. Light is produced in the presence of the complete reaction mixture and absence of both •NO and ATP (Figure 3A). By eliminating GAPDH, no light is produced, confirming that ATP is produced *via* the coupled reactions. Addition of •NO significantly reduced ($p < 0.05$) light output. At 1 nM •NO, light is reduced to about 93% of that of the control, and the percentage is reduced to only 25% when •NO concentration is raised to 1 μM (Figure 3B). However, when raising again the •NO concentration to 1 mM, the percentage remains at 25% of the control, probably due to enzyme saturation at the tested concentrations of reagents and enzymes (Figure 3B). Thus, the possible working range for •NO quantitation, using the method's chosen conditions, lies between the nanomolar up to the low micromolar range.

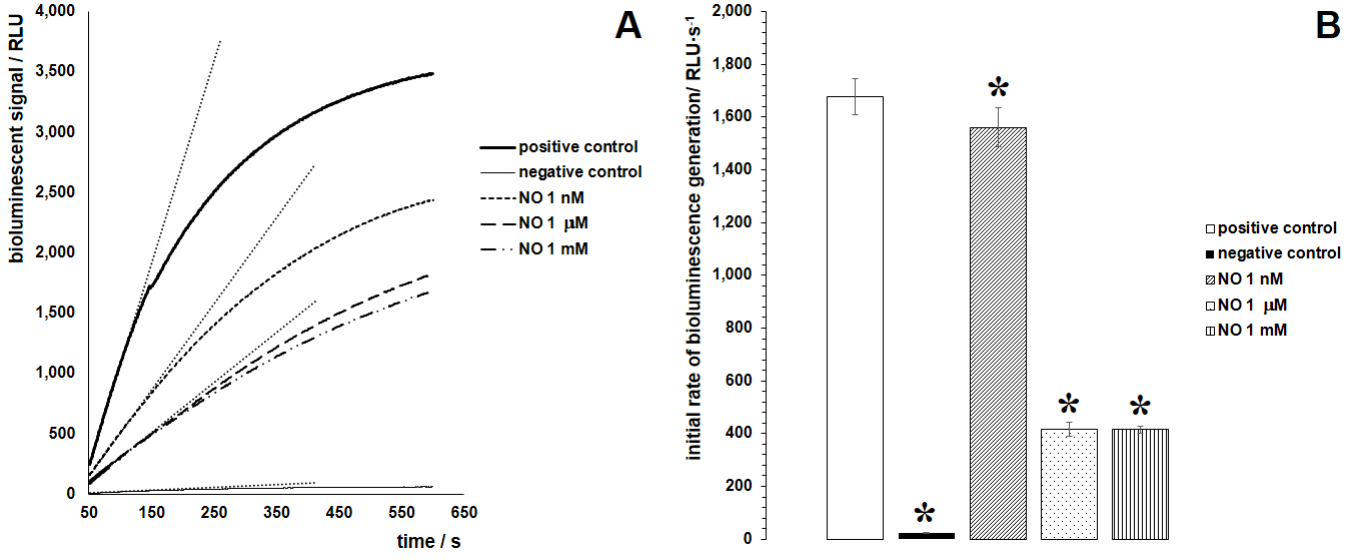

Figure 3. Preliminary evaluation of the enzymatic reactions coupling and the effect of •NO on GAPDH. (A) Representative coupled bioluminescent assay luminograms and (B) the corresponding values of initial rate of bioluminescence generation. Positive controls were made in the absence of •NO, while negative controls were made in the absence of GAPDH. Asterisks indicate statistically significant difference as compared with the positive control ($p < 0.05$). The dashed lines in (A) indicate the linear portion of the luminograms, whose slopes correspond to the initial rates of bioluminescence generation (see Experimental for further details). RLU, relative light units.

3.2. Experimental designs

On the basis of the preliminary results, the method was optimized using an experimental design methodology. The overall optimization process included two steps, a screening, to identify which factors have statistically the most influence on the method's response, and the subsequent determination of the levels at which these factors must be kept to optimize the method's response. Taking into account the various reagents and steps in the method, eleven factors were initially selected for screening and a Plackett-Burman design was selected (Table 2). The concentrations of the factors (reagents and enzymes) were the same as in the preliminary coupled assay, but volumes and the percentage of Pi were reduced, from a final volume of 1,000 μL to a final volume of 100 μL, and to 45% of Pi (v/v) to 25%, respectively. When testing the effect of DEA-NONOate on LUC activity, a relatively large volume of this compound was tested, 20 μL in 100-μL final reaction volume, or a 1:5 dilution factor. However, the •NO releasing conditions in the experimental design assay require a higher dilution factor: DEA-NONOate is diluted 1:20 in Pi, then 5 μL of this solution is assayed in a final reaction volume of 100 μL. These conditions are expected to reduce the interfering effect on LUC. Because PGK was injected using an automatic burette, it was not possible to largely reduce its volume, so that the volume of PGK was altered from 50 μL in the preliminary assay to 30 μL. Furthermore, the time of reaction was reduced from 10 minutes in the preliminary assay to 3 minutes and 30 seconds in the experimental design assay, because it was verified that a direct proportion of light production over time only occurs in the first minutes of reaction. Results showed that, in the presence of 5 nM of •NO and using the testing method Center, the concentrations of Pi (--), G3P (-), ADP (++), $MgCl_2$ (+), and the pre-incubation time (-) were likely the most significant factors (Supplementary data, Table S2). The factors with minus signal exerted a negative influence, that is, the higher their value, the lower was the response, whereas the plus signal indicated that the higher their value, the higher was the response. The number of minus or plus signals indicates the extension of their effects. Overall, the factors that could boost light generation (ADP and $MgCl_2$) revealed a positive effect, whereas those which could impair ATP generation (preincubation time) had a negative one. Once again the negative influence of Pi over the method's response was verified, together with a negative effect from G3P, which does not have a clear pattern in either enhancing or reducing the ATP generation (Table S2).

With this information, a Box Behnken optimization design was built to uncover the best Pi, G3P, ADP and $MgCl_2$ concentrations, together with the best preincubation time,

and to discover if their interactions are also important for the method's response. The remaining factors were kept at their intermediary concentrations. From the ANOVA table (Supplementary data, Table S3), it was verified that only the ADP concentration ([ADP], C), the preincubation time (E) and the quadratic factor preincubation time x preincubation time (EE) are important factors, showing significant *F*-ratios ($p<0.05$). According to their *F*-ratios, the model is significant whereas the lack of fit is not ($p<0.05$ and $p>0.05$, respectively), which shows that the experimental measurements fit the model. The response surface curve (Supplementary data, Figure S4) shows that the concentration of ADP should be kept at the highest value tested (0.36 mM) to obtain the maximum signal (bioluminescence emission), whereas the preincubation time should be kept to a minimum. Taking these into consideration, the concentrations were kept to the central values tested in the screening design with the exceptions of ADP, whose concentration was raised to 0.3 mM, and Pi which, although not considered a significant factor according to the ANOVA results, the concentration was lowered to 30 mM to avoid any inhibitory effect. To the sake of simplicity, preincubation was excluded from the optimized protocol.

3.3. Optimized coupled bioluminescent assay

Using the optimized conditions, the coupled bioluminescent assay was characterized in terms of linear range, LOD and LOQ and repeatability at low, medium and high concentrations of •NO.

The preliminary assay (Figure 3) indicated that the method is responsive in the nano- to low micromolar range, yet the precise interval was not known. To account for it, exploratory calibration curves in a relatively enlarged interval (0 to 1,000 μM of •NO) were performed (Figure 4). It was verified that a linear trend occurs between 0 to 100 nM (Figure 4, inset). Novel curves were set up in this interval, to which LOD and LOQ were calculated as 6.5 and 17.5 nM of •NO, respectively. The repeatability of the method was estimated from the relative standard deviation, and showed values of 3.84% at 20 nM, 5.70% at 50 nM and 4.28% at 100 nM of •NO (Supplementary data, Figure S5).

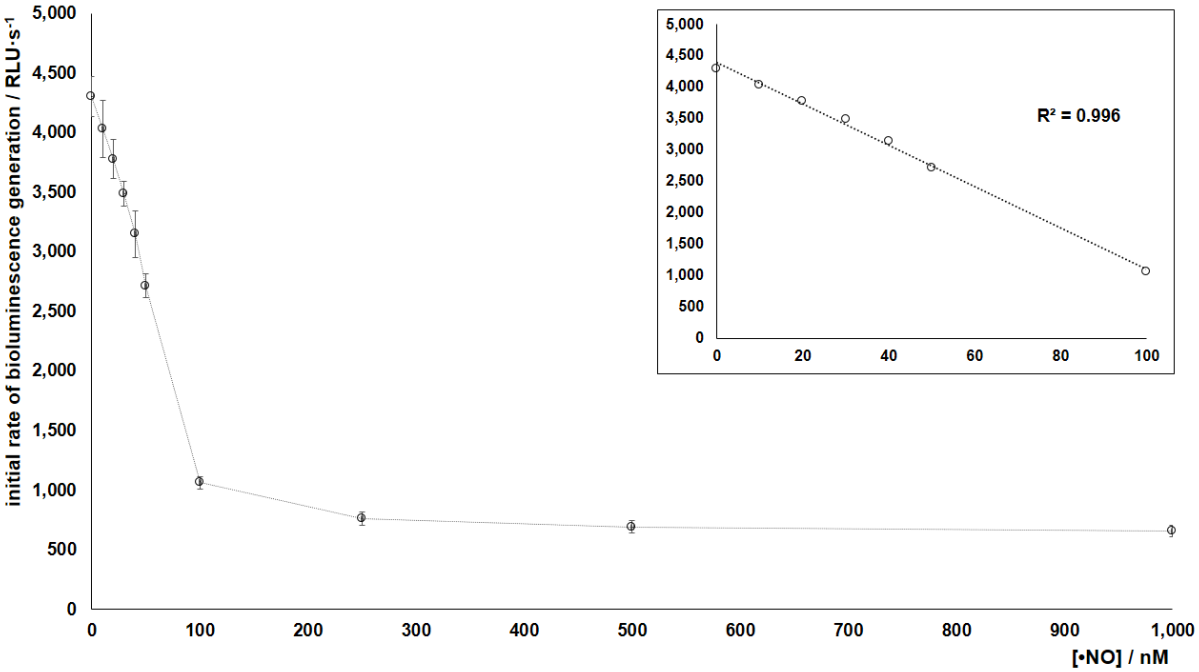

Figure 4. Representative exploratory curve for •NO. *Inset* Amplification of the zone with linear response. RLU, relative light units.

As a proof-of-principle, human whole saliva and microalgae culture medium were assayed using this new optimized method. These samples were chosen as examples of a clinical application, in the case of saliva, and as an important technological and biological product, the microalgae. Proceeding like in the preliminary assays, those samples were tested for their possible effect on LUC activity and their content in ATP through ATP calibration curves (Figure 2B). No interference in LUC activity was observed (data not shown). On the other hand, and as expected, their content in ATP is in the low micromolar range, 916 nM for saliva and 864 nM for microalgae culture medium. Before the quantitation of •NO, samples were subjected to an enzymatic assay to remove ATP. After the reaction, the ATP content dropped to 19 nM in saliva and 7 nM in microalgae culture medium (data not shown), which could still interfere with the method. To test if this or other interference were exerted by the samples' matrices, the coupled bioluminescent assay was performed by either plain calibration curves and curves set up by the method of standard additions (Figure 5, example for microalgae culture medium). The •NO content is presented in Table 3. The results obtained by either method (calibration curve or standard additions) are statistically different ($p<0.05$), which confirms matrix effects. To avoid such effects, it is recommended that biological samples be quantified by the method of standard additions. The LOD and LOQ for the curves obtained by this methodology are similar to the values

obtained in the method's characterization using simple calibration curves, 5 and 16 nM for saliva and 4 and 14 nM for microalgae culture medium, respectively.

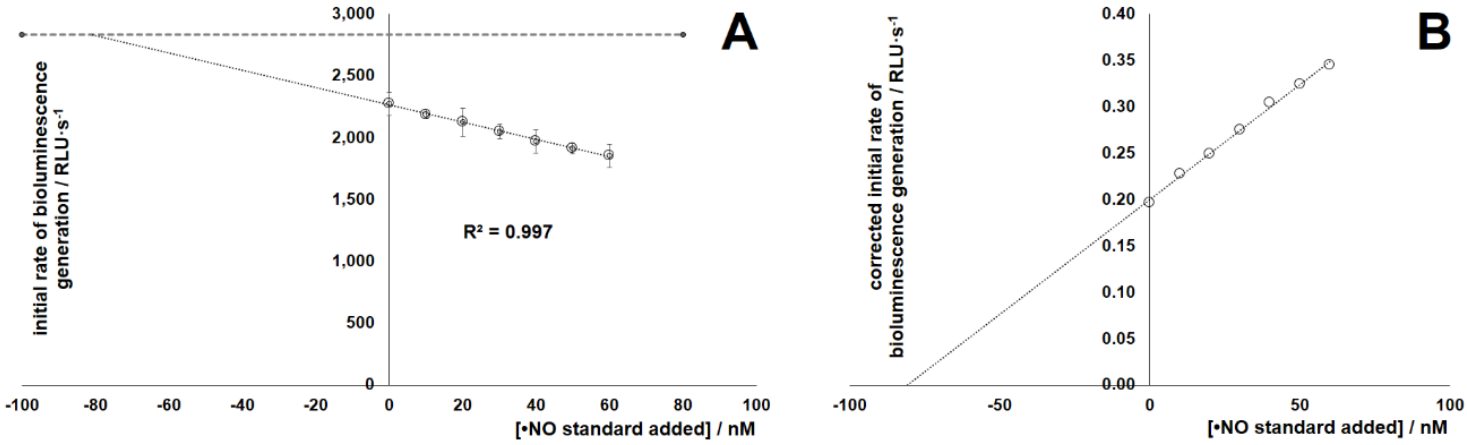

Figure 5. Representative standard additions curves for the •NO assay in microalgae culture medium. (A) Standard additions curve using the initial rate of bioluminescence generation. (B) Standard additions curve using the corrected initial rate of bioluminescence generation. The horizontal dashed line in (A) indicates the value of the blank (without both sample and DEA-NONOate standard addition). RLU, relative light units.

Finally, for comparison purposes, samples were tested using a commercial •NO detection kit. This kit is an indirect spectrophotometric method relying on the conversion of nitrate to nitrite followed by the Griess reaction. As the method measures total nitrate/nitrite, higher values compared to the bioluminescent assay were expected. In fact, from calibration curves, the total nitrate/nitrite content in samples were in the micromolar range (Table 3). The LOD and LOQ of the curves were calculated as 0.8 and 2.7 μM, respectively, which are close to the LOD value of 1 μM according to the manufacturer. The large difference in •NO amount obtained by the two methods stresses the importance of direct methods to measure •NO, instead of its metabolite products. Furthermore the method, albeit simple to perform, is much less sensitive compared to the presented method, demands more volume of reagents and takes a longer time to be concluded.

Table 3. •NO quantitation in samples using the optimized coupled bioluminescent assay and a commercial kit

Sample	•NO / total nitrate and nitrite concentration		
	Coupled bioluminescent assay / nM		Commercial kit / μM
	Calibration curve	Standard additions	Calibration curve
Saliva	67.24 ± 0.03	60.79 ± 7.13	22.00 ± 0.02
Microalgae culture medium	85.30 ± 0.04	80.75 ± 7.39	69.71 ± 0.06

4. Conclusions

This chapter presented the establishment of an optimized coupled bioluminescent assay for •NO quantitation. The novelty of this assay is not only the use of coupled enzymatic reactions with detection by luminometry, but also its optimization based on an experimental design methodology and test in real samples. This optimized method is sensitive, safe, simple to perform and economic despite the use of several reagents and enzymes because of their reduced volumes. All reagents and enzymes are commercially available, do not need further purification prior to use and their solutions are stable for several months when stored at -20 ºC. Although we used a single-tube luminometer, the method is applicable to multiplate assay. Portability of the assay for *in situ* analysis is also possible, albeit preferentially for samples with simpler matrices, like water, to avoid or minimize the pre-treatment steps.

References

(1) Butler, A.; Nicholson, R. *Life*, *Death and Nitric Oxide*; The Royal Society of Chemistry: Padstow, 2003.

(2) Bredt, D. S. Endogenous nitric oxide synthesis: biological functions and pathophysiology. *Free Radic*. *Res*. **1999**, *31*, 577-596.

(3) Lamattina, L.; García-Mata, C.; Graziano, M.; Pagnussat, G. Nitric oxide: the versatility of an extensive signal molecule. *Annu*. *Rev*. *Plant Biol*. **2003**, *54*, 109-136.

(4) Thomas, D. D.; Ridnour, L. A.; Isenberg, J. S.; W. Flores-Santana, W.; Switzer, C. H.; Donzelli, S.; Hussain, P.; Vecoli, C.; Paolocci, N.; Ambs, S.; Colton, C. A.; Harris, C. C.; Roberts, D. D.; Wink, D. A. The chemical biology of nitric oxide: implications in cellular signaling. *Free Radic*. *Biol*. *Med*. **2008**, *45*, 18-31.

(5) Nicholas, D. J. D.; Nason, A. Determination of nitrate and nitrite. *Methods Enzymol*. **1957**, *3*, 981-984.

(6) Gilchrist, M.; Winyard, P. G.; Benjamin, N. Dietary nitrate – good or bad?. *Nitric Oxide-Biol*. *Chem*. **2010**, *22*, 104-109.

(7) Simões, E. F. C.; Leitão, J. M. M.; Esteves da Silva, J. C. G. NO fluorescence sensing by europium tetracyclines complexes in the presence of H_2O_2. *J*. *Fluoresc*. **2013**, *23*, 681-688.

(8) Ridnour, L. A.; Sim, J. E.; Hayward, M. A.; Wink, D. A.; Martin, S. M.; Buettner, G. R.; Spitz, D. R. A spectrophotometric method for the direct detection and quantitation of nitric oxide, nitrite, and nitrate in cell culture media. *Anal*. *Biochem*. **2000**, *281*, 223-229.

(9) Borgmann, S. Electrochemical quantification of reactive oxygen and nitrogen: challenges and opportunities. *Anal*. *Bioanal*. *Chem*. **2009**, *394*, 95-105.

(10) Trouillon, R. Biological applications of the electrochemical sensing of nitric oxide: fundamentals and recent developments. *Biol*. *Chem*. **2012**, *394*, 17-33.

(11) Bedioui, F.; Griveau, S. Electrochemical detection of nitric oxide: assessement of twenty years of strategies. *Electroanalysis* **2013**, *25*, 587-600.

(12) Fontijn, A.; Sabadell, A. J.; Ronco, R. J. Homogeneous chemiluminescent measurement of nitric oxide with ozone. Implications for continuous selective monitoring of gaseous air pollutants. *Anal*. *Chem*. **1970**, *42*, 575-579.

(13) Bates, J. N. Nitric oxide measurement by chemiluminescence detection. *Neuroprotocols* **1992**, *1*, 141-149.

(14) Tsuchiya, K.; Takasugi, M.; Minakuchi, K.; Fukuzawa, K. Sensitive quantitation of nitric oxide by EPR spectroscopy. *Free Radic*. *Biol*. *Med*. **1996**, *21*, 733-737.

(15) van Faassen, E.; Vanin, A. NO trapping in biological systems with a functionalized zeolite network. *Nitric Oxide-Biol*. *Chem*. **2006**, *15*, 233-240.

(16) Silverman, D. N.; Tu, C. Aqueous measurement of nitric oxide using membrane inlet mass spectrometry. *Methods*. *Mol*. *Biol*. **2011**, *704*, 105-114.

(17) Kannan, P.; John, S. A. Highly sensitive electrochemical determination of nitric oxide using fused spherical gold nanoparticles modified ITO electrode. *Electrochim*. *Acta* **2010**, *55*, 3497-3503.

(18) Madasamy, T.; Pandiaraj, M.; Balamurugan, M.; Karnewar, S.; Benjamin, A. R.; Venkatesh, K. A.; Vairamani, K.; Kotamraju, S.; Karunakaran, C. Virtual electrochemical nitric oxide analyzer using copper, zinc superoxide dismutase immobilized on carbon nanotubes in polypyrrole matrix. *Talanta* **2012**, *100*, 168-174.

(19) Yap, C. M.; Xu, G. Q.; Ang, S. G. Amperometric nitric oxide sensor based on nanoporous platinum phthalocyanine modified electrodes. *Anal*. *Chem*. **2013**, *85*, 107-113.

(20) Zan, X.; Fang, Z.; Wu, J.; Xiao, F.; Huo, F.; Duan, H. Freestanding graphene paper decorated with 2D-assembly of Au@Pt nanoparticles as flexible biosensors to monitor live cell secretion of nitric oxide. *Biosens*. *Bioelectron*. **2013**, *49*, 71-78.

(21) Wang, L.; Hu, P.; Deng, X.; Wang, F.; Chen, Z. Fabrication of electrochemical NO sensor based on nanostructured film and its application in drug screening. *Biosens*. *Bioelectron*. **2013**, *50*, 57-61.

(22) Kumar, N.; Bhalla, V.; Kumar, M. Recent developments of fluorescent probes for the detection of gasotransmitters (NO, CO and H_2S), *Coord*. *Chem*. *Rev*. **2013**, *257*, 2335-2347.

(23) Chen, J. – B.; Zhang, H. – X.; Guo, X. – F.; Wang, H.; Zhang, H. – S. "Off-on" red-emitting fluorescent probes with large Stokes shifts for nitric oxide imaging in living cells. *Anal*. *Bioanal*. *Chem*. DOI 10.1007/s00216-013-7177-6.

(24) Hong, H.; Sun, J.; Cai, W. Multimodality imaging of nitric oxide and nitric oxide synthases. *Free Radic*. *Biol*. *Med*. **2009**, *47*, 684-698.

(25) Woldman, Y. Y.; Sun, J.; Zweier, J. L.; Khramtsov, V. V. Direct chemiluminescence detection of nitric oxide in aqueous solutions using the natural nitric oxide target soluble guanylyl cyclase. *Free Radic*. *Biol*. *Med*. **2009**, *47*, 339-1345.

(26) Zhang, X.; Kim, W. – S.; Hatcher, N.; Potgieter, K.; Moroz, L. L.; Gillette, R.; Sweedler, J. V. Interfering with nitric oxide measurements - 4,5-diaminofluorescein reacts with dehydroascorbic acid and ascorbic acid. *J*. *Biol*. *Chem*. **2002**, *277*, 48472-48478.

(27) Uhlenhut, K.; Högger, P. Pitfalls and limitations in using 4,5-diaminofluorescein for evaluating the influence of polyphenols on nitric oxide release from endothelial cells. *Free Radic*. *Biol*. *Med*. **2012**, *52*, 2266-2275.

(28) Sharifi, S.; Behzadi, S.; Laurent, S.; Forrest, M. L.; Stroeve, P.; Mahmoudi, M. Toxicity of nanomaterials. *Chem*. *Soc*. *Rev*. **2012**, *41*, 2323-2343.

(29) Pelaz, B.; Charron, G.; Pfeiffer, C.; Zhao, Y.; de la Fuente, J. M.; Liang, X. – J.; Parak, W. J.; del Pino, P. Interfacing engineered nanoparticles with biological systems: anticipating adverse nano-bio interactions. *Small* **2013**, *9*, 1573-1584.

(30) Corey, M. J. *Coupled Bioluminescent Assays – Methods*, *Evaluations*, *and Applications*; John Wiley and Sons: Hoboken, N.J., 2009.

(31) Dimmeler, S.; Lottspeich, F.; Brüne, B. Nitric oxide causes ADP-ribosylation and inhibition of glyceraldehyde-3-phosphate dehydrogenase. *J*. *Biol*. *Chem*. **1992**, *267*, 16771-16774.

(32) Dimmeler, S.; Brüne, B. Nitric oxide preferentially stimulates auto-ADP-ribosylation of glyceraldehyde-3-phosphate dehydrogenase compared to alcohol or lactate dehydrogenase. *FEBS Lett*. **1993**, *315*, 21-24.

(33) Mohr, S.; Stamler, J. S.; Brüne, B. Mechanism of covalent modification of glyceraldehyde-3-phosphate dehydrogenase at its active site thiol by nitric oxide, peroxynitrite and related nitrosating agents. *FEBS Lett*. **1994**, *348*, 223-227.

(34) Itoga, M.; Tsuchiya, M.; Ishino, H.; Shimoyama, M. Nitric oxide-induced modification of glyceraldehyde-3-phosphate dehydrogenase with NAD^+ is not ADP-ribosylation. *J*. *Biochem*. **1997**, *121*, 1041-1046.

(35) Mohr, S.; Hallak, H.; de Boitte, A.; Lapetina, E. G.; Brüne, B. Nitric oxide-induced *S*-glutathionylation and inactivation of glyceraldehyde-3-phosphate dehydrogenase. *J*. *Biol*. *Chem*. **1999**, *274*, 9427-9430.

(36) Broniowska, K. A.; Hogg, N. Differential mechanisms of inhibition of glyceraldehyde-3-phosphate dehydrogenase by *S*-nitrosothiols and NO in cellular and cell-free conditions. *Am*. *J*. *Physiol*.-*Heart Circul*. *Physiol*. **2010**, *299*, H1212-H1219.

(37) Marques, S. M.; Esteves da Silva, J. C. G. An optimized bioluminescent assay for inorganic sulfate quantitation in freshwater. *Anal*. *Methods* **2013**, *5*, 1317-1327.

(38) Fontes, R.; Fernandes, D.; Peralta, F.; Fraga, H.; Maio, I.; Esteves da Silva, J. C. G. Pyrophosphate and tripolyphosphate affect firefly luciferase luminescence because they act as substrates and not as allosteric effectors. *FEBS J*. **2008**, *275*, 1500-1509.

(39) Miller, J. N.; Miller, J. C. *Statistics and Chemometrics for Analytical Chemistry*, 5th ed.; Pearson Prentice Hall: Gosport, 2005.

(40) Keefer, L. K.; Nims, R. W.; Davies, K. M.; Wink, D. A. “NONOates” (1-substituted diazen-1-ium-1, 2-diolates) as nitric oxide donors: convenient nitric oxide dosage forms. *Methods Enzymol*. **1996**, *268*, 281-293.

(41) Li, Q.; Lancaster Jr., J. R. Calibration of nitric oxide flux generation from diazeniumdiolate ·NO donors. *Nitric Oxide-Biol*. *Chem*. **2009**, *21*, 69-75.

(42) Bowie, L. J. Synthesis of firefly luciferin and structural analogs. *Methods Enzymol*. **1978**, *57*, 15-28.

(43) Fan, X.; Roy, E.; Zhu, L.; Murphy, T. C.; Kozlowski, M.; Nanes, M. S.; Rubin, J. Nitric oxide donors inhibit luciferase expression in a promoter-independent fashion. *J*. *Biol*. *Chem*. **2003**, *278*, 10232-10238.

(44) Trimmer, B. A.; Aprille, J. R.; Dudzinski, D. M.; Lagace, C. J.; Lewis, S. M.; Michel, T.; Qazi, S.; Zayas, R. M. Nitric oxide and the control of firefly flashing. *Science* **2001**, *292*, 2486-2488.

(45) Greenfiel, M. D. Missing link in firefly bioluminescence revealed: NO regulation of photocyte respiration. *Bioessays* **2001**, *23*, 992-995.

(46) Timmins, G. S.; Robb, F. J.; Wilmot, C. M.; Jackson, S. K.; Swartz, H. M. Firefly flashing is controlled by gating oxygen to light-emitting cells. *J*. *Exp*. *Biol*. **2001**, *204*, 2795-2801.

(47) Ghiradella, H.; Schmidt, J. T. Fireflies at one hundred plus: a new look at flash control. *Integr*. *Comp*. *Biol*. **2004**, *44*, 203-212.

(48) Aprille, J. R.; Lagace, C. J.; Modica-Napolitano, J.; Trimmer, B. A. Role of nitric oxide and mitochondria in control of firefly flash. *Integr*. *Comp*. *Biol*. **2004**, *44*, 213-219.

(49) van Lune, H.; Bruggeman, J. J. Luciferase assay system. Patent EP 1724359 A1, November 22, 2006.

(50) Barnes, W. M.; Rowlyk, K. R. Magnesium precipitate methods for magnesium dependent enzymes. U. S. Patent application 2003/0027,196, February 6, 2003.

Nitric oxide quantitative assay by a glyceraldehyde 3-phosphate dehydrogenase/phosphoglycerate kinase/firefly luciferase optimized coupled bioluminescent assay

SUPPLEMENTARY DATA

Content

Table S1. Evaluation of the ATP contamination in the reagents and enzymes used in the coupled bioluminescent assay

Reagent or enzyme	**Bioluminescence / RLU[a]**	**% of the control (ATP)**
ATP	1,062,116 ± 51,808	100
D-LH_2 without LUC	12 ± 2	0.001
D-LH_2	13 ± 2	0.001
DEA-NONOate	694 ± 42	0.07
Pi	21 ± 2	0.002
G3P	1,305 ± 34	0.12
NAD^+	81 ± 9	0.01
ADP	7,522 ± 134	0.71
$MgCl_2$	387 ± 24	0.04
Glycine	98 ± 8	0.01
GAPDH	85 ± 4	0.008
PGK	76 ± 3	0.01

[a] Values are expressed as mean ± SD (n = 3).

Table S2. Center significance testing method results for the Plackett-Burman screening design

Factor	Effect in the presence of •NO 5 nM[a]
[Pi] / mM	--
[G3P] / mM	-
[NAD^+] / mM	NS
[ADP] / mM	++
[$MgCl_2$] / mM	+
[Glycine] / mM	NS
[GAPDH] / $\mu g \cdot mL^{-1}$	NS
[D-LH_2] / μM	NS
[PGK] / $\mu g \cdot mL^{-1}$	NS
[LUC] / $\mu g \cdot mL^{-1}$	NS
Preincubation time / minutes	-

[a] Significance of each effect at 95% level: NS, not significant; from + to +++, positive effect; from - to - - -, negative effect.

Table S3. Analysis of Variance (ANOVA) table for the Box Behnken optimization design

	SS[a]	DF	MS	*F*-ratio	*p*-value	*B*-coefficient	SE_b
Summary							
Model	4.580×10^5	20	2.290×10^4	4.350	0.0004		
Error	1.263×10^5	24	5.264×10^3				
Adjusted total	5.843×10^5	44	1.328×10^4				
Variable							
Intercept	1.453×10^6	1	1.453×10^6	275.944	0.0000	539.000	32.447
[Pi] (A)	7.439×10^3	1	7.439×10^3	1.413	0.2462	-0.532	0.448
[G3P] (B)	0.250	1	0.250	4.749×10^{-5}	0.9946	-0.185	26.872
[ADP] (C)	2.318×10^5	1	2.318×10^5	44.042	0.0000	743.055	111.967
[$MgCl_2$] (D)	60.062	1	60.062	1.141×10^{-2}	0.9158	0.567	5.304
Preincubation time (E)	1.665×10^5	1	1.665×10^5	31.622	0.0000	-13.600	2.418
AB	6.250	1	6.250	1.187×10^{-3}	0.9728	-0.455	13.192
AC	650.250	1	650.250	0.124	0.7283	4.636	13.192
AD	156.250	1	156.250	2.968×10^{-2}	0.8647	2.273	13.192
AE	1.225×10^3	1	1.225×10^3	0.233	0.6339	-6.364	13.192
BC	9.000	1	9.000	1.710×10^{-3}	0.9674	0.545	13.192
BD	182.250	1	182.250	3.462×10^{-2}	0.8540	-2.455	13.192
BE	16.000	1	16.000	3.039×10^{-3}	0.9565	-0.727	13.192
CD	42.250	1	42.250	8.062×10^{-3}	0.9294	-1.182	13.192
CE	121.000	1	121.000	2.299×10^{-2}	0.8808	2.000	13.192
DE	25.000	1	25.000	4.749×10^{-3}	0.9456	-0.909	13.192
AA	2.438×10^3	1	2.438×10^3	0.463	0.5026	-6.295	9.250
BB	4.975×10^3	1	4.975×10^3	0.945	0.3407	-8.992	9.250
CC	1.905×10^4	1	1.905×10^4	3.620	0.0692	-17.598	9.250
DD	1.415×10^3	1	1.415×10^3	0.269	0.6089	4.795	9.250
EE	2.649×10^4	1	2.649×10^4	5.032	0.0344	-20.750	9.250
Model check							
Main	4.058×10^5	5	8.116×10^4				
Int	2.433×10^3	10	243.325	4.622×10^{-2}	1.0000		
Int + squ	4.973×10^4	5	9.947×10^3	1.890	0.1336		
Squ	4.973×10^4	5	9.947×10^3		0.1336		
Error	1.263×10^5	24	5.264×10^3				
Lack of fit							
Lack of fit	1.201×10^5	20	6.007×10^3	3.879	0.0985		
Pure error	6.194×10^3	4	1.549×10^3				
Total error	1.263×10^5	24	5.264×10^3				

[a] SS, Sum of squares; DF, degrees of freedom; MS, mean squares (ratio between SS and DF); *F*-ratio, ratio between 'between-measures' MS and 'within-measures' (residual) MS; *p*-value, probability of getting the *F*-ratio under the null hypothesis at 95%; *B*-coefficient, regression coefficient from a multiple linear regression analysis; SE_b, standard error of b.

.

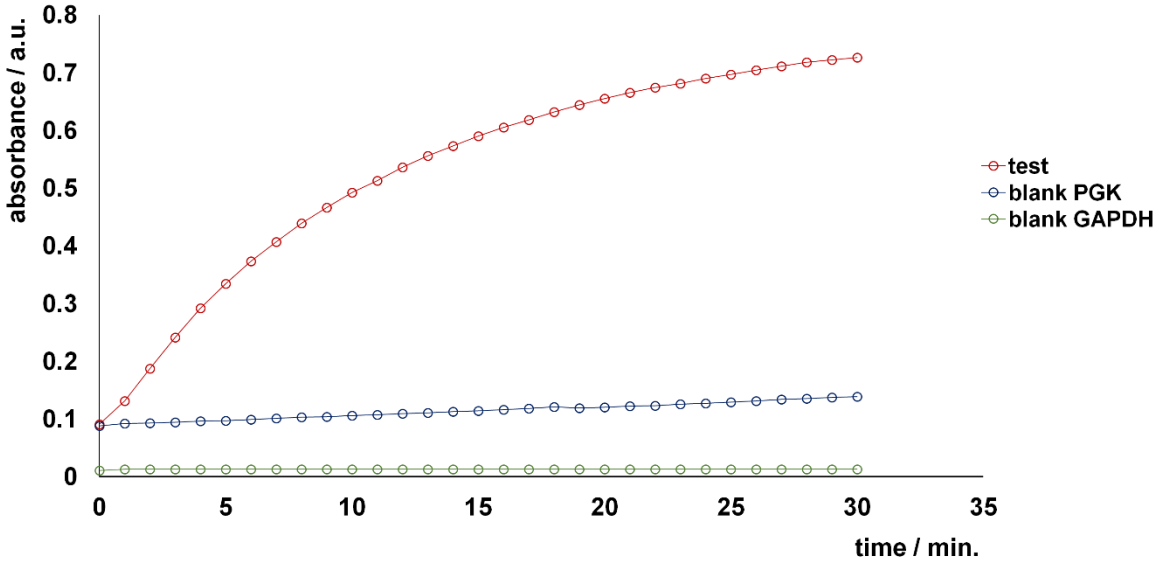

Figure S1. UV-vis absorbance spectra of GAPDH and PGK coupled reactions generating NADH + H^+. a.u., arbitrary units.

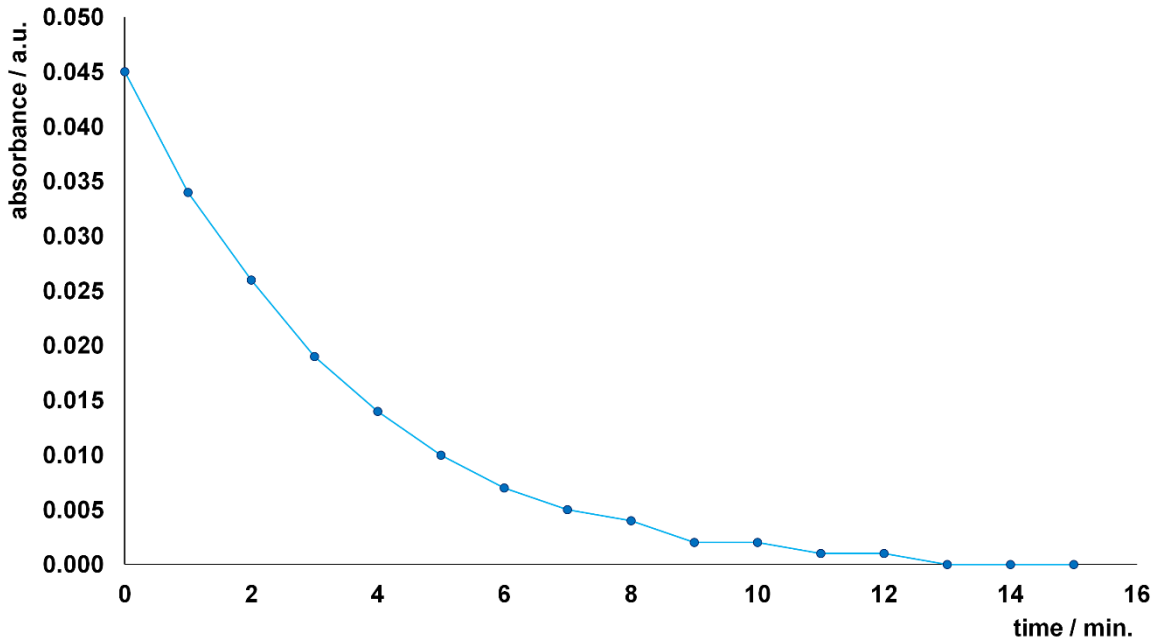

Figure S2. UV-vis absorbance spectrum of the decomposition of DEA-NONOate. a.u., arbitrary units.

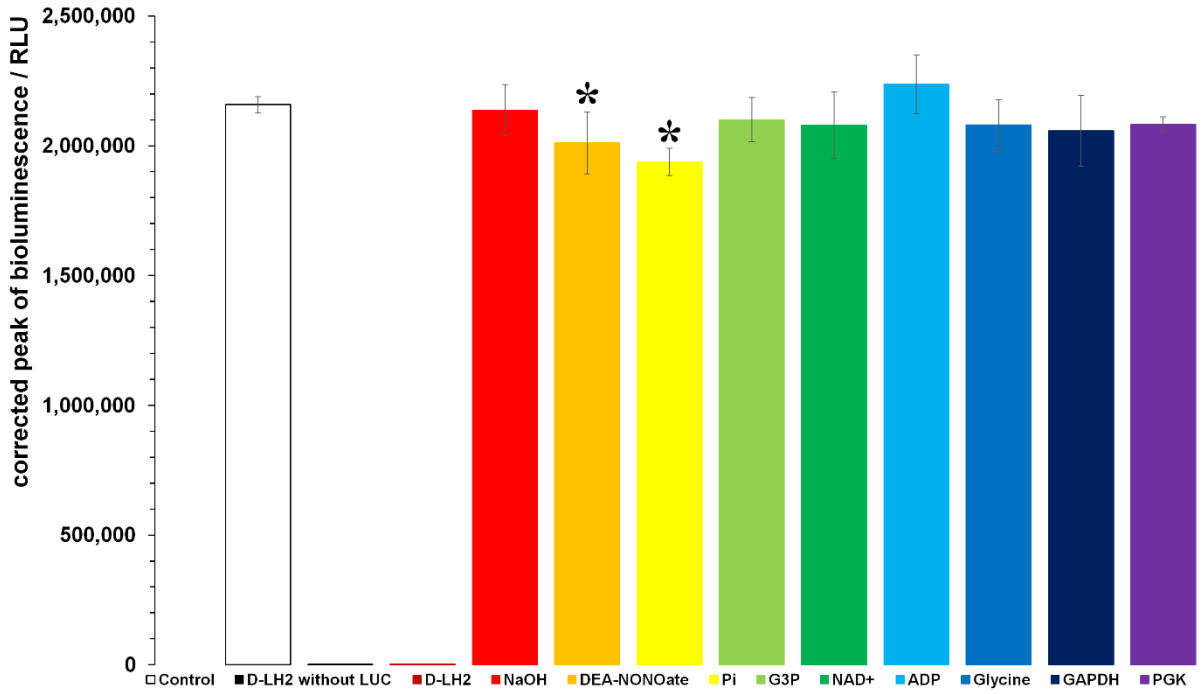

Figure S3. Evaluation of reagents and enzymes influence on LUC activity. Control was made in the absence of any reagent or enzyme. Asterisks indicate statistically significant difference as compared with the control ($p < 0.05$). RLU, relative light units.

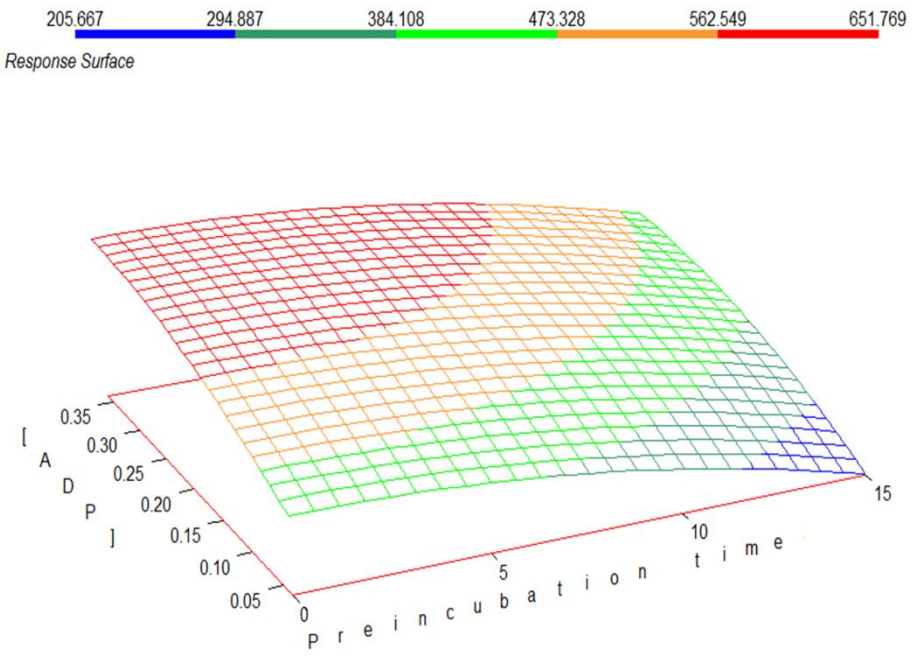

Figure S4. Response surface landscape plot for the most important method's factors, the concentration of ADP ([ADP]) and the preincubation time, tested in a Box Behnken design.

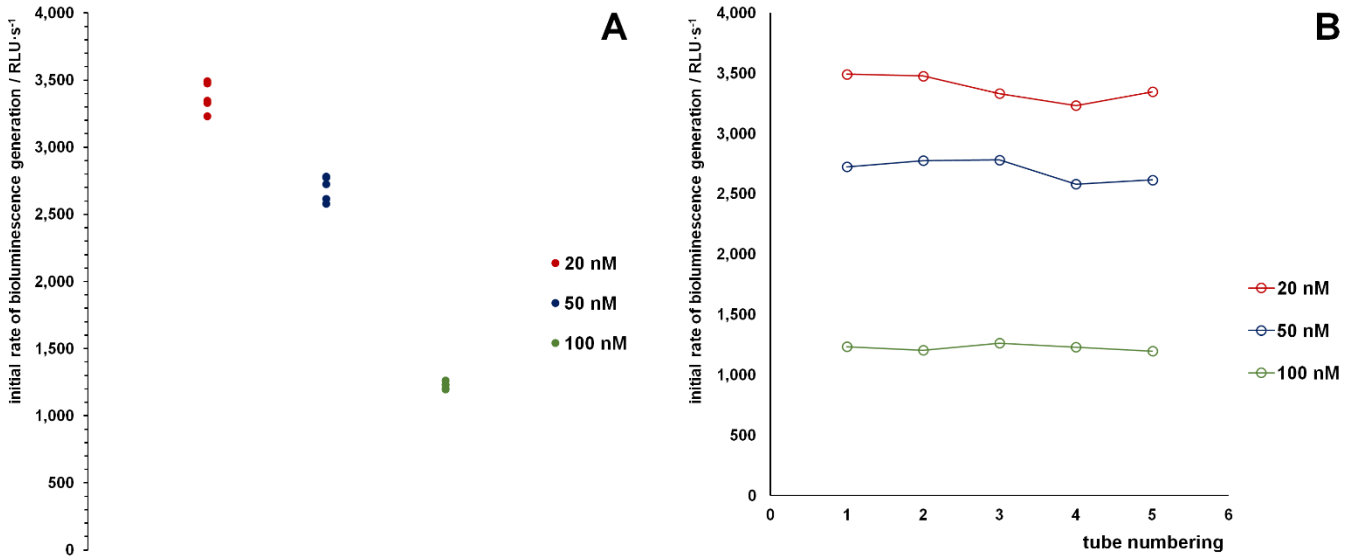

Figure S5. Evaluation of the optimized coupled bioluminescent assay repeatability. (A) Presentation of the experimental values by each •NO concentration tested. (B) Presentation of the experimental values by individual tubes within each concentration. RLU, relative light units.

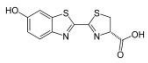

Chapter five

An optimized firefly luciferase bioluminescent assay for free fatty acids quantitation in biological samples

The scientific work leading to this chapter was integrally performed within the host institution, the Chemometric Research of Chemical, Environmental, Forensic and Biological Systems group, from the Chemistry Research Center of the University of Porto (*Centro de Investigação em Química da Universidade do Porto*, *CIQ-UP*), Department of Chemistry and Biochemistry, Faculty of Sciences, University of Porto. Simone Marques was responsible for bibliographic search, protocols set up, experimental execution, data treatment and manuscript writing, under the supervision of Joaquim Esteves da Silva.

An optimized firefly luciferase bioluminescent assay for free fatty acids quantitation in biological samples

A firefly luciferase (LUC) based bioluminescent assay for free fatty acids (FFA) is presented. LUC converts FFA into fatty acyl-adenylates, with consumption of adenosine 5'-triphosphate (ATP). Posteriorly, by adding LUC's substrate, firefly D-luciferin (D-LH_2), any remaining ATP can be quantified. A linear decrease in the bioluminescent signal is proportional to the amount of FFA. Using FFA standard mixtures containing myristic (14:0), palmitic (16:0), stearic (18:0), oleic (18:1) and arachidonic acid (20:4) in ethanol, the assay was optimized through statistical experimental design methodology, namely fractional factorial (screening) and central composite (optimization) designs. The optimized method requires 2 μL of sample *per* tube in a final reaction volume of 50 μL. It is linear in the range from 1 to 20 μM, with limits of detection (LOD) and quantitation (LOQ) of 1.3 and 4.5 μM, respectively. As a proof-of-principle, a fingertip drop of blood plasma was assayed by calibration curves. The method proved to be simple to perform, demands low reagent volumes, it is sensitive and robust and may be adapted to high-throughput screening.

Keywords: Analytical biochemistry; Luminometry; Experimental design; Enzymatic assay

1. Introduction

Firefly luciferase [*Photinus*-luciferin: oxygen 4-oxidoreductase (decarboxylating, ATP-hydrolyzing), EC 1.13.12.7] (LUC), which catalyzes a bioluminescent reaction, is an important bioanalytical tool.[1-3] The reaction proceeds thought two steps, the conversion of its natural substrate, firefly D-luciferin (D-LH_2), into the intermediate D-luciferyl-adenylate (D-LH_2-AMP) with the consumption of adenosine 5'-triphosphate (ATP) and the release of inorganic pyrophosphate (PPi), and the subsequent oxidative decarboxylation of D-LH_2-AMP into oxyluciferin, carbon dioxide (CO_2), free adenosine 5'-monophosphate (AMP) and photons of visible light (Scheme 1A).[1-3] Oba *et al*. have demonstrated the ability of LUC to synthesize fatty acyl-coenzyme A in the presence of fatty acids, ATP and coenzyme A (CoA) *via* the intermediate fatty acyl-adenylate (Scheme 1B).[4] This reaction consumes ATP, albeit not generating light, which prompted us to develop a bioluminescent method for the detection and quantitation of free fatty acids (FFA) by measuring the decrease in the bioluminescent signal after the addition of D-LH_2 to solutions with increasing amounts of fatty acids. To the best of our knowledge, this is the first bioluminescent method for FFA quantitation.

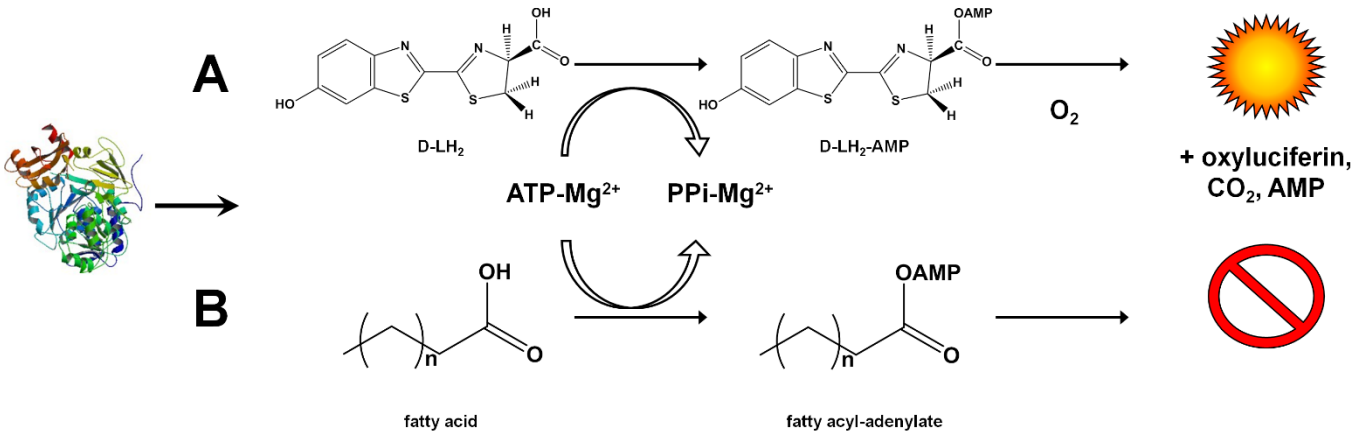

Scheme 1. Schematic representation of firefly luciferase (LUC) catalyzed reactions. (A) In the presence of its natural substrate, firefly D-luciferin (D-LH_2). (B) In the presence of a fatty acid.

Fatty acids are carboxylic acids with a hydrocarbon chain, and they include the saturated (without double bonds) lauric (12:0), myristic (14:0), palmitic (16:0) and stearic (18:0) acids and the unsaturated (with one or more double bonds) palmitoleic (16:1), oleic

(18:1), linoleic (18:2), linolenic (18:3) and arachidonic (20:4) acids, among others.[5] These biomolecules play important biological, clinical and biotechnological roles. For example, fatty acids are a source of energy in living organisms,[6] whereas arachidonic acid is a precursor of the eicosanoids paracrine hormones,[7, 8] and their circulation in blood is considered a nutritional status marker.[9] They are applied in energy storage and releasing devices such as solar heating and air-conditioning systems,[10] thermoplastic polymers[11] and biodiesel.[12] In this sense their detection, profiling and quantitation is paramount. The methods described in the literature are mainly based on instrumental techniques, namely high-performance liquid chromatography (HPLC) and gas chromatography (GC), sometimes coupled to mass spectrometry (MS).[13-17] These methods are very sensitive and allow the profiling of the different FFA present in complex samples such as blood. However, they demand specialized equipment, which may involve high costs of acquisition and maintenance, and also require specialized personnel to operate. Furthermore, they consume large volumes of potentially harmful eluents. The proposed method was conceived to avoid these drawbacks. It was optimized through a statistical experimental design methodology, characterized in terms of linear range and limits of detection (LOD) and quantitation (LOQ), and tested in human fingertip blood plasma as a proof-of-principle for biological samples.

2. Experimental

Note: All glass material was rinsed with acetone to avoid contamination. All experiments were performed at room temperature (approximately 20 ºC). Concentration values are final.

2.1. Reagents and solutions

2.1.1. Reagents

LUC (product code L9506, lot SLBD4220) and the reagents 4-(2-hydroxyethyl)piperazine-1-ethanesulfonic acid (HEPES, H3375), ATP (A2383), D-LH_2 (L9504), magnesium chloride ($MgCl_2$, 63064) and myristic (M3128), palmitic (P0500), oleic (O1008), stearic (85680) and arachidonic (10929) acids were purchased from Sigma-

Aldrich® (Steinheim, Germany). Nitrogen (Alphagaz™ Smartop N_2) was obtained from Air Liquide Portugal (Algés, Portugal). Acetone was obtained from Fisher Chemical (Loughborough, U.K.). Ethanol was from Panreac (Barcelona, Spain). Hexane was obtained from VWR (Fontenay Sous Bois, France).

A commercial FFA quantitation kit, 'Free Fatty Acid Quantitication Kit', ab65341, was purchased from Abcam® (Cambridge, U.K.).

2.1.2. Solutions

All reagents were used without further purification. A stock solution of LUC was prepared by dissolving the whole flask content in HEPES buffer 0.5 M, pH 7.5. The concentration was confirmed by ultraviolet-visible (UV-vis) spectrophotometry using an Unicam Helios γ spectrophotometer (Cambridge, U.K.), and considering a molar extinction coefficient of 39,310 $L \cdot mol^{-1} \cdot cm^{-1}$ at the maximum wavelength (λ_{max}) of 280 nm and a molecular mass of 60,745 Da. HEPES was prepared by dissolving the corresponding mass in deionized water, and the pH was adjusted to 7.5 by using a 10 M NaOH solution. Stock solutions of ATP and $MgCl_2$ were prepared in deionized water without pH adjustment. D-LH_2 stock solutions were prepared in deionized water with intense stirring for about 1 hour protected from the air and from the light. Concentration was confirmed by UV-vis spectrophotometry considering a molar extinction coefficient of 18,200 $L \cdot mol^{-1} \cdot cm^{-1}$ at λ_{max} 327 nm. FFA standard solutions were prepared by dissolving the corresponding masses in ethanol.

To ensure that the same conditions were achieved throughout the work, and also to avoid multiple freezing-thawing cycles, stock solutions were prepared in large volumes, aliquoted in small volumes and stored at -20 ºC.

2.2. Experimental designs formulation

Experimental designs were created using The Unscrambler® version 9.2 from CAMO (Oslo, Norway). A screening design was created using a fractional factorial design with five continuous variables at two levels and one nondesign (response) variable, which was set as a 1 μM FFA standard mixture. For the experimental procedure, one replication *per* experiment and three centre (control) experiments were chosen, with a total of eleven testing experiments plus the three control experiments. The factors and their levels were as following: preincubation time, 0 to 30 minutes; preincubation temperature, room temperature to 30 ºC; ATP concentration, 5 to 25 μM; LUC concentration, 5 to 25 nM; and

D-LH_2 concentration, 5 to 25 μM. When appropriate, tubes were incubated in a water bath using an IMLAB ET Basic Yellow Line immersion thermostat (Boutersem, Belgium). An optimization design was created using a central composite design with two continuous variables at two levels and one nondesign variable, which was set as a 1 μM FFA standard mixture. The star point distance from centre was settled at 1.41.For the experimental procedure, one replication *per* experiment and three centre experiments were chosen, with a total of eleven testing experiments plus the three control experiments. The factors and their levels were as following: ATP concentration, 5 to 25 μM; and D-LH_2 concentration, 5 to 25 μM.

2.3. Optimized bioluminescent assays

2.3.1. General optimized protocol

Bioluminescent assays were performed by luminometry using a homemade luminometer with a Hamamatsu HCL35 photomultiplier tube (Middlesex, N.J., U.S.A.) inside a light-tight dark chamber coupled to a Crison MicroBU 2030 automatic microburette (Barcelona, Spain) equipped with a 2.5 mL Hamilton GASTIGHT® 1002 glass syringe (Bonaduz, Switzerland).

The stock solutions of reagents, FFA standard mixtures and LUC were diluted in deionized water, ethanol or HEPES buffer 0.5 M, pH 7.5, respectively, and kept on ice until use.

The optimized bioluminescent assay is performed as follow: pipette 2.00 μL of sample or FFA standard mixture to a polypropylene transparent test tube and add 6.50 μL of ATP (18 μM) and 6.50 μL of $MgCl_2$ (4 mM). Set a chronometer to start at the moment of addition of 5.00 μL of LUC (5 nM), insert the tube into the luminometer and start to record the bioluminescent signal. One minute after the addition of LUC, inject 30 μL of D-LH_2 (17 μM) and record the light output for another 30 seconds, at an integration interval of 0.1 seconds.

Calibration curves were made according to the procedure described above using FFA standard mixtures with concentrations from 1 to 20 μM (each point measured in triplicate).

2.3.2. Samples' assays

Blood fingertip drops were freshly collected after an overnight fasting period. The forefinger was cleaned up with alcohol 70% and the finger was minced with a disposable lancet. The drop was collected with a micropipette and poured into a capped polypropylene tube. Plasma was obtained by centrifugation at 2,500 *x g* for 10 minutes using an Eppendorf 5415D workbench centrifuge (Hamburg, Germany). FFA were extracted according to a previously described procedure with the following modification: the organic phase was dried by passing a stream of nitrogen and reconstituted in ethanol.[18, 19]

Assays were performed under the optimized conditions described in subsection 2.3.1. through calibration curves. Samples were also assayed using a commercial kit under the manufacturer's instructions.

2.5. Statistical analysis

2.5.1. Experimental designs calculations

Data obtained from the experimental designs was analyzed using The Unscrambler® software. For the fractional factorial screening design, an analysis of effect was performed. Results were expressed as effects overview, using the significance testing methods center and higher order interaction effects (HOIE). For the central composite optimization design, a response surface analysis, which includes a two-way analysis of variance (ANOVA) table, was applied. From the ANOVA table, the analyzed parameters were the summary (evaluation of the global model), the variable (evaluation of the significance of each of the variables tested), the model check (evaluation of the global quadratic model) and the lack of fit (degree of misfitting of the experimental data to the model). All those parameters were evaluated through the *F*-ratios and the corresponding *p*-values. A p-value <0.05 was considered as statistically significant.

2.5.2. Optimized bioluminescent assays

Note: Data treatment and calculations were performed with a Microsoft® Excel® spreadsheet.

Calibration curves, for obtaining the method's figures of merit and for quantitation of FFA, were set up by the method of least squares by plotting the bioluminescence peak values as a function of the FFA standard mixtures concentration. The bioluminescence

peaks are obtained by selecting the maxima in the luminograms, corresponding to the moment at which D-LH_2 is injected into the reactional mixture (Figure 1A), and are expressed in relative light units (RLU). LOD and LOQ were calculated using the following criteria: LOD = (a + 3$S_{y/x}$) and LOQ = (a + 10$S_{y/x}$), where a is the intercept of the calibration curves and $S_{y/x}$ is the random error in the y-direction.[20] Calibration curve points are presented as mean ± standard deviation (SD) (n = 3), and sample concentrations as concentration ± 95% confident limits (95% CL) of the concentration. Using the commercial kit, the FFA content in samples was assayed by a calibration curve by plotting the absorbance as a function of the concentration of palmitic acid standards. Results are presented as FFA concentration ± 95% CL of the concentration. To test whether there was a significant difference between the results obtained by both methods, a paired t-test was performed.[20]

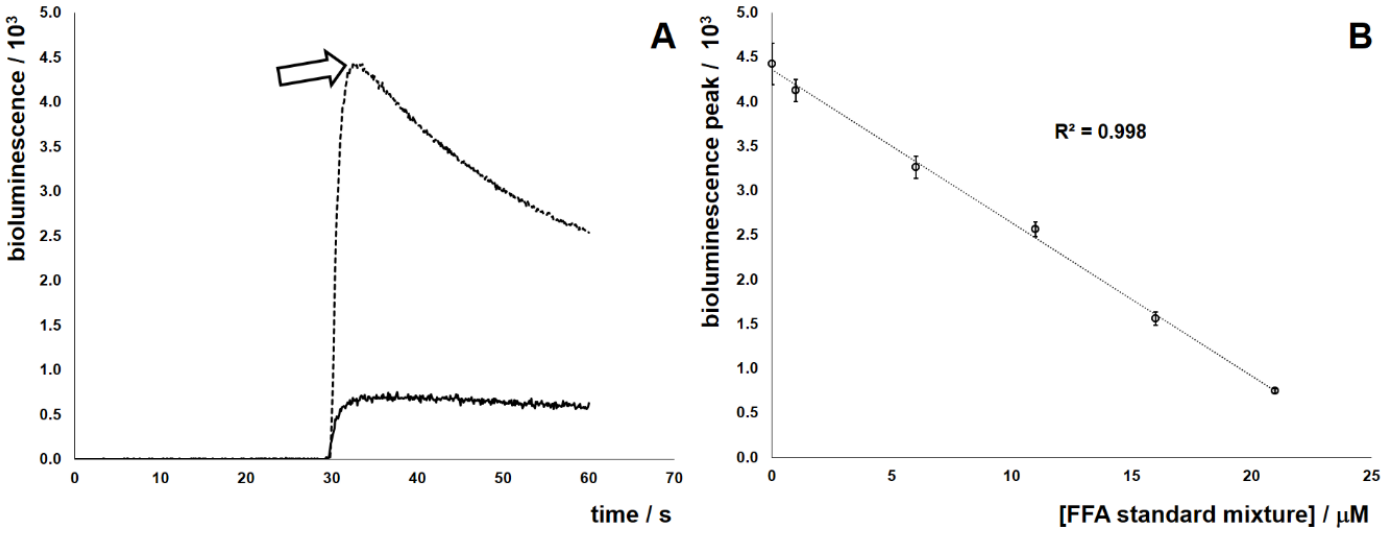

Figure 1. The bioluminescent assay light signal registration as a luminogram and the calibration curve setup. (A) A typical luminogram. The arrow indicates the bioluminescence peak due to D-LH_2 injection. The dashed luminogram represents a fatty acid standard mixture with a concentration of 0 μM, whereas the solid luminogram represents a fatty acid standard mixture with a concentration of 20 μM. (B) A typical calibration curve for free fatty acids (FFA) quantitation.

3. Results and discussion

The method was optimized using an experimental design methodology. The overall optimization process included two steps, a screening, to identify which factors have statistically the most influence on the method's response, and the subsequent determination of the levels at which these factors must be kept to optimize the method's response. Taking into account the various reagents and steps in the method, five factors

were initially selected for screening and a fractional factorial design was selected. Results showed that, in the presence of a 1 μM FFA standard mixture and using the testing methods center and HOIE, the ATP and D-LH_2 concentrations were the most significant factors (data not shown). Both factors exerted a positive influence, that is, the higher their concentrations, the higher was the bioluminescent signal (data not shown). With this information, a central composite optimization design was built to uncover the best ATP and D-LH_2 concentrations, and also to verify if their interactions were important for the method's response. The remaining factors were kept at their most convenient disposition, which corresponded to the minimum concentrations values, no preincubation and assay at room temperature. From the ANOVA table it was verified that both ATP and D-LH_2 concentrations, as well as their quadratic interactions, were important factors, showing significant *F*-ratios (p<0.05) (data not shown). According to their *F*-ratios, the model was significant whereas the lack of fit was not (p<0.05 and p>0.05, respectively), which showed that the experimental measurements fit the model (data not shown). The response surface curve (Figure 2) showed a maximum at which the concentrations of ATP and D-LH_2 should be kept to obtain the most robust response, about 18 μM for ATP and about 17 μM for D-LH_2.

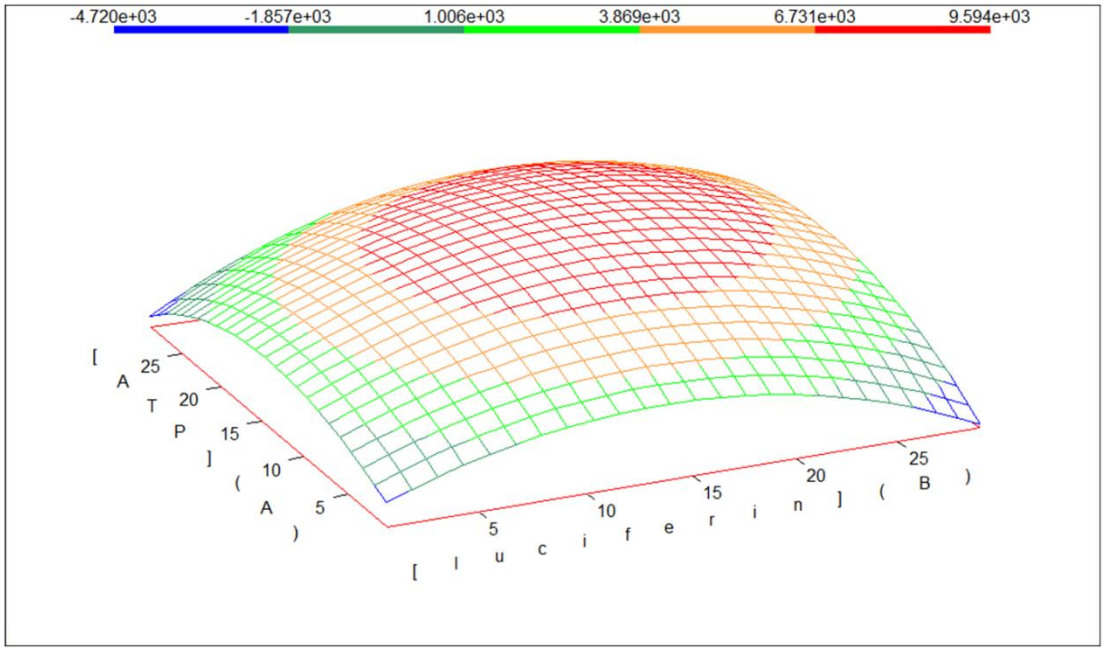

Figure 2. Response surface landscape plot for the factors tested in the central composite design. The factors were the concentrations of ATP, denoted as '[ATP] (A)', and D-LH_2, denoted as '[luciferin] (B)'.

Using the optimized conditions, the bioluminescent assay was characterized in terms of linear range, LOD and LOQ. It was verified that a linear trend occurred between 1 to 20 μM (Figure 1B), and LOD and LOQ were calculated as 1.3 and 4.5 μM, respectively.

As a proof-of-principle, plasma from a fingertip blood drop was assayed for its FFA content using this new optimized method. A value of 8.77 ± 0.21 μM was obtained. For comparison purposes, this sample was simultaneously tested using a commercial FFA detection kit. This kit is based on the enzymatic production and posterior oxidation of fatty acyl-CoAs, giving rise to a bright pink product that can be measured by either spectrophotometry or fluorometry. From spectrophotometric measurements, the sample FFA content was 8.90 ± 0.82 μM. No significant differences (p<0.05) were found between these values. Comparing those two methods, it is clear that the commercial kit is simple to perform and demands low volumes of samples and reagents, but it takes a longer time (one hour for incubations plus sample preparation and spectrophotometric reading) and it is slightly less sensitive (LOD 2 μM versus 1.3 μM for the bioluminescent assay).

Some caveats must be addressed. The presented method is based on ATP depletion due to the synthesis of fatty acyl-adenylates by LUC. Depletion methods are based on the measurement of small changes in the bioluminescent signal in the presence of a more or less large pool of ATP still unconsumed, which makes the methodology slightly less sensitive compared to other enzymatic reactions, from which LODs are in the nanomolar range. Nonetheless, it is still in the range of FFA concentration in biological samples. Another drawback is that the method does not allow the profile and quantitation of individual fatty acids, but rather the quantitation of total FFA. In this case, the method must be regarded as a screening methodology to obtain general information about the FFA amount. If further profiling is needed, a chromatographic method described in the literature must be selected. A major interfering in the assay is the presence of ATP, since this compound is ubiquitous in biological samples. The methodologies for fatty acids extraction separate the organic layer enriched in fatty acids from the aqueous layer with ATP, thus eliminating this contaminant. Finally, LUC may lose some activity in the course of the assay. To avoid this, it is recommended that the enzyme be kept on ice. Furthermore, if the storage time or the activity status of the enzyme are unknown, or if longer assay times are expected (more than two hours), the addition of additives to stabilize LUC, for example polyvynylpyrrolidone, glycine or dithiothreitol, is advised. LUC is also inhibited by alcohols.[21] Nonetheless, in this method, both the ethanol amount (2 μL) and LUC exposure time to ethanol (1 minute and 30 seconds) are reduced and, therefore, no effects are expected to occur.

4. Conclusions

In conclusion, despite the caveats described above, this method presents interesting features for the analyst, namely its safety, robustness, simplicity to perform and quickness. All reagents are commercially available, nontoxic, do not need further purification prior to use and their solutions are stable for several months when stored at -20 ºC. After their extraction from samples, FFA are assayed without further treatment, namely derivatization to become fluorescent. Although we used a single-tube luminometer, the method is applicable to multiplate assay. The proof-of-principle quantitation of FFA in plasma obtained from a fingertip drop of blood confirmed its applicability to real samples. Plasma was selected because of the clinical importance of FFA quantitation, however it is expected that other biological, environmental and chemical samples can be successfully assayed, because the extraction procedure reduces matrix complexity.

References

(1) Marques, S. M.; Esteves da Silva, J. C. G. Firefly bioluminescence: a mechanistic approach of luciferase catalysed reactions. *IUBMB Life* **2009**, *61*, 6-17.

(2) Inouye, S. Firefly luciferase: an adenylate-forming enzyme for multicatalytic functions. *Cell*. *Mol*. *Life Sci*. **2010**, *67*, 387-404.

(3) Marques, S. M.; Esteves da Silva, J. C. G. There's plenty of light at the bottom: bioanalytical and biomedical applications of luciferases. *Glob*. *J*. *Anal*. *Chem*. **2011**, *2*, 241-271.

(4) Oba, Y.; Ojika, M.; Inouye, S. Firefly luciferase is a bifunctional enzyme: ATP-dependent monooxygenase and a long chain fatty acyl-CoA synthetase. *FEBS Lett*. **2003**, *540*, 251-254.

(5) Nelson, D. L.; Cox, M. M. *Lehninger Principles of Biochemistry*, 4th ed.; W. H. Freeman and Company: New York (N.Y.), 2005.

(6) Manteiga, S.; Choi, K.; Jayaraman, A.; Lee, K. Systems biology of adipose tissue metabolism: regulation of growth, signaling and inflammation. *Wiley Interdiscip*. *Rev*.-*Syst*. *Biol*. *Med*. **2013**, *5*, 425-447.

(7) Brash, A. R. Arachidonic acid as a bioactive molecule. *J*. *Clin*. *Invest*. **2001**, *107*, 1339-1345.

(8) Hammond, V. J.; O'Donnell, V. B. Esterified eicosanoids: generation, characterization and function. *Biochim*. *Biophys*. *Acta-Biomembr*. **2012**, *1818*, 2403-2412.

(9) Hodson, L.; Skeaff, C. M.; Fielding, B. A. Fatty acid composition of adipose tissue and blood in humans and its use as a biomarker of dietary intake. *Prog*. *Lipid Res*. **2008**, *47*, 348-380.

(10) Yuan, Y.; Zhang, N.; Tao, W.; Cao, X.; He, Y. Fatty acids as phase change materials: a review. *Renew*. *Sust*. *Energ*. *Rev*. **2014**, *29*, 482-498.

(11) Maisonneuve, L.; Lebarbé, T.; Grau, E.; Cramail, H. Structure-properties relationship of fatty acid-based thermoplastics as synthetic polymer mimics. *Polym*. *Chem*. **2013**, *4*, 5472-5517.

(12) Hoekman, S. K.; Broch, A.; Robbins, C.; Ceniceros, E.; Natarajan, M. Review of biodiesel composition, properties, and specifications. *Renew*. *Sust*. *Energ*. *Rev*. **2012**, *16*, 143-169.

(13) Wang, F. – H.; Xiong, X. – J.; Guo, X. – F.; Wang, H.; Zhang, H. – S. Determination of fatty acids in bio-samples based on the pre-column fluorescence derivatization with 1,3,5,7-tetramethyl-8-butyrethylenediamine-difluoroboradiaza-s-indacene by high performance liquid chromatography. *J*. *Chromatogr*. *A* **2013**, *1291*, 84-91.

(14) Khoomrung, S.; Chumnanpuen, P.; Jansa-Ard, S.; Ståhlman, M.; Nookaew, I.; Borén, J.; Nielsen, J. Rapid quantitation of yeast lipid using microwave-assisted total lipid extraction and HPLC-CAD. *Anal*. *Chem*. **2013**, *85*, 4912-4919.

(15) Ubhayasekera, S. J. K. A.; Staaf, J.; Forslund, A.; Bergsten, P.; Bergquist, J. Free fatty acid determination in plasma by GC-MS after conversion to Weinreb amides, *Anal*. *Bioanal*. *Chem*. **2013**, *405*, 1929-1935.

(16) Chu, B. – S.; Nagy, K. Enrichment and quantitation of monoacylglycerols and free fatty acids by solid phase extraction and liquid chromatography-mass spectrometry. *J*. *Chromatogr*. *B* **2013**, *932*, 50-58.

(17) Amer, B.; Nebel, C.; Bertram, H. C.; Mortensen, G.; Hermansen, K.; Dalsgaard, T. K. Novel method for quantitation of individual free fatty acids in milk using an in-

solution derivatisation approach and gas chromatography-mass spectrometry, *Int*. *Dairy J*. **2013**, *32*, 199-203.

(18) Patterson, B. W.; Zhao, G.; Elias, N.; Hachey, D. L.; Klein, S. Validation of a new procedure to determine plasma fatty acid concentration and isotopic enrichment, *J*. *Lipid Res*. **1999**, *40*, 2118-2124.

(19) Yu, H.; Lopez, E.; Young, S. W.; Luo, J.; Tian, H.; Cao, P. Quantitative analysis of free fatty acids in rat plasma using matrix-assisted laser desorption/ionization time-of-flight mass spectrometry with *meso*-tetrakis porphyrin as matrix, *Anal*. *Biochem*. **2006**, *354*, 182-191.

(20) Miller, J. N.; Miller, J. C. *Statistics and Chemometrics for Analytical Chemistry*, 5th ed.; Pearson Prentice Hall: Gosport, 2005.

(21) Leitão, J. M. M.; Esteves da Silva, J. C. G. Firefly luciferase inhibition, *J*. *Photochem*. *Photobiol*. *B-Biol*. **2010**, *101*, 1-8.

Section three

Study of luciferin-related compounds from *Fridericia heliota*

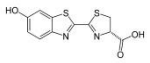

Chapter six

LC-MS and microscale NMR analysis of luciferin-related compounds from the bioluminescent earthworm *Fridericia heliota*

Simone M. Marques, Valentin N. Petushkov, Natalja S. Rodionova, Joaquim C.G. Esteves da Silva

J. Photochem. Photobiol. B – Biol. 102 (2011) 218-223

The scientific work leading to this paper was achieved in collaboration with Valentin N. Petushkov and his team at the Laboratory of Photobiology, Institute of Biophysics, Siberian branch of the Russian Academy of Sciences, Akademgorodok, Krasnoyarsk, Russia. Valentin Petshukov and Natalja Rodionova were responsible for collecting living specimens of the earthworm *Fridericia heliota*, separating and purifying different extracts and obtaining preliminary ultraviolet-visible and chromatographic properties. The extracts were sent to Portugal, where they were subjected to high-performance liquid chromatography coupled to mass spectrometry (HPLC-MS) analysis by Simone Marques, with the assistance of Zélia Azevedo and supervision of Joaquim Esteves da Silva at the host institution, the Chemometric Research of Chemical, Environmental, Forensic and Biological Systems group, from the Chemistry Research Center of the University of Porto (*Centro de Investigação em Química da Universidade do Porto*, *CIQ-UP*), Department of Chemistry and Biochemistry, Faculty of Sciences, University of Porto. All the authors were responsible for data interpretation and paper writing.

Journal of Photochemistry and Photobiology B: Biology 102 (2011) 218–223

Contents lists available at ScienceDirect

Journal of Photochemistry and Photobiology B: Biology

journal homepage: www.elsevier.com/locate/jphotobiol

LC–MS and microscale NMR analysis of luciferin-related compounds from the bioluminescent earthworm *Fridericia heliota*

Simone M. Marques [a], Valentin N. Petushkov [b], Natalja S. Rodionova [b], Joaquim C.G. Esteves da Silva [a,*]

[a] Centro de Investigação em Química (CIQ), Department of Chemistry and Biochemistry, Faculty of Sciences, Universidade do Porto, Rua do Campo Alegre 687, 4169-007 Porto, Portugal
[b] Laboratory of Photobiology, Institute of Biophysics, Siberian Branch of the Russian Academy of Sciences, Akademgorodok, 660036 Krasnoyarsk, Russia

ARTICLE INFO

Article history:
Received 5 October 2010
Received in revised form 6 December 2010
Accepted 10 December 2010
Available online 21 December 2010

Keywords:
Bioluminescence
Earthworm
Fridericia heliota
Luciferin
Microscale NMR
RP-HPLC–MS

ABSTRACT

This paper presents the main results of RP-HPLC–MS and microscale NMR analysis performed on Accompanying similar to Luciferin (AsLn(x)), compounds present in extracts of the bioluminescent earthworm *Fridericia heliota* that display similarities with *Fridericia*'s luciferin, the substrate of the bioluminescent reaction. Three isomers of AsLn were discovered, AsLn(1), AsLn(2) and AsLn(3), all of which present a molecular weight of 529 Da. Their UV–Vis absorption spectra show maxima at 235 nm for AsLn(1), 238 and 295 nm for AsLn(2) and 241 and 295 nm for AsLn(3). MS^n fragmentation patterns suggest the existence of carboxylic acid and hydroxyl moieties, and possibly chemical groups found in other luciferins like pterin or benzothiazole. The major isomer, AsLn(2), presents an aromatic ring and alkene and alkyl moieties. These luciferin-like compounds can be used as models that could give further insights into the structure of this newly discovered luciferin.

1. Introduction

Bioluminescence refers to a process in which an enzyme, luciferase, catalyses the oxidation of its substrate, luciferin, generating photons of visible light [1,2]. The most studied bioluminescent system is that of the North American firefly *Photinus pyralis* but other systems are known, like those of bacteria and coelenterates, which have important applications in basic and applied research [1,2].

Recently a new bioluminescent Siberian earthworm was described, *Fridericia heliota* (*Annelida*: *Clitellata*: *Oligochaeta*: *Enchytraeidae*) [3]. Besides the basic components, luciferase, luciferin and oxygen, its bioluminescent reaction requires the co-factors ATP and Mg^{2+}, similarly to fireflies, emitting a blue–green light with a maximum at 478 nm [4]. The presence of anions, cations of divalent metals, detergents and certain lipids, as well as changes in pH and temperature, may alter the emission profile *in vitro* [5].

Little is known about the structures of luciferase and luciferin, as well as the whole bioluminescent mechanism. Preliminary results on gel-filtration chromatography have assigned a molecular weight (MW) close to 70,000 and 500 Da to luciferase and luciferin, respectively [6]. A major drawback in the study of *F. heliota*'s bioluminescent system is the extreme difficulty in obtaining extracts of luciferase and luciferin. *F. heliota* has a reduced size (no more than 2 cm each worm) and a reduced luciferin content (0.5–0.7 μg/g of biomass, approximately 500 worms) [5]. Furthermore, the collection process is laborious, demanding the picking up of the earthworms one by one from soil by hand, in the dark and only during summer (2–3 months per year in Siberia). As a result it is common to get only 30–50 g of wet clean worms per season. Since many extraction and purification steps need to be performed, the luciferin loss is significant. Taking these facts into account it is useful to find model molecules, similar to luciferin in terms of structure and chemical properties but present in higher concentration than luciferin in extracts, and such was the purpose of the present work.

2. Materials and methods

2.1. Preparation of F. heliota extracts

The separation and purification of different fractions were achieved according to Scheme 1. Briefly, to obtain a crude total luciferin fraction 70 mL of crude total extract (cell-free extract) of *F. heliota*, prepared from 9.0 g of wet worms, was loaded onto a column (16 mm × 200 mm) packed with diethylaminoethyl (DEAE) Sepharose™ Fast Flow (Pharmacia Biotech, Uppsala, Sweden) coupled to the BioLogic™ LP chromatography system (BIO-RAD Laboratories, Hercules, USA). The column was equilibrated with tris(hydroxymethyl)-aminomethane-hydrochloric acid (Tris-HCl) buffer 10 mM, pH 8.1 (Serva Electrophoresis, Heidelberg, Germany). Elution was done by a linear gradient elution program of sodium chloride from 0 to 1 M. Before the second chromatographic step,

* Corresponding author. Tel.: +351 220 402 569; fax: +351 220 402 659.
E-mail address: jcsilva@fc.up.pt (J.C.G. Esteves da Silva).

1011-1344/$ - see front matter © 2010 Elsevier B.V. All rights reserved.
doi:10.1016/j.jphotobiol.2010.12.006

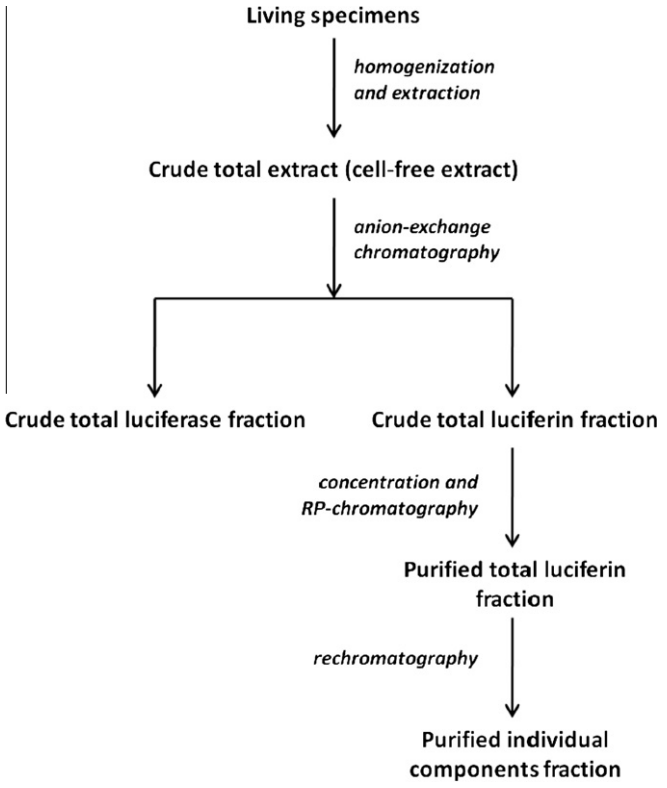

Scheme 1. Sequential chromatographic steps to obtain total and individual fractions from *Fridericia heliota*.

to obtain purified total luciferin fractions, the main luciferin fractions were acidified to pH 3 by adding hydrochloric acid and concentrated in a 3 mL disposable C_{16} extraction cartridge (Diapack-C_{16}, BioChemMak S&T, Moscow, Russia) which was previously equilibrated using hydrochloric acid 10 mM with acetonitrile 3%. The cartridge was rinsed with 15 mL of the equilibration solution, luciferin was washed off with 3 mL of acetonitrile 75% and then concentrated to 0.8 mL by vacuum (Vac-Rotor Concentrator Type 350P, Unipan Scientific Instruments, Warsaw, Poland). Reversed-phase liquid chromatography (RP-LC) was performed using a Mili-Chrom A-02 chromatograph (EcoNova, Novosibirsk, Russia) with a 2 mm × 75 mm column packed with ProntoSil® 120-5-C_{18} (EcoNova Novosibirsk, Russia). Elution was performed using a gradient elution program. Eluent A was a solution of ammonium formate 0.1%, pH 5, obtained by adding the corresponding acid to deionized water and dropping ammonium hydroxide to the desired pH. Eluent B was acetonitrile. The standard gradient program was 5–40% B for 28 min. Both the column and solvents were maintained at 40 °C, with a flow rate of 0.1 mL/min. Absorbance was monitored at 210, 230, 250, 270, 290, 310, 330 and 360 nm. To obtain purified individual component fractions, fractions of each luciferin-like component obtained from identical chromatograms were collected, evaporated to minimal volume under low pressure and subjected to rechromatography under conditions previously described.

2.2. Luciferase activity measurement

The reaction mixture to locate luciferin in chromatograms of purified total luciferin fractions by measuring luciferase activity (in arbitrary units) was composed of adenosine 5′-triphosphate 10 mM (ATP, 2.5 μL), magnesium chloride 100 mM (2.5 μL), Triton® X-100 10% (10 μL) (Sigma–Aldrich, St. Louis, USA), Tris-HCl buffer 20 mM, pH 8.1 (180 μL) and anion-exchange purified luciferase extract (10 μL). The reaction was initiated by adding luciferin fractions (1 μL) and was performed on a custom-made luminometer (Oberon, Krasnoyarsk, Russia). Each time before the addition of luciferin fractions the background luminescence was measured for 20s and subtracted from the total measurement.

2.3. RP-HPLC analysis

The characterization of purified individual AsLn fractions employed a chromatographic system composed of a HPLC pump (Finnigan™ Surveyor™ LC Pump Plus), an autosampler (Finnigan™ Surveyor™ Autosampler Plus) and a photodiode array detector equipped with a LightPipe™ flowcell (Finnigan™ Surveyor™ PDA Plus Detector) (all instrumentation from Thermo Electron Corporation, Waltham, USA), together with a silica-based C_{18} reversed-phase column (Hypersil™ GOLD Column 2.1 mm × 150 mm, particle size 5.0 μm, pore diameter 175 Å, Thermo Scientific, Waltham, USA). In each run 10 μL of samples were injected. The mobile phase consisted of (A) LC–MS grade deionized water with formic acid 0.1% and (B) LC–MS grade acetonitrile. Elutions were performed at a constant flow rate of 0.3 mL/min under a gradient elution program: 0–14 min, 5% B; 14–38 min, 40% B; 38–39 min, 80% B; 39–50 min, 100% B, and 51–60 min, 5% B, and absorbance was monitored at a total scan mode from 220 to 750 nm.

2.4. MS analysis

The mass spectrometer was a Finnigan™ LCQ™ Deca XP Max (Thermo Electron Corporation, Waltham, USA) coupled to the HPLC system. This device was equipped with an electrospray interface as ionization source and a quadrupole ion trap for MS^n experiments, and was operated both in positive and negative ion modes with the following conditions: spray voltage, 5 kV; capillary voltage, −15 V or 15 V in negative and positive ion modes, respectively; capillary temperature, 300 °C. Full-scan spectra were acquired over a mass range from 250 to 1500 Da in MS mode, from 135 to 540 Da in MS^2 mode and from 120 to 495 Da in MS^3 mode, all in negative ion mode; from 250 to 1500 Da in MS mode, from 135 to 545 Da in MS^2 mode and from 115 to 480 Da or 85 to 360 Da in MS^3 mode for AsLn(1) or AsLn(2), respectively, all in positive ion mode. The system was controlled by Xcalibur™ version 1.4 SR1 and data was treated using QualBrowser version 1.4 SR1 (both Thermo Electron Corporation, Waltham, USA). Assignment of some of the main fragments generated during MS^n experiences was done using the open database for mass spectrometry MassBank [7].

2.5. NMR analysis

Nuclear magnetic resonance measurements were performed at RIAIDT (Rede de Infraestruturas de Apoio à Investigação e ao Desenvolvimento Tecnológico), Unity of Magnetic Resonance, Section of Nuclear Magnetic Resonance, CACTUS Building at University of Santiago de Compostela (Spain) on a Bruker Avance DRX-500 NMR spectrometer (Bruker Corporation, Billerica, USA) operating at 500 MHz. Purified individual AsLn fractions (see subsection 2.1.) were lyophilized and ^1H and COSY data was recorded in hexadeuterated dimethyl sulfoxide (DMSO-d6, CD_3SOCD_3) with a 1 mm microprobe. Chemical shifts are given in parts per million (ppm) and were referenced to the solvent signal at 2.50 ppm. Data was treated using MestReNova Lite version 6.1.1-6384 (Mestrelab Research, Santiago de Compostela, Spain).

3. Results

Previous results have shown the presence of at least two compounds in total luciferin fractions, luciferin itself and a

non-identified compound informally called Component X [6]. By comparing spectral characteristics of peaks after chromatographic steps (data not shown) a new luciferin-like compound termed Accompanying similar to Luciferin (AsLn) was identified (Fig. 1A). Both Component X and AsLn have no luminescence activity with *F. heliota* luciferase (data not shown). However, as they have similar UV–Vis spectral parameters, they could share a similar structure with luciferin. Due to its reduced concentration luciferin was not observed in chromatograms. To detect luciferin in those fractions *Fridericia*'s luciferase was added and its activity measured. A defined and non-superimposed luciferin peak was obtained (Fig. 1A).

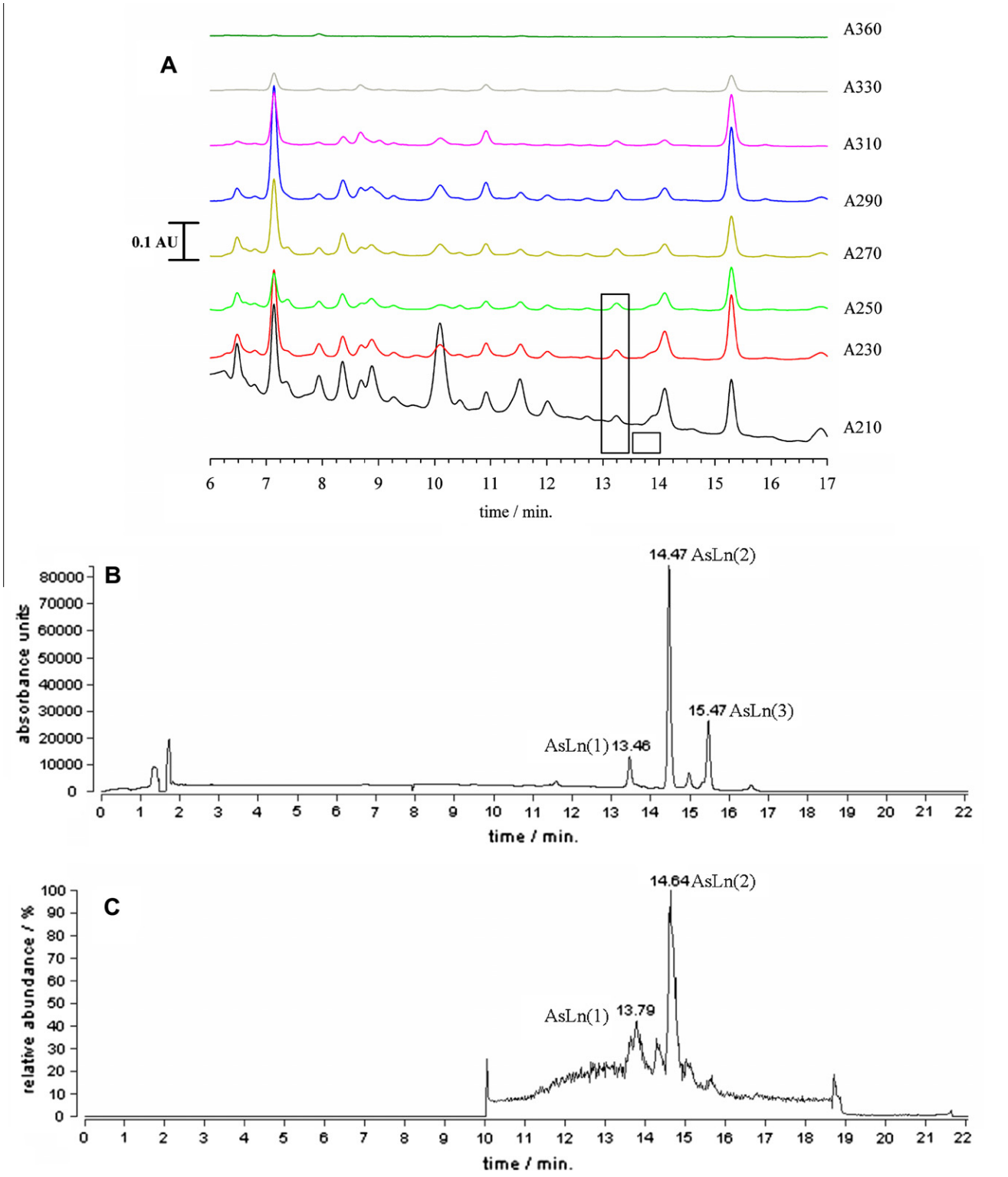

Fig. 1. (A) Representative chromatogram of purified total luciferin fraction at different absorbance wavelengths (A) with location of *F. heliota*'s luciferin. The black rectangles correspond to luciferin. Peak at 7.2 min corresponds to Component X and peak at 15.4 min was assigned to AsLn. (B) Representative chromatogram of purified individual AsLn fraction. (C) The corresponding MS spectrum in total ion count (TIC) and positive ion mode for sample in (B). AU, absorbance units.

Having established the luciferin model, AsLn, an attempt to uncover its structure was made. Table 1 resumes the main findings regarding chromatographic and mass spectrometric characterization of AsLn(x) in purified individual fractions. Based on retention time values and UV–Vis spectra, three isomers of AsLn were found (Fig. 1B). AsLn(1) is the first isomer that appears using RP-HPLC conditions, with retention times about 13 min. Its UV–Vis spectrum has a maximum at 235–238 nm with a shoulder at 268 nm (Fig. 2). The predominant isomer is AsLn(2), with retention times about 14 min but a completely different UV–Vis spectrum compared to AsLn(1), presenting two maxima, one at 238 nm (minor) and the other at 295 nm (major) (Fig. 2). Finally the isomer AsLn(3) could be detected at retention times about 15–16 min. This compound has a UV–Vis spectrum similar to AsLn(2), with two maxima at 241 nm (minor) and 295 nm (major) (Fig. 2). In MS analysis, as a first approach, a total ion count (TIC) analysis was performed, where a correlation between LC and MS peaks was observed (Fig. 1C). As a result a molecular weight (MW) of 529 Da based on $[M+H]^+$ and $[M-H]^-$ molecular ions was assigned to AsLn(1) (see Supplementary data, Fig. S1), a value similar to that preliminary reported for luciferin [6]. For AsLn(2), the obtained MW was also 529 Da (Fig. S2). Contrary to AsLn(1) and AsLn(2), AsLn(3)'s MW was not obtained with the current eluent A (formic acid 0.1%) (Fig. 1C). However, when using ammonium formate 10 mM, pH 5, a MW of 529 Da was assigned (Fig. S3). MS^n fragmentation patterns were obtained for AsLn(1) and AsLn(2) (Figs. S1 and S2). For AsLn(1) it was found that MS^2 and MS^3 fragmentation patterns are quite different in negative or positive ion modes (Fig. S1). The same trend was observed for AsLn(2) (Fig. S2), but remarkably AsLn(1) and AsLn(2) share a very similar pattern in negative ion mode (Table 1 and Figs. S1 and S2). The assignment of some chemical groups correlating to the observed fragmentation pattern was achieved. Both AsLn(1) and AsLn(2) present a 44 Da fragment (528–484 Da) in MS^2 spectra in negative ion mode which could be attributed to a carboxylate group (COO^-). AsLn(1) presents a 61 Da fragment (528–467 Da) which could correspond to the simultaneous departure of COO^- and a hydroxyl (HO) or ammonia (NH_3) group (44 + 17 Da). This fragment is not detected in AsLn(2). In MS^3 spectra both compounds present another 61 Da fragment (484–423 Da). Additionally a 163 Da fragment is seen (484–321 Da), which is the same mass of pterin ($C_6H_5N_5O$). Regarding positive ion mode, it was verified a 18 Da fragment in MS^2 spectrum for AsLn(1) (530–512 Da) and MS^3 spectrum for AsLn(2) (349–331 Da), which could be attributed to a water molecule (H_2O) or to an ammonium cation (NH_4^+). Two other common fragments to AsLn(1) and AsLn(2) in MS^2 spectra are 46 Da (530–484 Da) and 63 Da (530–467 Da), possibly corresponding to formic acid ($COOH_2$) or a combination of $COOH_2$/HO or $COOH_2/NH_3$ (46 + 17 Da), respectively. For AsLn(1) in MS^3 spectrum and AsLn(2) in MS^2 spectrum it was observed a 181 Da fragment (467–286 Da and 530–349 Da, respectively) with the same mass of 2-methylmercaptobenzothiazole and a similar mass to D-(+)-

Table 1
RP-HPLC–MS results from the analysis of AsLn(x).

Compound	UV–Vis maximum absorbance (nm)	Ion mode	Experimental $[M\pm H]^\pm$	Fragments derived from MS^2 (m/z)	Fragments derived from MS^3 (m/z)
AsLn(1)	235	Negative Positive	528.27 530.27	321; 467; 484[a] 356; 421; 449; 467[a]; 484; 512	484 → 321[a]; 338; 423; 425; 467 467 → 268; 286; 356; 421[a]
AsLn(2)	238/295	Negative Positive	528.20 530.20	321; 484[a] 331; 349[a]; 367; 467; 484; 498	484 → 321[a]; 338; 423; 452 349 → 205; 270; 286; 331[a]
AsLn(3)	241/295	Negative/positive	528.33/530.07	–	–

[a] Major fragment.

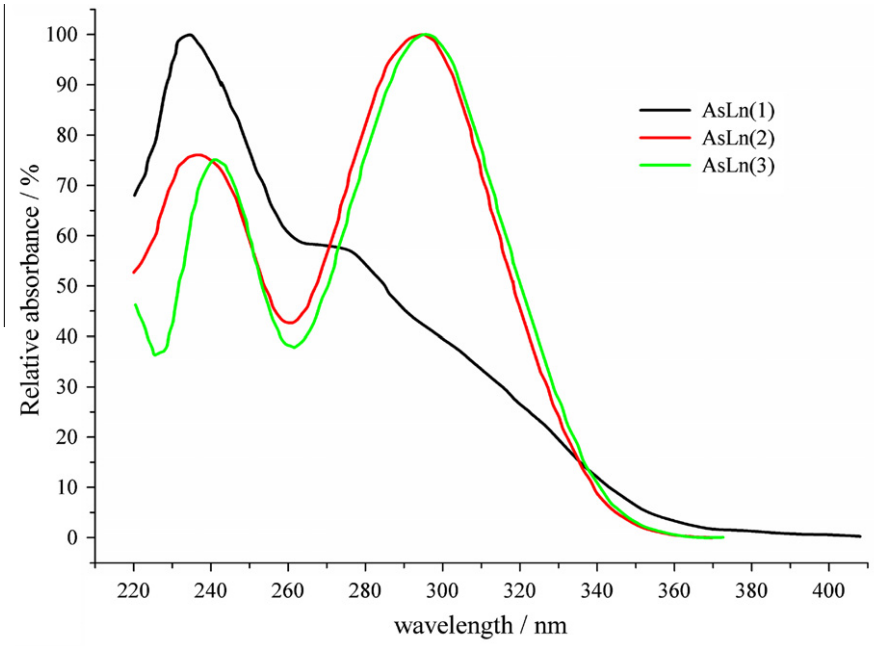

Fig. 2. UV–Vis absorbance spectra of AsLn(1), AsLn(2) and AsLn(3). These spectra were acquired using QualBrowser v. 1.4 SR1.

mannose, D-(+)-glucose, D-(+)-fructose and D-(+)-galactose (180 Da each). Finally the previously described 163 Da fragment was observed for AsLn(2) in its MS^2 spectrum (530–367 Da).

Purified individual AsLn(2) fractions were subjected to microscale NMR analysis. The ^1H NMR spectrum was characterized by three regions, a deshielded region from 8.5 to 6.5 ppm with signal

Table 2
^1H microscale NMR chemical shifts for AsLn(2) (500 MHz, CD_3SOCD_3).

Proton number in Fig. 3A	1	2	3	4	5	6	7	8	9	10	11	12	13	14
Chemical shift (ppm)	0.85	1.09	1.15	1.23	1.56	4.44	5.39	6.58	6.65	6.81	7.08	7.56	7.94	8.42

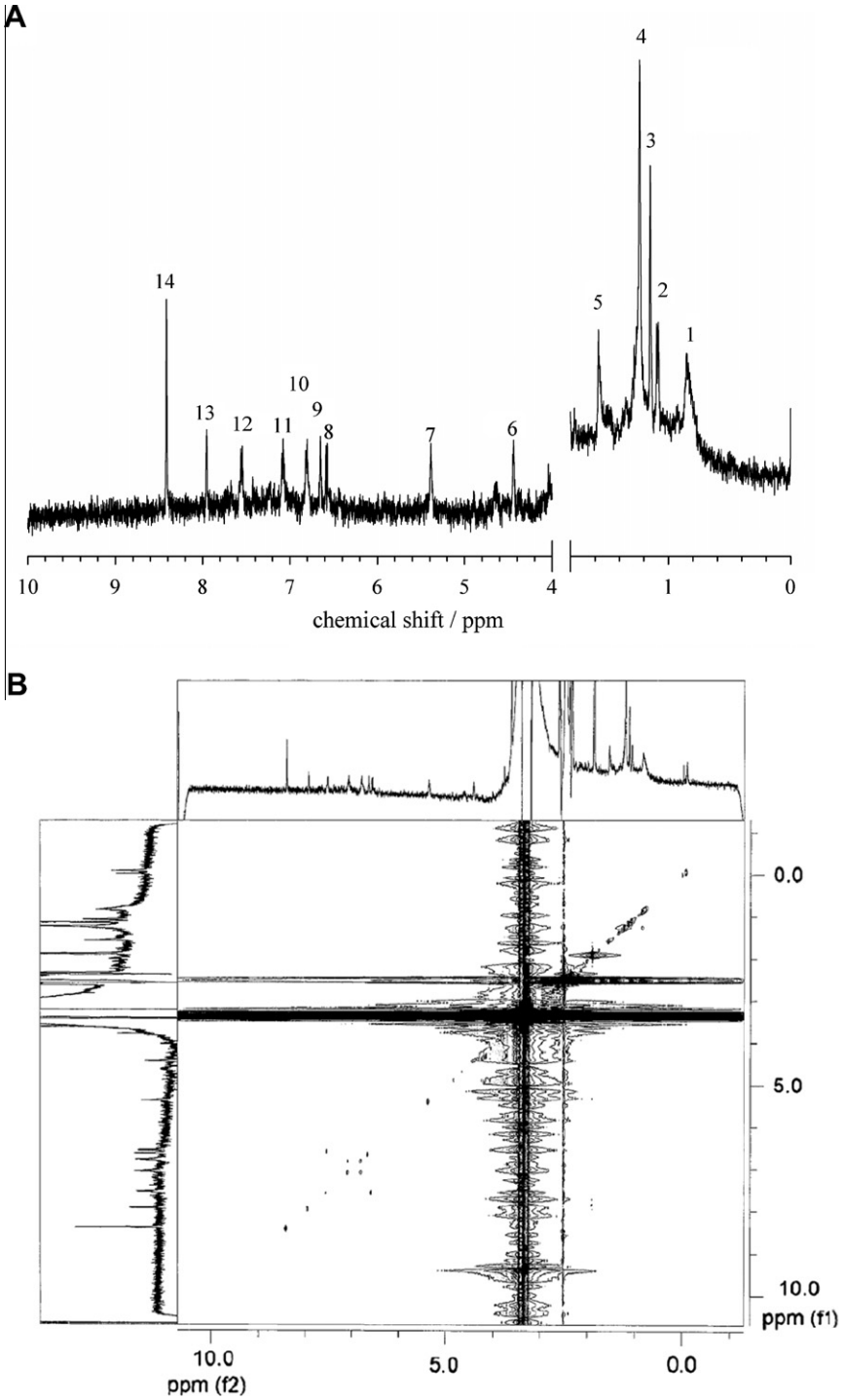

Fig. 3. (A) ^1H NMR and (B) COSY spectra of AsLn(2) in CD_3SOCD_3 (500 MHz).

typical of aromatic protons, a mid-low field region from 6.5 to 4.5 ppm due to alkene protons and a downfield region assigned to alkyl groups (Table 2 and Fig. 3A). Because of the low sample content it was not possible to unambiguously assign peak multiplicity and coupling constants, as well as perform ^{13}C analysis. A COSY spectrum showed a possible correlation between protons 1 and 5, 8 and 12 and 10 and 11 (Fig. 3B).

4. Discussion

In this paper an instrumental analysis of the *F. heliota* luciferin-like compound AsLn was presented. The first studies about this new bioluminescent system focused on luciferin, however no reliable data was obtained, since luciferin is present in minute amounts. This fact prompted us to discover compounds related to luciferin to act as models in providing useful information about its structure. The main evidence that AsLn(x) could be good models for luciferin is, besides the resemblance in spectroscopic data, their appearance in all purified extracts of luciferin. This suggests that AsLn(x) could be metabolites of luciferin, either their precursor or products resulting from the bioluminescent reaction. In fact, in the *P. pyralis* bioluminescent system dehydroluciferin (L) and its adenylated form, dehydroluciferyl-adenylate (L-AMP), are oxidized forms of luciferin that do not produce light and act as inhibitors of the bioluminescent reaction, as also occurs for oxyluciferin, the product of oxidative decarboxylation of luciferin [8–10]. Another hypothesis is that AsLn(x) could be enantiomers of luciferin, like D-luciferin and L-luciferin from *P. pyralis*, the former being the natural substrate for the bioluminescent reaction and the latter behaving as an inhibitor [8].

From MS^n spectra a few information regarding AsLn(x)' chemical structures could be inferred, namely the probable presence of carboxylic acid and hydroxyl groups. Two fragments with 163 (same mass of pterin) and 181 Da (same mass of 2-methylmercaptobenzothiazole) could be interpreted by analyzing other known luciferins. In the first case the luciferin from the bioluminescent millipede *Luminodesmus sequoiae* presents a pterin moiety [11], whereas firefly's luciferin has a benzothiazole moiety [8]. A possible drawback of these hypotheses is the distant phylogenetic relationship between millipedes, fireflies and earthworms. Nonetheless it was verified that *F. heliota*'s luciferin seems to be unrelated to other bioluminescent earthworms, as the cross-reaction of *F. heliota*'s luciferase with luciferin from *Diplocardia longa*, *N*-isovaleryl-3-aminopropanal, that acts as a common substrate for other bioluminescent worms, gave a negative result [12,13]. The other hypothesis is that the 181 Da fragment could be a sugar, like glucose or mannose although, to the best of our knowledge, no glycosylated luciferin was found yet.

NMR is a powerful technique for assessing chemical structures but, in the present work, it was necessary to apply a more sensitive method, microscale NMR [14]. Even so the concentration of AsLn(2) did not allow to obtain a complete structure, but rather to propose that aromatic, alkene and alkyl groups could be present. The minimum compound amount for a 1D proton analysis was estimated as 10–20 μg, but a fully structural analysis demands more experiments in multidimensional modes, in which samples' amount must be in the minimum limit of 50 μg for proton analysis and 150 μg for ^{13}C analysis, like HMQC or HMBC. Our estimation points out to about 5–10 μg of AsLn per fraction.

The ongoing work focuses on obtaining enriched samples of AsLn, or even Component X or luciferin, to confirm and complete these results.

Acknowledgements

The authors wish to thank Zélia Azevedo for the able technical assistance in LC–MS experiments and Jose Enrique Borges for the support in analyzing NMR spectra. This work was supported by Grants 08-04-01790-a from the Russian Foundation for Basic Research and PTDC/QUI/71366/2006 from the Portuguese Fundação para a Ciência e a Tecnologia (FCT). A Ph.D. grant to Simone M. Marques (SFRH/BD/65109/2009), co-funded by the European Social Fund (FSE) (through Programa Operacional Potencial Humano of the Quadro de Referência Estratégico Nacional [POPH-QREN]) and by FCT, is also acknowledged.

Appendix A. Supplementary material

Supplementary data (MS^n spectra for AsLn(1), AsLn(2) and AsLn(3)) associated with this article can be found, in the online version, at doi:10.1016/j.jphotobiol.2010.12.006.

References

[1] T. Wilson, J.W. Hastings, Bioluminescence, Annu. Rev. Cell Dev. Biol. 14 (1998) 197–230.
[2] O. Shimomura, Bioluminescence – Chemical Principles and Methods, World Scientific Publishing, Singapore, 2006.
[3] E. Rota, N.T. Zalesskaja, N.S. Rodionova, V.N. Petushkov, Redescription of *Fridericia heliota* (Annelida, Clitellata: Enchytraeidae), a luminous worm from the Siberian taiga, with a review of bioluminescence in the Oligochaeta, J. Zool. 260 (2003) 291–299.
[4] N.S. Rodionova, V.S. Bondar', V.N. Petushkov, ATP is a cosubstrate of the luciferase of the earthworm *Fridericia heliota* (Annelida: Clitellata: Oligochaeta: Enchytraeidae), Dokl. Biochem. Biophys. 392 (2003) 253–255.
[5] N.S. Rodionova, V.N. Petushkov, Effect of different salts and detergents on luciferin–luciferase luminescence of the enchytraeid *Fridericia heliota*, J. Photochem. Photobiol. B-Biol. 83 (2006) 123–128.
[6] V.N. Petushkov, N.S. Rodionova, Purification and partial spectral characterization of a novel luciferin from the luminous enchytraeid *Fridericia heliota*, J. Photochem. Photobiol. B-Biol. 87 (2007) 130–136.
[7] H. Horai, M. Arita, S. Kanaya, Y. Nihei, T. Ikeda, K. Suwa, Y. Ojima, K. Tanaka, S. Tanaka, K. Aoshima, Y. Oda, Y. Kakazu, M. Kusano, T. Tohge, F. Matsuda, Y. Sawada, M.Y. Hirai, H. Nakanishi, K. Ikeda, N. Akimoto, T. Maoka, H. Takahashi, T. Ara, N. Sakurai, H. Suzuki, D. Shibata, S. Neumann, T. Iida, K. Tanaka, K. Funatsu, F. Matsuura, T. Soga, R. Taguchi, K. Saito, T. Nishioka, MassBank: a public repository for sharing mass spectral data for life sciences, J. Mass Spectrom. 45 (2010) 703–714 at www.massbank.jp (accessed 12.03.10).
[8] S.M. Marques, J.C.G. Esteves da Silva, Firefly bioluminescence: a mechanistic approach of luciferase catalyzed reactions, IUBMB Life 61 (2009) 6–17.
[9] J.C.G. Esteves da Silva, J.M.C.S. Magalhães, R. Fontes, Identification of enzyme produced firefly oxyluciferin by reverse phase HPLC, Tetrahedron Lett. 42 (2001) 8173–8176.
[10] H. Fraga, D. Fernandes, J. Novotny, R. Fontes, J.C.G. Esteves da Silva, Firefly luciferase produces hydrogen peroxide as a coproduct in dehydroluciferyl adenylate formation, ChemBioChem 7 (2006) 929–935.
[11] M. Kuse, A. Kanakubo, S. Suwan, K. Koga, M. Isobe, O. Shimomura, 7, 8-Dihydropterin-6-carboxylic acid as light emitter of luminous millipede, *Luminodesmus sequoiae*, Bioorg. Med. Chem. Lett. 11 (2001) 1037–1040.
[12] V.N. Petushkov, N.S. Rodionova, New types of luminescent systems of soil enchytraeids (Annelida: Clitellata: Oligochaeta: Enchytraeidae), Dokl. Biochem. Biophys. 401 (2005) 115–118.
[13] E. Rota, in: V.B. Meyer-Rochow (Ed.), Bioluminescence in Focus – A Collection of Illuminating Essays, Research Signpost, Trivandrum, 2009, pp. 105–138.
[14] T.F. Molinski, NMR of natural products at the 'nanomole-scale', Nat. Prod. Rep. 27 (2010) 321–329.

Supplementary data

LC-MS and microscale NMR analysis of luciferin-related compounds from the bioluminescent earthworm *Fridericia heliota*

Simone M. Marques [a], Valentin N. Petushkov [b], Natalja S. Rodionova [b], Joaquim C.G. Esteves da Silva [a, *]

[a] *Centro de Investigação em Química* (*CIQ*), *Department of Chemistry and Biochemistry, Faculty of Sciences, University of Porto, Rua do Campo Alegre 687, 4169-007 Porto, Portugal*

[b] *Laboratory of Photobiology, Institute of Biophysics, Siberian Branch of the Russian Academy of Sciences, Akademgorodok, 660036 Krasnoyarsk, Russia*

* Corresponding author at: *Centro de Investigação em Química* (*CIQ*), Department of Chemistry and Biochemistry, Faculty of Sciences, University of Porto, Rua do Campo Alegre 687, 4169-007 Porto, Portugal. Tel.: +351-220-402-569; fax: +351-220-402-659.

E-mail address: jcsilva@fc.up.pt (J.C.G. Esteves da Silva).

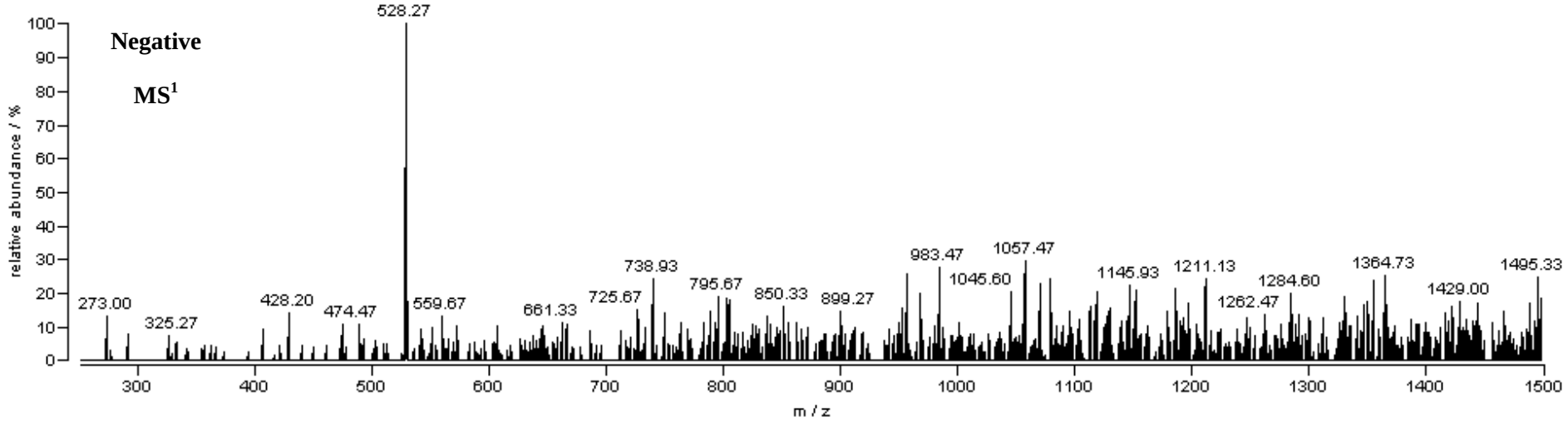
Negative
MS1
528.27
273.00
325.27
428.20
474.47
559.67
661.33
725.67
738.93
795.67
850.33
899.27
983.47
1045.60
1057.47
1145.93
1211.13
1262.47
1284.60
1364.73
1429.00
1495.33
relative abundance / %
m / z

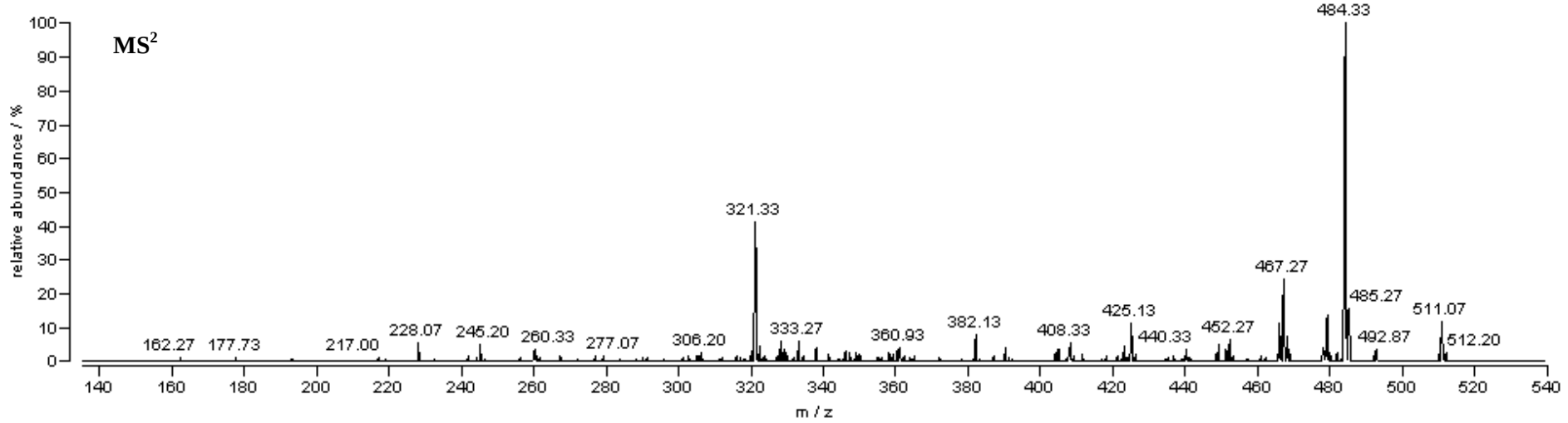
MS2
484.33
321.33
467.27
485.27
511.07
492.87
512.20
425.13
440.33
452.27
382.13
408.33
333.27
360.93
162.27
177.73
217.00
228.07
245.20
260.33
277.07
306.20
relative abundance / %
m / z

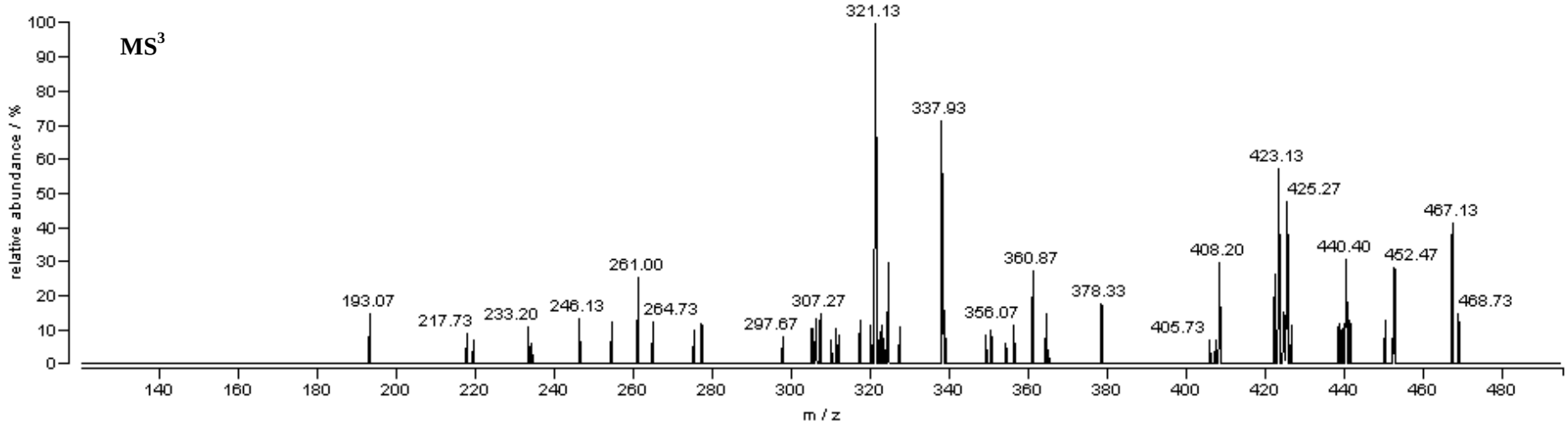
MS3
relative abundance / %
m / z
321.13
337.93
423.13
425.27
467.13
261.00
360.87
408.20
440.40
452.47
193.07
378.33
468.73
307.27
217.73
233.20
246.13
264.73
297.67
356.07
405.73

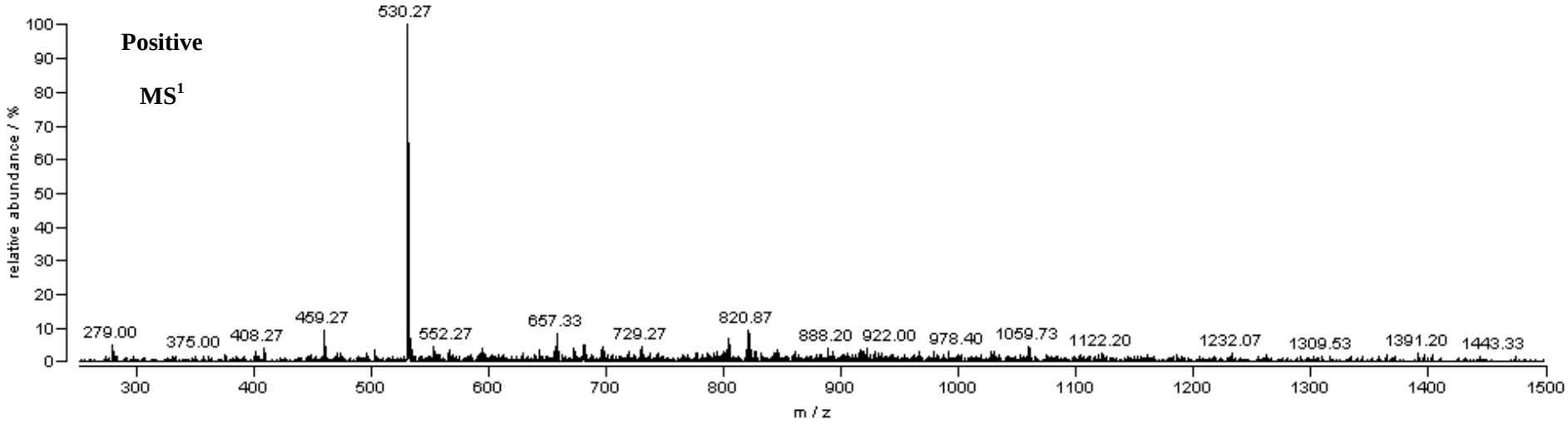
Positive
MS1
relative abundance / %
m / z
530.27
279.00
375.00
408.27
459.27
552.27
657.33
729.27
820.87
888.20
922.00
978.40
1059.73
1122.20
1232.07
1309.53
1391.20
1443.33

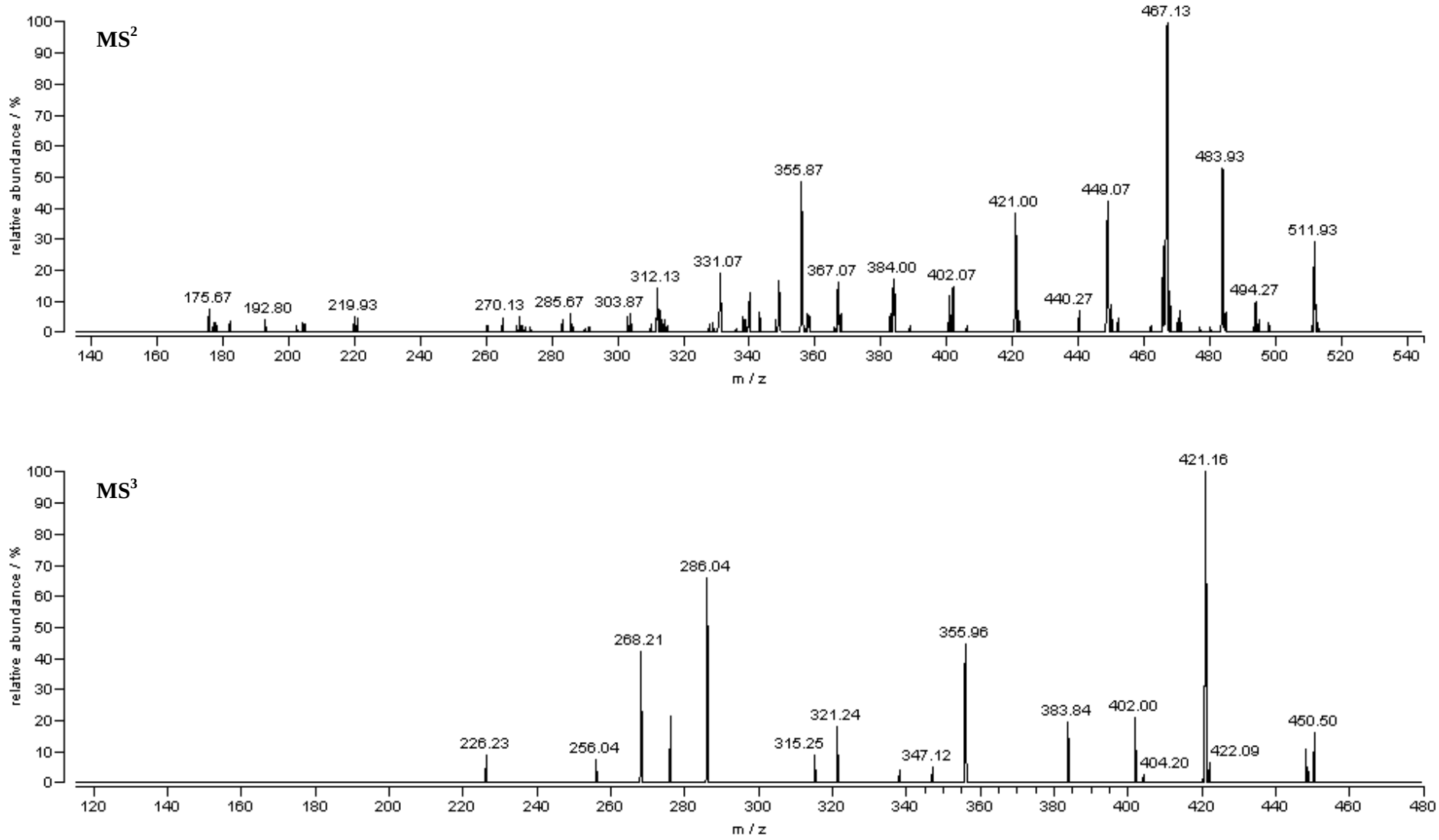

Fig. S1. MS^n spectra of AsLn(1) in negative and positive ion modes.

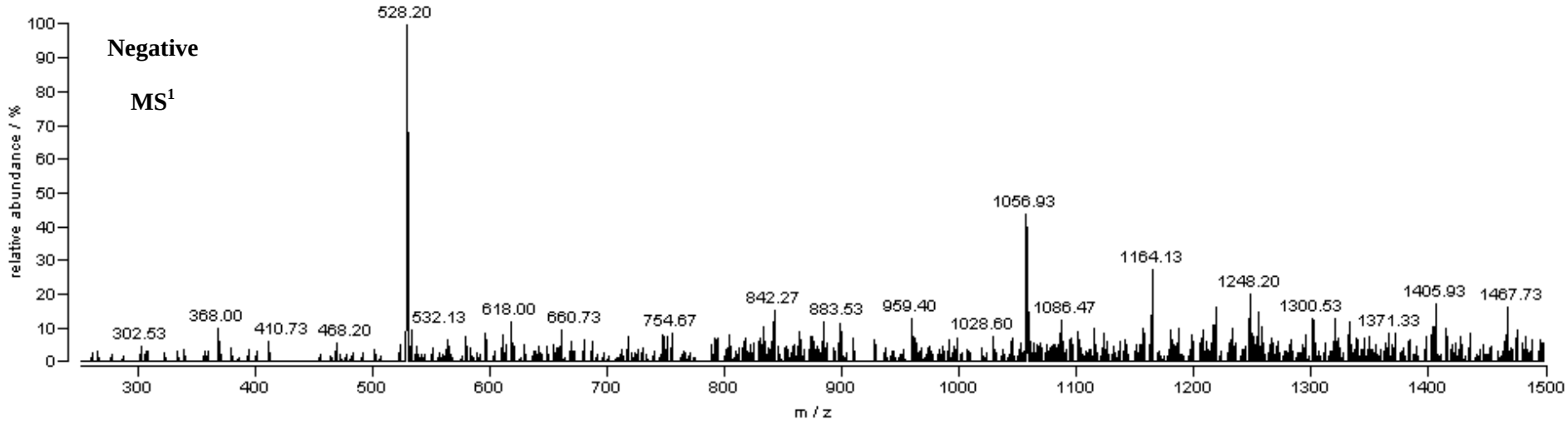
Negative
MS1
528.20
1056.93
1164.13
1248.20
1405.93
1467.73
1300.53
1371.33
842.27
883.53
959.40
1028.60
1086.47
754.67
618.00
660.73
532.13
368.00
410.73
468.20
302.53
relative abundance / %
m / z

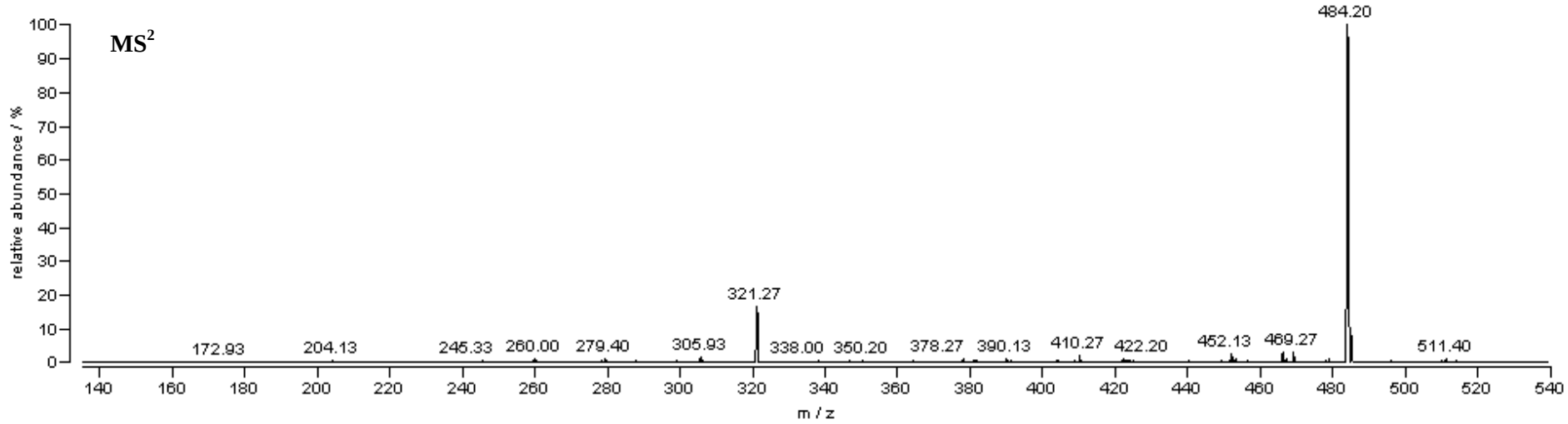
MS2
484.20
321.27
172.93
204.13
245.33
260.00
279.40
305.93
338.00
350.20
378.27
390.13
410.27
422.20
452.13
469.27
511.40
relative abundance / %
m / z

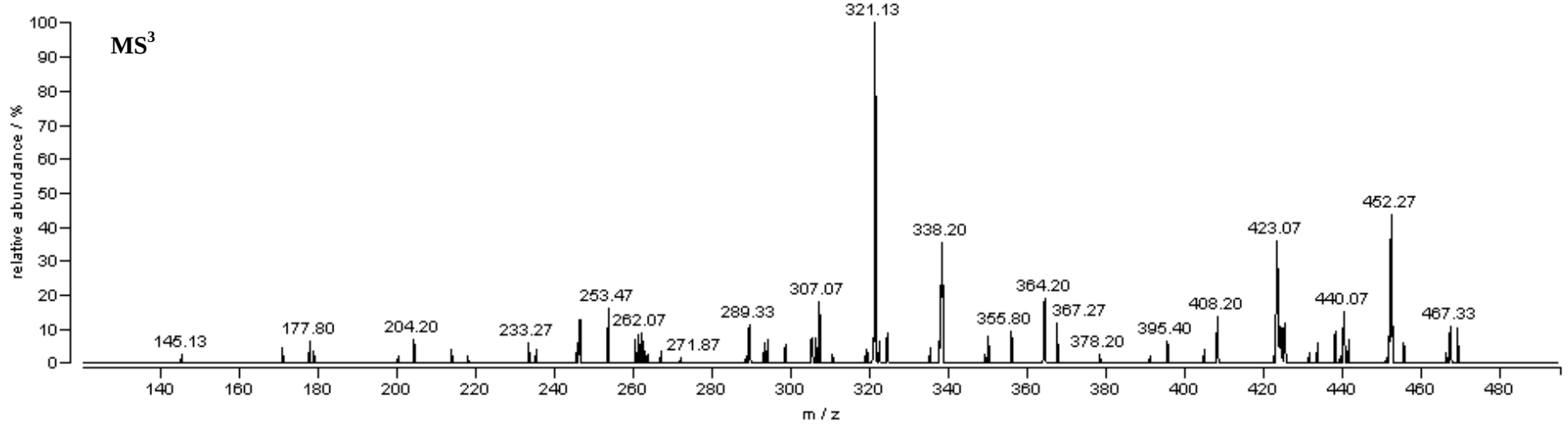
MS3
relative abundance / %
m / z
321.13
452.27
338.20
423.07
364.20
307.07
253.47
440.07
408.20
289.33
262.07
355.80
367.27
467.33
204.20
177.80
233.27
395.40
145.13
271.87
378.20

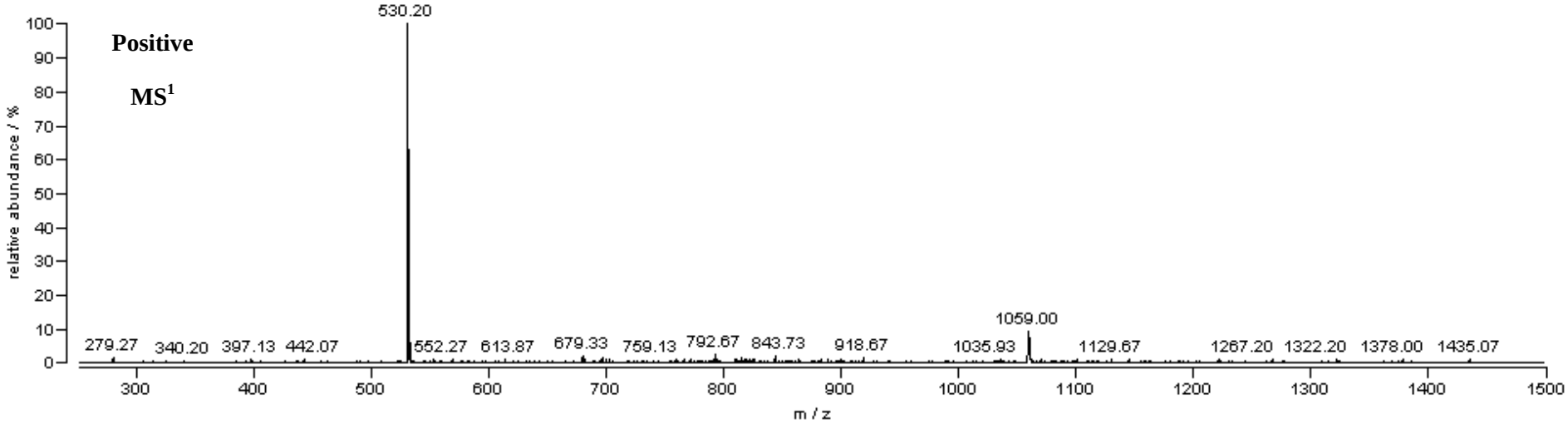
Positive
MS1
relative abundance / %
m / z
530.20
1059.00
279.27
340.20
397.13
442.07
552.27
613.87
679.33
759.13
792.67
843.73
918.67
1035.93
1129.67
1267.20
1322.20
1378.00
1435.07

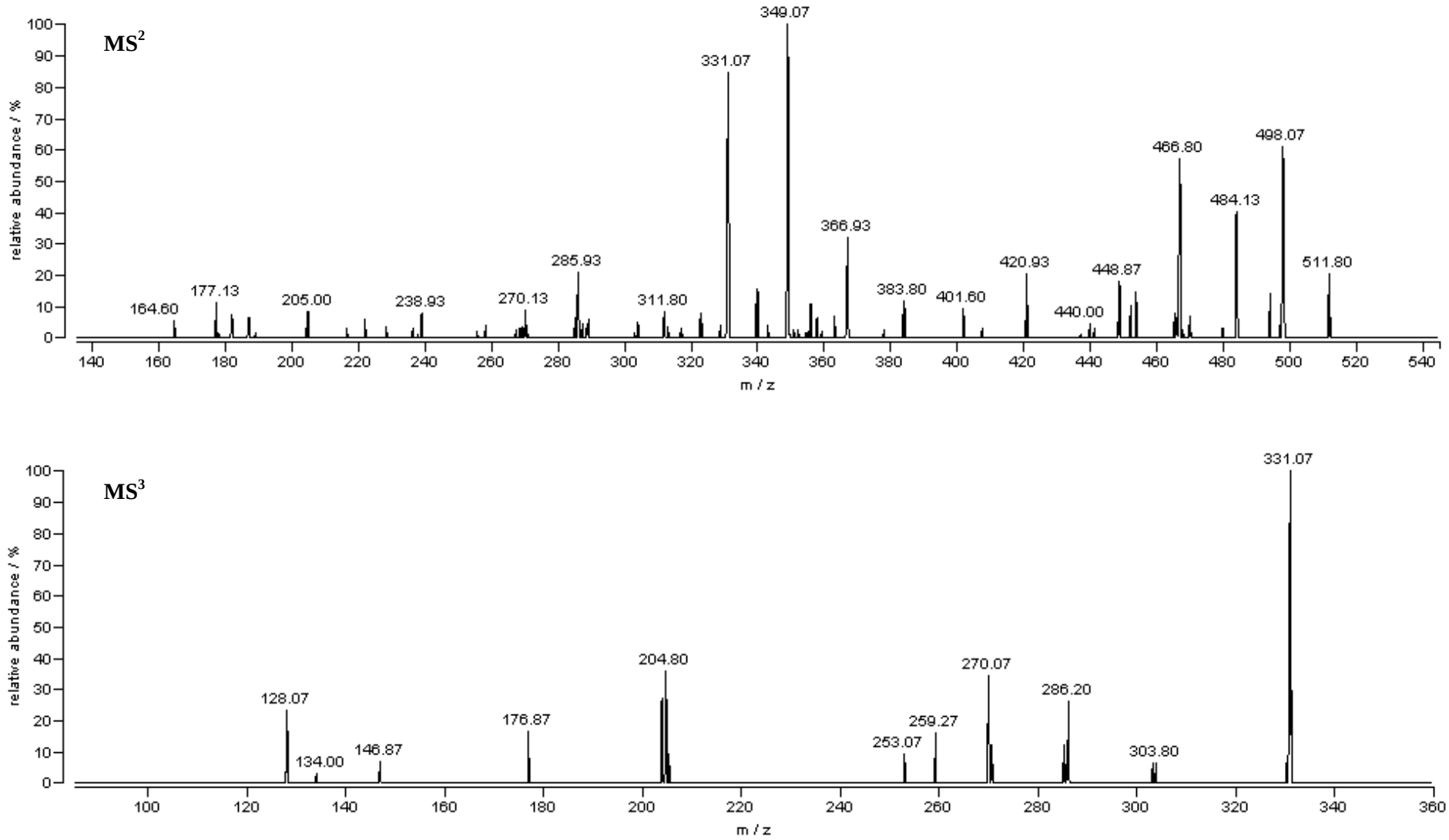

Fig. S2. MS^n spectra of AsLn(2) in negative and positive ion modes.

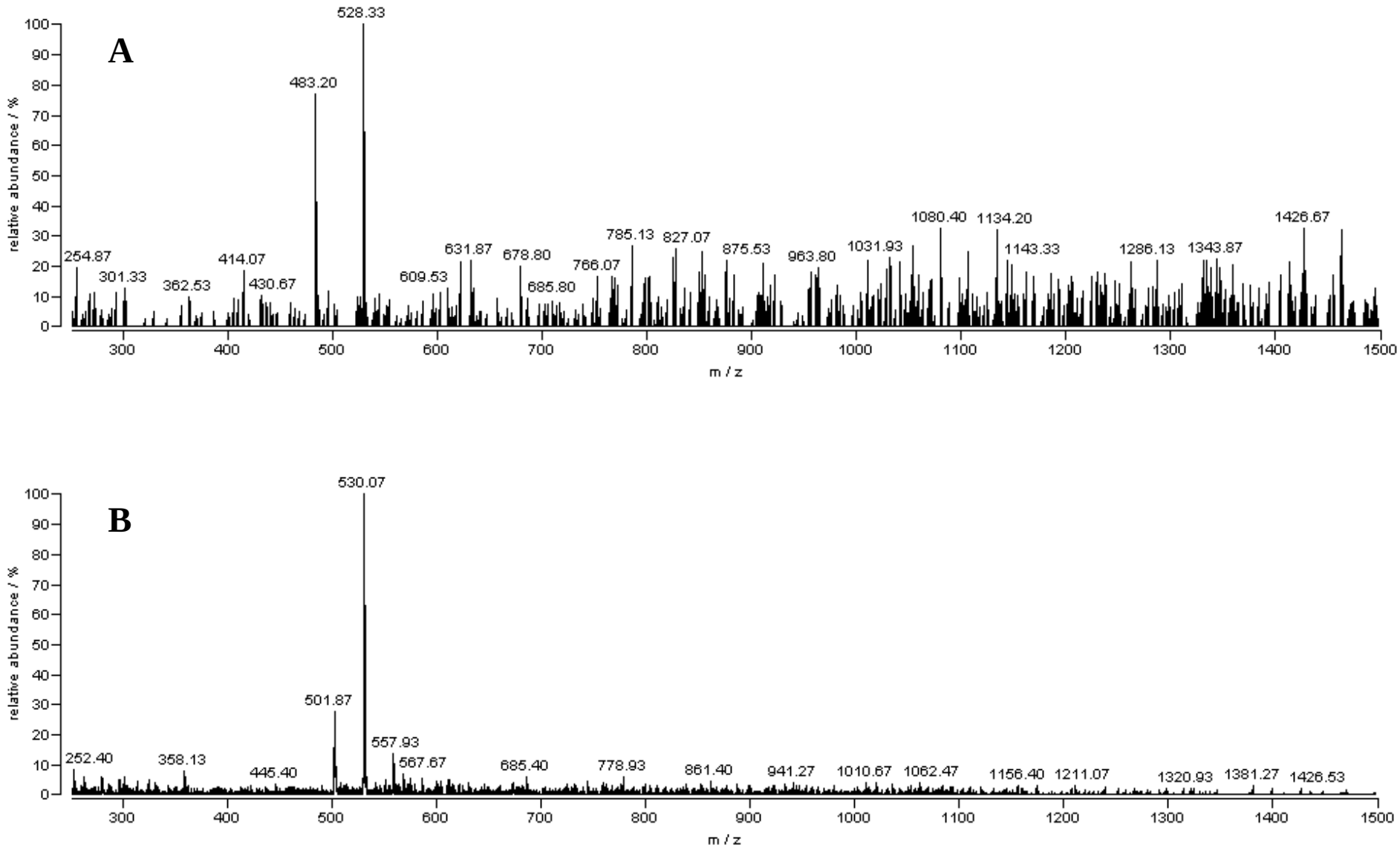

Fig. S3. MS^1 spectra of AsLn(3) in (A) negative and (B) positive ion modes.

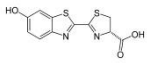

Chapter seven

CompX, a luciferin-related tyrosine derivative from the bioluminescent earthworm *Fridericia heliota*. Structure elucidation and total synthesis

Valentin N. Petushkov, Aleksandra S. Tsarkova, Maxim A. Dubinnyi, Natalja S. Rodionova, Simone M. Marques, Joaquim C.G. Esteves da Silva, Osamu Shimomura, Ilia V. Yampolsky

Tetrahedron Lett. 55 (2014) 460-462

This paper is the first part of the analysis of the luciferin-related compounds CompX and AsLn(2). Following the progresses in luciferin-related compounds study, improved techniques were required, which implied a new consortium with specialized analysts in high-resolution mass spectrometry (HR-MS) and nuclear magnetic resonance (NMR). HR-MS and NMR execution and interpretation and CompX total synthesis were performed by Aleksandra Tsarkova, Maxim Dubinnyi and Ilia Yamposlky By its turn, Valentin Petushkov and Natalja Rodionova were responsible for collecting living specimens of the earthworm *Fridericia heliota*, separating and purifying different extracts and coordinating the groups. Simone Marques was responsible for checking extracts purification and concentration by low-resolution MS and data gathering, under the supervision of Joaquim Esteves da Silva at the host institution, the Chemometric Research of Chemical, Environmental, Forensic and Biological Systems group, from the Chemistry Research Center of the University of Porto (*Centro de Investigação em Química da Universidade do Porto*, *CIQ-UP*), Department of Chemistry and Biochemistry, Faculty of Sciences, University of Porto. Osamu Shimomura was responsible for supervision and suggestions. All the authors were responsible for paper writing.

Tetrahedron Letters 55 (2014) 460–462

Contents lists available at ScienceDirect

Tetrahedron Letters

journal homepage: www.elsevier.com/locate/tetlet

CompX, a luciferin-related tyrosine derivative from the bioluminescent earthworm *Fridericia heliota*. Structure elucidation and total synthesis

Valentin N. Petushkov [a,b], Aleksandra S. Tsarkova [c], Maxim A. Dubinnyi [c], Natalja S. Rodionova [a,b], Simone M. Marques [d], Joaquim C. G. Esteves da Silva [d], Osamu Shimomura [a], Ilia V. Yampolsky [c,*]

[a] *Laboratory of Bioluminescent Biotechnologies, Institute of Fundamental Biology and Biotechnology, Siberian Federal University, pr. Svobodnyi, 79, Krasnoyarsk 660041, Russia*
[b] *Laboratory of Photobiology, Institute of Biophysics, Siberian Branch of the Russian Academy of Sciences, Akademgorodok, Krasnoyarsk 660036, Russia*
[c] *Institute of Bioorganic Chemistry, Russian Academy of Sciences, Miklukho-Maklaya 16/10, Moscow 117997, Russia*
[d] *Chemistry Research Center of the University of Porto (CIQ-UP), Department of Chemistry and Biochemistry, Faculty of Sciences, University of Porto, Campo Alegre St. 687, Porto 4169-007, Portugal*

ARTICLE INFO

Article history:
Available online 22 November 2013

Keywords:
Bioluminescence
Enchytraeid
Luciferin
Total synthesis

ABSTRACT

A luciferin analog, CompX, was isolated from the extracts of the bioluminescent earthworm *Fridericia heliota*. Its structure was determined as (*Z*)-5-(2-carboxy-2-methoxyvinyl)-2-hydroxybenzoic acid by spectroscopic data analysis and was confirmed by total synthesis. The (*Z*)-configuration of the double bond was established by comparing the ROESY spectra of CompX with those of its synthetic (*E*)-isomer. CompX represents a tyrosine analog, not previously found in natural sources, and is probably derived from tyrosine by deamination, O-methylation of the resulting alpha-keto acid, and carboxylation at the aromatic core.

Bioluminescence is caused by a biochemical reaction in which an enzyme, generically termed luciferase, promotes the oxidation of the substrate, luciferin, resulting in the emission of visible light.[1] Several bioluminescence mechanisms have been established, for example, those of beetles, coelenterates, and bacteria, which have led to their applications in biotechnology, molecular and cellular biology, and biomedicine.[1b]

Fridericia heliota Zalesskaja, 1990 (Annelida: Clitellata: Oligochaeta: Enchytraeidae) is a small (15–20 mm in length, 0.5 mm in diameter and ~2 mg in weight), white–yellowish Siberian earthworm which emits blue light when gently stimulated.[2] Although the species was first identified in 1990,[3] further studies were not performed until 2003. Initial studies focused on the taxonomic description[2] and in vitro characterization of the bioluminescent reaction between raw extracts of luciferase and luciferin.[4] So far, it has been demonstrated that the system requires at least five components, a 70 kDa luciferase, a 0.5 kDa luciferin, atmospheric oxygen magnesium ions, and adenosine 5′-triphosphate (ATP) to produce visible light with a maximum wavelength (λ_{max}) at 478 nm.[4a,b] The system is pH- and temperature-sensitive, achieving the optimum rate at pH 8.2 and 33 °C, respectively.[4c] It can be stimulated by nonionic detergents, such as Triton X-100, and inhibited by anionic detergents, and several anions.[4d]

Presently, our research is focused on the isolation and structural characterization of *Fridericia heliota* luciferin.[5] Extracts of luciferin contained unidentified substances, designated CompX,[5a] AsLn1, AsLn2, and AsLn3.[5b] These compounds demonstrated chromatographic behavior and UV spectral properties similar to those of luciferin. However, none of them exhibited luminescent activity when mixed with *F. heliota* luciferase or any other luciferase. We hypothesized that these compounds could represent the inactive analogs of luciferin, for example, its metabolic precursors or degradation products. Taking into account the extremely low luciferin content in the earthworm (0.5–0.7 μg/g of biomass),[5b] whereas the content of CompX is more than ten-fold that of luciferin, we decided to undertake its structural characterization and synthesis.

A consecutive series of chromatographic experiments allowed isolation of 0.15 mg of pure CompX from 90 g of *F. heliota* biomass (see Supplementary data). The UV–vis spectra (Fig. 1a) demonstrate pH-dependence in the pH range 2.8–5.0. At pH 2.8, the maxima are observed at 234 (local maximum) and 296 nm, whereas at pH 4.0, the λ_{max} are 230 (local maximum) and 294 nm, and at pH 5.0, the λ_{max} are 228 (local maximum) and 288 nm, which suggests the presence of an ionizable group with a pK_a of about 4. CompX is fluorescent (Fig. 1b), with a maximum emission wavelength (λ_{em}) in the blue range of the visible spectrum. The fluorescence spectra

* Corresponding author. Tel./fax: +7 499 724 81 22.
E-mail address: ivyamp@ibch.ru (I.V. Yampolsky).

0040-4039/$ - see front matter © 2013 Elsevier Ltd. All rights reserved.
http://dx.doi.org/10.1016/j.tetlet.2013.11.064

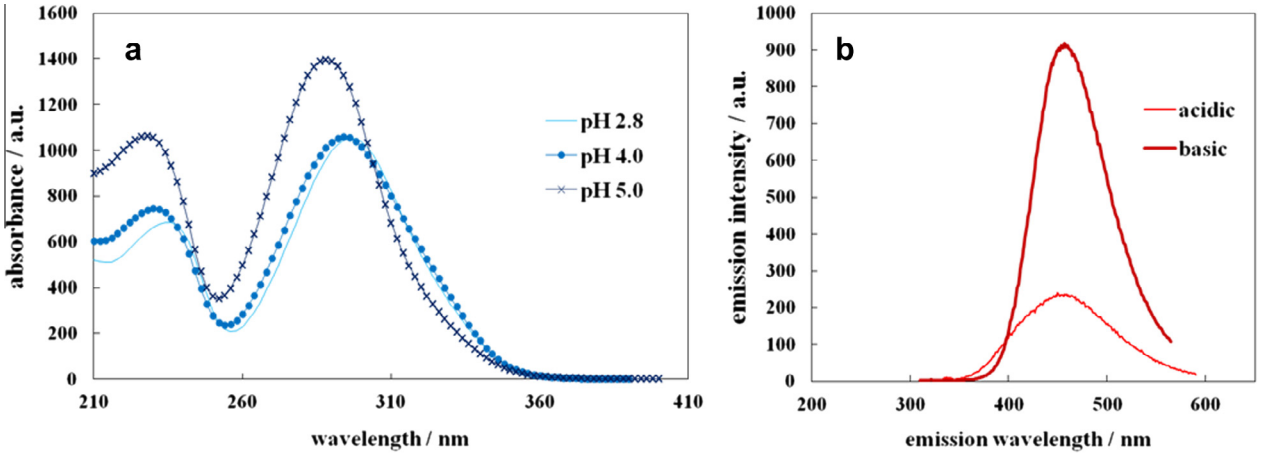

Figure 1. (a) UV–vis and (b) fluorescence emission spectra of CompX at different pH. In (a), the spectra were measured in ammonium formate 0.1% at pH 2.8 (thin line), 4.0 (dotted line), and 5.0 (asterisks line). In (b), the spectra were measured under basic (thick line) and acidic (thin line) conditions. The excitation wavelengths are 290 nm in basic medium and 310 nm in acidic medium. Spectra were acquired using an Agilent 1260 Infinity LC and Agilent Cary Eclipse software, respectively. a.u., arbitrary units.

show λ_{em} 460 nm in acidic aqueous solution (excitation at 310 nm), and λ_{em} = 457 nm in basic aqueous solution (λ_{ex} = 290 nm). The Stokes shift is large in both acidic (150 nm) and basic media (167 nm), suggesting extensive electronic delocalization.

The ESI-HRMS of pure CompX showed a molecular ion with *m*/*z* 239.0598, the closest molecular formula being $C_{11}O_6H_{11}^+$, (calcd *m*/*z* 239.0550). The ^{1}H NMR spectrum of CompX showed a characteristic pattern of three resonances in the aromatic region (Table 1), a small doublet (2.2 Hz, H-5), a large doublet (8.5 Hz, H-8), and a doublet of doublets (2.2 and 8.5 Hz, H-9), all with the same integral value. This pattern is typical of a phenol ring with three protons, two neighboring protons (large coupling), and the third in a *meta*-position with respect to the first and a *para*-position with respect to the second, leading to a small coupling and to the absence of spin–spin coupling, respectively. Two other proton signals occurred as a weak-field singlet at δ 6.89 (one proton, C-3) and a methoxy group at δ 3.71 (three protons, C-11) (Table 1). Thus seven of the ten protons were observable in the ^{1}H NMR spectrum. The ^{1}H NMR spectra of CompX are strongly pH-dependent (data not shown). All eleven carbon atoms were observed in the 2D HSQC and the 2D HMBC spectra, which showed eight aromatic/olefinic, two carboxylic, and one methoxy carbons. An HMBC cross-peak identified C-2 as the location of the methoxy group. The same carbon is among HMBC cross-peaks from the singlet proton H-3, which, in turn, gave cross-peaks to carbons 1, 2, 5, and 9 (Fig. 2a). The carboxylic group C-10 exhibits a cross-peak with

Table 1
^{1}H (800 MHz) and ^{13}C (200 MHz) chemical shifts and proton multiplicities of CompX and the synthetic CompX (*E*)-isomer (D_2O, pH 4.2)

	CompX		CompX (*E*)-isomer	
	δ_H	δ_C	δ_H	δ_C
Position				
1	—	170.4	—	171.0
2	—	146.5	—	151.1
3	6.89 (s)	122.1	5.96 (s)	103.9
4	—	117.8	—	116.1
5	8.15 (d, 2.2 Hz)	132.3	7.70 (d, 2.4 Hz)	129.9
6	—	124.7	—	126.5
7	—	160.4	—	158.4
8	6.95 (d, 8.5 Hz)	116.9	6.86 (d, 8.5 Hz)	116.4
9	7.82 (dd, 2.2 and 8.5 Hz)	135.4	7.35 (dd, 2.4 and 8.5 Hz)	134.0
10	—	174.9	—	174.3
11	3.71 (s)	58.6	3.69 (s)	55.6

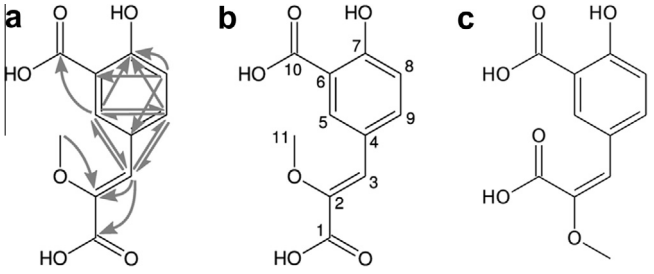

Figure 2. Structures of CompX and the CompX (*E*)-isomer. (a) The observed HMBC correlations in natural CompX. (b) Carbon atom numbering in CompX as in Table 1. (c) The synthetic CompX (*E*)-isomer with the opposite configuration of the C2–3 double bond.

the H-5 doublet only. Assuming that a HMBC cross-peak should not be observed through more than three bonds, although weak four-bond couplings are sometimes visible,[6] the only structure which conforms with the NMR and the mass spectra is that of 5-(2-carboxy-2-methoxyvinyl)-2-hydroxybenzoic acid (Fig. 2b). The three protons not observed in the NMR spectrum are those of the two carboxylic groups and that of a phenolic OH. To determine the configuration of the trisubstituted double bond we decided to synthesize both the *E*- and *Z*-isomers and compare their ROESY spectra.

The key synthetic step, the Horner–Wadsworth–Emmons olefination provided both isomers of CompX in a 2:1 (*Z*/*E*) ratio (Scheme 1).[7] The major *Z*-isomer was identical to the natural sample according to NMR, UV, and chromatography, whereas the minor *E*-isomer demonstrated significantly different properties. The most remarkable differences were the chemical shifts of C-3 and the attached proton (Δ 18.2 and 0.93 ppm, respectively, Table 1). Also, the unnatural double bond isomer of CompX was non-fluorescent.

The absolute (*Z*)-configuration of the CompX double bond was deduced from the absence of a H3–H11 cross peak in the ROESY spectrum of CompX and the presence of the corresponding cross-peak in the ROESY spectrum of its unnatural isomer (Supplementary data, Fig. S3).

Most probably, CompX is derived from tyrosine via three modifications, namely deamination to a keto-acid, enolate O-methylation, and carboxylation *ortho* to the phenolic hydroxyl. Our further studies on the *F. heliota* bioluminescent system will be focused on structural characterization of the bioluminescent reaction substrate, luciferin. This task, however, is heavily hampered by

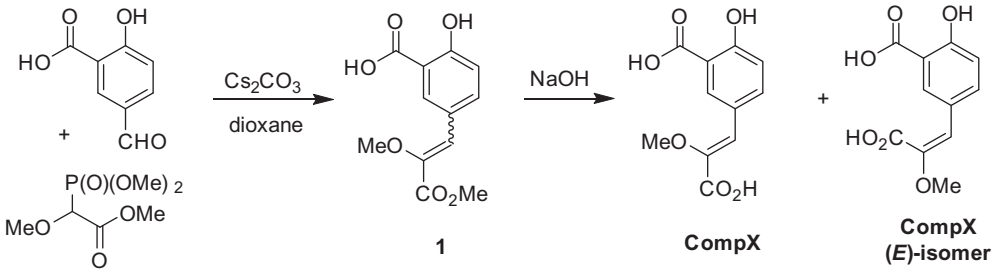

Scheme 1. Synthesis of CompX and its unnatural *E*-isomer.

the very low quantity of luciferin available from the earthworm. Preliminary NMR experiments gave evidence that substituted CompX is a part of the luciferin chemical structure. Namely, the ^{1}H NMR spectrum of *F. heliota* luciferin revealed the same aromatic fragment as in CompX. Further isolation and structural characterization of other CompX analogs (AsLn1-3) from *F. heliota* will hopefully shed light on their biosynthetic origin.

Acknowledgments

The Krasnoyarsk and Moscow groups acknowledge support from the Program of the Government of the Russian Federation 'Measures to Attract Leading Scientists to Russian Educational Institutions' (Grant No. 11.G34.31.0058), 'Molecular and Cellular Biology' of RAS, President of the Russian Federation 'Leading Science School' (Grant 3951.2012.4) and the Russian Foundation for Basic Research (Grant No. 11-04-01293-a). S.M.M. is grateful for a Ph.D. scholarship (reference SFRH/BD/65109/2009), co-funded by ESF, through POPH-QREN, and by national funds from FCT, I.P.

Supplementary data

Supplementary data associated with this article can be found, in the online version, at http://dx.doi.org/10.1016/j.tetlet.2013.11.064.

References and notes

1. (a) Wilson, T.; Hastings, J. W. *Annu. Rev. Cell Dev. Biol.* **1998**, *14*, 197; (b) Marques, S. M.; Esteves da Silva, J. C. G. *Global J. Anal. Chem.* **2011**, *2*, 241; (c) Shimomura, O. *Bioluminescence: Chemical Principles and Methods*; World Scientific Publishing: Singapore, 2006.
2. Rota, E.; Zalesskaja, N. T.; Rodionova, N. S.; Petushkov, V. N. *J. Zool.* **2003**, *260*, 291.
3. Zalesskaja, N. T.; Petushkov, V. N.; Rodionova, N. S. *Dokl. Biol. Sci.* **1990**, *310*, 141.
4. (a) Petushkov, V. N.; Rodionova, N. S.; Bondar', V. S. *Dokl. Biochem. Biophys.* **2003**, *391*, 204; (b) Rodionova, N. S.; Bondar', V. S.; Petushkov, V. N. *Dokl. Biochem. Biophys.* **2003**, *392*, 253; (c) Petushkov, V. N.; Rodionova, N. S. *Dokl. Biochem. Biophys.* **2005**, *401*, 115; (d) Rodionova, N. S.; Petushkov, V. N. *J. Photochem. Photobiol. B-Biol.* **2006**, *83*, 123.
5. (a) Petushkov, V. N.; Rodionova, N. S. *J. Photochem. Photobiol. B-Biol.* **2007**, *87*, 130; (b) Marques, S. M.; Petushkov, V. N.; Rodionova, N. S.; Esteves da Silva, J. C. G. *J. Photochem. Photobiol. B-Biol.* **2011**, *102*, 218.
6. Dubinnyi, M. A.; Osmakov, D. I.; Koshelev, S. G.; Kozlov, S. A.; Andreev, Y. A.; Zakaryan, N. A.; Dyachenko, I. A.; Bondarenko, D. A.; Arseniev, A. S.; Grishin, E. V. *J. Biol. Chem.* **2012**, *287*, 32993.
7. (a) Synthesis of (*E*/*Z*)-5-(2,3-dimethoxy-3-oxoprop-1-en-1-yl)-2-hydroxybenzoic acid (**1**): A suspension of methyl 2-(dimethoxyphosphoryl)-2-methoxyacetate (obtained according to the procedure described in Lowell, A. N.; Wall, P. D.; Waters, S. P.; Kozlowski, M. C. *Tetrahedron* **2010**, *66*, 5573) (19.5 g, 92 mmol), commercially available 5-formyl-2-hydroxybenzoic acid (13 g, 78 mmol), and Cs_2CO_3 (76.6 g, 235 mmol) in dioxane (100 mL) was stirred for 44 h at 60 °C. The mixture was acidified to pH 3.0 with aqueous HCl and extracted with EtOAc (3 × 150 mL). The solvent was evaporated under reduced pressure and the residue was subjected to chromatography on silica gel ($CHCl_3$/MeOH/AcOH, 93:5:2) to give compound **1** (3.84 g, 20%) as a 2:1 mixture of (*E*)- and (*Z*)-isomers (white solid). (*E*) ^{1}H NMR (700 MHz, DMSO-d_6) δ 8.19 (d, J = 2.1 Hz, 1H, ArH), 7.83 (dd, J = 8.7, 2.2 Hz, 1H, ArH), 6.91 (d, J = 8.7 Hz, 1H, ArH), 6.87 (s, 1H, CH), 3.70 (s, 3H, OCH_3), 3.66 (s, 3H, OCH_3). (*Z*) ^{1}H NMR (700 MHz, DMSO-d_6) δ 7.58 (d, J = 2.2 Hz, 1H, ArH), 7.27 (dd, J = 8.6, 2.3 Hz, 1H, ArH), 6.83 (d, J = 8.6 Hz, 1H, ArH), 6.14 (s, 1H, CH). 3.61 (s, 3H, OCH_3), 3.57 (s, 3H, OCH_3).; (b) *Synthesis of CompX [(Z)-5-(2-carboxy-2-methoxyvinyl)-2-hydroxybenzoic acid] and CompX (E)-isomer [(E)-5-(2-carboxy-2-methoxyvinyl)-2-hydroxybenzoic acid]*: A solution of NaOH (2 M, 5 mL) was added to (*E*/*Z*)-5-(2,3-dimethoxy-3-oxoprop-1-en-1-yl)-2-hydroxybenzoic acid (**1**) (30 mg, 0.12 mmol), and the mixture was stirred for 2 h at 50 °C. After completion of the hydrolysis (TLC), the mixture was acidified to pH 3.0 with aqueous HCl and extracted with EtOAc (2 × 15 mL). The solvent was evaporated in vacuo and the residue was chromatographed on silica gel ($CHCl_3$/MeOH/AcOH, 97:2:1) to give CompX (14 mg, 49%) and CompX (*E*)-isomer (7 mg, 25%) as white crystalline solids.

Pergamon

TETRAHEDRON
LETTERS

CompX, a luciferin-related tyrosine derivative from the bioluminescent earthworm *Fridericia heliota.* Structure elucidation and total synthesis

Valentin N. Petushkov[a,b,*], Aleksandra S. Tsarkova[c], Maxim A. Dubinnyi[c], Natalja S. Rodionova[a,b], Simone M. Marques[d], Joaquim C.G. Esteves da Silva[d], Osamu Shimomura[a], Ilia V. Yampolsky[c,*]

[a] *Laboratory of Bioluminescent Biotechnologies, Institute of Fundamental Biology and Biotechnology, Siberian Federal University, pr. Svobodnyi, 79, Krasnoyarsk 660041, Russia*

[b] *Laboratory of Photobiology, Institute of Biophysics, Siberian Branch of the Russian Academy of Sciences, Akademgorodok, Krasnoyarsk 660036, Russia*

[c] *Institute of Bioorganic Chemistry, Russian Academy of Sciences, Miklukho-Maklaya 16/10, Moscow 117997, Russia*

[d] *Chemistry Research Center of the University of Porto (*CIQ-UP*), Department of Chemistry and Biochemistry, Faculty of Sciences, University of Porto, Campo Alegre St. 687, Porto 4169-007, Portugal*

Supplementary Data

GENERAL

UV-vis spectra were obtained on the Agilent 1260 Infinity LC chromatograph software. Fluorescence spectra were acquired on an Agilent Cary Eclipse spectrophotometer (Agilent Technologies, Moscow, Russia) equipped with a Xenon flash lamp in fluorescence mode. The excitation wavelength was set at 290 and 310 nm in basic and acidic medium, respectively, and the emission wavelength was scanned from 300 nm to 700 nm. The scan rate was set to 120 nm/min, with a 5-nm excitation and emission slits.

High-resolution mass spectra were obtained on an Agilent 6224 TOF LC/MS System (Agilent Technologies, Santa Clara, CA, USA) equipped with a dual-nebulizer ESI source. Data acquisition and analysis was performed by the MassHunter Workstation software (Agilent Technologies, Santa Clara, CA, USA).

NMR spectra of natural CompX were acquired in D_2O, pH 4.2 at 30 °C on a Bruker Avance III 800 spectrometer equipped with a 5-mm CPTXI cryoprobe (Bruker Corporation, Billerica, MA, USA). Spectra of synthetic CompX and its double bond isomer were acquired under the same conditions (solvent, pH, temperature) on a Bruker Avance 700 spectrometer equipped with a 5-mm PATXI warm probe (Bruker Corporation, Billerica, MA, USA). The following spectra were used to elucidate structure: ^{1}H, 2D ^{1}H-^{13}C HSQC, 2D ^{1}H-^{13}C HMBC (J_{long} = 6 Hz) and 2D ROESY (200 ms). FID resolution for indirect dimensions was at least 40 Hz (^{13}C) and 30 Hz (^{1}H). Chemical shifts are given in parts per million (ppm). Data acquisition and analysis were performed using Bruker TopSpin software.

COLLECTION OF BIOMATERIAL AND COMPX ISOLATION AND PURIFICATION

Specimens of *Fridericia heliota* were individually hand-collected overnight in the soil forest from Krasnoyarsk (Russia) form June to November 2012. The total amount of earthworms (wet weight) collected was ~ 90 g, which corresponds to more than 100,000 worms. Before the extraction procedures, the cleaned wet earthworms were frozen at -20 °C. Fractions containing CompX were obtained by anion-exchange chromatography. A cell-free extract of *F. heliota*, prepared from ~ 20 g wet worms, was loaded onto a column (16 mm x 200 mm) packed with diethylaminoethyl (DEAE) Sepharose™ Fast Flow (Pharmacia Biotech, Uppsala, Sweden) coupled with the BioLogic™ LP chromatography system (BIO-RAD Laboratories, Hercules, CA, USA). The column was equilibrated by 15 mM tris(hydroxymethyl)-aminomethane-hydrochloric acid (Tris-HCl) buffer, pH 8.1 (Serva Electrophoresis GmbH, Heidelberg, Germany). Elution was done by a linear gradient elution program of sodium chloride 0-1 M. The main fractions obtained (~ 18 mL) were concentrated by solid-phase extraction. These fractions were acidified to pH 3 by adding hydrochloric acid and added to a 3-mL disposable C_{16} extraction cartridge (Diapack-C_{16}, BioChemMak S&T, Moscow, Russia). The column was washed with HCl 10mM containing 3% MeCN (10 mL), then eluted with 75% aqueous MeCN and the eluate was concentrated to the volume of 2 mL at the rotary evaporator. The concentrated solution obtained was submitted to a three-stages of reversed-phase chromatography at different pHs. A semi-preparative column (9.4 mm x 250 mm), ZORBAX Eclipse XDB-C_{18} (Agilent Technologies, Moscow, Russia) was coupled with the Agilent 1260 Infinity LC chromatograph (Agilent Technologies, Moscow, Russia). Elution was performed on a gradient elution program. In each chromatography, solvent A was 0.1% ammonium formate, pH 2.8,

4.0 or 5.0, and solvent B was acetonitrile. The gradient program was 5-40% B during 20 min. Both the column and solvents were maintained at at 25 °C, with a flow rate of 3 mL/min. Absorbance was monitored at 210, 230, 250, 270, 290, 310, 330 and 360 nm.

INHIBITORY EFFECT OF COMPX ON THE F. HELIOTA BIOLUMINESCENT REACTION *IN VITRO*

Inhibitory effect of CompX on the reaction between F. heliota luciferin, luciferase, ATP and oxygen was measured in a buffer, containing 20 мM Tris-HCl pH 8.2, 2.5 mM $MgCl_2$, 0.1 mM ATP and 0.5% Triton X100. Addition of 1000-fold excess of CompX with respect to luciferin led to decrease of luminescent signal by 73% (360 arbitrary units before addition, 100 arbitrary units after addition). These data suggest that CompX is a weak inhibitor of *F. heliota* luciferase.

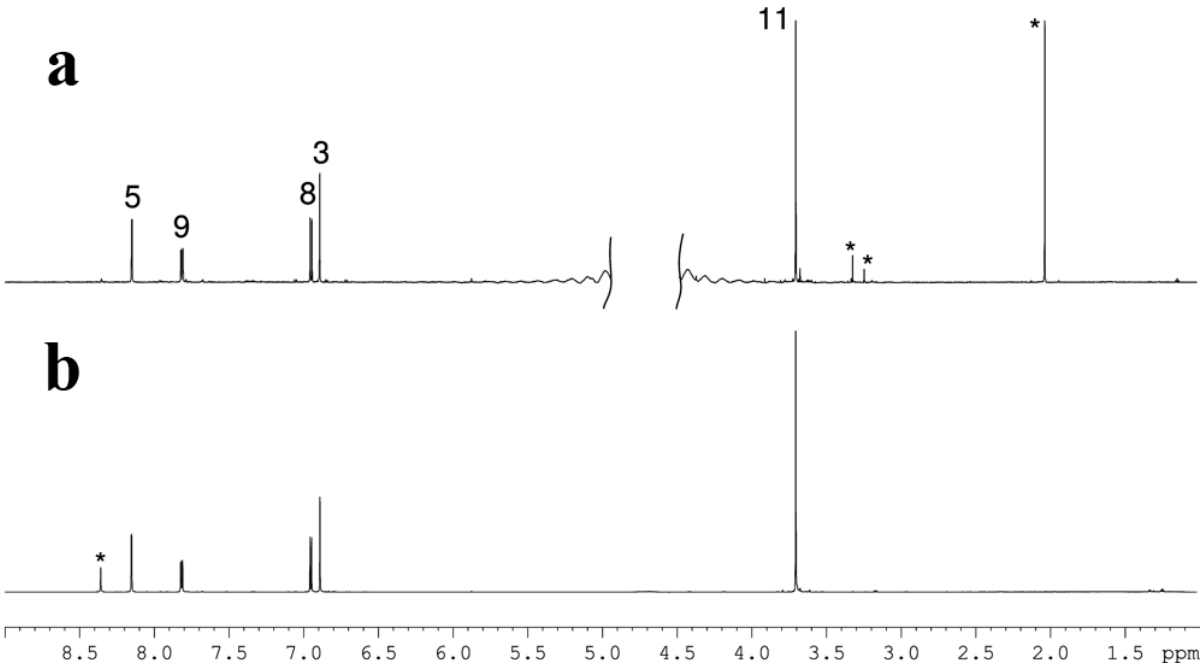

Figure S1. Comparison of ^{1}H NMR spectra: (a) synthetic CompX and (b) natural CompX. Impurities are indicated by asterisks, and digits designate atom numbers as indicated in Table 1 and Figure 2b.

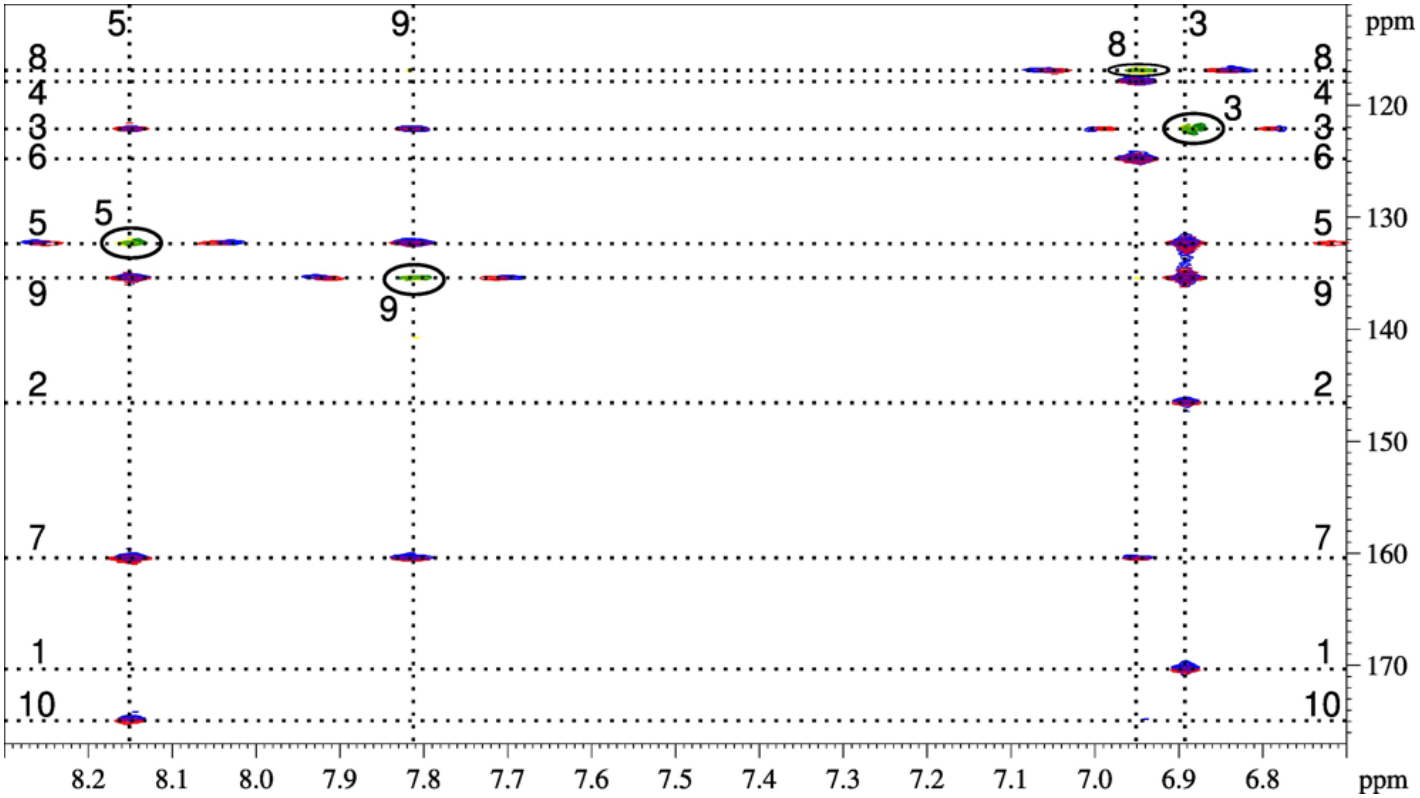

Figure S2. Comparison of the aromatic region of 2D spectra of natural CompX and synthetic CompX. Carbon numbers and the corresponding attached protons are assigned by digits as in Table 1 and Figure 2b. The colors refer to: yellow, HSQC of natural CompX; Green, HSQC of synthetic CompX; red, HMBC of natural CompX; blue, HMBC of synthetic CompX. Spectra were acquired under the conditions described in the notes.[9] Note that NMR spectra of natural CompX were obtained at 800 MHz whereas those of synthetic CompX were obtained at 700 MHz.

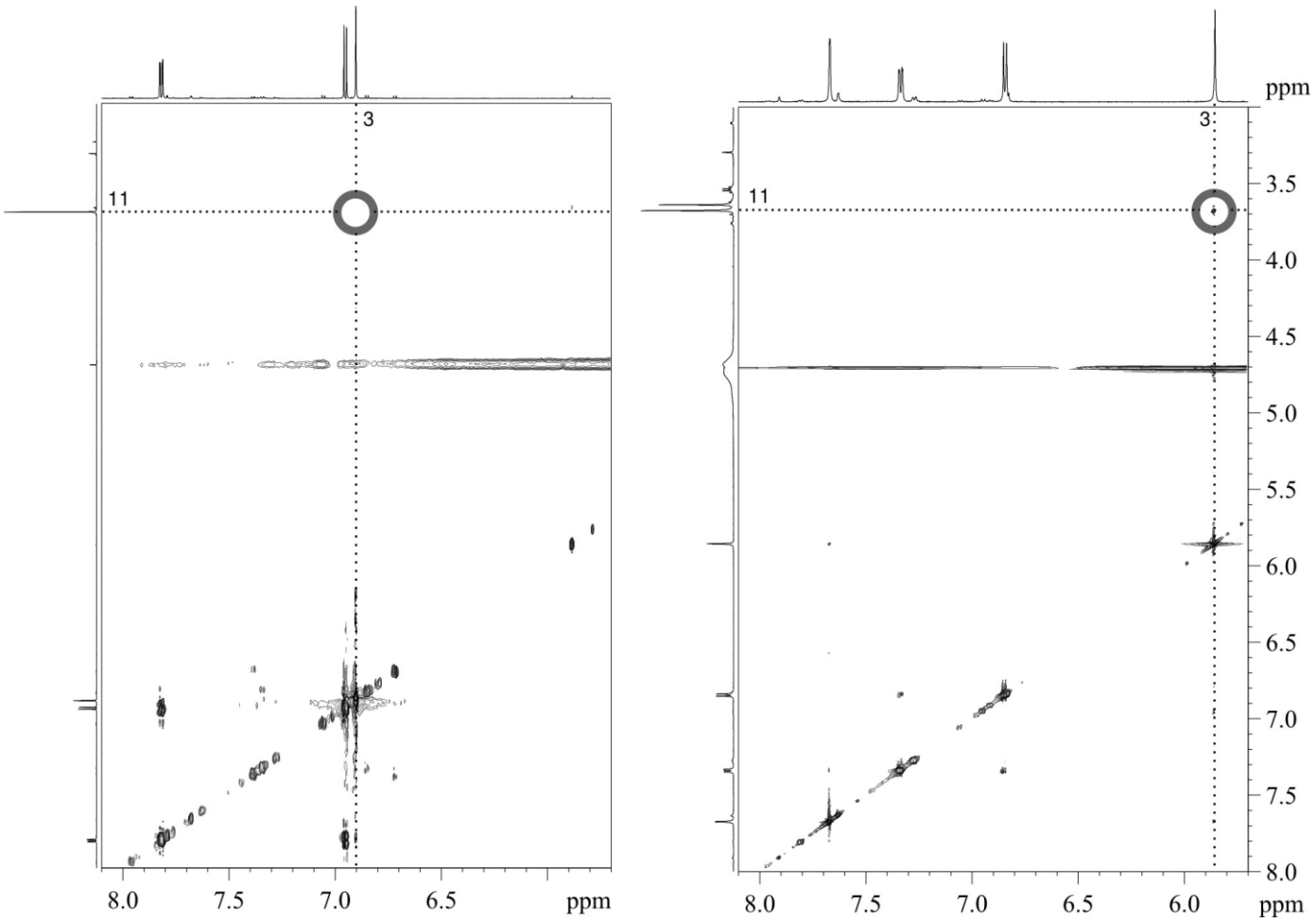

Figure S3. Comparison of the ROESY spectra of synthetic CompX (left) and CompX (*E*)-isomer (right). Positions of the observed 3-11 cross-peak in CompX (*E*)-isomer and the absent 3-11 cross-peak in CompX-s are highlighted by circles.

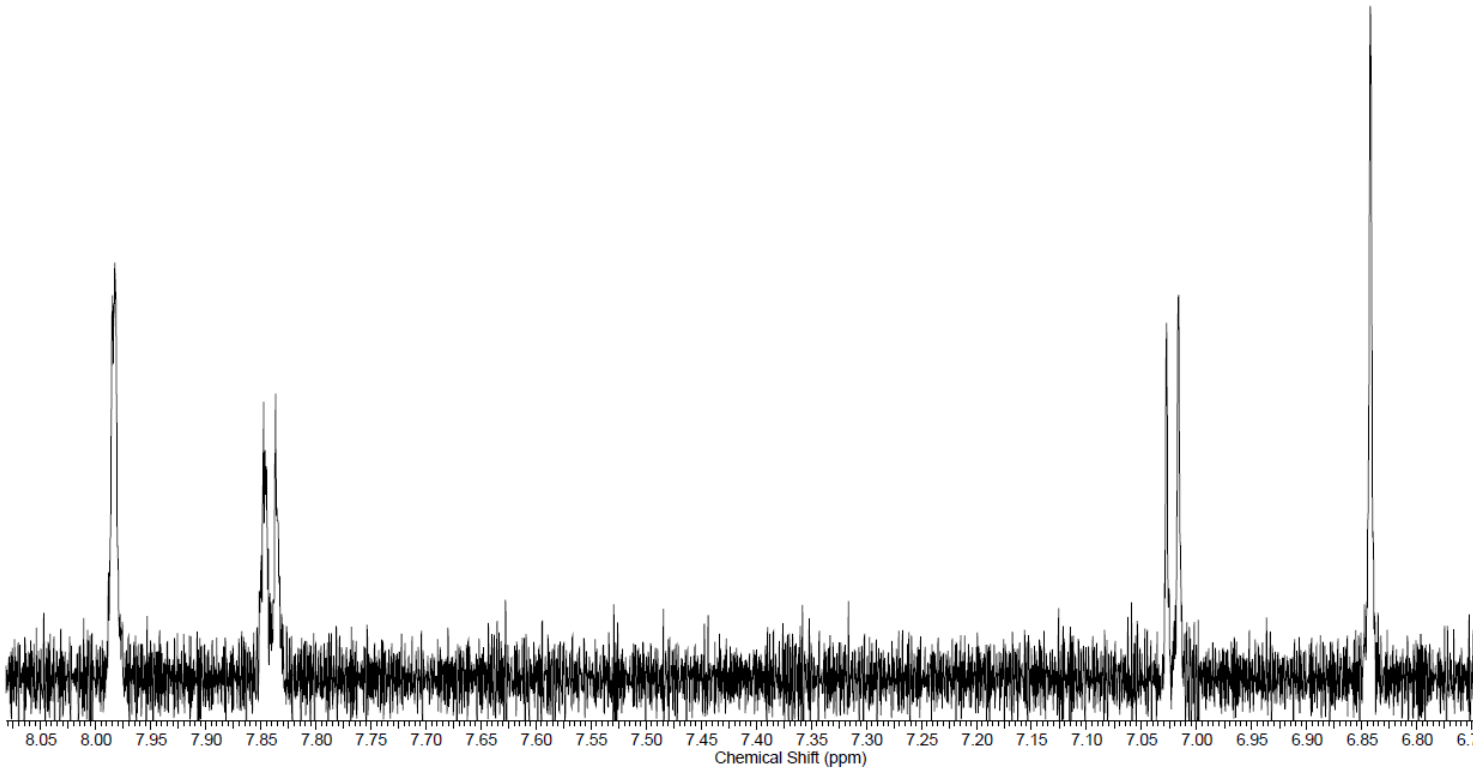

Figure S4. ^{1}H NMR spectrum (800 MHz, aromatic region) of *F. heliota* luciferin in D_2O.

Chapter eight

AsLn2, a luciferin-related modified tripeptide from the bioluminescent earthworm *Fridericia heliota*

Valentin N. Petushkov, Maxim A. Dubinnyi, Natalja S. Rodionova, Kirill D. Nadezhdin, Simone M. Marques, Joaquim C.G. Esteves da Silva, Osamu Shimomura, Ilia V. Yampolsky

Tetrahedron Lett. 55 (2014) 463-465

This paper is the second part of the analysis of the luciferin-related compounds CompX and AsLn(2). High-resolution mass spectrometry (HR-MS) and nuclear magnetic resonance (NMR) analysis execution and interpretation were performed by Maxim Dubinnyi, Kirill Nadezhdin and Ilia Yampolsky. By its turn, Valentin Petushkov and Natalja Rodionova were responsible for collecting living specimens of the earthworm *Fridericia heliota*, separating and purifying different extracts and coordinating the groups. Simone Marques was responsible for checking extracts purification and concentration by low-resolution MS and NMR and data gathering, under the supervision of Joaquim Esteves da Silva at the host institution, the Chemometric Research of Chemical, Environmental, Forensic and Biological Systems group, from the Chemistry Research Center of the University of Porto (*Centro de Investigação em Química da Universidade do Porto*, *CIQ-UP*), Department of Chemistry and Biochemistry, Faculty of Sciences, University of Porto. Osamu Shimomura was responsible for supervision and suggestions. All the authors were responsible for paper writing.

Tetrahedron Letters 55 (2014) 463–465

Contents lists available at ScienceDirect

Tetrahedron Letters

journal homepage: www.elsevier.com/locate/tetlet

AsLn2, a luciferin-related modified tripeptide from the bioluminescent earthworm *Fridericia heliota*

Valentin N. Petushkov [a,b], Maxim A. Dubinnyi [c], Natalja S. Rodionova [a,b], Kirill D. Nadezhdin [c], Simone M. Marques [d], Joaquim C. G. Esteves da Silva [d], Osamu Shimomura [a], Ilia V. Yampolsky [c,*]

[a] *Laboratory of Bioluminescent Biotechnologies, Institute of Fundamental Biology and Biotechnology, Siberian Federal University, pr. Svobodnyi, 79, Krasnoyarsk 660041, Russia*
[b] *Laboratory of Photobiology, Institute of Biophysics, Siberian Branch of the Russian Academy of Sciences, Akademgorodok, Krasnoyarsk 660036, Russia*
[c] *Institute of Bioorganic Chemistry, Russian Academy of Sciences, Miklukho-Maklaya 16/10, Moscow 117997, Russia*
[d] *Chemistry Research Center of the University of Porto (CIQ-UP), Department of Chemistry and Biochemistry, Faculty of Sciences, University of Porto, Campo Alegre St. 687, Porto 4169-007, Portugal*

ARTICLE INFO

Article history:
Available online 23 November 2013

Keywords:
Bioluminescence
Fridericia heliota
Luciferin
Modified peptide

ABSTRACT

AsLn2, an unusual modified peptide, was isolated from the bioluminescent earthworm *Fridericia heliota* (Enchytraeidae). Its structure, elucidated by NMR and mass spectrometry, includes residues of tyrosine, CompX (a novel tyrosine modification product, reported in the accompanying paper), and N(omega)-acylated lysine. Chromatography, UV, and ^{1}H NMR data imply a close structural similarity of AsLn2 with *F. heliota* luciferin. AsLn2 appears to be an intermediate or by-product in *F. heliota* luciferin biosynthesis.

The bioluminescence of earthworms has been insufficiently investigated. Bioluminescent genera are found in three oligochaeta families: Megascolecidae, Lumbricidae, and Enchytraeidae.[1] Among them, only the bioluminescence mechanism of Diplocardia longa (Megascolecidae) has been established in terms of the chemistry of its luciferin.

The Siberian luminous earthworm (*Fridericia heliota*, only recently described) belongs to the Enchytraeidae oligochaeta family.[2] Five components were found to be essential for the luminescence of F. heliota: Fridericia luciferase, Fridericia luciferin, adenosine 5′-triphosphate, Mg^{2+}, and atmospheric oxygen.[3] Cross-reactions of luciferase or luciferin from Fridericia with luciferins and luciferases from other organisms, including firefly *Photinus*, earthworms *Microscolex*, *Diplocardia*, and *Henlea*, were all negative, showing the unique nature of the F. heliota bioluminescent system.

An aim of our long-term project is the structural characterization of *F. heliota* luciferin. However, this task has been seriously hampered by the scarcity of the earthworm biomass (manual harvesting gives about 30 g/year), and the low content of luciferin (~0.5 μg per gram of wet biomass). In the course of our extensive efforts on purifying *F. heliota* luciferin, we observed two components, the chromatographic and UV spectral properties of which resembled luciferin, and designated them CompX and AsLn2.[4–6] Both these components are more than tenfold abundant compared to luciferin, which allowed us to study their structures. The present Letter is focused on the structural characterization of AsLn2, whereas the accompanying Letter[4] reports the structure of CompX.

The isolation and purification of AsLn2 were based on anion-exchange chromatography of crude extracts, obtained from 90 g of frozen worms, followed by three-stage reverse-phase chromatography (Supplementary data, Fig. S1) and gave ~0.1 mg of pure AsLn2. As mentioned above, the UV–vis spectra of AsLn2 and luciferin were similar (Fig. 1a, Table 1).[5] Both AsLn2 and luciferin are fluorescent (Fig. 1b, Table 1), with emission maxima in the visible range.

A HRMS study of pure AsLn2 gave an $[M+H]^{+}$ molecular ion with $m/z = 530.2146$, to which the molecular formula $C_{26}H_{31}N_3O_9$ matches with an uncertainty of 0.0013 Da (Supplementary data, Figure S2). The following NMR experiments were used to elucidate the structure of AsLn2: ^{1}H, ^{13}C, ^{1}H–^{1}H COSY, ^{1}H–^{13}C HSQC, ^{1}H–^{13}C HMBC, and ^{1}H–^{15}N HMBC. An analysis of the proton NMR spectra (Supplementary data, Fig. S3) indicated the presence of an aliphatic chain ($CH–CH_2–CH_2–CH_2–CH_2$), one AMX spin system, one spin system of two aromatic doublets (2H each), and five protons very close to those found in the data of CompX (Fig. 2a, see accompanying paper). Characteristic ^{1}H and ^{13}C chemical shifts (Supplementary data, Fig. S4) together with 2D HMBC connectivities (Fig. 2b)

* Corresponding author. Tel./fax: +7 499 724 81 22.
E-mail address: ivyamp@ibch.ru (I.V. Yampolsky).

0040-4039/$ - see front matter © 2013 Elsevier Ltd. All rights reserved.
http://dx.doi.org/10.1016/j.tetlet.2013.11.061

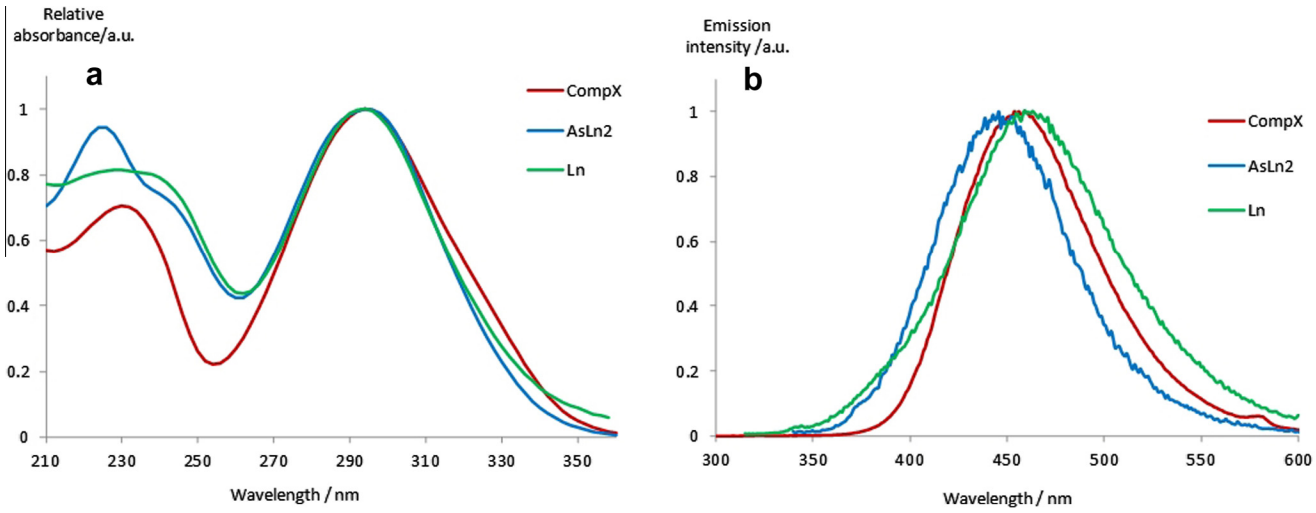

Figure 1. (a) UV–vis, and (b) fluorescence emission spectra of Fridericia luciferin (Ln) (green), AsLn2 (blue) and CompX (red) at pH 4.0 in water.

Table 1
UV–vis and fluorescence maxima of AsLn2 and *Fridericia* luciferin at different pH values[a]

Compound	Absorption		Fluorescence	
	λ_{max} (local)	λ_{max}	$\lambda_{excitation}$	$\lambda_{emission}$
Luciferin pH 7.0	228	294	290	466
AsLn2 pH 4.0	226	294	330	446
AsLn2 pH 2.8	226	294	290	464

[a] All values in nm.

identified the aliphatic chain as part of a lysine moiety and the AMX system with two aromatic doublets as a tyrosine residue (Table 2). The 2D ^{15}N HMBC spectrum displayed only two cross peaks from the 3″ protons of tyrosine to its nitrogen atom (δ 121.24, Table 2). The ^{15}N chemical shift provided unambiguous proof that the tyrosine nitrogen was involved in a peptide bond. Two other nitrogens were not directly observed due to the very low sensitivity of ^{15}N NMR spectra, the broad ^{15}N line shape of free NH_2 group, and/or the multiplicities of the protons of the lysine chain. The ^{1}H and ^{13}C NMR chemical shifts of five protons and ten carbons, which were not a part of the lysine or tyrosine residues, were closely similar to the corresponding atoms in CompX.[4] Therefore, substituted CompX was postulated to be a part of the structure of AsLn2. The three fragments, lysine, CompX, and tyrosine, were connected via two peptide bonds, as supported by four three-bond ^{1}H–^{13}C HMBC connectivities (Fig. 2b). The configuration of the double bond in AsLn2 is postulated to be the same as in CompX for two reasons. Firstly, the chemical shift of vinylic proton H-3′ is 6.74 ppm, whereas the opposite geometry of the double bond would give about 1 ppm lower value. Secondly, AsLn2 is fluorescent, while the (*E*)-isomer of CompX as well as its derivatives at the carboxylic group (esters and amides) is not (data not shown). The proposed structure, (*Z*)-N^6-(5-(3-((1-carboxy-2-(4-hydroxyphenyl)ethyl)amino)-2-methoxy-3-oxoprop-1-en-1-yl)-2-hydroxybenzoyl)lysine, is in agreement with all the NMR data and the observed molecular ion. Determination of the configurations of the two stereogenic centers in AsLn2 will be a subject of our further research.

In conclusion, preliminary NMR experiments on Fridericia luciferin have shown that the substituted CompX moiety constitutes a part of its structure (Supplementary data, Fig. S5). Also, the

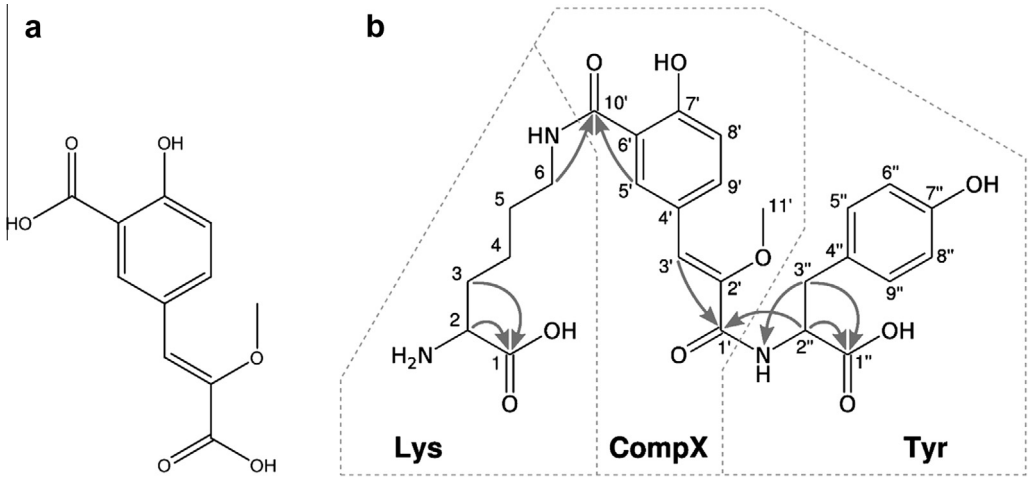

Figure 2. Structures of (a) CompX[4] and (b) AsLn2 with atom numbering as in Table 2. Gray arrows outline important ^{1}H → ^{13}C and ^{1}H → ^{15}N HMBC connectivities used to elucidate the structure of AsLn2.

Table 2
NMR chemical shifts and proton multiplicities of AsLn2 in D_2O, pH 7.0 at 30 °C (600 MHz for ^1H and 150 MHz for ^{13}C)

Fragment	Carbon	^1H chemical shift and multiplicity and ^{13}C chemical shift		
		δ_H		δ_C
Lys	1	—	—	174.70
	2	3.72	dd (5.6 Hz, 6.8 Hz)	54.77
	3	1.93, 1.88	m, m	30.19
	4	1.46	m	22.02
	5	1.67	quint (7.2 Hz)	28.21
	6	3.41	t (7.0 Hz)	39.09
CompX	1′	—	—	165.40
	2′	—	—	146.09
	3′	6.74	s	120.19
	4′	—	—	117.81
	5′	7.97	d (1.7 Hz)	130.66
	6′	—	—	123.41
	7′	—	—	[a]
	8′	6.95	d (8.7 Hz)	118.54
	9′	7.74	dd (1.7 Hz, 8.7 Hz)	134.77
	10′	—	—	169.41
	11′	3.47	s	59.27
Tyr	1″	—	—	177.79
	NH	[a]	—	^{15}N: 121.24
	2″	4.53	dd (5.1 Hz, 8.2 Hz)	56.24
	3″	3.23	dd (5.1 Hz, 14.1 Hz)	36.72
		2.97	dd (8.2 Hz, 14.1 Hz)	
	4″	—	—	129.49
	5″, 9″	7.14	d (8.4 Hz)	130.59
	6″, 8″	6.82	d (8.4 Hz)	115.30
	7″	—	—	154.12

[a] Not observed.

presence of a lysine residue and the absence of a tyrosine residue can be deduced from comparison of NMR spectra of AsLn2 and luciferin. However, neither CompX, nor AsLn2 exhibit luminescence activity. These facts suggest that these compounds may be involved in luciferin biosynthesis or degradation. Their biological role, biosynthetic origin, and relation to luciferin will be the subjects of our further studies.

Acknowledgments

The authors wish to thank Dr. Alexander O. Chizhov for recording mass spectra. The Krasnoyarsk and Moscow groups acknowledge support from the Program of the Government of the Russian Federation 'Measures to attract leading scientists to Russian educational institutions' (Grant no. 11. G34.31.0058), 'Molecular and Cellular Biology' of RAS, President of the Russian Federation 'Leading science school' (Grant 3951.2012.4) and the Russian Foundation for Basic Research (Grant no. 11-04-01293-a). S.M.M. is grateful to a Ph. D. scholarship (reference SFRH/BD/65109/2009), co-funded by ESF, through POPH-QREN, and by national funds from FCT, I.P.

Supplementary data

Supplementary data associated with this article can be found, in the online version, at http://dx.doi.org/10.1016/j.tetlet.2013.11.061.

References and notes

1. (a) Wilson, T.; Hastings, J. W. *Annu. Rev. Cell. Dev. Biol.* **1998**, *14*, 197; (b) Marques, S. M. Esteves da Silva *J. C. G. Glob. J. Anal. Chem.* **2011**, *2*, 241; (c) Shimomura, O. *Bioluminescence: Chemical Principles and Methods*; World Scientific Publishing: Singapore, 2006.
2. Rota, E.; Zalesskaja, N. T.; Rodionova, N. S.; Petushkov, V. N. *J. Zool.* **2003**, *260*, 291.
3. (a) Petushkov, V. N.; Rodionova, N. S.; Bondar', V. S. *Dokl. Biochem. Biophys.* **2003**, *391*, 204; (b) Rodionova, N. S.; Bondar', V. S.; Petushkov, V. N. *Dokl. Biochem. Biophys.* **2003**, *392*, 253.
4. For the accompanying paper, see: Petushkov, V. N.; Tsarkova, A. S.; Dubinnyi, M. A.; Rodionova, N. S.; Marques, S. M.; Esteves da Silva, J. C. G.; Shimomura, O.; Yampolsky, V. *Tetrahedron Lett.* **2013**. volume, first page.
5. (a) Rodionova, N. S.; Petushkov, V. N. J. *Photochem. Photobiol. B-Biol.* **2006**, *83*, 123; (b) Petushkov, V. N.; Rodionova, N. S. J. *Photochem. Photobiol. B-Biol.* **2007**, *87*, 130.
6. Marques, S. M.; Petushkov, V. N.; Rodionova, N. S.; Esteves da Silva, J. C. G. J. *Photochem. Photobiol. B Biol.* **2011**, *102*, 218.

o
Pergamon

TETRAHEDRON
LETTERS

AsLn2, a luciferin-related modified tripeptide from the bioluminescent earthworm *Fridericia heliota*

Valentin N. Petushkov[a,b], Maxim A. Dubinnyi[c], Natalja S. Rodionova[a,b], Kirill D. Nadezhdin[c], Simone M. Marques[d], Joaquim C.G. Esteves da Silva[d], Osamu Shimomura[a], Ilia V. Yampolsky[c,*]

[a] *Laboratory of Bioluminescent Biotechnologies, Institute of Fundamental Biology and Biotechnology, Siberian Federal University, pr. Svobodnyi, 79, Krasnoyarsk 660041, Russia*

[b] *Laboratory of Photobiology, Institute of Biophysics, Siberian Branch of the Russian Academy of Sciences, Akademgorodok, Krasnoyarsk 660036, Russia*

[c] *Institute of Bioorganic Chemistry, Russian Academy of Sciences, Miklukho-Maklaya 16/10, Moscow 117997, Russia*

[d] *Chemistry Research Center of the University of Porto (*CIQ-UP*), Department of Chemistry and Biochemistry, Faculty of Sciences, University of Porto, Campo Alegre St. 687, Porto 4169-007, Portugal*

Supplementary Material

GENERAL

UV-Vis spectra were obtained using the Agilent 1260 Infinity LC chromatograph software in 0.1% formic acid pH 2.8 and 4.0 for AsLn2 and pH 7.0 for luciferin. The pH was adjusted using ammonium hydroxide. Fluorescence spectra were acquired on an Agilent Cary Eclipse spectrophotometer (Agilent Technologies, Moscow, Russia) equipped with a Xenon flash lamp in fluorescence mode in 0.1% formic acid, pH 2.8 and 4.0, for AsLn2, and pH 7.0 for luciferin. The pH was adjusted using ammonium hydroxide. The excitation wavelength was set at 290 nm for luciferin, pH 7.0, for AsLn2, pH 2.8, and 330 nm, and for AsLn2, pH 4.0. The emission was scanned from 300 nm to 600 nm for luciferin pH 7.0, from 300 nm to 700 nm for AsLn2, pH 2.8, and from 340 nm to 700 nm for AsLn2, pH 4.0. The scan rate was set to 120 nm/min, with a 5-nm excitation and emission slits.

High-resolution mass spectra were obtained on an Agilent 6224 TOF LC/MS System (Agilent Technologies, Santa Clara, CA, USA) equipped with a dual-nebulizer ESI source. Data acquisition and analysis was performed by the MassHunter Workstation software (Agilent Technologies, Santa Clara, CA, USA).

NMR spectra of AsLn2 were acquired in D_2O, pH 7.0 (as pH-meter readings) at 30 ^oC on a Bruker Avance III 800 MHz NMR spectrometer equipped with 5 mm CPTXI cryoprobe (Bruker Corporation, Billerica, MA, USA). The following spectra were used to identify the chemical structure: ^1H, ^{13}C, 2D COSY, 2D ^1H-^{13}C HSQC, 2D ^1H-^{13}C HMBC (J_{long}=7 Hz) and 2D ^1H-^{15}N HMBC (J_{long}=5 Hz). Free Induced Decay (FID) resolution for indirect dimensions was 30 Hz for ^{13}C, 6 Hz for ^1H and 95 Hz for ^{15}N. Chemical shifts are given in parts per million (ppm). Data acquisition and analysis were performed using Bruker TopSpin software.

COLLECTION OF BIOMATERIAL AND COMPX ISOLATION AND PURIFICATION

Specimens of *Fridericia heliota* were individually hand-collected overnight in the soil forest from Krasnoyarsk (Russia) form June to November 2012. The total amount of earthworms (wet weight) collected was ~ 90 g, which corresponds to more than 100,000 worms. Before extraction, the cleaned wet earthworms were frozen at -20 ^oC. A cell-free extract of *F. heliota*, prepared from ~ 20 g wet worms, was loaded onto a column (16 mm x 200 mm) packed with diethylaminoethyl (DEAE) Sepharose™ Fast Flow (Pharmacia Biotech, Uppsala, Sweden) coupled to the BioLogic™ LP chromatography system (BIO-RAD Laboratories, Hercules, CA, USA). The column was equilibrated by 15 mM tris(hydroxymethyl)-aminomethane-hydrochloric acid (Tris-HCl) buffer, pH 8.1 (Serva Electrophoresis GmbH, Heidelberg, Germany). Elution was done by a linear gradient elution program of sodium chloride 0-1 M. The main fractions obtained (~ 18 mL) were concentrated by solid-phase extraction. These fractions were acidified to pH 3 by adding hydrochloric acid and then added to a 3-mL disposable C_{16} extraction cartridge (Diapack-C_{16}, BioChemMak S&T, Moscow, Russia). Further purification was performed using a semi-preparative column (9.4 mm x 250 mm), ZORBAX Eclipse XDB-C_{18} (Agilent Technologies, Moscow, Russia) coupled to the Agilent 1260 Infinity LC chromatograph (Agilent Technologies, Moscow, Russia). Elution was done using a gradient elution program. Solvent A was 0.1% ammonium formate, pH 5 and solvent B was acetonitrile. The standard gradient

program was 5-40% B during 20 min. Both the column and solvents were maintained at 25 ºC, with a flow rate of 3 mL/min. Absorbance was monitored at 210, 230, 250, 270, 290, 310, 330 and 360 nm. Each fraction was rechromatographed on the same system with solvent A being 0.1% formic acid pH 2.8, 4.0 and 7.0. When necessary, the pH was adjusted using ammonium hydroxide. To evaluate component content in these fractions, 10 µl of each fraction was run on a 3.0 mm x 150 mm-ZORBAX Eclipse XDB-C18 column, with the same program described above, to integrate the respective peaks at λ = 290 nm. Identification of the peaks as CompX or AsLn2 was inferred by their retention times and their specific UV-Vis spectra, and the content of components by their optical density.

LUCIFERIN ACTIVITY ASSAY

Identification and quantification of luciferase and luciferin fractions was done through enzymatic reaction. The reaction mixture for measuring luciferase activity and luciferin content (in arbitrary units) was composed of 10 mM ATP (2.5 µL), 100 mM magnesium chloride (2.5 µL), 10% Triton® X-100 (10 µL) (Sigma-Aldrich, St. Louis, USA), 20 mM Tris-HCl buffer pH 8.1 (180 µL) and anion-exchange purified luciferin or luciferase extracts, respectively (10 µL). The reaction was initiated by adding luciferin or luciferase fractions and was performed on a custom-made luminometer (Oberon, Krasnoyarsk, Russia). Each time before the addition of luciferin or luciferase fractions, the background luminescence was measured for 20 seconds and subtracted from the total measurement.

AsLn2 showed no appreciable inhibitory activity on bioluminescence reaction at concentrations 1000-fold higher than those of luciferin.

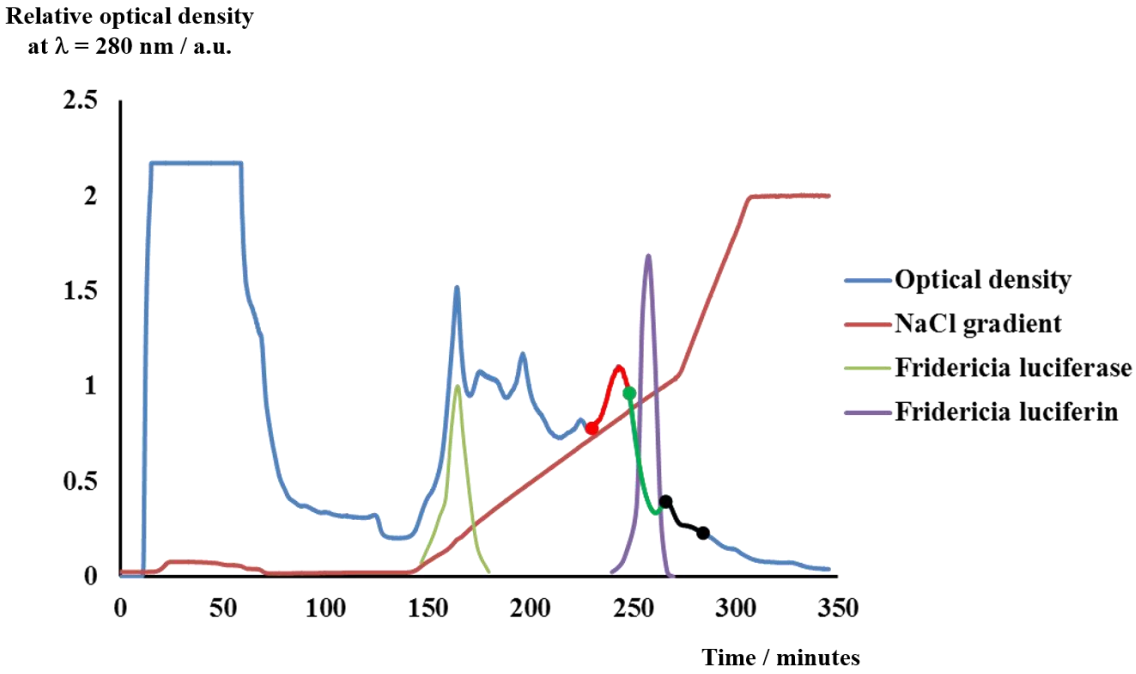

Figure S1. Anion-exchange chromatogram of cell-free extract (~ 20g worms), using a 16 mm diameter x 200 mm long column packed with DEAE Sepharose and equilibrated by 15 mM Tris-HCl buffer, pH 8.1. Elution was done by a linear gradient elution program of sodium chloride (NaCl) 0-1 M. *Fridericia* luciferase and *Fridericia* luciferin peaks were assigned through their chemical reaction (page S2). Colored segments correspond to collected fractions enriched in CompX, AsLn2 or luciferin. 230-248 minutes, red segment; fraction 248-266 minutes, dark green segment; fraction 266-284 minutes, black segment. a.u., arbitrary units.

Table S1. Total content of components in the fractions collected after anion-exchange chromatography.

Fraction / minutes	Component / optical units		
	CompX	AsLn2	Luciferin
230-248	0.09	0.330	0.01
248-266	2.170	1.850	0.137
266-284	3.050	0.08	0.006
Total amount	5.310	2.260	0.153

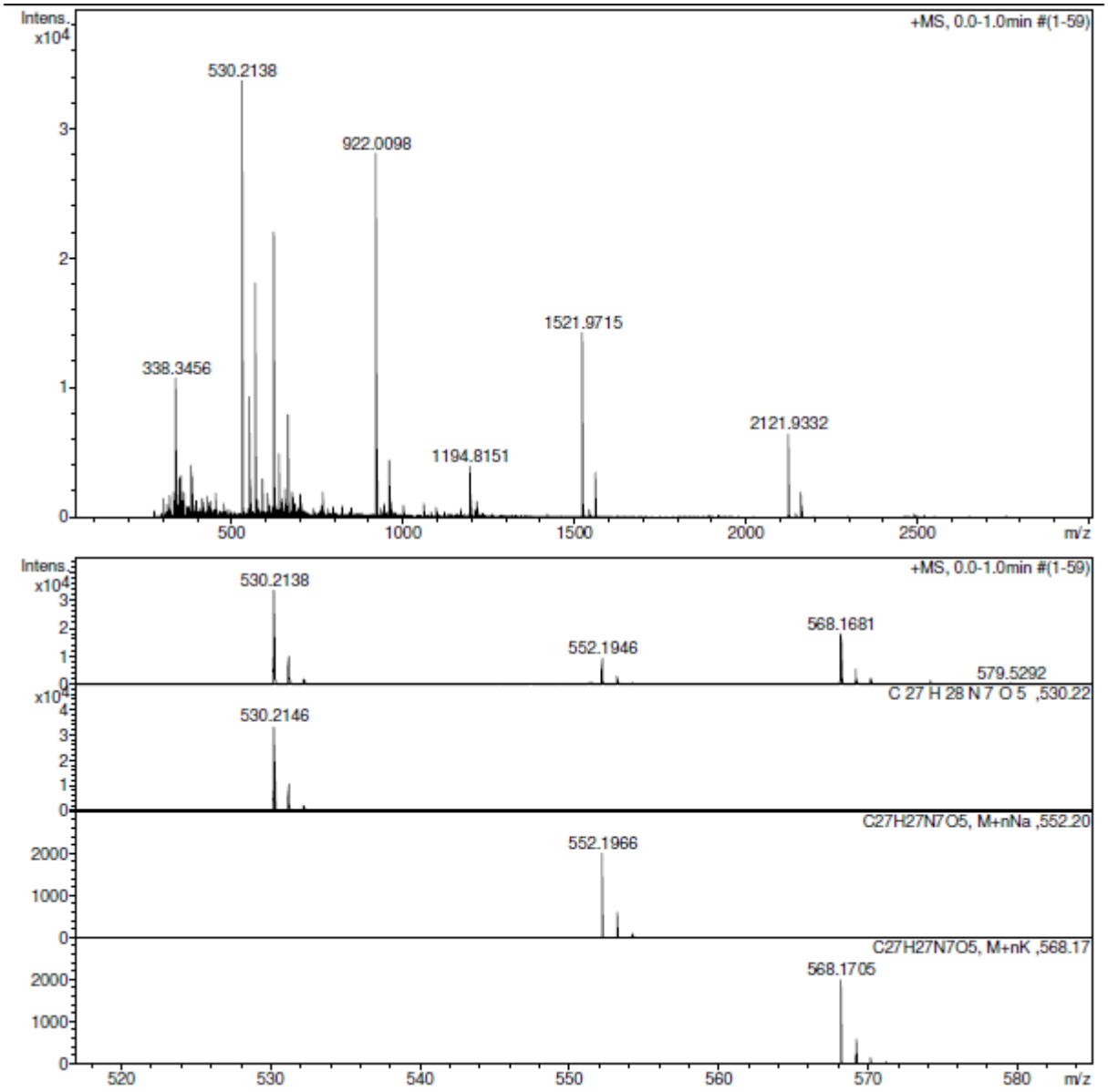

Figure S2. HRMS spectrum of AsLn2 in positive ion mode.

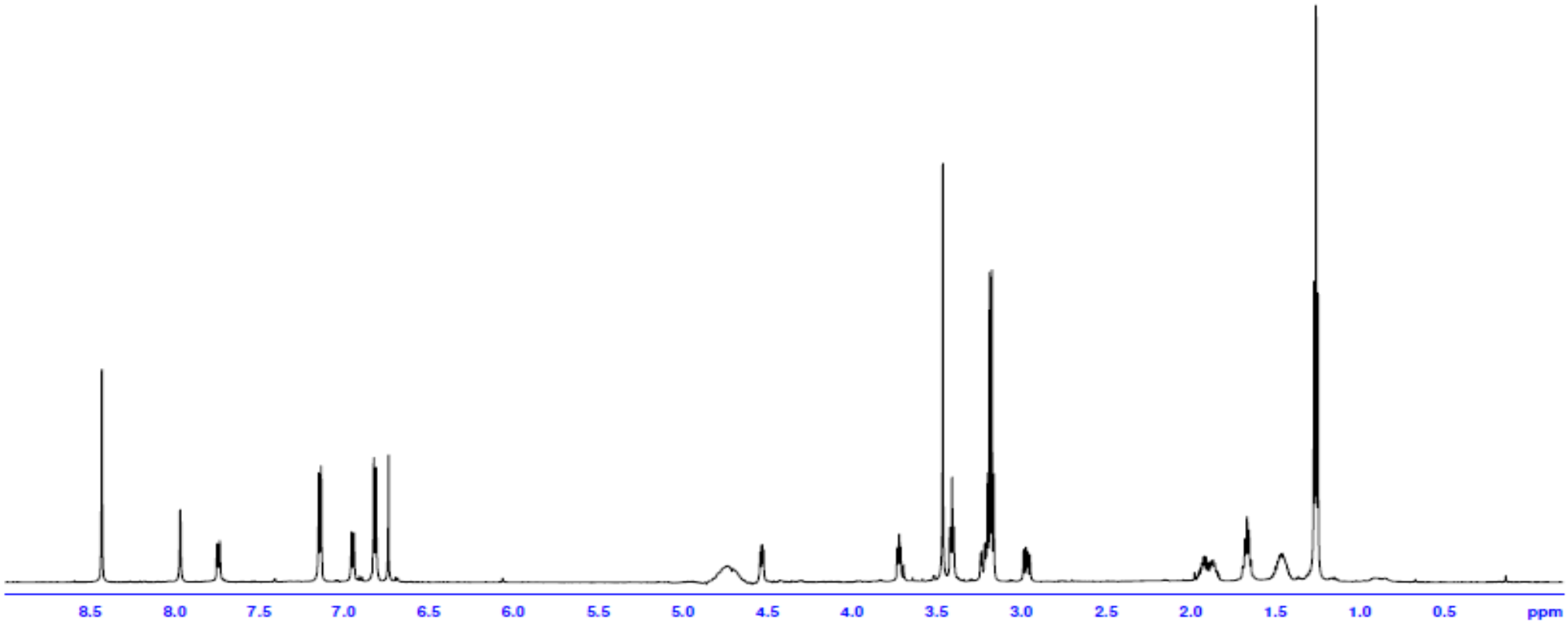

Figure S3 ^{1}H NMR spectrum of AsLn2 in D_2O, pH 7.0 at 30 ^{o}C.

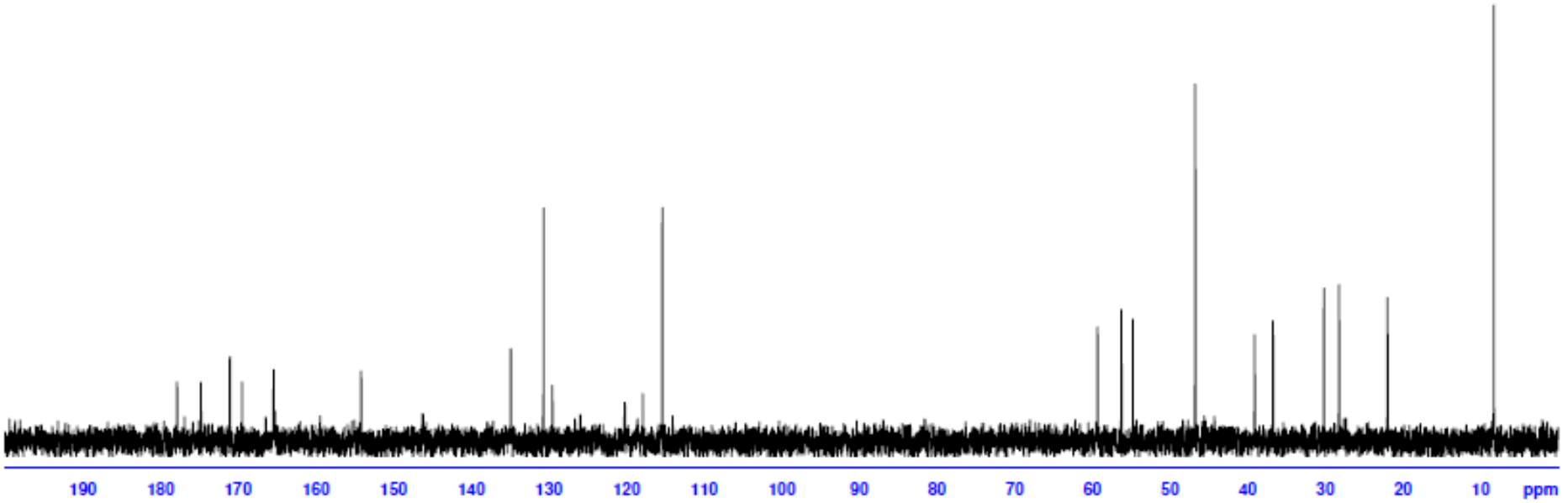

Figure S4. ^{13}C NMR spectrum of AsLn2 in D_2O, pH 7.0 at 30 °C.

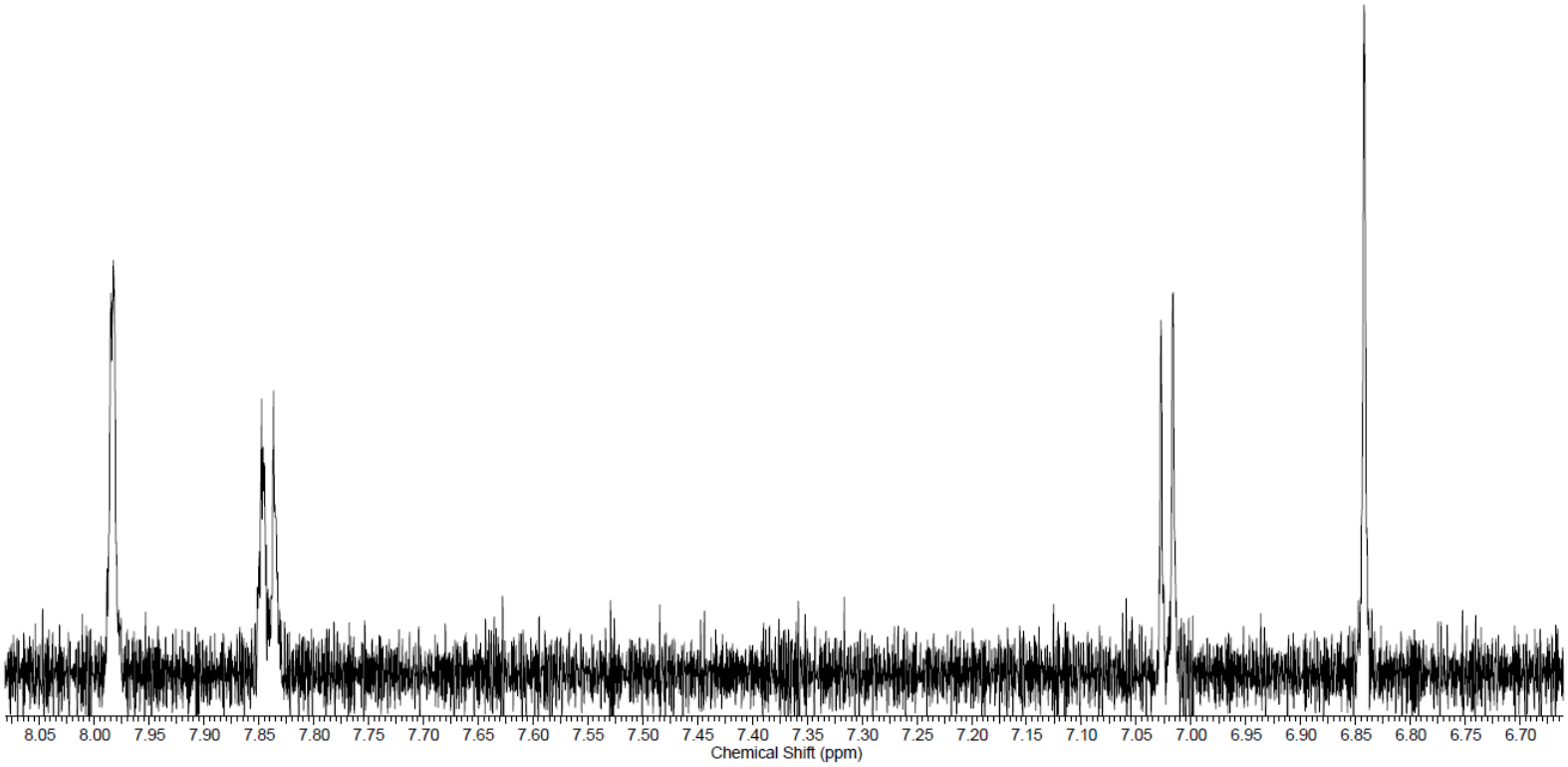

Figure S5. ^{1}H NMR spectrum (aromatic region) of *F. heliota* luciferin in D_2O.

Section four

Future perspectives and conclusions

Future perspectives

As the need for improved methods for an ever growing number of analytes continues, novel proposals are expected. Novel methods may rely on luciferase alone or coupled reactions, which greatly enhances their scope. Statistical experimental designs for screening and optimization of a method's factors are a valuable tool that offers robustness, celerity and reduced costs. Even currently established bioluminescent methods may be improved with new bioluminescent systems, such as that from *Fridericia heliota*.

The characterization of *Fridericia heliota*'s bioluminescent system is still at its dawn, however the foundations for new developments were set up. Following the structural characterization of *F. heliota*'s luciferin, including its chemical synthesis in a large scale, the next focus will be on luciferase. Purified *F. heliota*'s luciferase may be subjected to structural characterization as well, through X-ray diffraction, for example, followed by the cloning of its gene and the biotechnological production of the recombinant enzyme in large amounts. The reaction's features like thermal stability and color emission may also be improved by means of genetic engineering or the chemical modification of luciferin.

Finally, the rapidly growing fields of nanochemistry and nanotechnology have led to new bioluminescent methods due to the successful coupling of nanomaterials with luciferases. This topic will be further described in the next chapter.

Chapter nine

New methodologies based on the coupling of luciferase with nanomaterials

Simone M. Marques, Joaquim C.G. Esteves da Silva, *in*: D.J. Rodgerson (ed.), Bioluminescence – Characteristics, Adaptations and Biotechnology, Nova Science Publishers, New York (N.Y.), 2011, pp. 29-48.

The text was integrally written by Simone Marques within the host institution, the Chemometric Research of Chemical, Environmental, Forensic and Biological Systems group, from the Chemistry Research Center of the University of Porto (*Centro de Investigação em Química da Universidade do Porto*, *CIQ-UP*), Department of Chemistry and Biochemistry, Faculty of Sciences, University of Porto, under the supervision of Joaquim Esteves da Silva.

In: Bioluminescence
Editor: David J. Rodgerson, pp. 29-48
ISBN 978-1-61209-747-3

Chapter 2

NEW METHODOLOGIES BASED ON THE COUPLING OF LUCIFERASE WITH NANOMATERIALS

Simone M. Marques and Joaquim C. G. Esteves da Silva*
Centro de Investigação em Química, Department of Chemistry and Biochemistry,
Faculty of Sciences, Universidade do Porto, Rua do Campo Alegre 687,
4169-007 Porto, Portugal

ABSTRACT

Luciferase is a powerful tool in bioanalysis. Several well-established methods employ luciferases, particularly firefly and *Renilla* luciferases, as reporter genes or biosensors in environmental, biomedical and biochemical research. These techniques have interesting features for the analyst such as sensitivity, specificity and reduced assay time. Nanochemistry and Nanotechnology are disciplines that are gaining much attention and evolving rapidly. They allow the development of custom-made nanomaterials with the desired properties, starting from conventional bulk materials. Recently, the coupling of nanomaterials such as carbon nanotubes, mesoporous silica nanoparticles, metallic nanoparticles and quantum dots with luciferases led to new or improved methodologies for analyte quantification and enhanced gene delivery strategies. One of the principal scopes is to modulate or alter luciferase's bioluminescence emission, either by stabilizing it or tuning it to longer wavelengths. This chapter aims to present state-of-art articles regarding new methods based on the coupling of luciferases to nanomaterials, along with a brief introduction to Nanoscience.

Keywords: Luciferase; Nanochemistry; Nanomaterials; Nanoscience; Nanotechnology; Bioanalytical Chemistry; Bioimaging; Biomedicine; Carbon Nanotubes; Gold Nanoparticles; Nanodiamonds; Nanostructured Films; Quantum Dots; Silica Nanoparticles

* Tel: +351220402569. Fax: +351220402659. E-mail: jcsilva@fc.up.pt

INTRODUCTION

Basic Concepts about Nanoscience, Nanomaterials, Nanochemistry and Nanotechnology

Nanoscience is a current, although not really novel [1], topic of intense interest and, accordingly, of much research. The very first definition of Nanoscience was strictly based on size; any material within 1-100 nm would be under the remit of Nanoscience. Today, however, the scientific community does not hold this single definition. In fact, in 2004 the Royal Society and the Royal Academy of Engineering published a report in which a broader definition was proposed [2]:

> "Nanoscience is the study of phenomena and manipulation of materials at atomic, molecular and macromolecular scales, where properties differ significantly from those at a larger scale."

This definition highlights the concept of size-dependent properties of a given material. A nanomaterial has the same composition of the macroscopic, or bulk, material, but a whole different set of properties such as spectroscopic, mechanical, chemical reactivity, among others. Usually this shift in properties occurs at the nanometric scale, and then the "nano" designation. However, some materials already present bulk properties at a few nanometers in size, while others can be regarded as nanomaterials in the micrometer range, and that is one reason why the "size only" definition is not an ideal one and that an extended scale from 1 to 1000 nm is more realistic. Furthermore, at this scale, a defined structure can be observed with spectroscopic techniques in true nanomaterials or nanostructured materials (bulk materiais with defined forms at nanoscale, as in the case of zeolites), but not in bulk materials in general. For example, pure bulk metallic gold is a yellow and inert material whereas colloidal gold nanoparticles not only exhibit several different colours according to size and concentration but also present catalytic properties [3], as in the oxidation of carbon monoxide to carbon dioxide [4]. Beyond nanogold, the semiconductor nanoparticles known as "quantum dots" have receiving much attention due to their intense and stable fluorescence and wide variety of colours. These unique properties result from a quantic confinement of the nanocrystal not found in bulk semiconductors [5, 6].

Nanomaterials include, besides nanomaterials themselves and nanostructured materials already mentioned, the nanocomposites and nanohybrids. Nanocomposites are a combination of at least two different components into a single nanomaterial with final properties that can be the same of the original individual components or new ones can emerge. For example, the integration of zinc oxide nanoparticles in plain cellulosic paper led to an improved strain sensor [7]. By its turn, a nanohybrid is the result of coupling different nanomaterials in which their physical integrity is maintained in the final product and new or improved features are obtained [8]. As an example, the conjugation of single-walled carbon nanotubes with quantum dots not only allowed the study of photochemical processes in which they participate but also revealed their potential application in photovoltaic cells [9]. Another important attribute of nanomaterials is their high surface area-volume ratio, which is in the order of 100 to 1000 m^2/g. For this reason, mesoporous nano-sized silica is now being

preferred over bulk silica with the same porosity due to the higher superficial area of the nanomaterial.

In the nanoworld, surface is a very important aspect. In bulk materials, surfaces are a minor portion of their volume and can be ignored up to some point. But almost all of a nanomaterial is surface. To obtain a nanomaterial its size has to be strictly controlled, to avoid it becoming bulk. As a result of this control, an incomplete filling of the valence orbitals occurs. These "dangling bonds" raise the surface's energy and explain the extreme reactivity of nanomaterials' surfaces. This reactivity though is not only detrimental; by adding capping agents not only this energy is reduced and more stability is obtained but also the functionalization of the nanomaterial is achieved. Functionalization is the attachment of molecules through covalent or non-covalent (electrostatic, physical adsorption) interactions which confers new and improved characteristics to the nanomaterial. For example, the functionalization of single-walled carbon nanotube sensors with benzene enhanced their sensitivity towards gaseous species derived from sulphur hexafluoride [10].

Nanomaterials can be obtained by chemical or physical process. In this context, Nanochemistry can be regarded as "the utilization of synthetic chemistry to make nanoscale building blocks of different size and shape, composition and surface structure, charge and functionality" [11]. It is the contribution of Chemistry to Nanoscience. Traditionally, Chemistry deals with molecules, whose dimensions are inferior to nanometers, and so to obtain nanomaterials one needs to build it piece by piece, an approach known as "bottom-up". In Physics, on the other hand, one begins with "large" blocks of bulk material, in the micrometer range for example, which are then modelled to the desired nanomaterial towards miniaturization, a "top-down" approach compared to the sculpture of a statue. This division is not absolute, however, as top-down techniques can also be applied in the chemical preparation of nanomaterials. For instance, the exfoliation of clay results in separated lamellar sheets with different properties from the bulk clay and nanometric dimensions. It is also important to note that the real innovation is neither in the building block composition nor in the synthesis process but rather in the manner they arrange. In Nanoscience an important process is the self-assembly, regarded as the spontaneous generation of higher-order systems from pre-existing components that already contain the information for their self-assembly, leading to the synthesis of nanomaterials with new or betters properties in relation to the starting building blocks [12, 13]. In Nature, the phenomenon of self-assembly occurs in scales from the folding of proteins, for example, to the existence of galaxies. Self-assembly is also a reversible process, implying the adjustment of the interactions according to novel conditions. In Nanochemistry's bottom up methods, the most popular self-assembly process is the molecular self-assembly of atoms, molecules or ions into bigger and ordered structures based in commonly known chemical interactions such as ionic, metallic, covalent, electrostatic, hydrogen bridges, Van der Waals forces and π-π stacking. However, self-assembly is not limited to small molecules aggregates. Non-molecular self-assembly leads to even bigger species, from nano to the micrometer range. In this case other forces come into play, like capillary effects, Van der Waals and London forces and elastic, electric and magnetic interactions, that is, forces that do not hold for individual molecules but requires cooperativity among them. In equilibrium, and without external forces, self-assembly occurs by minimizing the system's energy, the so-called static self-assembly. Once formed, the system is stable and it is at global or local energy minima [12, 13]. On the other hand, out of equilibrium and in the presence of external forces applied to the system, it undergoes a dynamic self-assembly

[14]. Usually, these forces are mild, so that in their absence the system does not disaggregate. As the research has focused on static self-assembly much is known about it [12, 13]. In contrast, dynamic self-assembly demands more studies about its theoretical basis and practical applications [14].

In Nanoscience research, one theoretically designs a certain nanomaterial with already defined characteristics, like enhanced luminescence or mechanical resistence, which is then fabricated or synthesized and characterized by appropriate techniques and so, unlike other disciplines, fundamental science is in mutual association with experimental science. In fact Nanoscience and Nanotechnology evolved almost at the same time, having existed a delay in Nanotechnology outcome just due to the need of improved instrumental devices. The big challenge is, so, to attribute practical use to them, creating new devices, structures and systems for general use through commercial distribution and industrial scale-up.

Why Nanomaterials-Luciferase Coupling?

Luciferase is a key tool in biomedical and bioanalytical chemistry [15]. Many efforts are made towards improving its features, namely increased catalytic efficiency [16], higher luminescence intensity and stability [17-19], new light colours emission [20, 21], and enhanced resistance to proteolysis [22] and to elevated temperatures and pH variations [23]. So far, these features were mainly accomplished through genetic engineering, mainly by mutagenesis in selected amino acid [16-20], by fusion with other enzymes [24] or biomolecules [25] and by splitting luciferase into two or more fragments which regain activity through protein-protein interactions between the proteins attached to each of the luciferase's portions [26, 27]. In some cases, other improvements were obtained through the use of biological or chemical adjuvants which can enhance the biochemical reaction and the corresponding light output, for example α-synuclein [28], inorganic pyrophosphate [29], coenzyme A [30], liposomes [31, 32], magnesium sulfate [33] and other osmolites [34]. Chemically modified luciferins also confer distinctive patterns to the bioluminescent reaction [35, 36].

Regarding Nanoscience and the respective nanomaterials and nanodevices, it soon became evident their potential in biological applications [37]. Bionanotechnology encompass the study, characterization and application of nanomaterials in living entities. Some applications already proposed include photothermal therapy for cancer [38], novel vectors for gene delivery [39] and novel probes for bioimaging [40], just to quote a few.

Following these ideas a logical step would be to bring luciferase and nanomaterials together as nanohybrids, improving luciferase's properties and expanding its range of applications, as will now be exposed.

NEW METHODOLOGIES BASED ON THE COUPLING OF LUCIFERASE WITH NANOMATERIALS

Carbon-Based Nanomaterials

Carbon Nanotubes

Carbon is an eclectic element concerning nanomaterial production. It appears in several forms:

i) graphene nanoribbons, a one atom-thick sheet of conjugated sp^2-hybridized carbon atoms [41- 44];
ii) filamentous carbon (nanotubes if hollow, nanofibers if filled), which can be regarded as a graphene sheet rolled around itself to form a cylinder with 0.4-3 nm in diameter if composed of only one sheet (a single-walled carbon nanotube), or 2-100 nm in diameter if composed of several concentric sheets (a multi-walled carbon nanotube), and lengths from nanometers up to micrometers or even several centimetres [41, 44, 45];
iii) fullerenes, spherical C_{60} or higher [41, 46];
iv) nanodiamonds [41, 47]; and
v) nanostructured porous carbon replicas, structures based on the utilization of templates, commonly mesoporous silica, where the self-assembly of carbon occurs; posteriorly, the template is removed and the material will present the inverse of the shape of the template and a specific pore size [48-50].

Carbon nanotubes are a particularly successful carbon-based nanomaterial. They present very attractive characteristics like high mechanical strength, excellent chemical, electronic and optoelectronic performances, low density, and good heat transmission capacity [41, 44, 45]. Another important feature is the great diversity of functionalization processes they allow, especially at the edges and defects. There is also the possibility of polymer wrapping and endohedral encapsulation of molecules by inserting molecular components inside them and allowing their self-assembly [51-54]. These processes are exclusive of nanotubes [51-54]. Taken together with the high surface areas they possess, the possibilities are astonishing. Those improvements have rendered several interesting applications for carbon nanotubes as catalysts [55], in electric circuits and devices [56], in solar cells [9], as sensors [10], among others. Biomedicine gives much attention to the evolution of these nanomaterials [44, 57, 58], and current studies are focused on their biocompatibility [59] and improving their solubility in organic solvents and water [60].

A biosensor for cellular ATP based on carbon nanotubes and luciferase was proposed [61]. It relies upon the immobilization of luciferase into near-infrared fluorescence emitting nanotubes through carboxylated poly-ethylene glycol phospholipids wrapped around commercial single-walled nanotubes. When the bioluminescent reaction catalyzed by luciferase takes place, with concomitant consume of cellular ATP and exogenously-added luciferin, the resulting product, oxyluciferin, will adhere to the nanotubes and quench their fluorescent emission. It allows the quantification of ATP in roughly 10 minutes at room temperature, it is sensitive and selective to ATP, as it does not respond neither to closely

related nucleotides as ADP, CTP and GTP nor to the bioluminescent reaction by-products AMP and inorganic pyrophosphate, and it allows the spatial and temporal quantification of ATP in living cells. On the other hand, it is an irreversible sensor that cannot be regenerated after the bioluminescent reaction takes place. With further optimizations this could be a useful optical biosensor for ATP. The principal contribution of the nanomaterial in relation to previously proposed methods is the enhancement in sensitivity, simplicity and stability that they confer to the biosensor [61].

Nanodiamonds

Nanodiamonds are allotropes of carbon, with an average diameter of 5 nm, formed from the detonation of carbon-bearing explosives such as a mixture of trinitrotoluene (TNT) and hexogen, and so they are also called detonation nanodiamonds or ultrafine-dispersed diamonds (UDD) [41, 47]. They possess interesting characteristic, namely a large surface area, optical transparency and luminescence, increased mechanical strength, and enhanced magnetic and electrochemical properties [41, 47, 62]. Their core is composed of crystalline carbon with some nitrogen atoms derived from the precursor that, together with a nearby lattice vacancy can be regarded as defects responsible for their photoluminescence [47, 63, 64]. Nanodiamonds are already produced in commercial scale, for example by ALIT, Inc., at Kiev (Ukraine) [65]. Recently, however, they are being recruited to biomedical applications as drugs, genes and proteins carriers [66, 67], as a cellular scaffold [68], as a bioimaging probe [69] and as biosensors [70, 71], provided that they are non-cytotoxic; in fact, they are considered the most biocompatible of all carbon nanomaterials [47], and more applications are likely to be proposed as they are prone to form nanocomposites and nanohybrid materials and to be subjected to further functionalizations [56].

A proof-of-principle bioluminescent sensor based on nanodiamonds and bacterial luciferase is described in the literature [72]. A biochip was developed by adsorbing the nanodiamod-luciferase complex into an aluminium oxide film, and a bioluminescent signal was detected. Although this is a preliminary study it points out that the nanodiamonds-luciferase coupling holds potential for bioanalytical applications.

Metallic Nanoparticles

Metals in their nanometric scale are among the first materials to get practical applications and posteriorly recognized as materials different from bulk with size-depending properties [1, 73]. This kind of nanomaterial can be obtained in a variety of shapes and sizes [74-76] and their interesting properties grant them lots of studies and proposed applications. The most common metallic nanoparticles are made from noble metals like gold, silver, platinum and palladium. In the bulk form they are little reactive, but they became reactive in nano form [4, 73]. On the other hand, metals which are already reactive in the bulk form become so reactive as nanometals that are very difficult to work with them. The principal applications are based on their optical, magnetic and catalytic properties [73]. For example, the use of silver nanoprisms in solar cells enhanced their light harvesting potential [77]. In biological applications gold nanoparticles is undoubtedly one of those that receive plenty of attention and studies [78-80].

Gold Nanoparticles

The nanochemistry of gold nanoparticles, or colloidal gold, has old roots, being used since ancient times for decoration and as a medicine, for example [1, 81]. Gold nanoparticles are formed by metallic gold with dangling bonds at the surface, like other nanomaterials. The most distinctive characteristic of their surface chemistry is the high affinity for thiol groups. This leads to the formation of self-assembled monolayers (SAM), especially of alkanethiols, which stabilized the surface atoms and confers new functionalities to the surface [82]. Furthermore, it is possible the synthesis of hybrid nanoparticles, like a silver core covered by a gold layer [83], gold nanoparticles conjugate with platinum clusters at their surface [84] or the trapping of iron oxide inside gold nanoparticles [85], which enhances their features and augment the field of applications.

In metallic surfaces, the existence of free electrons in movement generates an electric dipole at the surfaces, which induces their collective oscillation, the so-called plasmons [86]. By irradiating the particles with light at a specific wavelength, they can resonate, giving rise to absorption of the radiation and detection of a plasmonic band, responsible for the intense color of gold nanoparticles. The frequency at which this plasmonic band occurs depends on the shape and size of the nanoparticles, but for gold it is in the visible to near-infrared range. For instance, in a recent study, oligonucleotides were immobilized onto gold nanoparticles [87]. By shedding light at the plasmonic frequency, the light was absorbed and led to an electronic transition from ground state to an excited state. The non-radiative decay to the fundamental state released energy as heat. The heat so generated denatured the oligonucleotide chains which then exerted their intended activity in this study, gene silencing [87]. In phototherapy, nanoparticles could be directed to cancer cells [88] or bacteria [89]; their exposition to near-infrared emitting gold nanoparticles causes cellular lysis. Gold nanoparticles also present magnetic properties, which could be applied for data storage [90].

Many achievements could be obtained with gold nanoparticles' functionalization with biomolecules. For example, the coupling of the enzyme tyrosinase onto gold nanoparticles led to a biosensor for phenolic compounds [91]. A biosensor for proteases based on luciferase-gold nanoparticles is already described [92]. It is based on the quenching, by the nanoparticles, of the light emitted by luciferase. A blue-emitting, eight-mutation variant with enhanced stability in serum and higher catalytic efficiency luciferase from *Renilla reniformis*, termed Luc8 [17], was coupled to 5 nm-diameter gold nanoparticles previously functionalized with carboxylic oligo(ethylene glycol) through a short amino acid sequence recognized by matrix metalloproteinase-2 (MMP-2), which was chosen as a test protease due to its relevant cellular roles, namely in tumor invasion and metastasis [93]. By acting on its substrate, MMP-2 will promote the separation between luciferase and the nanoparticles, thus raising the light emission [92]. Protease concentrations ranging from 50 ng mL^{-1} to 1 μg mL^{-1} were assessed. This example represents an easy and sensitive way to determine MMP-2 concentration, but other proteases could be assayed by just changing the amino acid sequence. Furthermore, it relies upon desired features conferred by the nanoparticles such as photostability, biocompatibility and large surface area to attach luciferase, which are not easily obtained with traditional chemical quenchers.

Quantum Dots

Quantum dots (QD) is the common designation of semiconductor colloidal nanocrystals, generally measuring 2-6 nm, composed of elements from the periodic groups II and VI (e.g. CdSe, CdTe, CdS, ZnSe) or III and V (e.g. InP, InAs), sometimes with a core-shell structure like CdSe/ZnS or CdTe/CdS or dopped with another compound, such as Mn: ZnS/ZnS [94]. Recently, the production of carbon-dots, the carbon-based counterpart of inorganic QDs [95, 96], is another bid on QDs' versatility. They present several unique optical and electronic features, like size- and composition-tunable light emission from visible to near-infrared wavelengths, broad absorption spectra, narrow and symmetric emission spectra, very high levels of brightness and photostability, high quantum yields and high molar extinction coefficients [94], being one of the most popular nanomaterial to date.

QDs have so many applications that refer all of them is beyond the scope of this chapter. Illustrative examples include latent fingerprinting detection [97, 98], biosensor for hydrogen peroxide [99], and artificial light harvester in solar energy systems [100]. But it is in the biomedical field that QDs really stand out [40, 101-105]. They are applied as probes for *in vitro* and *in vivo* imaging [106-108], in real-time biomolecule tracking [109-111], as biosensors for kinases and phosphatases [112] and glucose [113], and so on. However, for these biological applications, the issue of biocompatibility and toxicity is always under attention. Current studies suggest that QDs can insert cellular damages [114-118], but deleterious effects can be diminished through capping with an additional shell, like in the core/shell QDs [108], functionalization with ligands [115, 119] and water-soluble QDs formulation [107]. Another strategy is the synthesis of QDs devoided of toxic elements, especially cadmium [103, 108, 120, 121].

Bioimaging is observing an intense development. Application of luciferases as probes are desired due to simplicity, costs and versatility. However, a major drawback is encountered: the way light interacts with tissues. In biological systems, chromophores molecules like hemoglobin, colagen and water could absorb light in certain wavelengths, which are then transmitted or scattered [122]. In this way little light can penetrate more than a few inches, except for red or near-infrared radiation [122]. Green- or blue-emitting luciferase, like those from fireflies and *Renilla*, are inadequate for such *in vivo* bioimaging studies. The cloning of red light-emitting luciferases or the genetic engineering of the green-emitting ones was a possible solution [20, 21]. Recently, however, a novel proposal was made, based on the bioluminescence resonance energy transfer (BRET) from the eight-mutation luciferase Luc8 [17] to a red-emitting quantum dot [123]. Resonant energy transfer is a long-recognized phenomenon. A theory to explain it was proposed by the German scientist Theodor Förster, and hence the acronym Förster Resonant Energy Transfer, FRET, commonly used [124-126]. It involves two chromophores, a donor and an acceptor. The donor, initially in an electronically excited state, can transfer the energy to an acceptor as long as they are close to each other, between 1-10 nm, and that the donor's emission spectrum overlaps the acceptor's absorption spectrum. This transfer occurs through dipole-dipole coupling, and not by electron transfer, whereby it is non-radiative, or resonant [125, 126]. When both the chromophores are fluorescent the term Fluorescent Resonance Energy Transfer applies. If the energy comes from a bioluminescent reaction it is called Bioluminescence Resonance Energy Transfer [127-129]. There are numerous examples of FRET involving QDs and fluorophores [130], fluorescent proteins [131] or nanomaterials [132].

In the proposed system [123], Luc8 (emission maximum at 480 nm) acted as the donor molecule and commercial red-emitting QDs (CdSe/ZnS core-shell QDs with emission peak at 605 and 655 nm, and CdTe/ZnS at 705 and 800 nm) were the acceptors. These QDs have a maximum absorption in the blue range, hence a good energy transfer would be expected.

The QD-Luc8 conjugates were initially characterized regarding coupling efficiency and effective BRET occurrence. By adding coelenterazine, a peak at 480 nm was indeed registered along with a second peak at 605-800 nm due to BRET. Then they were injected in solution in nude mice and the BRET signal was detected with a proper camera. It was verified that not only BRET occurred *in vivo* but also deeper intramuscular injections allowed a recordable signal from only 5 pmol of conjugates, compared to little signal registered for 30 pmol of bare luciferase bioluminescence at the same locations or at subcutaneous injections. The same animals were tested for QD-Luc8 fluorescent emission and, although a signal could be obtained in subcutaneous injections, as expected, it was very faint in intramuscular injections, confirming that bioluminescence detection is more sensitive than fluorescence *in vivo*. At the same study, nude mice were injected simultaneously with QD-Luc8 conjugates with different emission maxima, from 605 to 800 nm, and the corresponding signals were sequentially detected by using adequate filters to each wavelength, thus confirming the possibility of multiplex imaging. Finally it was tested the possibility of monitoring cells transfected with those conjugates *in vivo*, instead of injecting the conjugates in solution or buffers. To achieve it, C6 glioma cells were incubated *in vitro* with QD655-Luc8 conjugates and posteriorly injected in nude mice. A strong BRET signal was obtained both *in vitro* and *in vivo* from these cells, but no fluorescence from the QDs was detected.

In subsequent studies the system was improved regarding the QD-Luc8 coupling, by using HaloTag- [133] and intein-mediated conjugation [134], and enhancing the long-term stability of Luc8 by encapsulation in a polyacrylamide gel [135]. Another improvement is the luciferase-templated formation of near-infrared emitting (800-1050 nm) PbS QDs [136]. This process, biomineralization, involves the incubation of QDs precursors with a solution of Luc8, which will serve as template for the self-assembly of the QD-Luc8 nanohybrid, without the need of other coupling methods. By BRET the blue light emitted by Luc8 is transferred to the so-formed QD and near-infrared light is emitted [136].

Initially the QD-Luc system was proposed for applications in bioimaging, but posteriorly it was suggested as bio-nanosensor for proteases [134, 137] and nucleic acids [138]. In the first case, Luc8 is coupled to the QDs through an animo acid sequence recognized by the protease. Without protease, the BRET signal will be detected; in its presence, the cleavage of the sequence will release Luc8 from QD and BRET ceases. In the second case, two oligonucleotide probes are assembled *in vitro*, one containing luciferase and the other a QD, being the QD-oligonucleotide sequence complementary to the target nucleic acid. Without nucleic acid, the two probes will hybridize, under certain conditions, and a BRET signal will be produced. In the presence of target nucleic acid, there will be a competition between the target and the Luc-probe to hybridize with QD-probe. The more target nucleic acid the more extensive will be its hybridization with QD-probe and lesser BRET signal will be produced.

All of these methods proved to be highly sensitive (limits of detection for the proteases of 1 ng mL^{-1} for MMP-2, 5 ng mL^{-1} for MMP-7 and 500 ng mL^{-1} for urokinase-type plasminogen activator [134], and 20 nM for nucleic acids [138]), simple and rapid (demanding one hour of incubation for protease detection and 30 minutes for nucleic acids assay) compared to other corresponding methods. They are also versatile, as other proteases

and several oligonucleotides can be assayed just by changing the amino acid sequence between the luciferase and the QD or the nucleotidic sequence of the nucleic acid. Regarding bioimaging, it allowed the record of signals in a region of the electromagnetic spectrum where the light is less absorbed by tissues (red to near infrared), leading to improved signal-to-noise ratio and analysis at deeper locations inside living subjects, without performing any genetic alterations in luciferase. In fact, the QD-Luc8 self-illuminating system is so successful that are now commercially produced by Zymera, Inc, at San Jose, CA (USA) under the designation BRET-Qdot® [139].

Nanostructured Materials

Mesoporous Silica Nanoparticles

Silica, actually silicon dioxide, is one of the most common substances on Earth. It is present in rocks and soil and has important function in life, like in the diatoms. A broad range of applications involve silica, from basic pottery to photonic crystals (the self-assembly of spherical silica nanoparticles in a compact and periodic arrangement at nanometric scale that leads to diffraction of the incident light, resulting in different colours) [140-142].

In Nanoscience, silica is important in its colloidal state, in which silica particles (1-1000 nm) are dispersed in a continuous phase. If this phase is liquid, the system is called a sol. By aggregating these particles into a solid structure enclosing a continuous liquid phase the system is now called a gel [140]. These concepts are the basis of the sol-gel technology widely applied to prepare colloidal silica, for example the Stöber method, based on the basic hydrolysis of a silica precursor, leading to spherical and amorphous particles within 0.05-2 μm initially, but can be reduced up to 100-400 nm [140, 143].

Compared to other nanomaterials, for example carbon, silica is somehow limited in terms of functionalization, being the principal kind of functionalization related to organosilanes that will react with silanol groups (free hydroxyl groups derived from non-compensated, polymerized $Si(HO)_4$ at the surface) at silica's surface [140, 144, 145]. When using bifunctional organosilanes, one end will react with silanol and the other could have any functional group, so enhancing the applications. Furthermore, with a fine control of the synthesis process it can be attained the control of particle and pores' size and morphology, along with the insertion of functionalizations [140, 144, 145]. For example, porosity could be induced and controlled by using templates, generally surfactants, which are posteriorly removed [140, 144, 145]. Hybrid silica nanoparticles are also available, generally consisting in the coating of other nanoparticles with silica, for example magnetic hematite [146], or the production of nanocomposites, like copper-coated silica nanoparticles for odor removal [147] or gold-doped silica nanoparticles for biosensing [148].

Regarding luciferase, another method for ATP detection based on the immobilization of firefly luciferase into sugar-silica materials prepared form the sol-gel process was created [149]. The main improvement in this new method was that luciferase maintained a relatively high and stable light emission compared to other matrices like agarose beads and sepharose, a characteristic conferred by the covalent linkage of sugars (D-gluconolactone and D-maltonolactone) to the structure of the chosen silica precursor, (aminopropyl)triethoxysilane. The gel-containing luciferase can be re-used after several catalytical cycles, a unique feature

compared to other systems, and it proved to be very sensitive, being able to detect 1 pM of ATP. In fact, the issue of enzyme stability upon immobilization needs attention, because this factor hampers the development of biosensors and bioreactors. A theoretical study analyzed the influence of temperature and composition of nanometric silica upon firefly luciferase's active site [150]. Using molecular dynamics simulation it was observed that nanoporous (6 nm width) hydrophilic silica can indeed help to stabilize luciferase at room (27 ºC) and high (60 ºC) temperatures.

Nanostructured Film

Another optical biosensor using nanospheres covered with a nanostructured film in which luciferase is embedded was proposed [151]. The film's assembly is based on the layer-by-layer method, which is based on the alternate adsorption of polycations and polyanions in solution to a desired template or substrate, which leads to the formation of multilayers whose composition and thickness can be finely controlled [152]. In this example [151], firefly luciferase and cationic poly(dimethyldiallyl ammonium chloride) were added to polystyrene sulfonated spheres with 520 nm of diameter and, through electrostatic interactions, several layers were deposited. Within 15 minutes, a monolayer was assembled. Results [151] showed that the immobilized luciferase retained about 70% of its activity compared to free enzymes. Furthermore, a sustained bioluminescence was detected during a 7-day analysis, especially if the outermost layer is composed of the cation, albeit with a reduced enzymatic activity in this particular case. Finally, these nanospheres were exposed to commercial solutions with different concentrations of ATP, and a response proportional to the ATP content was observed, suggesting a role as ATP sensor.

CONCLUSION

Nanoscience in general, and nanomaterials in particular, are the hot topics for the XXI century investigation. If it is true that a lot of work is already done, it is also true that many efforts are waiting to be solved out. For example, the interaction of nanoparticles with biomolecules within cells is poorly understood, although it is of paramount importance as more and more nanomaterials are being requested for biomedical applications [153, 154].

Although Bionanotechnology (or Nanobiotechnology) is taking its first steps it is already regarded as an area with a huge future ahead. In this context, the coupling of luciferases with nanomaterials can be regarded as a fruitful partnership. In fact, major advances have been observed in luciferase's enzymatic mechanism and biotechnology, which opened new areas for applications of the highly sensitive and selective luciferase-based bioanalytical methodologies. The main achievements so far were towards biosensing for ATP, nucleic acids and proteases, and bioimaging, but other applications are likely to arise. Carbon-based nanomaterials have the most promising potential for biological applications because of their biocompatibility and nontoxicity. Coupling these materials with well-established luciferase methodologies will undoubtedly be a good bet, not only for the optimization of already existing bioanalytical methodologies but also for the designing of new ones.

In conclusion nanomaterials, tiny entities which occupy "the region between the atomistic and the macroscopic worlds" [8], and luciferase, an indispensable bioanalytical tool, coupled to each other, represent the future of Bioanalytical Chemistry and Biomedicine.

REFERENCES

[1] Edwards, P. P. & Thomas, J. M. (2007). Gold in a metallic divided state-from Faraday to present-day nanoscience. *Angew. Chem.-Int. Edit.*, *46*, 5480-5486.

[2] The Royal Society & The Royal Academy of Engineering. Nanoscience and Nanotechnologies: opportunities and uncertainties. July 2004 [consulted at 10/13/2010]. Available from: http://www.nanotec.org.uk/finalReport.htm.

[3] Daniel, M.-C. & Astruc, D. (2004). Gold nanoparticles: assembly, supramolecular chemistry, quantum-size-related properties, and applications toward biology, catalysis, and nanotechnology. *Chem. Rev.*, *104*, 293-346.

[4] Valden, M., Lai, X. & Goodman, D. W. (1998). Onset of catalytic activity of gold clusters on titania with the appearance of nonmetallic properties. *Science*, *281*, 1647-1650.

[5] Brus, L. (1986). Electronic wave functions in semiconductor clusters: experiment and theory. *J. Phys. Chem.*, *90*, 2555-2560.

[6] Smith, A. M. & Nie, S. (2010). Semiconductor nanocrystals: structure, properties, and band gap engineering. *Accounts Chem. Res.*, *43*, 190-200.

[7] Gullapalli, H., Vemuru, V. S. M., Kumar, A., Botello-Mendez, A., Vajtai, R., Terrones, M., Nagarajaiah, S. & Ajayan, P. M. (2010). Flexible piezoelectric ZnO–paper nanocomposite strain sensor. *Small*, *6*, 1641-1646.

[8] Costi, R., Saunders, A. E. & Banin, U. (2010). Colloidal hybrid nanostructures: a new type of functional materials. *Angew. Chem.-Int. Edit.*, *49*, 4878-4897.

[9] Schulz-Drost, C., Sgobba, V., Gerhards, C., Leubner, S., Calderon, R. M. K., Ruland, A. & Guldi, D. M. (2010). Innovative inorganic–organic nanohybrid materials: coupling quantum dots to carbon nanotubes. *Angew. Chem.-Int. Edit.*, *49*, 6425-6429.

[10] Kang, H., Lim, S., Park, N., Chun, K.-Y. & Baik, S. (2010). Improving the sensitivity of carbon nanotube sensors by benzene functionalization. *Sens. Actuator B-Chem.*, *147*, 316-321.

[11] Ozin, G. A., Arsenault, A. C., & Cademartiri, L. (2009). *Nanochemistry - A Chemical Approach to Nanomaterials* (2nd edition). Cambridge, The Royal Society of Chemistry.

[12] Whitesides, G. M. & Boncheva, M. (2002). Beyond molecules: self-assembly of mesoscopic and macroscopic components. *Proc. Natl. Acad. Sci. U. S. A.*, *99*, 4769-4774.

[13] Whitesides, G. M. & Grzybowski, B. (2002). Self-assembly at all scales. *Science*, *295*, 2418-2421.

[14] Fialkowski, M., Bishop, K. J. M., Klajn, R., Smoukov, S. K., Campbell, C. J. & Grzybowski, B. A. (2006). Principles and implementations of dissipative (dynamic) self-assembly. *J. Phys. Chem. B*, *110*, 2482-2496.

[15] Roda, A., Guardigli, M., Michelini, E. & Mirasoli, M. (2009). Bioluminescence in analytical chemistry and *in vivo* imaging. *Trends Anal. Chem.*, *28*, 307-322.

[16] Hirokawa, K., Kajiyama, N. & Murakami, S. (2002). Improved practical usefulness of firefly luciferase by gene chimerization and random mutagenesis. *Biochim. Biophys. Acta-Protein Struct. Mol. Enzymol., 1597*, 271-279.

[17] Loening, A. M., Fenn, T. D., Wu, A. M. & Gambhir, S. S. (2006). Consensus guided mutagenesis of *Renilla* luciferase yields enhanced stability and light output. *Protein Eng. Des. Sel., 19*, 391-400.

[18] Fujii, H., Noda, K., Asami, Y., Kuroda, A., Sakata, M. & Tokida, A. (2007). Increase in bioluminescence intensity of firefly luciferase using genetic modification. *Anal. Biochem., 366*, 131-136.

[19] Welsh, J. P., Patel, K. G., Manthiram, K. & Swartz, J. R. (2009). Multiply mutated *Gaussia* luciferases provide prolonged and intense bioluminescence. *Biochem. Biophys. Res. Commun., 389*, 563-568.

[20] Caysa, H., Jacob, R., Müther, N., Branchini, B., Messerle, M. & Söling, A. (2009). A redshifted codon-optimized firefly luciferase is a sensitive reporter for bioluminescence imaging. *Photochem. Photobiol. Sci., 8*, 52-56.

[21] Branchini, B. R., Ablamsky, D. M., Davis, A. L., Southworth, T. L., Butler, B. Fan, F., Jathoul, A. P. & Pule, M. A. (2010). Red-emitting luciferases for bioluminescence reporter and imaging applications. *Anal. Biochem., 396*, 290–297.

[22] Riahi-Madvar, A. & Hosseinkhani, S. (2009). Design and characterization of novel trypsin-resistant firefly luciferases by site-directed mutagenesis. *Protein Eng. Des. Sel., 22*, 655-663.

[23] Imani, M., Hosseinkhani, S., Ahmadian, S. & Nazari, M. (2010). Design and introduction of a disulfide bridge in firefly luciferase: increase of thermostability and decrease of pH sensitivity. *Photochem. Photobiol. Sci., 9*, 1167-1177.

[24] Taneoka, A., Sakaguchi-Mikami, A., Yamazaki, T., Tsugawa, W. & Sode, K. (2009). The construction of a glucose-sensing luciferase. *Biosens. Bioelectron., 25*, 76-81.

[25] Zhang, Y., Phillips, G. J., Li, Q. & Yeung, E. S. (2008). Imaging localized astrocyte ATP release with firefly luciferase beads attached to the cell surface. *Anal. Chem., 80*, 9316-9325.

[26] Villalobos, V., Naik, S. & Piwnica-Worms, D. (2007). Current state of imaging protein-protein interactions *in vivo* with genetically encoded reporters. *Annu. Rev. Biomed. Eng., 9*, 321-49.

[27] Luker, K. E., Gupta, M. & Luker, G. D. (2008). Imaging CXCR4 signaling with firefly luciferase complementation. *Anal. Chem., 80*, 5565-5573.

[28] Kim, J., Moon, C. H., Jung, S. & Paik, S. R. (2009). α-Synuclein enhances bioluminescent activity of firefly luciferase by facilitating luciferin localization. *Biochim. Biophys. Acta – Proteins Proteomics, 1794*, 309-314.

[29] Fontes, R., Fernandes, D., Peralta, F., Fraga, H., Maio, I. & Esteves da Silva, J. C. G. (2008). Pyrophosphate and tripolyphosphate affect firefly luciferase luminescence because they act as substrates and not as allosteric effectors. *FEBS J., 275*, 1500-1509.

[30] Fraga, H., Fernandes, D., Fontes, R. & Esteves da Silva, J. C. G. (2005). Coenzyme A affects firefly luciferase luminescence because it acts as a substrate and not as an allosteric effector. *FEBS J., 272*, 5206-5216.

[31] Nakata, N., Ishida, A., Tani, H., Kamidate, T. (2003). Cationic liposomes enhanced firefly bioluminescent assay of bacterial ATP in the presence of an ATP extractant. *Anal. Sci., 19*, 1183-1185.

[32] Kheirolomoom, A., Kruse, D. E., Qin, S., Watson, K. E., Lai, C.-Y., Young, L. J. T., Cardiff, R. D. & Ferrara, K. W. (2010). Enhanced *in vivo* bioluminescence imaging using liposomal luciferin delivery system. *J. Control. Release*, 141, 128-136.

[33] Ganjalikhany, M. R., Ranjbar, B., Hosseinkhani, S., Khalifeh, K. & Hassani, L. (2010). Roles of trehalose and magnesium sulfate on structural and functional stability of firefly luciferase. *J. Mol. Catal. B-Enzym., 62*, 127-132.

[34] Ataei, F., Hosseinkhani, S. & Khajeh, K. (2009). Luciferase protection against proteolytic degradation: a key for improving signal in nano-system biology. *J. Biotechnol., 144*, 83-88.

[35] Shinde, R., Perkins, J. & Contag, C. H. (2006). Luciferin derivatives for enhanced *in vitro* and *in vivo* bioluminescence assays. *Biochemistry, 45*, 11103-11112.

[36] Shao, Q., Jiang, T., Ren, G., Cheng, Z. & Xing, B. (2009). Photoactivable bioluminescent probes for imaging luciferase activity. *Chem. Commun., 27*, 4028-4030.

[37] Gao, J. & Xu, B. (2009). Applications of nanomaterials inside cells. *Nano Today, 4*, 37-51.

[38] Sharma, P., Brown, S. C., Singh, A., Iwakuma, N., Pyrgiotakis, G., Krishna, V., Knapik, J. A., Barr, K., Moudgil, B. M. & Grobmyer, S. R. (2010). Near-infrared absorbing and luminescent gold speckled silica nanoparticles for photothermal therapy. *J. Mater. Chem., 20*, 5182-5185.

[39] Isobe, H., Nakanishi, W., Tomita, N., Jinno, S., Hiroto Okayama, H. & Nakamura, E. (2006). Nonviral gene delivery by tetraamino fullerene. *Mol. Pharm., 3*, 124-134.

[40] Frasco, M. F. & Chaniotakis, N. (2010). Bioconjugated quantum dots as fluorescent probes for bioanalytical applications. *Anal. Bioanal. Chem., 396*, 229-240.

[41] Krueger, A. (2010). *Carbon Materials and Nanotechnology*. Weinheim, Wiley-VHC.

[42] Loh, K. P., Bao, Q., Ang, P. K. & Yang, J. (2010). The chemistry of graphene. *J. Mater. Chem., 20*, 2277-2289.

[43] Soldano, C., Mahmood, A. & Dujardin, E. (2010). Production, properties and potential of graphene. *Carbon, 48*, 2127-2150.

[44] Yang, W., Ratinac, K. R., Ringer, S. P., Thordarson, P., Gooding, J. J. & Braet, F. (2010). Carbon nanomaterials in biosensors: should you use nanotubes or graphene?. *Angew. Chem.-Int. Edit., 49*, 2114-2138.

[45] Dresselhaus, M. S., Dresselhaus, G., & Avouris, P. Eds (2001). *Carbon Nanotubes - Synthesis, Structure, Properties, and Applications*. Leipzig, Springer.

[46] Santos, L. J., Rocha, G. P., Alves, R. B. & Freitas, R. P. (2010). Fulereno[C_{60}]: química e aplicações. *Quim. Nova, 33*, 680-693.

[47] Barnard, A. S. (2009). Diamond standard in diagnostics: nanodiamond biolabels make their mark. *Analyst*, 134, 1751-1764.

[48] Ryoo, R., Joo, S. H. & Jun, S. (1999). Synthesis of highly ordered carbon molecular sieves via template-mediated structural transformation. *J. Phys. Chem. B, 103*, 7743-7746.

[49] Ryoo, R., Joo, S. H., Kruk, M. & Jaroniec, M. (2001). Ordered mesoporous carbons. *Adv. Mater., 13*, 677-681.

[50] Stein, A., Wang, Z. & Fierke, M. A. (2009). Functionalization of porous carbon materials with designed pore architecture. *Adv. Mater., 21*, 265-293.

[51] Hirsch, A. (2002). Functionalization of single-walled carbon nanotubes. *Angew. Chem.-Int. Edit., 41*, 1853-1859.

[52] Balasubramanian, K. & Burghard, M. (2005). Chemically functionalized carbon nanotubes. *Small, 1*, 180-192.

[53] Tasis, D., Tagmatarchis, N., Bianco, A. & Prato, M. (2006). Chemistry of carbon nanotubes. *Chem. Rev., 106*, 1105-1136.

[54] Zhao, Y.-L. & Stoddart, J. F. (2009) Noncovalent functionalization of single-walled carbon nanotubes. *Accounts Chem. Res., 42*, 1161-1171.

[55] Serp, P., & Figueiredo, J. L. Eds (2009). *Carbon Materials for Catalysis*. Hoboken, John Wiley & Sons.

[56] Guglielmotti, V., Chieppa, S., Orlanducci, S., Tamburri, E., Toschi, F., Terranova, M. L. & Rossi, M. (2009). Carbon nanotube/nanodiamond structures: an innovative concept for stable and ready-to-start electron emitters. *Appl. Phys. Lett., 95*, 222113-222113-3.

[57] Lin, Y., Taylor, S., Li, H., Fernando, K. A. S., Qu, L., Wang, W., Gu, L., Zhou, B. & Sun, Y.-P. (2004). Advances toward bioapplications of carbon nanotubes. *J. Mater. Chem., 14*, 527-541.

[58] Katz, E. & Willner, I. (2004). Biomolecule-functionalized carbon nanotubes: applications in nanobioelectronics. *ChemPhysChem, 5*, 1084-1104.

[59] Cui, H.-F., Vashist, S. K., Al-Rubeaan, K., Luong, J. H. T. & Sheu, F.-S. (2010). Interfacing carbon nanotubes with living mammalian cells and cytotoxicity issues. *Chem. Res. Toxicol., 23*, 1131-1147.

[60] Tasis, D., Tagmatarchis, N., Georgakilas, V. & Prato, M. (2003). Soluble carbon nanotubes. *Chem.-Eur. J., 9*, 4000-4008.

[61] Kim, J.-H., Ahn, J.-H., Barone, P. W., Jin, H., Zhang, J., Heller, D. A. & Strano, M. S. (2010). A luciferase/single-walled carbon nanotube conjugate for near-infrared fluorescent detection of cellular ATP. *Angew. Chem.-Int. Edit., 49*, 1456-1459.

[62] Holt, K. B. (2010). Undoped diamond nanoparticles: origins of surface redox chemistry. *Phys. Chem. Chem. Phys., 12*, 2048-2058.

[63] Pichot, V., Stephan, O., Comet, M., Fousson, E., Mory, J., March, K. & Spitzer, D. (2010). High nitrogen doping of detonation nanodiamonds. *J. Phys. Chem. C, 114*, 10082-10087.

[64] Vlasov, I. I., Shenderova, O., Turner, S., Lebedev, O. I., Basov, A. A., Sildos, I., Rähn, M., Shiryaev, A. A. & Van Tendeloo, G. (2010). Nitrogen and luminescent nitrogen-vacancy defects in detonation nanodiamond. *Small, 6*, 687-694.

[65] http://www.alit.kiev.ua/index.htm. Consulted at 11/08/2010.

[66] Shimkunas, R. A., Robinson, E., Lam, R., Lu, S., Xu, X., Zhang, X.-Q., Huang, H., Osawa, E. & Ho, D. (2009). Nanodiamond-insulin complexes as pH-dependent protein delivery vehicles. *Biomaterials, 30*, 5720-5728.

[67] Li, J., Zhu, Y., Li, W., Zhang, X., Peng, Y. & Huang, Q. (2010). Nanodiamonds as intracellular transporters of chemotherapeutic drug. *Biomaterials, 31*, 8410-8418.

[68] Zhang, Q., Mochalin, V. N., Neitzel, I., Knoke, I. Y., Han, J., Klug, C. A., Zhou, J. G., Lelkes, P. I. & Gogotsi, Y. (2011). Fluorescent PLLA-nanodiamond composites for bone tissue engineering. *Biomaterials, 32*, 87-94.

[69] Fu, C.-C., Lee, H.-Y., Chen, K., Lim, T.-S., Wu, H.-Y., Lin, P.-K., Wei, P.-K., Tsao, P.-H., Chang, H.-C. & Fann, W. (2007). Characterization and application of single fluorescent nanodiamonds as cellular biomarkers. *Proc. Natl. Acad. Sci. U. S. A., 104*, 727-732.

[70] Zhao, W., Xu, J.-J., Qiu, Q.-Q. & Chen, H.-Y. (2006). Nanocrystalline diamond modified gold electrode for glucose biosensing. *Biosens*. *Bioelectron*., *22*, 649-655.

[71] Raina, S., Kang, W. P. & Davidson, J. L. (2010). Fabrication of nitrogen-incorporated nanodiamond ultra-microelectrode array for dopamine detection. *Diam*. *Relat*. *Mat*., *19*, 256-259.

[72] Puzyr', A. P., Pozdnyakova, I. O. & Bondar', V. S. (2004). Design of a luminescent biochip with nanodiamonds and bacterial luciferase. *Phys. Solid State*, *46*, 761-763.

[73] Feldheim, D. L., & Foss Jr., C. A. Eds (2002). *Metal Nanoparticles – Synthesis, Characterization, and Applications*. New York, Marcel Dekker.

[74] Lisiecki I. (2005). Size, shape, and structural control of metallic nanocrystals. *J. Phys. Chem. B*, *109*, 12231-12244.

[75] Grzelczak, M., Pérez-Juste, J., Mulvaney, P. & Liz-Marzán, L. M. (2008). Shape control in gold nanoparticle synthesis. *Chem*. *Soc*. *Rev*., *37*, 1783-1791.

[76] Meng, X. K., Tang, S. C. & Vongehr, S. (2010). A review on diverse silver nanostructures. *J. Mater*. *Sci*. *Technol*., *26*, 487-522.

[77] Kulkarni, A. P., Noone, K. M., Munechika, K., Guyer, S. R. & Ginger, D. S. (2010). Plasmon-enhanced charge carrier generation in organic photovoltaic films using silver nanoprisms. *Nano Lett*., *10*, 1501-1505.

[78] Chow, P. E. Ed (2010). *Gold Nanoparticles - Properties, Characterization and Fabrication*. Hauppauge, Nova Science Publishers.

[79] Panyala, N. R., Peña-Méndez, E. M. & Havel, J. (2009). Gold and nano-gold in medicine: overview, toxicology and perspectives. *J. Appl. Biomed*., *7*, 75-91.

[80] Giljohann, D. A., Seferos, D. S., Daniel, W. L., Massich, M. D., Patel, P. C. & Mirkin, C. A. (2010). Gold nanoparticles for biology and medicine. *Angew*. *Chem*.*-Int. Edit*., *49*, 3280-3294.

[81] Goesmann, H. & Feldmann, C. (2010). Nanoparticulate functional materials. *Angew*. *Chem*.*-Int*. *Edit*., *49*, 1362-1395.

[82] Love, J. C., Estroff, L. A., Kriebel, J. K., Nuzzo, R. G. & Whitesides, G. M. (2005). Self-assembled monolayers of thiolates on metals as a form of nanotechnology. *Chem*. *Rev*., *105*, 1103-1169.

[83] Tokonami, S., Morita, N., Takasaki, K. & Toshima, N. (2010). Novel synthesis, structure, and oxidation catalysis of Ag/Au bimetallic nanoparticles. *J. Phys*. *Chem*. *C*, *114*, 10336-10341.

[84] Zhang, S., Shao, Y., Yin, G. & Lin, Y. (2010). Electrostatic self-assembly of a Pt-around-Au nanocomposite with high activity towards formic acid oxidation. *Angew*. *Chem*.*-Int*. *Edit*., *49*, 2211-2214.

[85] Huang, C., Jiang, J., Muangphat, C., Sun, X. & Hao, Y. (2011). Trapping iron oxide into hollow gold nanoparticles. *Nanoscale Res*. *Lett*., *6*, 1-5.

[86] Aslan, K., Lakowicz, J. R. & Geddes, C. D. (2005). Plasmon light scattering in biology and medicine: new sensing approaches, visions and perspectives. *Curr*. *Opin*. *Chem*. *Biol*., *9*, 538-544.

[87] Lee, S. E., Liu, G. L., Kim, F. & Lee, L. P. (2009). Remote optical switch for localized and selective control of gene interference. *Nano Lett*., *9*, 562-570.

[88] Gobin, A. M., Watkins, E. M., Quevedo, E., Colvin, V. L. & West, J. L. (2010). Near-infrared-resonant gold/gold sulfide nanoparticles as a photothermal cancer therapeutic agent. *Small*, *6*, 745-752.

[89] Wang, S., Singh, A. K., Senapati, D., Neely, A., Yu, H. & Ray, P. C. (2010). Rapid colorimetric identification and targeted photothermal lysis of *Salmonella* bacteria by using bioconjugated oval-shaped gold nanoparticles. *Chem.-Eur. J., 16,* 5600-5606.

[90] Leong, W. L., Lee, P. S., Mhaisalkar, S. G., Chen, T. P, & Dodabalapur, A. (2007). Charging phenomena in pentacene-gold nanoparticle memory device. *Appl. Phys. Lett., 90,* 042906-042906-3.

[91] Cortez, J., Vorobieva, E., Gralheira, D., Osório, I., Soares, L., Vale, N., Pereira, E., Gomes, P. & Franco, R. Bionanoconjugates of tyrosinase and peptide-derivatised gold nanoparticles for biosensing of phenolic compounds. *J. Nanopart. Res.*, DOI: 10.1007/s11051-010-0099-8.

[92] Kim, Y.-P., Daniel, W. L., Xia, Z., Xie, H., Mirkin, C. A. & Rao, J. (2010). Bioluminescent nanosensors for protease detection based upon gold nanoparticle-luciferase conjugates. *Chem. Commun. 46,* 76-78.

[93] Fingleton, B. (2006). Matrix metalloproteinases: roles in cancer and metastasis. *Front. Biosci., 11,* 479-491.

[94] Bimberg, D., Grundmann, M., & Ledentsov, N. N. (1999). *Quantum Dot Heterostructures*. Salisbury, John Wiley & Sons.

[95] Sun, Y.-P., Zhou, B., Lin, Y., Wang, W., Fernando, K. A. S., Pathak, P., Meziani, M. J., Harruff, B. A., Wang, X., Wang, H., Luo, P. G., Yang, H., Kose, M. E., Chen, B., Veca, L. M. & Xie, S.-Y. (2006). Quantum-sized carbon dots for bright and colorful photoluminescence. *J. Am. Chem. Soc., 128,* 7756-7757.

[96] Baker, S. N. & Baker, G. A. (2010). Luminescent carbon nanodots: emergent nanolights. *Angew. Chem.-Int. Edit., 49,* 6721-6744.

[97] Yu-Juan, J., Yun-Jun, L., Guo-Ping, L., Jie, L., Yuan-Feng, W., Rui-Qin, Y. & Wen-Ting, L. (2008). Application of photoluminescent CdS/PAMAM nanocomposites in fingerprint detection. *Forensic Sci. Int., 179,* 34-38.

[98] Dilag, J., Kobus, H. & Ellis, A. V. (2009). Cadmium sulfide quantum dot/chitosan nanocomposites for latent fingermark detection. *Forensic Sci. Int., 187,* 97-102.

[99] Hu, X., Han, H., Hua, L. & Sheng, Z. (2010). Electrogenerated chemiluminescence of blue emitting ZnSe quantum dots and its biosensing for hydrogen peroxide. *Biosens. Bioelectron., 25,* 1843-1846.

[100] Nabiev, I., Rakovich, A., Sukhanova, A., Lukashev, E., Zagidullin, V., Pachenko, V., Rakovich, Y. P., Donegan, J. F., Rubin, A. B. & Govorov, A. O. (2010). Fluorescent quantum dots as artificial antennas for enhanced light harvesting and energy transfer to photosynthetic reaction centers. *Angew. Chem.-Int. Edit., 49,* 7217-7221.

[101] Bruchez Jr., M., Moronne, M., Gin, P., Weiss, S. & Alivisatos, A. P. (1998). Semiconductor nanocrystals as fluorescent biological labels. *Science, 281,* 2013-2016.

[102] Smith, A. M., Duan, H., Mohs, A. M. & Nie, S. (2008). Bioconjugated quantum dots for *in vivo* molecular and cellular imaging. *Adv. Drug Deliv. Rev., 60,* 1226-1240.

[103] Juzenas, P., Chen, W., Sun, Y.-P., Coelho, M. A. N., Generalov, R., Generalova, N. & Christensen, I. L. (2008). Quantum dots and nanoparticles for photodynamic and radiation therapies of cancer. *Adv. Drug Deliv. Rev., 60,* 1600-1614.

[104] Algar, W. R., Tavares, A. J. & Krull, U. J. (2010). Beyond labels: a review of the application of quantum dots as integrated components of assays, bioprobes, and biosensors utilizing optical transduction. *Anal. Chim. Acta, 673,* 1-25.

[105] Wagner, M. K., Li, F., Li, J., Li, X.-F. & Le, X. C. (2010). Use of quantum dots in the development of assays for cancer biomarkers. *Anal. Bioanal. Chem*., *397*, 3213-3224.

[106] Tholouli, E., Sweeney, E., Barrow, E., Clay, V., Hoyland, J. A. & Byers, J. R. (2008). Quantum dots light up pathology. *J. Pathol*., *216*, 275-285.

[107] Liu, W., Howarth, M., Greytak, A. B., Zheng, Y., Nocera, D. G., Ting, A. Y. & Bawendi, M. G. (2008). Compact biocompatible quantum dots functionalized for cellular imaging. *J. Am. Chem. Soc*., *130*, 1274-1284.

[108] Gao, J., Chen, K., Xie, R., Xie, J., Lee, S., Cheng, Z., Peng, X. & Chen, X. (2010). Ultrasmall near-infrared non-cadmium quantum dots for *in vivo* tumor imaging. *Small*, *6*, 256-261.

[109] Crane, J. M., Van Hoek, A. N., Skach, W. R. & Verkman, A. S. (2008). Aquaporin-4 dynamics in orthogonal arrays in live cells visualized by quantum dot single particle tracking. *Mol. Biol. Cell*, *19*, 3369-3378.

[110] You, C., Wilmes, S., Beutel, O., Löchte, S., Podoplelowa, Y., Roder, F., Richter, C., Seine, T., Schaible, D., Uzé, G., Clarke, S., Pinaud, F., Dahan, M. & and Piehler, J. (2010). Self-controlled monofunctionalization of quantum dots for multiplexed protein tracking in live cells. *Angew. Chem.-Int. Edit*., *49*, 4108-4112.

[111] Luo, K., Li, S., Xie, M., Wu, D., Wang, W., Chen, R., Huang, L., Huang, T., Pang, D. & Xiao, G. (2010). Real-time visualization of prion transport in single live cells using quantum dots. *Biochem. Biophys. Res. Commun*., *394*, 493-497.

[112] Freeman, R., Finder, T., Gill, R. & Willner, I. (2010). Probing protein kinase (CK2) and alkaline phosphatase with CdSe/ZnS quantum dots. *Nano Lett*., *10*, 2192-2196.

[113] Wu, P., He, Y., Wang, H.-F. & Yan, X.-P. (2010). Conjugation of glucose oxidase onto Mn-doped ZnS quantum dots for phosphorescent sensing of glucose in biological fluids. *Anal. Chem*., *82*, 1427-1433.

[114] Derfus, A. M., Chan, W. C. W. & Bhatia, S. N. (2004). Probing the cytotoxicity of semiconductor quantum dots. *Nano Lett*., *4*, 11-18.

[115] Hoshino, A., Fujioka, K., Oku, T., Suga, M., Sasaki, Y. F., Ohta, T., Yasuhara, M., Suzuki, K. & Yamamoto, K. (2004). Physicochemical properties and cellular toxicity of nanocrystal quantum dots depend on their surface modification. *Nano Lett*., *4*, 2163-2169.

[116] Lovrić, J., Cho, S. J., Winnik, F. M. & Maysinger, D. (2005). Unmodified cadmium telluride quantum dots induce reactive oxygen species formation leading to multiple organelle damage and cell death. *Chem. Biol*., *12*, 1227-1234.

[117] Lovrić, J., Bazzi, H. S., Cuie, Y., Fortin, G. R. A., Winnik, F. M. & Maysinger, D. (2005). Differences in subcellular distribution and toxicity of green and red emitting CdTe quantum dots. *J. Mol. Med*., *83*, 377-385.

[118] Cho, S. J., Maysinger, D., Jain, M., Röder, B., Hackbarth, S. & Winnik, F. M. (2007). Long-term exposure to CdTe quantum dots causes functional impairments in live cells. *Langmuir*, *23*, 1974-1980.

[119] Susumu, K., Uyeda, H. T., Medintz, I. L., Pons, T., Delehanty, J. B. & Mattoussi, H. (2007). Enhancing the stability and biological functionalities of quantum dots via compact multifunctional ligands. *J. Am. Chem. Soc*., *129*, 13987-13996.

[120] Pradhan, N., Goorskey, D., Thessing, J., & Peng, X. (2005). An alternative of CdSe nanocrystal emitters: pure and tunable impurity emissions in ZnSe nanocrystals. *J. Am. Chem. Soc*., *127*, 17586-17587.

[121] Cai, W., Hsu, A. R., Li, Z.-B. & Chen, X. (2007). Are quantum dots ready for in vivo imaging in human subjects?. *Nanoscale Res. Lett.*, *2*, 265-281.

[122] Hale, G. M. & Querry, M. R. (1973). Optical constants of water in the 200-nm to 200-μm wavelength region. *Appl. Optics*, *12*, 555-563.

[123] So, M.-K., Xu, C., Loening, A. M., Gambhir, S. S. & Rao, J. (2006). Self-illuminating quantum dot conjugates for *in vivo* imaging. *Nat. Biotechnol.*, *24*, 339-343.

[124] Förster, T. (1948). Zwischenmolekulare energiewanderung und fluoreszenz. *Ann. Phys. – Berlin*, *437*, 55-75.

[125] Roda, A., Guardigli, M., Michelini, E. & Mirasoli, M. (2009). Nanobioanalytical luminescence: Förster-type energy transfer methods. *Anal. Bioanal. Chem.*, *393*, 109-123.

[126] Medintz, I. L. & Mattoussi, H. (2009). Quantum dot-based resonance energy transfer and its growing application in biology. *Phys. Chem. Chem. Phys.*, *11*, 17-45.

[127] Xu, Y., Piston, D. W. & Johnson, C. H. (1999). A bioluminescence resonance energy transfer (BRET) system: application to interacting circadian clock proteins. *Proc. Natl. Acad. Sci. U. S. A.*, *96*, 151-156.

[128] Bacart, J., Corbel, C., Jockers, R., Bach, S. & Couturier, C. (2008). The BRET technology and its application to screening assays. *Biotechnol. J.*, *3*, 311-324.

[129] Xia, Z. & Rao, J. (2009). Biosensing and imaging based on bioluminescence resonance energy transfer. *Curr. Opin. Biotechnol.*, *20*, 37-44.

[130] Chen, L., Algar, W. R., Tavares, A. J. & Krull, U. J. (2011). Toward a solid-phase nucleic acid hybridization assay within microfluidic channels using immobilized quantum dots as donors in fluorescence resonance energy transfer. *Anal. Bioanal. Chem.*, *399*, 133-141.

[131] Hering, V. R., Gibson, G., Schumacher, R. I., Faljoni-Alario, A. & Politi, M. J. (2007). Energy transfer between CdSe/ZnS core/shell quantum dots and fluorescent proteins. *Bioconjugate Chem.*, *18*, 1705-1708.

[132] Dong, H., Gao, W., Yan, F., Ji, H. & Ju, H. (2010). Fluorescence resonance energy transfer between quantum dots and graphene oxide for sensing biomolecules. *Anal. Chem.*, *82*, 5511-5517.

[133] Zhang, Y., So, M.-K., Loening, A. M., Yao, H., Gambhir, S. S. & Rao, J. (2006). HaloTag protein-mediated site-specific conjugation of bioluminescent proteins to quantum dots. *Angew. Chem.-Int. Edit.*, *45*, 4936-4940.

[134] Xia, Z., Xing, Y., So, M.-K., Koh, A. L., Sinclair, R. & Rao, J. (2008). Multiplex detection of protease activity with quantum dot nanosensors prepared by intein-mediated specific bioconjugation. *Anal. Chem.*, *80*, 8649-8655.

[135] Xing, Y., So, M.-K., Koh, A. L., Sinclair, R. & Rao, J. (2008). Improved QD-BRET conjugates for detection and imaging. *Biochem. Biophys. Res. Commun.*, *372*, 388-394.

[136] Ma, N., Marshall, A. F. & Rao, J. (2010). Near-infrared light emitting luciferase *via* biomineralization. *J. Am. Chem. Soc.*, *132*, 6884-6885.

[137] Yao, H., Zhang, Y., Xiao, F., Xia, Z. & Rao, J. (2007). Quantum dot/bioluminescence resonance energy transfer based highly sensitive detection of proteases. *Angew. Chem.-Int. Edit.*, *46*, 4346-4349.

[138] Cissell, K. A., Campbell, S. & Deo, S. K. (2008). Rapid, single-step nucleic acid detection. *Anal. Bioanal. Chem.*, *391*, 2577-2581.

[139] http://www.zymera.com/. Consulted at 11/09/2010.

[140] Bergna, H. E. & Roberts, W. O. Eds (2006). *Colloidal Silica - Fundamentals and Applications*. Boca Raton, Taylor & Francis.

[141] Norris, D. J., Arlinghaus, E. G., Meng, L., Heiny, R. & Scriven, L. E. (2004). Opaline photonic crystals: how does self-assembly work?. *Adv. Mater., 16*, 1393-1399.

[142] Bardosova, M. & R. H. Tredgold, R. H. (2002). Ordered layers of monodispersive colloids. *J. Mater. Chem., 12*, 2835-2842.

[143] Stöber, W., Fink, A. & Bohn, E. (1968). Controlled growth of monodisperse silica spheres in the micron size range. *J. Colloid Interface Sci., 26*, 62-69.

[144] Fryxell, G. E. (2006). The synthesis of functional mesoporous materials. *Inorg. Chem. Commun., 9*, 1141-1150.

[145] Slowing, I. I., Vivero-Escoto, J. L., Trewny, B. G. & Lin, V. S.-Y. (2010). Mesoporous silica nanoparticles: structural design and applications. *J. Mater. Chem., 20*, 7924-7937.

[146] Zhang, J., Thurber, A., Hanna, C. & Punnoose, A. (2010). Highly shape-selective synthesis, silica coating, self-assembly, and magnetic hydrogen sensing of hematite nanoparticles. *Langmuir, 26*, 5273-5278.

[147] Singh, A., Krishna, V., Angerhofer, A., Do, B., MacDonald, G. & Moudgil, B. (2010). Copper coated silica nanoparticles for odor removal. *Langmuir, 26*, 15837-15844.

[148] Lee, K. G., Wi, R., Park, T. J., Yoon, S. H., Lee, J., Lee, S. J. & Kim, D. H. (2010). Synthesis and characterization of gold-deposited red, green and blue fluorescent silica nanoparticles for biosensor application. *Chem. Commun., 46*, 6374-6376.

[149] Cruz-Aguado, J. A., Chen, Y., Zhang, Z., Elowe, N. H., Brook, M. A. & Brennan, J. D. (2004). Ultrasensitive ATP detection using firefly luciferase entrapped in sugar-modified sol-gel-derived silica. *J. Am. Chem. Soc., 126*, 6878-6879.

[150] Nishiyama, K. (2008). Thermal behavior of luciferase on nanofabricated hydrophilic Si surface. *Biomacromolecules, 9*, 1081-1083.

[151] Pastorino, L., Disawal, S., Nicolini, C., Lvov, Y. M. & Erokhin, V. V. (2003). Complex catalytic colloids on the basis of firefly luciferase as optical nanosensor platform. *Biotechnol. Bioeng. 84*, 286-291.

[152] Siqueira Jr., J. R., Caseli, L., Crespilho, F. N., Zucolotto, V. & Oliveira Jr, O. N. (2010). Immobilization of biomolecules on nanostructured films for biosensing. *Biosens. Bioelectron., 25*, 1254-1263.

[153] Lynch, I., Cedervall, T., Lundqvist, M., Cabaleiro-Lago, C., Linse, S. & Dawson, K. A. (2007). The nanoparticles-protein complex as a biological entity; a complex fluids and surface science challenge for the 21st century. *Adv. Colloid Interface Sci., 134-135*, 167-174.

[154] Mailänder, V. & Landfester, K. (2009). Interaction of nanoparticles with cells. *Biomacromolecules, 10*, 2379-2400.

Conclusions

Two major conclusions for this project may be delineated. On the one hand, four novel firefly luciferase-based bioluminescent methods were developed, optimized, characterized and tested in real samples. On the other hand, the original aim of uncovering the chemical structure of *Fridericia heliota*'s luciferin and the testing of this bioluminescent system as the basis for novel methods was not achieved. This can be explained by the very low amount of this compound in a tiny earthworm. Nonetheless the identification, structure elucidation and chemical synthesis of model compounds, CompX and AsLn(2), which share features with the authentic luciferin, shed lights on this elusive molecule.

Analytical chemistry is one of the pillars of modern society. From the simplest techniques up to the high-technology state-of-the-art equipment, it is present in food analysis, industrial production checkpoints, clinical medicine, environmental monitoring, basic research, and so on. The development and application of novel, improved methodologies is of utmost importance for the continuous evolution of this discipline.

Attractive features must be encountered in all new proposed methods, such as sensitivity, reduced costs, facility of analysis, low assay time, robustness. Of course there is not a perfect method, rather each analyst must select and adapt a methodology to her/his needs. In this sense, the purposes of this project were fulfilled, and the novel methods here presented may certainly constitute valuable tools for the scientific community, and beyond.